Elucidating cellular signaling mechanisms of *anoikis* resistance

by

Tony Ling Tin Ng

B.Sc., Simon Fraser University, 2002
M.D., The University of British Columbia, 2004

A THESIS SUBMITTED IN PARTIAL FULFILLMENT OF
THE REQUIREMENTS FOR THE DEGREE OF

DOCTOR OF PHILOSOPHY

in

The Faculty of Graduate and Postdoctoral Studies

(Pathology and Laboratory Medicine)

THE UNIVERSITY OF BRITISH COLUMBIA

(Vancouver)

April 2014

Abstract

Anoikis, which describes a physiologic apoptotic mechanism of non-hematopoietic cells that is triggered following detachment of cells from their native extracellular matrix, functions as a key process to prevent unwanted dissemination of cells from their intended organ site. Cancer cells, in contrast, develop mechanisms to suppress *anoikis*, allowing them to metastasize through the lymphovascular system to secondary organ sites. In this thesis, we utilized screening methodologies to identify novel signaling mechanisms of *anoikis* resistance in cancer cells. While a functional approach using an siRNA-based screen of Ewing sarcoma cells did not yield validatable hits, use of gene expression profiling demonstrated a remarkable resemblance of the cellular detachment process to various prototypical forms of cellular and bioenergetic stress, such as nutrient deprivation, hypoxia and endoplasmic reticulum stress. Correspondingly, activation of various cellular stress response pathways was demonstrated, which appear critical for mitigating this stress. In particular, two pathways were shown to play a role in *anoikis* resistance, mediated by TXNIP and AMPK. TXNIP, which has been shown to play a homeostatic role to modulate glucose metabolism, redox status and proliferation during stress states, was shown to be rapidly up-regulated following cellular detachment, and promotes *anoikis* in certain cell line models. AMPK is also rapidly activated, activating multiple downstream pathways to restore the bioenergetic status of detached cells, which show marked reduction in ATP levels following detachment. In particular, AMPK-mediated suppression of the mTORC1 pathway plays a particularly important role through the suppression of total protein synthesis levels,

an otherwise energetically-costly anabolic process. Blockade of the AMPK pathway or restoration of mTORC1 activation in cancer cells help to restore *anoikis*, while direct inhibition of protein synthesis in AMPK-deficient cancer cells restores their ability to suppress *anoikis*. Overall, we show that activation of energy-conserving pathways, normally considered "tumor suppressive" in nature, in fact promotes survival of cancer cells in this early stage of metastasis. This highlights the ambiguous role of many such pathways, which can both promote and suppress tumor progression in a context-dependent manner.

Preface

All of the work presented henceforth was conducted in the British Columbia Cancer Research Centre in Vancouver, British Columbia.

Portions of Chapters 3 and 4 have been published [Ng T. L., Leprivier G., Robertson M.D., Martin M.J., Laderoute K.R., Davicioni E., Triche T.J., Sorensen P.H. The AMPK stress response pathway mediates anoikis resistance through inhibition of mTOR and suppression of protein synthesis. Cell Death Diff. 2012 Mar; 19(3):501-10.]. I was the lead investigator, responsible for all major areas of concept formation, data collection and analysis, as well as manuscript composition. Leprivier G. was involved in the early stages of concept formation and contributed to manuscript edits. Robertson M.D. provided technical assistance with experiments and data analysis. Martin M.J. performed the technical aspects of an expression profiling experiment in Chapter 3. Laderoute K.R. provided the AMPK knockout cell line. Davicioni E. provided advice on expression profile data analysis. Triche T.J. contributed to manuscript edits. Sorensen P.H. was the supervisory author on this project and was involved in concept formation and manuscript composition.

I was the lead investigator for the projects described in Chapter 2 and the remainder of Chapter 3, where I was responsible for all major areas of concept formation, data collection and analysis, as well as the majority of manuscript composition. Robertson M.D. provided technical assistance with experiments and data analysis. Sorensen P.H. was the supervisory author on this project and was involved throughout the project in concept formation and manuscript composition.

Table of Contents

List of Tables

List of Figures

Acknowledgements

I would like to thank all the members of the laboratory, past and present, who has supported and guided me through the years. In particular, I thank Dr. Gabriel Leprivier, Dr. Barak Rotblat, Dr. Cristina Tognon, Dr. Naniye Cetinbas, Dr. Fan Zhang, Dr. Valentina Evdokimova, Adi Barokas and Amy Li, all of whom have provided invaluable scientific and personal guidance through my years of training. I would also like to acknowledge Matthew Robertson and all the students who have provided technical support during their training in the laboratory. I would also like to thank Dr. Blake Gilks, Dr. Torsten Nielsen and the Anatomical Pathology residency program at the University of British Columbia, who supported and mentored me throughout this invaluable opportunity.

I am also grateful to Dr. Poul Sorensen for his guidance, and for this opportunity to freely delve into basic science research, as well as the guidance of my graduate committee, Drs. Samuel Aparicio, Torsten Nielsen and Calvin Roskelley.

Finally, I would like to thank my family and friends for their love and support. In particular, I thank Jean, Gavin, Julia, my parents and my parents-in-law for their unwavering and unconditional support.

The work contained herein has been financially supported by training fellowships from the Clinician Investigator Program of the Royal College of Physicians of Canada, the Canadian Institutes of Health Research, and the Michael Smith Foundation for Health Research, as well as research grants from the US Department of Defense, the British Columbia Cancer Foundation and the Canadian Institutes for Health Research.

Dedication

To Jean, Gavin and Julia

who loved and supported me

through every moment of this journey

Chapter 1 INTRODUCTION

1.1 SYNOPSIS AND RATIONALE FOR THESIS

Tumor metastasis represents a clinically- and biologically-critical step in cancer development. However, our understanding of the metastatic process remains in its infancy, in part because tumor metastasis represents a complex and multi-step process that requires numerous cellular and molecular adaptations by tumor cells (1). One of the initial properties that tumor cells must acquire in the metastatic cascade is the ability to separate away from the primary tumor, through a physical detachment of tumor cells from the familiar environment of other tumor cells and the native extracellular matrix (2). In contrast, normal cells and non-metastasizing tumor cells are unable to survive following such detachment, and instead undergo rapid apoptosis. Termed *anoikis*, this was initially described in 1994 as a physiologic cell death process of non-transformed cells that cancer cells must suppress to allow them to metastasize (3). Over the years, numerous mechanisms have been discovered that allow cancer cells to suppress *anoikis* (4). Ultimately, it is hoped that a greater understanding of such mechanisms will allow for therapeutic strategies that help restore the *anoikis* process in cancer cells as a method to prevent tumor metastasis.

However, much of our understanding of *anoikis* resistance relates to mechanisms relating to cell survival and death pathways that have been investigated since the early studies in *anoikis*. In particular, the studies have focused on pro-survival pathways governed by tyrosine kinases, as well as direct

modulators of the apoptotic machinery that promotes cell death (4). In recent years, however, we have gained a greater understanding of more non-canonical mechanisms governing cancer cell survival. In particular, it has become increasingly apparent that adaptations in cellular metabolic processes are critical for cancer cells to survive under various environmental states (5).

The rationale for this thesis is to reinvestigate cellular signaling mechanisms of *anoikis* resistance in the context of these recent insights in cancer biology, in the hopes of elucidating novel mechanistic pathways. Furthermore, the investigations in this thesis will be approached using non-biased techniques including gene expression profiling and high-throughput functional screening, such that the initial direction of the research will be hypothesis-generating rather than hypothesis-based. Overall, the aim is to elucidate novel and unexpected mechanisms into this critical step in cancer progression, and identify novel anti-metastatic therapeutic strategies involving non-canonical pathways.

1.2 GENERAL CONCEPTS IN CANCER BIOLOGY AND THERAPEUTICS

1.2.1 TRADITIONAL PARADIGM OF CANCER

Despite significant progress in our understanding of the biology of cancer progression, and the development of improved therapeutics as a result, cancer remains the second most common cause of mortality in developed nations (6). One possible explanation is that the overall approach to cancer therapy remains similar to that used for much of the previous century. Following the detection of a tumor, the initial treatment modality for the great majority of solid organ tumors is surgery.

When a tumor is deemed operable, usually in the absence of apparent systemic tumor spread, the entirety of a primary tumor is removed, with the patient clinically deemed "disease-free" (7). However, it is well understood that many such patients continue to have a risk of tumor recurrence, particularly those with high-risk clinical parameters such as large primary tumor size or lymph node metastasis (7). This is biologically explained by the presence of clinically undetectable residual tumor cells, either in the primary site or in secondary organ sites. Such tumor cells are thought to exist as either single cells or as microscopic tumor clusters, below the detection limits of powerful imaging techniques such as high-resolution magnetic resonance imaging (MRI), and even metabolism-based imaging modalities such as positron emission tomography (PET) (8, 9). Consequently, systemic chemotherapies are administered with the intention of eradicating these tumor cells to prevent the development of local or distant recurrent disease.

However, the success rates of such systemic therapies are often poor (10). One important reason is the toxicity of traditional chemotherapeutics, the vast majority of which are designed to target and non-discriminately kill rapidly proliferating tumor cells, thus also affecting normal cells that have high proliferation rate such as intestinal epithelial and hematolymphoid cells, putting the patients at risk for therapy-related morbidity and mortality (11). Just as importantly, despite administration of such highly toxic chemotherapy, many patients eventually develop tumor recurrence. This may occur shortly after the cessation of chemotherapy, often seen with the most lethal tumor types such as ovarian and lung cancer, or may occur remotely after initial disease (9). The ability of tumor cells to persist despite

exposure to these powerful therapies highlights an apparent although highly unresolved concept: such residual tumor cells are frequently resistant to such therapies, and it is unclear whether these cells inherently lack susceptibility or whether they secondarily develop chemoresistance (9). Overall, the search for a systemic therapy capable of eliminating such undetectable residual tumor cells represents the key goal of therapeutic development.

Even though such chemotherapies have relatively high failure rates, the currently available range of systemic therapies remains quite limited (12). Although the mechanisms of action are broad, such as DNA intercalation (anthracyclines), inhibition of microtubule assembly (vinca alkaloids), inhibition of topoisomerase (plant alkaloids) and DNA crosslinking (platinum-containing agents and alkylating agents), most of these agents target cells that are highly proliferative or metabolically active (12). In contrast, cells that are biologically indolent are able to survive despite systemic administration of such agents (9). Such agents have shown remarkable effectiveness in tumor types that display uniformly high rates of proliferation, such as lymphomas and certain childhood sarcomas (13). However, their effectiveness in the most common types of solid organ malignancies remains limited. Despite this and their known toxicities, these agents continue to be routinely used in these tumor types.

The biological basis for using such agents is the concept that cancer cells have significantly higher rates of cell division and DNA replication. This feature of tumor cells is best summarized in a landmark review article by Hanahan and Weinberg in 2000 titled “The Hallmarks of Cancer” (14). The authors highlighted six

critical features of cancer cells, emphasizing their autonomous and limitless ability for growth, in addition to their propensity to resist apoptosis and sustain angiogenesis. This article was reflective of the overall understanding of cancer at that period, and the study of cancer biology was heavily focused on the multitude of mechanisms used by cancer cells to persist in the cell cycle and avoid cell cycle inhibition, driven by various self-sufficient proliferation signals such as growth-promoting tyrosine kinases. This was described in the context of gain-of-function alterations in proto-oncogenes that most often lead to sustained cellular proliferation, and loss-of-function alterations in tumor suppressor genes that lead to resistance to apoptosis, loss of DNA damage repair mechanisms as well as increased tumor growth. As a result, the primary model used to study tumors has been tumor cell lines and tumor samples derived from the rapidly proliferating cells of primary tumors. Consequently, compounds were identified based on their ability to kill or inhibit growth of preclinical tumor models derived from these cells, such as rapidly-proliferating monolayer tissue cultures of tumor cell lines, or exponentially-growing xenografts in immunodeficient mice. While these models have reaffirmed the effectiveness of the traditional chemotherapeutic agents, novel compounds have and continue to be identified using these models. Although some agents identified over the last decade have shown clinical effectiveness, they are nearly always used in conjunction with traditional chemotherapeutics, which continue to be the standard of care for most cancers (15). The majority of these so-called targeted therapies that are currently in routine clinical use still aim to target the proliferating tumor cell, through inhibition of various classic oncogenes such as growth-

promoting tyrosine kinases (16). Despite the remarkable effectiveness of certain agents in specific tumor types, such as HER2 kinase inhibitors in breast cancer, and c-kit inhibitors in gastrointestinal stromal tumors, most of these novel agents show only modest therapeutic benefit for the vast majority of tumor types (16). Other agents have attempted to target the other noted cancer "hallmarks", such as angiogenesis inhibitors and promotion of apoptosis through proteasomal inhibition, but these agents have also shown very modest effect (17).

1.2.2 CELLULAR STRESS IN A MODIFIED PARADIGM OF CANCER

Over the past decade, there has been a significant shift in our understanding of cancer. One critical advance has been the understanding that cancer is a far more dynamic disease than previously thought. Many recent studies have shown that cancer cells exhibit various adaptive changes during the course of disease progression, rather than existing in a static state of relentless growth and survival (18). Instead, while it is likely true that most cells within a tumor exhibit the traditional "hallmarks" of cancer, there are many steps during progression of disease that cancer cells exhibit far different functional states. For example, cells away from the periphery of a large primary tumor often have poor access to blood supply, and thus suffer from oxygen and nutrient deprivation (19). Rapidly proliferating and genetically altered tumor cells must also adapt to and repair accumulating DNA mutations that would otherwise trigger cell death (18). In addition, when tumor cells have spread to secondary sites, they are forced to exist in a new tissue environment in the absence of familiar growth factors and extracellular matrix, and must adapt to a new tumor "microenvironment" before they are able to

establish growth of a significant metastatic lesion (1). Overall, tumor cells are subjected to a wide variety of stresses during their growth and progression to clinically significant disease, and must activate various stress response mechanisms to survive through such conditions (20). Therefore, such cellular response mechanisms may in fact be protective for cancer cells, and contribute to tumor survival and progression (20). The significance of these findings is such that the "hallmarks of cancer" have recently been revised by Hanahan and Weinberg to in part include these concepts of adaptation into their model, particularly with respect to metabolic adaptations in response to cellular metabolic stress (18).

While studies of the pro-tumorigenic effects of cellular stress responses have only recently become the focus of investigations, the importance of the cellular response to stress has been frequently demonstrated in the past, particular with regards various cancer-specific genes identified in the past decades. Most notably is the role of p53 in cancer. Its best-characterized function is as a tumor suppressor to counteract the initiation events that lead to cancer, through its ability to transcriptionally up-regulate genes that activate protective mechanisms such as cell cycle arrest and apoptosis (21). These functions of p53 are activated in response to various stresses such as DNA damage and hypoxia, through transcriptional and post-transcriptional up-regulation of p53 protein levels. While it has been shown that such up-regulation of wild-type p53 has a robust ability to suppress tumor development, the up-regulation of other stress response genes often results in activation of pathways that do not result in tumor suppression. For example, a critical gene in the response to hypoxia is the transcription factor HIF-1alpha (19).

Through the hypoxia-mediated inactivation of the VHL E3-ubiquitin ligase, HIF-1alpha protein is rapidly induced in conditions of low oxygen. Rather than triggering apoptotic pathways to eliminate cells burdened with such stress, HIF-1alpha up-regulates a number of adaptive mechanisms to promote survival, including a switch towards anaerobic metabolism and promotion of angiogenesis (22). Hence, while some stress response mechanisms have evolved to serve an adaptive role at the organism level by suppressing disease-causing tumor formation, many of the stress responses are adaptive at the single cell level, and consequently may serve to promote tumor survival and progression. This highlights the dependence of cancers not only on the genes and pathways required for the continued proliferation and expansion of the tumor, but also on mechanisms that allow tumor cells to survive the multitude of environmental challenges faced during cancer progression. This dependence on the genes and pathways required to make this metabolic and proliferative "switch" to a more indolent cellular state has been termed "non-oncogene addiction", referring to the fact that most of such genes participate in normal cellular functions rather than contributing to the "oncogenic" phenotype (20).

1.2.3 TUMOR DORMANCY

While the possible stress response mechanisms used by cancer cells are highly diverse, one common objective is for the cell to shut down the metabolically demanding functions in order to conserve cellular energy levels and divert resources to overcome such stresses (20). This is evident in certain stresses that directly impact the cellular metabolic state, such as hypoxia and nutrient

deprivation. Under oxygen-deprived conditions, cells instead utilize oxygen-independent catabolic processes such as glycolysis rather than oxidative metabolism (as mediated by HIF-1alpha) (19). Nutrient deprivation also forces cells to halt anabolic processes such as protein synthesis (as mediated by inhibition of the mTOR pathway) (23). However, shut down of these processes also prevents the ability to sustain the "hallmarks of cancer". Most importantly, cancer cells must be able to inhibit their usual proliferative state driven by sustained oncogenic function. Other stressors also trigger proliferation arrest, for example via p53-mediated up-regulation of p21 following DNA damage and GADD45a mediated cell cycle arrest during ER stress (24, 25).

The ability to activate such cellular quiescence despite sustained oncogene-driven proliferation signals relates to a concept termed tumor dormancy (9). This concept has re-emerged in the literature to mechanistically explain this phenomenon of cancer recurrence occurring after a prolonged period of clinically undetectable disease, where tumor cells enter a sustained period of reduced growth. Dormant tumor cells appear to occur at various stages in the course of tumor progression, existing either at the primary tumor site, as circulating tumor cells in the lymphovascular system, or as disseminated dormant tumor cells in secondary organ site, reflecting potential future sites of tumor recurrence (7).

1.3 TUMOR METASTASIS – A MULTISTEP PROCESS

Tumor cell metastasis represents a clinically critical process in the overall progression of metastasis, as it continues to represent the cause of mortality for greater than 90% of cases of the common solid organ cancers (26). Although its

importance was highlighted in the "Hallmarks of Cancer," its description in that paper as a single process belies the complexity of this phenomenon. In particular, because of the multitude of processes that is required for the development of metastases – from the local invasive spread away from the primary tumor, to the extension of tumors cells into the lymphovascular circulation, to the survival and growth of tumor cells at secondary organ sites – the cellular mechanisms required for a tumor to transition into a clinically-relevant metastasis are highly multifaceted. In fact, mechanisms required in the early stages of metastasis, when tumor cells are required to disseminate and survive for prolonged periods of time in foreign environments, appear to conflict with mechanisms in the later stages of metastasis that require tumor cells to undergo significant proliferation (1). Despite the intricate processes required for metastasis, the vast majority of common solid organ malignancies will ultimately develop metastases in their natural history, and the various localized and systemic therapies currently available to either prevent or treat metastatic disease continue to have high failure rates.

1.3.1 INTRAVASATION AND LYMPHOVASCULAR INVASION

The multistep process of metastasis begins with the initial departure of tumor cells from the primary tumor site, and this is represented by the ability of cells to enter and survive in the lymphatic or vascular circulation. The ability of tumor cells to enter these lymphovascular spaces has been apparent through the microscopic study of tumors by anatomical pathologists, illustrated best as tumor cell clusters within lymphovascular space in microscopic sections of tumor (27). Such lymphovascular invasion (LVI) can be seen either as an isolated, focal finding,

or may be seen widely within a given tumor, and is strongly associated with certain tumor types, such as micropapillary carcinoma of the breast or bladder, and the so-called inflammatory breast cancer (28, 29). Although the clinical significance of LVI is still controversial, there is significant evidence that the presence of LVI in various cancers (such as breast and urothelial carcinoma) is correlated with lymph node metastasis (30), disease recurrence and increased mortality (31). As a result, reporting of the presence of LVI is an important part of the pathologic assessment of many tumors, as its presence is used as a factor in determining the clinical management of the patient (32, 33).

To achieve intravasation, tumor cells must be able to cross the physical barrier of the vessel wall, including the cellular and extracellular matrix components. This ability has been shown to be mediated by both cancer cell signaling pathways such as Notch (34) and secreted factors such as TGFbeta (35). Mediators of epithelial-to-mesenchymal transition (EMT) such as Twist also appear to contribute to this (36). Cooperative cells in the tumor stroma may also play an important role, such as tumor-associated macrophages (37). The capacity for intravasation appears to be increased in the tumor setting in part due to the incomplete integrity and maturity of tumor blood and lymphatic vessels and the associated haphazard neovascularization seen in tumors (38).

Once in the lymphovascular circulation, tumor cells must be able to survive in this setting that is absent of survival signals that come from its native extracellular matrix environment. In addition to lymphovascular emboli that are observed in pathological tumor tissue specimens, this phenomenon is also seen in

the clinical setting as circulating tumor cells (CTCs). While the biological and clinical importance of CTCs is still being elucidated, there is emerging data that the presence of CTCs is associated with negative prognosis in multiple tumor types, including melanoma and lung cancer (8, 39). The ability to isolate CTCs has also allowed for preliminary studies into their biology. Genome-wide profiling of CTCs have characterized a number of up-regulated genes and pathways that presumably contribute to the survival of CTCs and subsequent metastases (40, 41), and have demonstrated both genotypic similarity to the primary tumor (42) as well as evidence of molecular evolution towards the metastatic tumor (43). Interestingly, the recent ability to isolate greater numbers of CTCs has allowed for more direct characterization of their biological behavior, including evidence of up-regulation of various anti-apoptotic pathways and activation of EMT programs (44, 45), as well as an unexpectedly high level of heterogeneity in their proliferation signatures (46). There is also recent data suggesting that CTCs may exist not only as single cells, but also as small tumor cell clusters, due to the ability to isolate CTCs without excessively disruptive microfiltration methods (8, 47). Surprisingly, such CTC clusters appear to have a significantly lower proliferation index compared to both the primary tumor and single CTCs based on Ki67 antibody labeling, suggesting increased cellular quiescence (8). This therefore may represent a source of disseminated tumor cells in a state of dormancy, and represent a subpopulation that would be resistant to therapeutic agents that target proliferative tumor cells.

It has been proposed that CTCs can be utilized not only for investigational purposes but also for more direct clinical use. While the supportive evidence

remains weak, the quantitation of CTCs has been shown to be useful as a predictive marker of response to systemic therapy in some studies. The monitoring of CTCs has also shown possible utility in predicting disease recurrence following surgical resection of the primary tumor (46). In addition, obtaining CTCs may serve as a so-called "liquid biopsy" to obtain cells that predict the genotype or phenotype of yet-to-develop metastases; as an example, targetable EGFR mutations have been detected in CTCs of non-small-cell lung cancer patients where no such mutations were noted in the primary tumor (48).

Some studies have attempted to directly characterize such lymphovascular emboli. One group has performed extensive studies on lymphovascular emboli using a model developed from a case of inflammatory breast carcinoma, which represents a clinicopathologically-defined breast cancer type with extensive lymphovascular invasion, particularly involving the dermis, resulting in an "inflammatory" erythematous appearance in the skin overlying the cancer (49). Their studies have shown the role of various mediators promoting the survival of such tumor cell emboli. One demonstrated mechanism is through the up-regulation of E-cadherin, promoting a homotypic cell-cell adhesion-mediated survival, with simultaneous down-regulation of the endothelium-binding glycoprotein sialyl-Lewis X (50, 51). More recent studies have shown that specific protease-mediated cleavage of E-cadherin is important to generate an isoform that mediates survival (52). This pro-survival role of E-cadherin is in contrast to the generally accepted tumor suppressive role of this protein. This group has also demonstrated that such emboli show stem cell-like features and dependence on a Notch3-mediated anti-apoptotic

pathway, supportive of a role of transdifferentiation to promote survival following lymphovascular invasion (49, 53), similar to the previously mentioned studies on CTCs. Overall, these studies provide support that mechanisms promoting early tumor metastasis mimic the mechanisms promoting survival of lymphovascular emboli.

1.3.2 TUMOR CELL DISSEMINATION AND EXTRAVASATION

Once tumor cells have survived the transition into the lymphovascular circulation, they are then able to disseminate to secondary organ sites. There is some support that this is an entirely passive process, where the distribution of tumor cells from the primary site is dictated entirely by the flow of the vasculature (1). As tumor cells, particularly from epithelial malignancies, have sizes greater than 20 microns, more than twice the diameter of the average capillary lumen, it is likely that tumor cells become passively entrapped in the first capillary beds they encounter once in circulation (1). However, there is also evidence that tumor cells have the propensity to target certain organs during their dissemination (54). This may be mediated by various secreted factors derived from the target organ sites such as chemokines, or various adhesion molecules on the tumor cells themselves that selectively bind to the vasculature in target organs (1). Furthermore, such passive entrapment in capillary beds is not an absolute limiting factor, since malignancies from any organ site are capable of developing metastases in essentially any secondary site (54).

While it has been suggested that such dissemination to and entrapment in the capillary beds of target organs occurs rapidly following intravasation, in the

order of minutes to a few hours (1), there are certain sites in the circulation where CTCs or disseminated tumor cells may persist for prolonged periods in the absence of attachment to the vascular wall, such as in the bone marrow (55). Such tumor cells have been repeatedly identified in a high proportion of clinically disease-free breast cancer patients, and their presence has been predictive of disease recurrence as subsequent metastases (56). These dormant bone marrow tumor cells have also demonstrated persistence and poor response following systemic chemotherapy (57). Therefore, the factors governing the survival of CTCs or disseminated tumor cells likely remain important in determining the capability a cancer to eventually develop overt metastatic disease.

Following arrival at a target organ, tumor cells must first achieve extravasation to allow for subsequent development of a metastatic mass. The mechanisms underlying extravasation from the target organ vasculature appear different from those identified for intravasating tumor cells. For example, in a mouse and rat model of lung metastases, tumor cells have been shown to have the capacity to proliferate directly within the lung vasculature rather than following a specific extravasation mechanism, destroying the underlying vascular wall in the process (58). Tumor cells have also demonstrated the ability to undergo a more definitive extravasation process, mediated through tumor cell secreted factors that increase vascular permeability such as angiopoetin-like-4, COX-2 and VEGF (59-61). Such factors may also contribute to the tropism of the tumor cells, as certain factors such as angiopoetin-like-4 (ANGPTL4) appear to have an effect specific to the vasculature of the lung (61). Interestingly though, there is evidence that the ability

of cancer cells to extravasate is not mediated by transforming oncogenes per se, as there is evidence that transformation with H-Ras does not affect the ability of cells to extravasate compared to non-transformed fibroblast controls (62), although this data relied on the model of intravenous injection into chicken embryo chorioallantoic membrane. Overall, based on the currently available literature data, there is not significant evidence to suggest a rate-limiting role for extravasation in tumor metastasis, although tumor secreted factors such as ANGPTL4 as well as the characteristics of the target organ vasculature may help dictate the preferred organ sites for metastasis for a particular cancer type.

1.3.3 DEVELOPMENT OF MICROMETASTASES

The ability of single disseminated tumor cells or tumor cell clusters to subsequently sustain survival as a micrometastasis appears to represent a key step in the overall development of a clinically relevant metastasis. Much of the literature has focused on determining how the factors in the so-called microenvironment of the secondary organ site contribute to or prevent the formation of micrometastases. The conceptual basis for this is the “seed and soil” hypothesis by Stephen Paget in 1889, which proposed that the tissue properties of the target organ site are key determinants in the ability of a metastasis to form. As such, it has been determined that various components of the metastatic site, such as the stromal cells, extracellular matrix and secreted factors, contribute either to the hospitability or the hostility of this microenvironment for the arriving tumor cell (1). Tumor cells are also capable of altering the hostile factors of the microenvironment to promote their survival, even prior to leaving the primary site. For example, primary tumors

are able to secrete factors such as the hypoxia-induced lysyl oxidase that reach the metastatic site, which stimulate stromal cells in the target organs to recruit circulating cells that ultimately alter the extracellular matrix microenvironment into a permissive state for later metastatic development. There is also dependence on survival signaling pathways in these micrometastatic cells to resist intrinsic and extrinsic triggers of apoptosis, such as Src kinase signaling in metastatic breast cancer cells in the bone marrow (63), and the SDF1/CXCL12 factor secreted by bone marrow mesenchymal cells that promote survival of breast cancer cells expressing the corresponding receptor CXCR4 (64). In summary, the development of micrometastases from single disseminated tumor cells depends on both cell autonomous and non-autonomous survival factors.

1.3.4 GROWTH INTO OVERT METASTASIS

It has been proposed that the final step in the metastatic cascade – outgrowth of a micrometastasis into a clinically-overt metastasis – represents the rate-limiting step in the overall metastatic process. This is supported by data in immunocompetent mice injected intravenously with a syngeneic mouse melanoma cell line, showing that while the efficiency rates of earlier steps are relatively high, with about 80% of potentially metastatic cells achieving extravasation and 3% of cells achieving formation of a micrometastasis, the proportion of cells eventually developing into a metastatic lesion is <0.02% (65). One important contributing factor to the low efficiency of developing overt metastatic lesions is the high rate of death of micrometastatic lesions that were able to survive initially. Hence, the

mechanisms governing growth and survival following extravasation appear to be critical in determining the metastatic ability of a cancer.

One proposed barrier to the emergence of growth from a micrometastasis is the relative inability to reactivate the proliferative signaling pathways that are active in the primary tumor setting, such as the integrin beta1-focal adhesion kinase axis (66). To escape from such lack of proliferative signals, there is evidence tumor cells recruit bone marrow-derived circulating cells that subsequently secrete pro-growth factors such as osteopontin (67). Another contributing factor is the level of angiogenesis in an early metastatic lesion. Tumor cells may secrete factors that suppress angiogenesis such as prosaposin (68), or promote vascularization such as angiopoetin-2 (69); the balance between pro- and anti-angiogenic factors may mediate a form of angiogenic dormancy in the metastatic lesion that suppresses growth until suitable microenvironmental conditions are present. Metastatic tumor cells may also secrete factors to directly modulate the organ environment to permit growth, such as breast cancer cell expression of IL-11 and Jagged1 that promote osteoclastic activity to allow for metastatic growth in the physically rigid bone environment (70). Overall, the mechanisms that promote metastatic outgrowth recapitulate that utilized in the primary tumor, with the added challenge of the hostile microenvironmental conditions encountered in a foreign organ site.

1.4 *ANOIKIS*

1.4.1 *ANOIKIS* AND ANCHORAGE INDEPENDENCE

It has long been recognized that the property of anchorage-independent growth and survival is critical to the cancer phenotype. In fact, the capability of prolonged survival and growth in a three-dimensional setting is essentially definitional for cellular transformation in the *in vitro* setting, correlating well with the ability to develop tumors in animal models (71). It is well-known that expression of various oncogenic proteins such as mutant Ras in otherwise immortalized but non-transformed cell lines is sufficient to confer this property of anchorage independence (72). However, for many years, the signaling mechanisms underlying this oncogene-mediated property were poorly understood.

In 1994, Frisch and colleagues identified a related phenomenon whereby epithelial cells would undergo rapid apoptosis following loss of cellular anchorage to an underlying extracellular matrix (3). This phenomenon was termed *anoikis*, a Greek term meaning "homelessness." Such *anoikis* death was achieved quite simply in the *in vitro* setting using immortalized cell lines that would proliferate indefinitely in a monolayer culture setting, but would undergo such rapid cell death when prevented from attaching to the plastic substratum on which it is normally cultured, and forced to exist in suspension conditions. *Anoikis* was most evident when epithelial cell lines were used, with fibroblasts showing relative *anoikis* resistance. Interestingly, when transforming oncogenes such as H-Ras, v-Src and transformation promoter agents such as phorbol ester were introduced, the level of

anoikis was markedly reduced (3). Therefore, *anoikis* resistance was conferred to cells by oncogenes and agents that also conferred anchorage independence.

As a result, early studies into *anoikis* utilized this *in vitro* phenomenon as readout of anchorage independence and therefore cellular transformation. Subsequent studies confirmed the ability of various classic oncogenes to confer *anoikis* resistance, and this was dependent on the downstream activation of pathways such as Raf/Erk and PI3K/Akt, correlating with their ability to form colonies in the soft agar assay (73). These data therefore served as evidence that the ability to cope with absent cellular attachment is critical in the development of three-dimensional colonies in a matrix-free environment.

1.4.2 *ANOIKIS* AND METASTASIS

Conceptually, the phenomenon of *anoikis* in normal epithelial cells would presumably serve to prevent cells from colonizing a foreign tissue environment if detached from the primary site (74). Therefore, overcoming *anoikis* susceptibility would be a critical first step for cancer cells to begin the metastatic cascade. However, while the early literature following the discovery of *anoikis* further established the validity of this phenomenon *in vitro*, studies were needed to correlate *anoikis* resistance with metastatic capability *in vivo*. Indeed, over the years, evidence accumulated supporting the relevance of *anoikis* in tumor metastasis (2). Although some doubt the relevance of *anoikis* in the clinical setting due to the suggestion that the time spent in circulation is transient (1), there is evidence that tumor cells can remain in suspension absent of extracellular matrix attachment for prolonged periods of time, particularly as tumor cell clusters (8), and in low-flow

circulatory sites such as the bone marrow. Furthermore, metastases within the peritoneal cavity also appear to depend on the availability of an attachment site for the tumor cells, either on the peritoneal surface itself following destruction of the mesothelial layer, or as multicellular clusters of tumor cells through homotypic cell-cell interactions (75).

Following the initial description of *anoikis* by Frisch, a number of *in vivo* correlates of this phenomenon were described in the literature, including matrix-dependent survival of breast epithelial cells (76). This dependence on matrix attachment for suppression of apoptosis was also described in non-epithelial cells such as myocytes and mouse embryonic fibroblasts (77). Such data supports a physiologic role for *anoikis*, both in metastasis suppression and as a means of cellular selection during tissue morphogenesis.

Subsequent papers gradually provided evidence to support a role of *anoikis* resistance in tumor dissemination. When gastric cancer cell lines were stably transfected with the *anoikis* suppressor Bcl-2, this resulted in increased peritoneal dissemination of tumor despite no effect on the proliferation rate or xenograft size (78). The converse was seen when caspase-8 was overexpressed in the same cells (79). Prostate cancer xenografts also demonstrated reduced numbers of metastases when levels of the *anoikis* suppressor FAK were knocked down by siRNA (80). There is also data supportive of a role for *anoikis* resistance in lung and breast cancer metastasis (81, 82), as well as non-epithelial cancers such as melanoma and neuroblastoma (83, 84).

A key piece of evidence in correlating *anoikis* resistance with metastasis was demonstrated by Douma et al., who used a genome-wide functional screen to identify novel suppressors of *anoikis* (85). Using rat intestinal epithelial (RIE) cells, a retroviral cDNA expression library was applied, and surviving clones were isolated following forced culture in suspension and multiple rounds of selection for survival. While normal RIE cells undergo massive apoptosis very shortly after cellular detachment, transformation using oncogenic Ras(V12) confers *anoikis* resistance and prolonged survival as multicellular spheroid clusters. Amongst the surviving clones from the cDNA overexpression screen, TrkB was identified as a potent suppressor of *anoikis*. This was shown to be dependent on hyperactivation of the PI3K/Akt pathway, although the role of pathways further downstream was not fully elucidated. Importantly, when these same cells were injected into the tail veins of immunodeficient mice, numerous metastases (predominantly in the lungs and heart) formed in mice injected with TrkB-overexpressing RIE cells, while unaltered RIE cells resulted in no metastases. Interestingly, when TrkB cells were further stimulated with the TrkB ligand BDNF, even greater numbers of metastases formed, including in sites such as bones, kidneys, liver and soft tissues. Therefore, *in vitro* resistance to *anoikis* correlates well with metastatic capability in an *in vivo* model of metastasis. Furthermore, the level of activation of *anoikis* suppressors such as TrkB appears to correlate with extent of metastatic disease, and the disease burden does not appear to be limited to the capillary bed that the tumor cells first encounter (i.e. the lung capillary bed following injection into the tail vein).

Subsequent studies further established the correlation between *anoikis* resistance and metastatic capability by the tail vein mouse model. This included further studies correlating TrkB mutation and overexpression with metastasis in breast carcinoma cell lines (86), as well as in other non-epithelial cancers such as melanomas and sarcomas (87, 88). Importantly, *anoikis* resistance was also shown to correlate with the rate of spontaneous metastasis from tumor xenografts (80, 89). Increased metastasis was also shown to correlate with suppression of *anoikis* mediated by loss of E-cadherin in a conditional knock-out mouse model of lobular breast cancer (90). Interestingly, a recent study was able to determine the expression profile of circulating tumor cells through isolation and characterization of CTCs from an endogenous mouse model of pancreatic adenocarcinoma using next-generation-based RNA sequencing and transcriptome profiling (40). Using this model, they identified Wnt2 as overexpressed in CTCs, and this overexpression resulted in suppression of *anoikis* through downstream activation of the TAK1 kinase. Overall, these studies lend support to the validity of investigating *anoikis* resistance as a mechanism promoting metastatic capability.

1.4.3 *ANOIKIS* IN RELATION TO OTHER *IN VIVO* PHENOMENA

While the focus of *anoikis* research has been in relation to metastasis, the *anoikis* phenomenon has been shown to correlate with other processes seen *in vivo.* For example, Debnath, Brugge and colleagues first showed that the lumen in breast acini are formed due to gradual apoptosis of luminal cells, and specifically result from *anoikis* death following detachment from the acinar basement membrane (91, 92). Suppression of *anoikis* would therefore result in sustained luminal proliferation

and filling, correlating with the pathological phenomenon of breast ductal carcinoma-in-situ (DCIS). The connection between this physiologic process in breast development, termed acinar morphogenesis, and *anoikis* was supported by numerous further studies by multiple groups (93-95).

Anoikis also appears to play a role in processes unrelated to cancer. Endothelial cells have also been shown to be dependent on attachment for survival, and this attachment appears to be disrupted by mechanical forces such as sheer stress secondary to hypertension (96). Vascular smooth muscle cellular attachment is also disrupted by hypertension through tensile forces. Therefore, mechanical forces appear to promote apoptosis of vascular cellular components, resulting in reduced vascular integrity and increased development of degenerative processes such as atherosclerosis (97). The phenomenon also appears to affect cardiac myocytes, and their susceptibility to *anoikis* may contribute to heart failure secondary to cardiac hypertrophy (96).

Such endothelial cell survival may also play a role in tumor vasculature (98). Furthermore, *anoikis* resistance in endothelial cells conferred by viral oncogenes such as vFLIP from HHV8 appears to be an important mechanisms of carcinogenesis mediated by these oncogenes (99). Overall, *anoikis* appears to contribute to various *in vivo* phenomena beyond its role as an anti-metastasis process.

1.5 MECHANISMS OF *ANOIKIS* RESISTANCE

1.5.1 *ANOIKIS* RESISTANCE MEDIATED BY PROTEIN KINASE PATHWAYS

Early studies by Frisch and colleagues following the initial discovery of *anoikis* focused on investigating various kinase-mediated signaling mechanisms that modulated *anoikis*. They identified various Jun N-terminal kinases (JNKs), also known as stress-activated protein kinase (SAPKs) in promoting *anoikis*, while anti-apoptotic pathways were mediated by integrins ultimately leading to the up-regulation of Bcl-2 (100). In addition, transformation by H-Ras(V12) suppressed JNK activation, correlating with reduced cell death. They further showed that JNK-mediated activation of the intermediary kinase MEKK-1 results in *anoikis* in a caspase-dependent manner, resulting in a positive feedback loop through MEKK-1 mediated activation of caspases (101). However, a subsequent study by Khwaja and Downward showed evidence to the contrary, demonstrating a lack of association between JNK activation (as well as activation of the related stress-activated kinase p38) and levels of *anoikis* death (102). Rather, cellular detachment was correlated to activation of PI3K/Akt in the context of H-Ras(V12) transformation. Another study by the same group further established a role for the PI3K/Akt pathway in the suppression of *anoikis*, showing that chemical inhibition of this pathway was sufficient to restore *anoikis*, despite the lack of hyperactivation of Akt following detachment (73). Another kinase shown in early studies to contribute to *anoikis* resistance was focal adhesion kinase (FAK), known to be a transducer of integrin function (103). In addition, integrin-linked kinase (ILK) activity was also associated with suppression of *anoikis*, again through activation of Akt (104). Overall, while

these early studies implicated a large number of prototypical kinase signaling pathways in both mediating *anoikis* susceptibility, they all appeared to converge on the PI3K/Akt pathway.

Subsequent studies demonstrated a role for numerous kinase pathways in *anoikis* resistance, particularly various receptor tyrosine kinases. This includes the EGFR receptor tyrosine kinase, which various groups have shown to promote *anoikis* resistance through the MAPK pathway and direct activation of Src (105, 106). Integrin-dependent activation of EGFR has also been demonstrated (107). Interestingly, ligand-independent EGFR activation has also been observed in squamous cell carcinoma, and this was dependent on cell-cell adhesion mediated by E-cadherin (108). We have previously shown a very similar mechanism through the ErbB4 tyrosine kinase, which promotes *anoikis* resistance in Ewing sarcoma cells dependent on cell-cell adhesion again mediated through E-cadherin (109). As previously discussed, the TrkB kinase also appears to play a critical role in numerous cancer types, as well as the other key members of the neurotrophin receptor kinase family TrkA and TrkC (110-112). Therefore, various receptor tyrosine kinases play an important role in *anoikis* resistance, both in a ligand-dependent and –independent manner.

One key receptor kinase pathway shown to contribute to *anoikis* in multiple cell types is that mediated by the insulin-like growth factor-1 receptor (IGF-1R). IGF-1R was first found by Valentinis et al. to mediate *anoikis* resistance through activation of FAK (113). Further studies by the same group using various mouse fibroblast models showed that IGF-1R also activates Akt to suppress *anoikis*,

mediated through the intermediary protein IRS-1 (114), with an alternative *anoikis* resistance pathway through a cell-cell adhesion-mediated activation of endogenous Ras (115). Interestingly, IGF-1R mediated *anoikis* resistance appears to play an important role in primary sarcoma cell lines, including Ewing sarcoma (88, 116). Our group has also previously shown a critical role for IGF-1R in the suppression of *anoikis* mediated by the congenital fibrosarcoma fusion oncogene ETV6-NTRK3 (EN) (117). We showed that IGF-1R is required for EN to localize to the plasma membrane to form polymerized complexes with the IRS-1 intermediary protein. Such complexes are required for the downstream hyperactivation of Akt by EN that is critical for the transformation phenotype (118, 119). Importantly, this phenotype was reproducible in a mouse model of secretory breast cancer that transgenically expressed the EN oncogene in breast epithelial cells under a tissue-specific promoter (120). Consequently, we have also shown that pharmacologic inhibition of IGF-1R is sufficient to block the *in vitro* and *in vivo* transformation phenotype of EN-overexpressing breast epithelial cells (121). Another group has shown that IGF-1R promotes tumor metastasis without altering rates of proliferation or growth in three-dimensional culture, and this can be inhibited using a pharmacologic inhibitory antibody to IGF-1R (122). Such metastasis may be mediated by the ability of IGF-1R activation to increase the ratio of the pro-metastatic LIP isoform of the CCAAT/Enhancer binding protein beta (C/EBPbeta) transcription factor (123).

Various non-receptor kinases also play a central role in *anoikis* resistance mediated by various upstream and downstream mechanisms. Following the initial discovery by Khwaja et al. of the role of Akt in *anoikis* resistance, Akt activation has

been found to be critical in numerous *anoikis* resistance pathways. For example, oncogenic kinases such as B-Raf (124), and non-kinase pathways activated by TGF-beta (125) and TIMP-1 (126), have all been found to be upstream activators of Akt following cellular detachment. In addition, direct constitutive Akt activation using a farnesylated form of the kinase is sufficient to suppress *anoikis* (127). Deletion of the PTEN tumor suppressor (which normally dephosphorylates PI3K and suppresses Akt activation) also results in *anoikis* resistance (128). Akt appears to activate multiple novel downstream pathways to promote *anoikis* resistance, such as down-regulation of RhoB (87) and inhibition of FOXO3a activity resulting in de-repression of the caspase-8 inhibitor FLIP (129).

The closely linked MAP kinase/Erk pathway is also frequently hyperactivated in various *anoikis* resistance pathways. Interestingly, while constitutive hyperactivation of intermediary kinases such as the Raf-MEK-Erk axis results in *anoikis* suppression, limited and moderate activation of the same pathway appears to instead promote *anoikis* (130). Also, endogenous Ras activation has been shown to suppress *anoikis* through mechanisms independent of the MAPK/Erk and PI3K/Akt pathways (131). Erk may also signal directly to inhibit activation of apoptosis through up-regulation of the anti-apoptotic protein Bcl-2 (132).

Src kinase represents another non-receptor tyrosine kinase with a role in *anoikis* resistance. Although downstream activation of Akt has been shown to be important in Src-mediate *anoikis* resistance (133), Src has also been shown to activate other downstream pathways such as Pyk2 (134). Conversely, Akt-mediated suppression of *anoikis* has been found to be dependent on Src activation (135). Src

also appears to suppress detachment-induced apoptosis by directly modulating the apoptotic machinery, such as its ability to phosphorylate Bif-1 to block Bif-1/Bax complexes that contribute to the initiation of apoptosis (136). Other kinases in the Src-related family of kinases (SFKs) have also been shown to contribute to *anoikis* resistance (137).

More recently, some alternative kinase pathways have also been found to play a role. Cheng, Zhao and colleagues showed that SIK1 kinase was necessary in *anoikis* death that results from p53 activity (138). SIK1 represents one of many kinases that are dependent on the constitutive kinase activity of the known tumor suppressor LKB1 (139). *In vivo* metastasis studies confirmed an anti-metastatic role for SIK1, and clinical breast cancer samples showed a negative correlation between SIK1 levels and metastatic recurrence.

In summary, numerous classical and emerging kinase pathways have been found to modulate *anoikis*. While many of these kinases act through their modulation of central intermediary kinase pathways such as PI3K/Akt and MAPK/Erk, novel kinase-mediated *anoikis* resistance pathways continue to be identified.

1.5.2 *ANOIKIS* RESISTANCE MEDIATED BY INHIBITION OF APOPTOSIS

While it is evident that *anoikis* is closely linked to the process of apoptosis, it was recognized early in the investigations into *anoikis* that direct suppression of the apoptotic machinery was a key mechanism in *anoikis* resistance. As mentioned, the initial studies by Frisch and colleagues described the role of key anti-apoptotic proteins such as Bcl-2 in suppressing *anoikis*. Numerous studies since have

described various mechanisms by which inhibition of the intrinsic apoptotic pathway is critical to *anoikis* resistance. Oncogenic Ras transformation results in down-regulation of the pro-apoptotic protein Bak through the PI3K pathway (140). The same group showed that while the anti-apoptotic protein Bcl-X(L) is down-regulated following cellular detachment, Ras transformation prevents this down-regulation by directly preventing the release of the mitochondrial apoptotic protein Omi/HtrA2 (141), independent of the PI3K and MAPK pathways (142). This sustained Bcl-X(L) levels was also shown in the context of Src-mediated *anoikis* resistance (143). Another key pro-apoptotic protein in *anoikis* is Bim, as Reginato, Brugge and colleagues showed that increased Bim levels are critical in the *anoikis* pathway, mediated by withdrawal of integrin signaling; resistance to *anoikis* was demonstrated through sustained activation of the Erk pathway that blocked the up-regulation of Bim (144). This was also demonstrated in a Bim knockout mouse model, showing abnormal clearance of the lumens of breast terminal units during puberty (145). Other groups also showed that such suppression of Bim levels plays a role in Raf-mediated *anoikis* resistance (146, 147). In addition, pro-apoptotic protein Bad is phosphorylated and consequently inhibited downstream of the B-Raf/MEK pathway (147). Bax and Bid also play an important role, both translocating to the mitochondrion within 15 minutes following cellular detachment, resulting in cytochrome c release and apoptosis within a few hours (148, 149).

Studies into *anoikis* have not only led to the identification of apoptotic mechanisms mediating this phenomenon, but have also resulted in the discovery of novel proteins involved in apoptosis more generally. Bit1 was identified as a pro-

apoptotic protein suppressed by cellular attachment, and acts in a complex with the Groucho/TLE family member AES to promote *anoikis* in a caspase-independent manner (150), through its ability to directly suppress activation of Erk (151). Another fundamental mechanism of *anoikis* was illustrated by Puthalakath, Strasser and colleagues, describing a central role of the pro-apoptotic protein Bmf (152). Under attachment conditions, Bmf is sequestered to the myosin V motor complex; following detachment, Bmf is released, promoting apoptosis in part by binding to and inhibiting Bcl-2. However, the complexity and specificity of the apoptotic system was illustrated by Schmelzle, Brugge and colleagues, as they showed that while Bmf is important in the *anoikis* resistance and acinar morphogenesis of breast epithelial cells, BH3-only pro-apoptotic proteins Bad and Bid specifically did not play a role in *anoikis* death in these cells, although they did contribute to apoptosis in response to other death stimuli (153).

Another family of apoptosis-modifying proteins is IAP (inhibitors of apoptosis). An interesting study isolated CTCs from mice bearing xenografts of prostate carcinoma cells and compared their behavior to the primary tumor xenograft cells, showing relative *anoikis* resistance in the CTCs (154). The CTCs were found to have higher levels of the IAP proteins XIAP, cIAP2 and survivin, and the *anoikis* resistance of these cells was found to be dependent on elevated levels of XIAP. Similar findings were demonstrated by another group, showing that Ras-mediated *anoikis* resistance was dependent on an ability to up-regulate XIAP and cIAP2 (155). This up-regulation relied on activation of the NF-kappaB pathway (156).

The Mcl-1 inhibitor of apoptosis has also been shown by multiple groups to suppress *anoikis*. Mcl-1 protein was found to be rapidly degraded following cellular detachment, and restoration of Mcl-1 levels promoted *anoikis* resistance (157). The *anoikis* resistance of a melanoma cell line was also shown to be reliant on sustained Mcl-1 levels following detachment, mediated by a hyperactivated B-Raf/MEK pathway (158). Caveolin-1 also suppresses *anoikis* through its ability to complex with and stabilize Mcl-1 levels following detachment (159).

In addition to the intrinsic apoptosis pathway, the extrinsic pathway has also been shown to play an important role. This was first recognized by Frisch, who showed that death-domain-containing proteins such as FADD act to promote *anoikis* directly downstream of death receptors (160). Through a high-throughput screen of chemical inhibitors to identify novel modulators of *anoikis*, Mawji, Schimmer and colleagues identified anisomycin as a novel sensitizer to *anoikis* in a prostate carcinoma cell line (161). The mechanism of anisomycin appears to act through its ability to increase levels of FLIP, which blocks apoptosis through the Fas/TRAIL death receptor pathway by inhibiting caspase-8 (162). Levels of the DR5 receptor of TRAIL also contribute to the *anoikis* resistance of colorectal cancer cells (163). Another pathway through the death receptor DAP3 promotes *anoikis* through downstream activation of FADD and caspase-8 (164, 165).

Interestingly, a study by Overholtzer, Brugge and colleagues illustrated a possible alternative death mechanism following cellular detachment (166). Termed "entosis," this process of death is mediated by the internalization of a cell by a neighboring host cell following cellular detachment. This was observed both *in vitro*

as well as *in vivo* in mouse breast tissue. Death results from release of lysosomal enzymes by the host cell, although the host cell can alternatively release the internalized cell still alive. This mechanism appears to act through an adherens junction-dependent, integrin-independent manner. Overall, these data show that *anoikis* resistance is frequently dependent on the direct modulation of various cell death processes, including the intrinsic and extrinsic apoptosis pathways as well as alternative non-apoptotic pathways.

1.5.3 *ANOIKIS* RESISTANCE MEDIATED BY CELLULAR ADHESION

The complexity of integrin-mediated signaling resulting from cell-to-extracellular matrix (ECM) interactions has been explored extensively since Frisch described the importance of integrins in *anoikis*. Many studies have shown that various cell types rely on specific integrin subtypes for *anoikis* activation and resistance. Squamous cell carcinoma cells show reliance on alphaVbeta6 integrin for *anoikis* resistance, while alphaVbeta5 or alpha-negative integrin-expressing cells show *anoikis* susceptibility (167). This is supported by other groups showing an *anoikis* sensitizing role for alphaV integrin in gastric carcinoma cells (168). In contrast, alpha5beta1 integrin appears to be important in the *anoikis* process of hepatocellular carcinoma cells (168). In melanoma, *anoikis* is promoted by alphaVbeta3, while alpha4 integrin promotes *anoikis* in osteosarcoma cells (169, 170).

Multiple studies have also shown a reliance on cell-cell interactions in mediating *anoikis* resistance in cancer cells, particularly through cadherin signaling. E-cadherin in particular has been shown to contribute to suppression of *anoikis* in

various epithelial cancer models. In normal intestinal epithelial cells, E-cadherin levels are lost in conjunction with the *anoikis* process; remarkably, this cell death can be inhibited using activating cross-linking antibodies to E-cadherin (171). Cancer cells such as squamous cell carcinomas in contrast are able to retain E-cadherin levels in suspension, and adhesion to other cells through homotypic E-cadherin interactions contributes to their *anoikis* resistance through an ability to activate EGFR in a ligand-independent manner (108).

However, such dependence on E-cadherin for *anoikis* resistance is not universal across cell types. In fact, E-cadherin is well known as a tumor suppressor in lobular breast and gastric carcinoma, as it is lost in both familial and sporadic forms of this cancer. Its role in *anoikis* resistance in lobular breast cancer was studied using a conditional knockout mouse model, in which E-cadherin and p53 were knocked out in the epithelium of transgenic mice expressing Cre recombinase under the cytokeratin 14 promoter (*K14cre;Cdh1*$^{F/F}$*;Trp53*$^{F/F}$) (90). The tumors that resulted in the breast were highly similar to human invasive lobular carcinomas, and were found to have a high rate of metastatic disease compared to mice with retained E-cadherin. Cells from these tumors showed significantly greater *anoikis* resistance compared to cells from tumors that retained E-cadherin expression, and *anoikis* susceptibility was restored after re-expression of E-cadherin. This is supported by work by others, including data showing that in esophageal squamous cell carcinoma, *anoikis* resistance is promoted by a switch from E-cadherin to N-cadherin, mediated in part by protein kinase casein kinase-2 (172). This cadherin switch is also seen in cells subjected to hypoxia, again associated with suppression

of *anoikis* (173). Onder, Weinberg and colleagues also showed that loss of E-cadherin was associated with increased metastatic disease (174). Interestingly, this resulted in a downstream elevation of various transcripts, including mediators of the epithelial-to-mesenchymal transition (EMT) such as Twist.

Many others have also shown that EMT plays a role in *anoikis* resistance. One group demonstrated that EMT and the associated down-regulation of surface E-cadherin contributed to suppression of *anoikis*, as this promoted the nuclear localization of the NRAGE protein that helps to transcriptionally repress *anoikis* promoting genes such as p14ARF (175). Other proteins that have been shown to activate EMT such as claudin-1, involved in cell-cell adhesion through tight junctions, also promote *anoikis* resistance by decreasing levels of E-cadherin through up-regulation of the EMT transcription factor ZEB1 (176). ZEB1-mediated EMT was also found to be important in the *anoikis* resistance mediated downstream of the aforementioned TrkB (176). Furthermore, as a corollary, restoration of an epithelial phenotype through inhibition of an EMT promoter, resulting in a mesenchymal-to-epithelial transition, was found to restore *anoikis* sensitivity in an otherwise highly resistant and metastatic breast cancer cell line (177).

In contrast, there appears to be a divergent role for cadherins in mediating *anoikis* resistance in non-epithelial cancers such as sarcomas. While early studies into *anoikis* resistance have demonstrated relative resistance of mesenchymal cells such as normal fibroblasts to *anoikis* (178), we have shown that *anoikis* can indeed be restored in various mesenchymal cancer models, such as Ewing sarcoma and congenital fibrosarcoma (109, 117). Paradoxically, we have demonstrated a role for

the epithelial E-cadherin in promoting *anoikis* resistance in Ewing sarcoma cells, while mesenchymal-type cadherins such as N-cadherin did not play a role (109). Indeed, the aforementioned early studies showed the ability to induce an epithelial phenotype (including up-regulation of E-cadherin expression) in various sarcoma cell types through the expression of E1a (178). Such "epithelialization" of mesenchymal cells promotes the cellular aggregation, although the role of this process in modulating *anoikis* was not well established (179). Therefore, one possible explanation for the unexpected role for E-cadherin in promoting sarcoma *anoikis* resistance is the requirement for a mesenchymal-to-epithelial transition (MET) and subsequent reliance on homotypic E-cadherin interactions for cell-cell adhesion that then promotes survival, in contrast to N-cadherin which appears to have a reduced capacity for mediation of such homotypic cell-cell adhesion (180). Overall, these data suggest that different cell and cancer types show divergent reliance on EMT, MET and cadherin type for *anoikis* resistance.

1.5.4 *ANOIKIS* RESISTANCE MEDIATED BY CELL CYCLE INHIBITION

As previously discussed, it has been long recognized that tumors possess proliferative heterogeneity, with a fraction of cells in a given tumor displaying features of quiescence and consequent resistance to standard chemotherapeutic agents (181). Subsequently, one mechanism found to mediate such proliferative quiescence is that of multicellular resistance, describing the cell cycle arrest seen in multicellular clusters through cell-cell adhesion mechanisms (182). In an important paper by St. Croix, Kerbel and colleagues in 1996, multicellular resistance was explored in the context of cellular detachment (183). Using breast carcinoma cells,

they showed that levels of the cell cycle inhibitor p27/KIP1 were rapidly elevated following detachment and persistence as multicellular clusters, with sustained elevation even days following detachment, and that this triggered cell cycle arrest. Using antisense oligonucleotides, suppression of p27 levels was found to restore the cell cycle and promote *in vitro* cell death in the detached cells, as well as reduce tumorigenicity in mice. Interestingly, a subsequent paper found that p27 up-regulation in suspension was dependent on the previously discussed E-cadherin interactions, and the survival benefit conferred by E-cadherin was abrogated when p27 elevation was blocked (184). These papers therefore illustrate that cell cycle arrest due to cell-cell adhesion is important in the survival of detached multicellular clusters, reminiscent of *anoikis* resistance mediated by E-cadherin. Although this link between multicellular resistance and *anoikis* resistance was not made in this paper, it illustrates that such "multicellular spheroids" depend on *anoikis* resistance mechanisms for survival. While the concepts of multicellular spheroids and *anoikis* resistance are not considered synonymous, both describe the ability of tumor cells to survive in a suspension state, with tumor cells nearly always opting to form such cellular clusters to regain the survival pathways mediated by cellular adhesion.

The ability of cell cycle arrest mechanisms to promote *anoikis* resistance was supported by a number of subsequent studies. Galectin-3 was found to suppress *anoikis* by mediating a G1 arrest following detachment through its ability to up-regulate p27 and the related inhibitor p21/CIP1, while down-regulating the G1/S cyclins E and A (185). *Anoikis* resistance was also conferred in breast epithelial cells when any of several cell cycle inhibitors were overexpressed, including p27, p21

and p16(INK4a) (186). Through a poorly understood mechanism, this cell cycle arrest results in reduced levels of Bim, and this was dependent on sustained Erk phosphorylation levels seen in these cells despite absent activity of the upstream kinases Raf and MEK. Another group also demonstrated that cell cycle arrest mediated downstream of TIMP-1, through p27 elevation and cyclin D1 down-regulation, contributes to *anoikis* resistance (187). These data all support the notion that *anoikis* resistance is promoted by mechanisms beyond those that modify survival or death signals, with multiple examples of how cell-cell adhesion-mediated cell cycle inhibition promotes survival in detached multicellular spheroids.

1.6 *ANOIKIS* AND CELLULAR STRESS

Since proliferative arrest is seen under numerous cellular stress states, the finding that cell cycle arrest contributes to *anoikis* resistance lends credence to the possibility that cellular stress plays a role during the *anoikis* process. However, such proliferative arrest would not be expected under conditions of hyperactivation of the Akt and MAPK pathways, which is readily demonstrated to be a key component of *anoikis* resistance in various cancer types (Figure 1.1). Therefore, mechanisms would be required to suppress cell growth and proliferation in the setting of Akt/MAPK pathway activation. In recent years, the roles of various cellular stress response pathways have been described in the literature, although it remains unclear what the relative contributions are of these pathways to *anoikis* susceptibility and resistance.

1.6.1 *ANOIKIS* AND OXIDATIVE STRESS

One of the first reports of cellular stress following cell detachment described the role of reactive oxygen species (ROS) in endothelial cells. Mitochondria-derived ROS levels were shown to rapidly increase following detachment, and this appeared to contribute to *anoikis* death (188). Treatment with inhibitors of ROS generation or scavengers of ROS appeared to modulate caspase activity and JNK pathway activation, and contributed to suppression of *anoikis*. These early pieces of data were supportive of the emerging idea that ROS not only leads to oxidative toxicity through its ability to generate free radicals that damage cellular macromolecules, but can also directly alter signaling pathways by serving as a non-enzymatic signaling molecule (189).

Further studies were supportive of an *anoikis*-promoting role of ROS. In detached gastric carcinoma cells, treatment with the ROS-producing natural compound emodin resulted in restoration of *anoikis* through its ability to down-regulate levels of the *anoikis* suppressor RhoA, a key component of focal adhesion complexes seen in detached cells (190). Another natural compound, curcumin, also helped to restore *anoikis* in lung carcinoma cells through promotion of superoxide levels and downstream suppression of Bcl-2. Reactive nitrogen species have also been found to promote *anoikis* by increasing microtubule depolymerization (191).

In contrast, some studies have shown that increased ROS instead contribute to *anoikis* resistance. One group showed that detached cells depend on Rac1-mediated ROS production for survival, based on a mechanism of ROS-mediated activation of Src kinase that ultimately activates EGFR in a ligand-independent

manner (192). The same mechanism was demonstrated in prostate cancer cells, and relied on the EGFR-mediated suppression of pro-apoptotic Bim (193). Nitric oxide was also shown to promote *anoikis* resistance in lung carcinoma cells through its ability to prevent degradation of the *anoikis* suppressor caveolin-1 (194). Hydrogen peroxide was shown to suppress *anoikis* through the same mechanism, and treatment with various ROS scavengers was associated with reduced caveolin-1 levels and thus partial restoration of *anoikis* (195). Interestingly, angiopoetin-like 4, a protein highly expressed in metastatic cancers, was shown to suppress *anoikis* through its ability to increase superoxide levels by activating NADPH oxidase, leading to ROS-mediated Src activation and downstream activation of the PI3K and MAPK pathways (196). Overall, based on data supporting both an *anoikis*-promoting and –suppressive role of ROS, the role of ROS in *anoikis* remains unresolved. Such discrepancies in the data remain unresolved, and may relate to the types of ROS being investigated, or the relative levels of ROS being used in the experimental systems.

1.6.2 *ANOIKIS* AND AUTOPHAGIC STRESS

Autophagy describes a catabolic process in which cells degrade intracellular components, particularly for the purposes of energy restoration during periods of cellular stress (197). Of the three forms of autophagy described, the most commonly observed is macroautophagy, referring to a degradation process involving the formation of a bilayered autophagosome, and is dependent on a number of proteins in the autophagy-related gene (Atg) family. Macroautophagy hereon will simply be referred to as autophagy. Although it would appear that such a process would be

activated only during periods of severe bioenergetic stress during which no other energy sources are available, autophagy has been shown to be involved in the early stages of various stresses, including ER stress and hypoxia (198-201). In addition, the role of autophagy in cancer is also diverse, with earlier studies demonstrating a pro-tumorigenic role by recycling bioenergetic molecules during periods of metabolic stress (202). However, autophagy at its end-stage also acts as a form of cell death, and recent data has shown a tumor suppressive role much like apoptotic death, seemingly in the context of p53 mutation status (203).

Debnath first described a role for autophagy in *anoikis* in 2008, demonstrating that autophagy is activated in the early stages following cellular detachment and helps to suppress *anoikis* (95, 204). Inhibition of autophagy resulted in reduced anchorage-independent growth in three-dimensional cultures of breast cancer cells, and increased luminal clearing in models of breast acinar morphogenesis. Subsequent studies by the same group showed that Ras-transformed breast cells also display significant levels of autophagy following detachment, and that inhibition of autophagy partially suppressed anchorage-independent growth in soft agar and marginally increased cell death in suspension (205). However, the capacity to activate autophagy also correlated with rates of proliferation and glucose metabolism, and it was unclear whether the effect on anchorage-independent growth was due to the small effect on *anoikis* or rather the proliferation rate during the prolonged growth in soft agar.

Interestingly, the same group demonstrated in a recent study that autophagy may have both pro- and anti-tumorigenic roles in three-dimensional culture

systems. While they show again that breast epithelial cells, this time transformed with an oncogenic form of PI3K, again show a dependence on autophagy for normal acinar luminal formation, they show that subsequent proliferation in three-dimensional culture requires suppression of the same autophagy (206). Such an anti-proliferative effect is of course in contrast with their previously discussed findings of a pro-proliferation effect of autophagy when the same cells are transformed with oncogenic Ras (205). These data again support the notion that stress response pathways such as autophagy can play opposing roles in tumor development based on the cell type and environmental context.

1.6.3 *ANOIKIS* AND HYPOXIC STRESS

A number of groups have also demonstrated a role for the hypoxic stress response in *anoikis*. While it would appear more evident that low oxygen tension plays a role in prolonged three-dimensional cultures where the central cells of large multicellular clusters would experience hypoxia, the role of the hypoxic response early following cellular attachment is unclear. Rohwer, Cramer and colleagues showed that the central player in the hypoxic response, HIF-1alpha, promotes *anoikis* resistance even in normoxic conditions, through a mechanism dependent on its ability to suppress levels of the *anoikis*-promoting alpha5-integrin (207). Another group showed that such HIF-1alpha-dependent *anoikis* resistance in normoxic conditions is dependent on the formation of lipid rafts, up-regulating HIF-1alpha transcript and protein levels in an EGFR- and MAPK/ERK pathway-dependent manner (208). More recently, true hypoxic stress has been demonstrated during the acinar morphogenesis of breast luminal cells. Under such conditions of detachment,

HIF-1alpha again was found to be critical for survival, this time shown to be dependent on its ability to suppress the pro-apoptotic factors Bim and Bmf in a MAPK/Erk pathway-dependent manner (209). Hypoxia also drives other *anoikis* suppressing mechanisms such as EMT and cadherin switching from E-cadherin to N-cadherin (173)

An intriguing finding was shown in bone marrow micrometastases derived from breast cancer patients. Gene expression profiling showed an up-regulation of genes in relation to the HIF-1alpha pathway (210). Similar findings were shown in other studies of more developed metastatic lesions (211). Hypoxia response pathways therefore appear to promote *anoikis* resistance in both normoxic and hypoxic conditions, with supportive evidence in relevant clinical samples.

1.6.4 *ANOIKIS* AND ENDOPLASMIC RETICULUM STRESS

Endoplasmic reticulum (ER) stress represents a form of cellular stress triggered by a variety of intracellular and extracellular stimuli. It is seen particularly as a result of metabolic stress, and the resulting decrease in bioenergetic status leads to an inability of cells to fully complete the process of protein synthesis, modification and folding, all of which are energy-demanding processes dependent on the ER (212). Amongst other consequences, there is a build-up of misfolded proteins, further disrupting the processes of the ER and the cell as a whole. As a result, the unfolded protein response (UPR) pathway is triggered, activating proteins regulating the two main arms of the pathway, namely the PERK kinase and the RNA-binding protein IRE-1alpha (213). These two pathways activate a series of processes that help to reverse ER stress, including inhibition of further protein

translation initiation through phosphorylation of eIF2alpha, up-regulation of chaperone proteins such as BiP, and increased levels of the transcription factors ATF4 and ATF6 (213). While such proteins function to promote protein folding and reduce further misfolded protein stress, prolonged activation of the UPR has been shown to trigger apoptosis, much like what occurs during prolonged activation of autophagy (213).

ER stress has also been demonstrated during the *anoikis* process, and a role for the UPR was first demonstrated by Sequeira, Aguirre-Ghiso and colleagues (214). In particular, PERK was shown to be activated following detachment, resulting in the expected inhibition of translation initiation, as well as the ATF4- and ATF6-mediated transcription of various factors such as pro-apoptotic CHOP. Although inhibition of PERK did not result in modulation of *anoikis* death, enforced and sustained PERK activation in suspension and three-dimensional cultures resulted in increased apoptosis.

However, later work from the same group demonstrated a role for PERK in the *anoikis* resistance of breast epithelial cells (215). This was shown to be due to a mechanism of PERK-mediated autophagy that is dependent on an eIF2alpha-mediated reduction in oxidative stress. Most recently, PERK was shown in the same cellular system to activate autophagy through a novel mechanism of PERK-induced AMPK activation and mTORC1 inhibition. Overall, detachment-induced activation of components of the UPR pathway have shown to have an *anoikis* suppressive role.

1.6.5 *ANOIKIS* AND METABOLIC STRESS

An important paper by Schafer, Brugge and colleagues in 2009 described a central role for metabolic stress and related stress response pathways in *anoikis* resistance (216). Surprisingly, cellular detachment alone resulted in reduced intracellular ATP levels in non-transformed breast epithelial cells as a result of decreased glucose uptake, and this could be rescued by overexpression of an oncogene such as *ERBB2*. This was mediated by oncogenic activation of PI3K through ligand-independent activation of EGFR, which restored glucose uptake levels. ROS was again found to play a role, as exogenous antioxidant treatment abrogated the detachment-induced reduction in ATP levels through its ability to prevent ROS-induced inhibition of catabolism through fatty acid oxidation. Endogenous antioxidants were then found to function in a similar manner, as the EGFR/PI3K-mediated glucose uptake was shown to result in increased cellular NAPDH antioxidant levels due to increased glucose flux through the pentose phosphate pathway, which also restored ATP levels through fatty acid oxidation. *In vivo* studies helped to confirm this, as detached cells during breast acinar morphogenesis showed increased ROS associated with luminal apoptosis, and such cell death was abrogated by antioxidant treatment. This paper represented one of the first demonstrations that cellular detachment results in bioenergetic stress due to reduced glucose uptake, promoting *anoikis* death. It also demonstrated a mechanistic link between seemingly divergent processes, including kinase signaling, ROS and glucose metabolism.

Another *anoikis* resistance pathway mediated by fatty acid oxidation regulation was recently discovered by Carracedo, Pandolfi and colleagues (217). They found that PML, a previously-described tumor suppressor, promoted ATP levels in detached cells through an ability to activate PPARalpha signaling and downstream fatty acid oxidation, thereby suppressing *anoikis*. This was confirmed by the ability of PML to suppress breast luminal clearing. PML was also found to be a negative prognostic marker in breast cancer, correlating with increased metastatic recurrence. This data therefore supports the findings by Schafer and colleagues that maintenance of cellular ATP levels is important in *anoikis* resistance, and this is conferred through activation of fatty acid oxidation by multiple *anoikis* resistance pathways.

Further recent studies have lent additional support to these findings. A metabolomics study of ovarian cancer cells showed that the metabolic rate of highly aggressive ovarian cancer cells was significantly higher than correspondingly less aggressive cells, with higher rates of pyruvate uptake and oxygen consumption (218). This increased metabolic rate corresponded with higher levels of ATP in detached cells, and was associated with increased invasion capacity. Another study identified a role for PDK4 in breast epithelial cell *anoikis* resistance (219). PDK4, a target of PPARalpha, phosphorylates and inhibits pyruvate dehydrogenase, promoting glucose flux through glycolysis rather than oxidative metabolism. The reduced oxidative respiration levels lead to decreased ROS levels, therefore suppressing ROS-induced *anoikis*. This data supports the concept of the Warburg

effect, where cancer cells have been shown to depend on a switch towards anaerobic metabolism for survival.

Altogether, these emerging data on the role of metabolism in *anoikis* resistance suggest that mitigation of bioenergetic stress is critical for survival. Such survival is best supported by energy-restoring catabolic processes that are less reliant on oxidative metabolism.

1.7 HYPOTHESIS

Although many *anoikis* resistance mechanisms have been elucidated, the majority of the identified pathways represent general mechanisms that govern survival under a broad range of cellular conditions, rather than mechanisms more specific to the process of *anoikis*. This is in part a result of the reliance of many previous studies on a hypothesis-driven approach, based on established knowledge of cellular survival and anti-apoptosis mechanisms, rather than an unbiased, screening-based, hypothesis-generating approach. Consequently, important but unexpected contributory mechanisms may remain undiscovered.

To work towards our objective of elucidating novel signaling mechanisms governing *anoikis* resistance in cancer cells, we will utilize hypothesis-generating experimental systems to attempt to identify novel insights into these mechanisms. We first hypothesize that a high-throughput, cell-based functional screen using siRNA libraries will allow us to identify specific proteins in signaling pathways that are critical to suppressing *anoikis* in cancer cells. Secondly, we hypothesize that analysis of gene expression alterations following cellular detachment will highlight specific proteins or broader signaling pathways that become activated or repressed,

and that such protein/pathway activation or repression will be functionally important for *anoikis* resistance. Well-established cell biology and biochemical methods will then be used for subsequent validation. Overall, we believe that this will lead to both novel biological insights into this critical initial step in tumor cell metastasis, and ultimately provide insight into therapeutic restoration of *anoikis* to suppress metastatic disease.

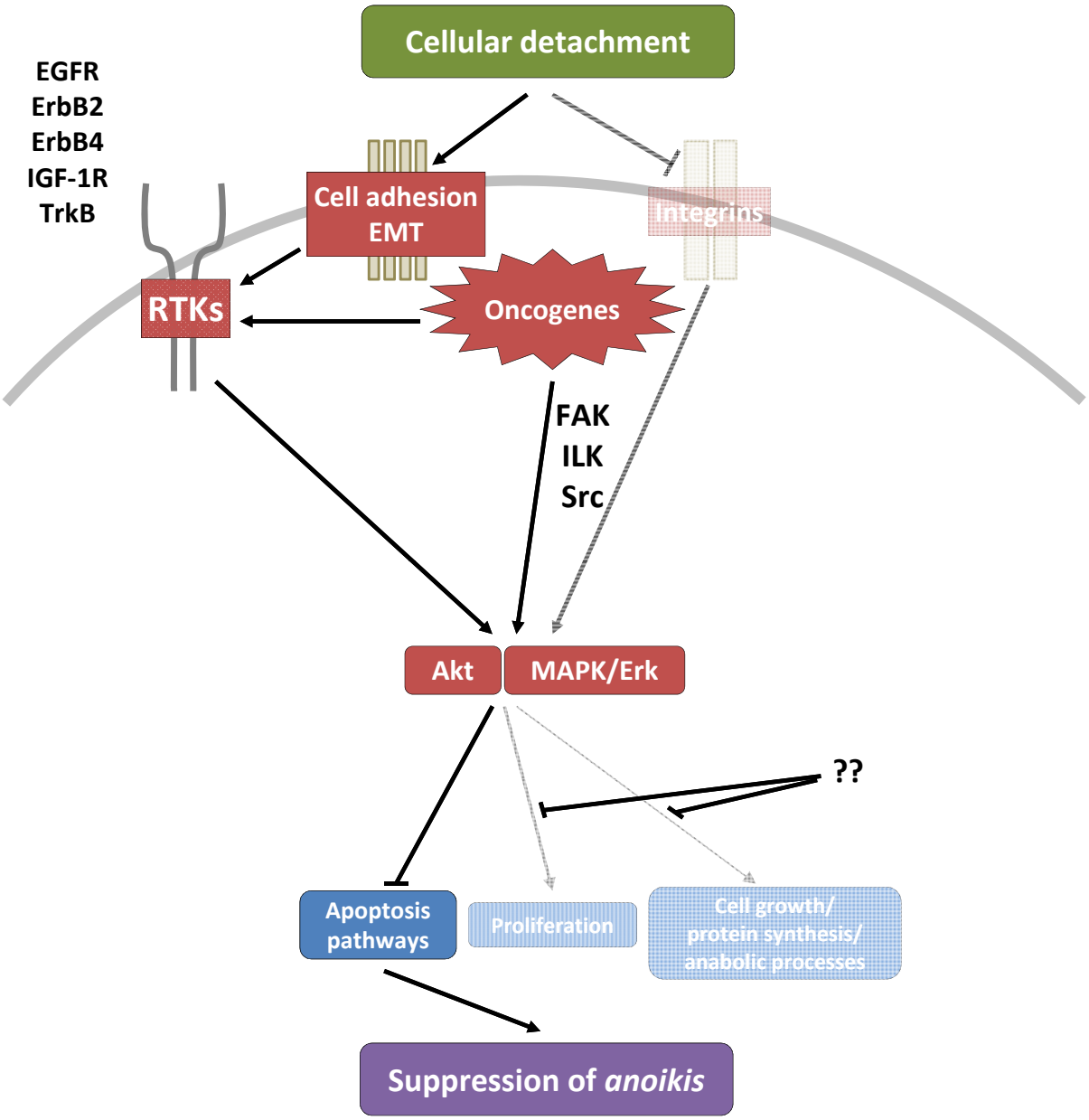

Figure 1.1. Schematic summary of *anoikis* resistance mechanisms mediated through the Akt and MAPK pathways. The question marks indicate the role of mechanisms not yet fully elucidated that help mediate cell cycle arrest during cellular detachment conditions.

Chapter 2 FUNCTIONAL SCREEN FOR NOVEL SUPPRESSORS OF *ANOIKIS* IN EWING SARCOMA

2.1 INTRODUCTION

Since the advent of RNA-interference (RNAi) technology for *in vitro* cell biology studies, RNAi has been utilized in a large number of functional screens to identify novel targets in cancer biology and therapy. Due to the relative ease of developing large RNAi libraries, using synthetic siRNAs or plasmid-based shRNAs, large panels of genes can be modulated to allow for the development of non-biased genetic screens, including genome-wide screens. By individually knocking down the levels of genes within a library, the consequences of the loss-of-function of each gene can be determined in an appropriate cellular context, in an attempt to reflect the effect of genetic loss in tumors due to deletions or inactivating mutations, or mimic the inhibition of the protein through small molecule inhibition. Those identified to have the most significant phenotypic effect in the screen are termed "hits," representing genes worthy of subsequent validation using alternative biochemical studies.

The feasibility of developing such large screens depends on a number of major factors, including a cell model system that can be cultured in a manner that allows for efficient delivery of the RNAi library, a phenotype that can be easily modulated by RNAi, and the availability of an assay for the phenotype that can be performed and read in a high-throughput manner. In addition, the phenotype being assayed

ideally should have a broad dynamic range, such that there are large differences expected in the assay readout for genes with a true biologic effect versus genes with no effect. In the absence of a significant range for the assayed phenotype, it becomes difficult to determine which genes have a true effect; since numerous genes are being assayed simultaneous, the rate of false positive hits increases proportionally, with true hits requiring a higher level of statistical significance to overcome the effect of such multiple comparisons.

RNAi screens have a number of significant advantages compared to other library-based screens. Prior to RNAi technology, genetic-based screens have relied on overexpression studies using cDNA libraries. However, the levels of overexpression seen using plasmid constructs of cDNA libraries are often many-fold greater than the expression levels seen physiologically or in tumors (220). Furthermore, overexpression studies usually require the use of non-transformed cellular models, with the objective of identifying hits that confer transformation or other cancer phenotypes to such cells; loss-of-function studies, in contrast, are usually performed in the context of cancer cells, and the identified hits would therefore represent possible targets for inhibitory therapy (221). Other studies have used chemical libraries as the method of screening. One obvious advantage of such libraries is that an identified hit would immediately represent a possible therapeutic approach. However, it has been rare that a chemical inhibitor identified at such an *in vitro* level has lead to the development of a clinically-useful therapeutic (222).

Despite the advantages of an RNAi-based screen, a multitude of challenges arise when interpreting the results of RNAi screens. One consideration is the non-

specificity of siRNAs and shRNAs (221). While use of RNAi has become ubiquitous in cell biology studies, the specific effect in an experimental system can often not be fully determined. This is because individual RNAi molecules, even when bioinformatically determined to complement specifically to a single mRNA species, may still have broader effects on expression due to the ability of RNAi molecules to affect the levels of other mRNAs that have incomplete complementarity (223). In addition, it has been shown that RNAi molecules may have unpredictable and even opposing effects on gene expression, such as during conditions of cell cycle arrest (224). Therefore, subsequent secondary screens using the subset of the most significantly positive hits are often needed, possibly using an alternative assay method. In addition, validation studies are critical, for example using RNAi molecules with alternative sequences, or using other forms of pathway analysis such as overexpression studies or chemical inhibitors. Despite this, the rate of false positive hits arising from RNAi-based screens remains quite high (225).

Another problem relates to the limitations in the experimental design possibilities when using different types of RNAi libraries. Screens using siRNA libraries require the delivery of a single siRNA type into each experimental sample. Therefore, the siRNA delivery and assay readout must be done in a high-throughput manner, often using cells cultured in a dense multiwell arrangement. This limits the possibilities of the assay method used, as it must be performed in formats such as arrayed 96-well or 384-well plates, ideally with a minimal number of assay reagents needed to be added, and with a readout capable of being analyzed efficiently such as using plate readers. Cost considerations are also essential, as one must factor in cell

culture plasticware and reagents, assay reagents, readout hardware and labor costs, which increase rapidly based on the siRNA library size. Assays performed in a multiwell configuration have other caveats, such as variations between wells of a plate, and variability between plates depending on the precise duration of the assay.

Screens using shRNA libraries have different advantages and challenges. While shRNAs can be transfected individually as with siRNAs, they are often delivered as a pooled library, with screens titrated such that cells within a pool are transfected at an approximate efficiency of one shRNA plasmid per cell. Each shRNA plasmid is often tagged with a unique barcode sequence. Positive hits are then usually identified by subjecting the cells to an experimental or stress condition that would select out clones expressing a particular shRNA. These clones are then identified by determining the sequence of the barcode. While such an experimental setup allows were far greater efficiency for performing the screen, one disadvantage is that the screen must be performed using such a pool of heterogeneous and polyclonal cells, reducing the capability of identifying cell-nonautonomous pathways. Furthermore, it is difficult to precisely transfect cells at a truly monoclonal manner, such that cells in the screen may often express less than or greater than one shRNA plasmid.

A number of groups have applied such screens to identify possible novel suppressors of *anoikis*. As previously mentioned, one of the first screens utilized a barcoded cDNA library to identify novel genes by overexpression, with positive hits isolated through selection of clones surviving detachment conditions (85). While this identified TrkB as a novel suppressor of *anoikis*, the survival mechanism

mediated by TrkB is primarily through well-known *anoikis* resistance pathways such as those mediated by oncogenic Ras, such as the MEK/Erk and PI3K/Akt pathways. The chemical screen performed by Mawji, Schimmer identified anisomycin as restoring *anoikis* sensitivity in part through suppressing the apoptosis inhibitor FLIP. However, anisomycin is a well known inducer of apoptosis, and also has been demonstrated to have myriad effects on signaling pathways, including activation of p38, up-regulation of Bim and potentiation of ROS (226-228).

Irie, Brugge and colleagues demonstrated the results of a screen that utilized an siRNA library against human protein kinases to identify novel suppressors of *anoikis* (229). Using MCF-10A breast cells overexpressing either IGF-1R or vector alone, they attempted to identify novel targets that specifically cooperated with IGF-1R-overexpression as compared to wild type MCF-10A cells. Cells were transfected in a 96-well format in a "reverse transfection" manner, and cell death was assayed using the Alamar Blue assay following 72 hours in suspension. A hit was considered positive when it showed significantly high ratio of cell death reduction in IGF-1R-overexpressing cells versus cell death reduction seen in vector-alone cells. A positive hit, protein tyrosine kinase 6 (PTK6), was validated using alternate cancer cell lines and the soft agar colony formation assay, although the validation studies showed only small effects on *anoikis* death in conjunction with PTK6 loss of function, and these effects were mostly demonstrated in the MCF-10A model only in the context of IGF-1R pathway hyperactivity.

Recently, an RNAi based screen using a genome-wide lentiviral-based shRNA library was performed on *anoikis*-sensitive prostate cancer cells to identify novel

promoters of *anoikis* (230). The library was delivered as a pool, and *anoikis*-resistant clones were isolated and characterized. Positive hits were identified as those with greatest proportional abundance in the surviving clones following prolonged selection for three weeks under suspension conditions. Alpha/beta hydrolase domain containing 4 (ABHD4) was identified and validated in alternate *anoikis*-sensitive cell line models such as OVCAR3, as knockdown of ABHD4 helped to suppress *anoikis*. However, similar to the previously described cDNA screen that identified TrkB, this screen again focused on identifying modulators of *anoikis* in *anoikis*-sensitive cell lines, and does not aim to identify true suppressors of *anoikis* in resistant cell lines that would represent the ideal targets for therapy.

Overall, previously described loss-of-function screens for novel suppressors of *anoikis* have only demonstrated limited novel targets, and the magnitude of effect seen in the identified hits has been modest. Furthermore, these screens have been limited to carcinoma models. We therefore wished to perform a similar siRNA-based screen on Ewing sarcoma cells, a representative childhood sarcoma with a high propensity for metastasis. Previously, we identified ErbB4 as a novel suppressor of *anoikis* in Ewing sarcoma through the use of a medium-throughput phosphorylation screen of tyrosine kinases utilizing a phospho-specific antibody array. However, broader screens for *anoikis* resistance genes in childhood sarcoma models have not been previously performed.

2.2 MATERIALS AND METHODS

Cell culture and DNA transfection. Ewing sarcoma cell lines TC-32 and TC-71 were obtained as previously described (231) and maintained in RPMI 1640 media supplemented with 10% fetal bovine serum. TC-32luc and TC-71luc cell lines were developed by transduction of the corresponding cell lines with supernatant derived from SMPU-R-MNCU3-LUC vector, as previously described (232). For suspension cultures, cells at subconfluence were detached by trypsinization and diluted to a concentration of 250,000 cells/mL, plated on polyHEMA-coated 10cm dishes or 6-/12-well plates, or precoated 96-well plates (Non-Binding Surface coated microplates, Corning, Lowell, MA) and incubated for the indicated timecourses. Chemical inhibitors were added to suspension cultures immediately following detachment and plating onto polyHEMA-coated plates to determine their effects on the early stages of the *anoikis* response.

For the siRNA screening protocols, TC-32luc and TC-71luc cells were cultured in standard 96-well plates in monolayer conditions, with or without siRNA treatment. Trypsinization was achieved by aspirating the media from each well, directly applying 0.25% trypsin with EDTA (1mM) with incubation for 1 minute (Life Technologies, Grand Island, NY), and neutralization of trypsin/EDTA with phenol red-free RPMI 1640 media containing 10% fetal bovine serum. The entire mixture was resuspended into a single cell suspension by gentle pipetting through a P200 tip, and transferred entirely into wells of the Non-Binding Surface coated 96-well plates. These were cultured for 48 hours in suspension prior to subsequent assays.

Antibodies and chemicals. Trypsin (0.25%) with EDTA (1mM) was obtained from Life Technologies (Grand Island, NY). LY294002 and U0126 inhibitors were obtained from Sigma-Aldrich (St. Louis, MO). Firefly luciferin (D-luciferin, K+ salt) was obtained from Perkin Elmer (Waltham, MA). Anti-lamin A/C, anti-PARP and anti-Grb2 antibodies were obtained from BD Biosciences (San Jose, CA), Anti-Twf2/PTK9L and anti-beta-actin antibodies were purchased from Santa Cruz Biotechnologies (Santa Cruz, CA)

siRNA, siRNA libraries and RNA transfection. All siRNAs were obtained from Dharmacon, Thermo Fisher Scientific (Pittsburgh, PA) against human targets, with the ON-TARGETplus modification. The libraries used were the insulin signaling pathway library, the tyrosine kinase library and the cell cycle regulation library. Negative control siRNAs used were siCNTRL2 and siCNTRL3 (scrambled controls), while positive control siRNAs were siLaminA/C (for validation of protein knockdown of an easily assayed protein product) and siTOX (which induces apoptotic cell death within 24 to 48 hours following successful transfection, for validation of transfection efficiency). Individual siRNAs against PLK1, ErbB4, IGF-1R, PTK9L, Rb1, RBL1, RBL2 and Syk were also obtained from Dharmacon, Thermo Fisher Scientific, as sets of four siRNAs. Transfection was performed using the Dharmafect 3 reagent (Thermo Fisher Scientific), with siRNA delivered at a concentration of 25 nM. The screen was performed using a reverse transfection protocol, with the cell suspension combined with the siRNA/transfection reagent mixture, and subsequently plated into the plate wells and cultured for 72 hours. Alternatively, forward transfection was used, with cells cultured at subconfluency

for 24 hours, transfection mixture applied subsequently, and monolayer culture continued for 72 hours.

Luminescence assay. Firefly luciferin was applied directly to monolayer or suspension culture wells at a concentration of 60 μg/mL, added to consecutive wells at one-second intervals, directly into the cell culture media, and incubated for 5 minutes at room temperature. White 96-well plates were used to optimize the luminescence readouts. Total luminescence from each well was read using the Safire 2 plate reader (Tecan, Mannedorf, Switzerland) using 1000 ms integration time for each well. Normalization to background control wells was not necessary, as background luminescence in wells where luciferin was not applied was negligible (<1% background-to-signal). If this luminescence assay was performed on monolayer cultures, and the cells were required for subsequent suspension culture, the cell culture media with luciferin reagent was aspirated off of the monolayer culture, and subsequent trypsinization and suspension culturing was performed.

MTS assay. The CellTiter 96 Aqueous One Solution Cell Proliferation Assay (MTS), based on the 3-(4,5-dimethylthiazol-2-yl)-5-(3-carboxymethoxyphenyl)-2-(4-sulfophenyl)-2H-tetrazolium, inner salt (MTS) compound highly similar to (MTT), was obtained from Promega (Madison, WI). The solubilized compound was added directly to 96-well plate cell culture wells, and incubated for 1-4 hours at 37°C. Absorbance at 490nm was measured as a readout of viable cell numbers in each well.

Statistical analysis. Following normalization of luminescence values to in-plate control wells subjected to transfection reagent only (no siRNA), generating

normalized monolayer and suspension readouts, a survival ratio was obtained for suspension cultures by dividing the luminescence readout in suspension by the readout in monolayer conditions. Student's t-test (Welch's t-test for samples of unequal variance) was performed between the suspension and monolayer readouts to determine significance of the survival ratio values. Dixon's Q-test was performed for outlier analysis.

2.3 RESULTS

Development of a luminescence-based assay for high-throughput readout of suppression of *anoikis*. As a first step in the development of a suppression of *anoikis* screen, we developed an assay to allow for high-throughput screening of tumor cell survival following cellular detachment. The aim of this is for the eventual development of an automated or semi-automated protocol that allows for the determination of *anoikis*-related cell death following the application of an siRNA library. While numerous assays of cell viability and cell death are available to assay for *anoikis*, we wished to develop a method that allows for rapid assaying of *anoikis* in a multi-well plate format (at least 96- or 384-well format) with minimal reagent handling, while retaining the important characteristics of an assay for high-throughput use, namely a broad but linear dynamic range, high sensitivity to small changes in the cellular phenotype (i.e. a steep slope in the linear range of the assay readout), and low background.

To do this, we utilized two Ewing sarcoma cell lines, TC-32 and TC-71, previously well-characterized in our laboratory to robustly suppress *anoikis* (109). We utilized a commercially-available 96-well plate type that forces cells into a

suspension culture through a coating with a polymer containing a nonionic hydrophilic tail that prevents cellular attachment to the well surface (Non-Binding Surface (NBS) plates, Corning, Tewksbury, MA). When the Ewing sarcoma cell lines were cultured on these plates under normal culture conditions, they formed multiple small spheroid clusters distributed in the wells (Figure 2.1A). By culturing cells under such suspension conditions for 48 to 72 hours, we were able to assess for relative *anoikis* resistance following cellular detachment. Importantly, we were able to culture cells in this suspension condition either by directly plating cells into the well, as well as by initially culturing cells in monolayer conditions in a 96-well format, then trypsinizing the cells directly in these wells, following by resuspension and plating the cells into a corresponding well in the NBS suspension plates (Figure 2.1A). Culturing first in monolayer conditions allows for the transfection of siRNAs in the usual monolayer conditions prior to subjecting cells to detachment conditions.

To then assay for the relative degree of *anoikis* in suspension conditions, we tested a number of commercially available assays designed for high-throughput screening of cell survival or cell death. One assay we considered was based on the MTS compound. This assay, as with the MTT assay, measures the total amount of oxidative activity in a culture as a surrogate measure of the number of living cells. Unlike the MTT assay, however, this only requires the addition of a single reagent, following which the total absorbance in the assay well at 490 nm is measured. However, we found that this assay showed relatively poor dynamic range, with a high signal-to-background ratio (data not shown). We also found that there was

relative variability between wells of cells despite plating of identical cell numbers, and there was considerable variability between plates of cells.

We therefore developed an assay based on TC-32 and TC-71 cell lines stably transduced using a lentiviral vector that overexpresses the firefly luciferase gene (TC-32luc and TC-71luc). While these cells were designed for *in vivo* use, we predicted that assaying these cells *in vitro* by applying the same firefly luciferin would allow for a readout of viable cell numbers in a similar fashion. Indeed, when we plated increasing numbers of these cells and cultured them in monolayer conditions, we were able to show a linear relationship between the initially plated cell numbers and the final readout by luminescence (Figure 2.2A and B). We also showed that this linear relationship is maintained when the cells are subsequently transferred to suspension culture (Figure 2.2C and D). We also evaluated whether a difference could be observed when comparing the method of cellular detachment. Overall, use of trypsin/EDTA appeared to result in a more linear relationship with initial cell number as compared to use of EDTA alone, with less variability between wells (Figure 2.2E and F). We also showed that treatment of these Ewing cells in suspension conditions with the PI3K/Akt pathway inhibitor LY294002 and MEK/ERK pathway inhibitor U0126 resulted in a reduction in the luminescence readout in an expected dose-dependent manner (Figures 2.3A to D). One observation we noted was consistently lower luminescence readout in the wells at the outer edges of the plate as compared to wells away from the edge. This "edge effect" is well recognized in high-throughput screens, and since we also observed this effect, we chose to only use culture wells away from the plate edge. Importantly,

application of the firefly luciferin reagent did not show appreciable toxicity in the cells, and the same cells could be subsequently utilized once the culture media and reagent was removed. Overall, we were able to demonstrate that this luminescence-based assay of viable cell numbers following cellular detachment is a feasible readout of *anoikis* sensitivity in Ewing sarcoma cells.

Development of a protocol for high-throughput delivery of siRNA in a suspension culture format. We then evaluated various possible protocols for the delivery of siRNA in this 96-well suspension culture format. First, we determined the effectiveness of direct delivery of siRNA into suspension cultures. This was achieved using a "reverse-transfection" method whereby the siRNA transfection mixture was combined directly with trypsinized cells and directly plated onto the non-binding surface plates. Using lysates directly from the 96-well plates, we showed that this transfection protocol was effective in protein knockdown using a control siRNA against the lamin A/C protein (Figure 2.4A). However, while this method of siRNA delivery represents the least labor-intensive protocol and the shortest time from siRNA transfection to assaying for *anoikis* resistance, we were concerned that this protocol does not in fact assess the effect of knocking down true suppressors of *anoikis*. Specifically, since there is a time period required for degradation of a protein following siRNA transfection and reduction of corresponding mRNA levels, varying from a few hours to 72 hours depending on the stability of the protein, we were concerned that such a reverse-transfection method would frequently not result in sufficient protein knockdown during the process of

anoikis-related cell death, since the process of *anoikis* would be expected to begin immediately following plating into suspension culture conditions.

Therefore, we wished to develop a protocol that achieved consistent protein knockdown by the time of cellular detachment. Instead of directly plating cells in suspension conditions following siRNA transfection, we instead cultured the transfected cells in usual monolayer conditions for 72 hours initially, allowing for protein knockdown prior to cellular detachment. Following trypsinization of these cells, we were able to show that cells sustained protein knockdown of the control lamin A/C (Figure 2.4A). Overall, delivery of siRNA in a 96-well format was effective both in "reverse transfection" format directly plated in suspension culture, and a "forward transfection" format initially plate in monolayer conditions and subsequently subjected to detachment.

Evaluation of the siRNA protocol as a high-throughput screen for novel suppressors of anoikis using an IGF-1R pathway-related siRNA library. Using the "forward transfection" protocol, we applied a small siRNA library to the TC-32luc and TC-71luc cell lines, which targets various components of the insulin receptor (IR)/insulin-like growth factor-1 receptor (IGF-1R) pathway. Taking into account the "edge effect," we arranged the delivery of siRNAs in various wells in the 96-well format (Figure 2.4B). We added additional wells that did not include siRNA in the transfection ("transfection reagent only"), which serve as control wells to assess for possible toxic effects related to the transfection reagent, and to serve as normalization values for the analysis of hits. Positive control siRNAs against PLK1, and a commercially available "siTOX", were also used to ensure transfection

efficiency, as both siRNAs are known to robustly promote cell death in these cells. Following transfection of the siRNA library into corresponding wells, and subsequent monolayer culture for 72 hours, we assayed for cell survival using the luminescence assay relative to transfection reagent-only wells, generating a "monolayer" readout of the siRNA effect, following normalization against control the "transfection reagent only" wells. We subsequently trypsinized and re-plated the cells on non-binding surface-coated plates, cultured in suspension for 48 hours, and assayed again for cell survival, generating a "suspension" readout, again normalized to the "transfection reagent only" wells. To control for the *a priori* effects of the siRNA in monolayer conditions, we used a "survival ratio" as the final metric of the siRNA effect, using the "suspension" readout as the numerator and the "monolayer" readout as the denominator (Figure 2.4C).

Analysis of the effects of the IR/IGF-1R library siRNAs in monolayer conditions demonstrated hits that affect cell numbers/survival both positively and negatively. For example, knockdown of TSC1 and TSC2, which are known to act as negative regulators of the mTORC1 pathway that normally promotes cellular proliferation (233), resulted in mildly increased cell numbers/survival relative to control wells as measured by the luminescence assay (Figure 2.5A). In contrast, knockdown of ribosomal protein S6, a key downstream component of the Akt/mTORC1 pathway, resulted in a significant reduction in cell survival. Knockdown of other proteins such as Xpo1 also resulted in a significant decrease in cell survival.

As expected in the analysis of the assay results following cellular detachment, knockdown of genes that showed a significant effect in monolayer conditions

resulted in similar effects in suspension conditions due to the significantly reduced cell numbers at the time of cellular detachment, as seen with siRNAs to RPS6 (ribosomal protein S6) and Xpo1 (Figure 2.5A). However, most interestingly, certain siRNAs showed minimal effect in monolayer conditions (with "monolayer" readouts near 1.0), but showed significant decrease in suspension conditions. For example, knockdown of IRS-1 or Akt1 resulted in a monolayer readout of 0.630 and 0.703, respectively, while in suspension cultures the readouts were 0.355 and 0.430 (Table 2.1), suggesting that the knockdown of these genes played a disproportionately greater role in suspension versus monolayer cultures. This correlates with our previous studies showing a role of the IR/IGF-1R pathway in the suppression of *anoikis* (117)

Therefore, when survival ratios were calculated (Figure 2.5B) and the siRNAs were ranked by increasing survival ratio (Figure 2.5C), we proposed that genes at the lowest end of this range would represent candidate suppressor of *anoikis* "hits" (Table 2.1). However, as expected, genes such as Xpo1 that demonstrate significant survival effect in monolayer conditions can also show a very low survival ratio due to the low value of the denominator monolayer readout. On the contrary, genes associated with the highest survival ratio would possibly represent promoters of *anoikis* death, such as PPP2R2B, which was shown to promote cell death under oxidative stress and autophagic conditions (234). Overall, the results of this screen demonstrated various possible hits representing suppressors and promoters of *anoikis* in Ewing sarcoma cells related to the IR/IGF-1R pathway, with the validity of the results supported by literature findings and previous results in our laboratory.

Screen for novel suppressors of anoikis using a tyrosine kinase siRNA library. To extend the screen to a larger set of genes, we utilized an siRNA library that targets the spectrum of tyrosine kinases in the human genome (Figure 2.6). This is a particularly useful set of genes as they represent possible therapeutic targets by small molecular kinase inhibitors. Using the TC-32luc and TC-71luc cell lines, we performed the screen against the 88 siRNAs in triplicate, following the same protocol as in the IR/IGF-1R pathway screen. In both cell lines, many genes showed significant inhibitory effect when knocked down in monolayer conditions (Figure 2.7A and B). In particular, knockdown of NTRK2, EphB2, LMTK2 and Hck showed a prominent effect commonly in both cell lines, represented in the top 10 hits in the results from the two screens (Table 2.2A and B). Taking into account these genes that showed already prominent effect in monolayer conditions, we then analyzed genes that showed the lowest survival ratio following cellular detachment when knocked down (Figure 2.7A and B). As expected, some genes that showed a prominent effect when knocked down in monolayer conditions also showed low survival ratio, such as with Hck. However, certain genes showed a significantly reduced survival ratio with relatively sustained survival under monolayer conditions. For example, knockdown of PTK9L in TC71luc cells showed a 0.620 survival in monolayer conditions, but only a 0.207 survival in suspension, with an overall survival ratio of 0.335 (Table 2.2C). This gene also appeared in the top hits in the screen of TC32luc cells. Using Student's t-scores as readouts of statistical significance, only a limited number of genes demonstrated t-scores exceeding the 95% confidence interval cutoff of t=2.132 (Figure 2.8A and B). Furthermore, when

we took into the consideration the effect of multiple comparisons, requiring an approximate confidence interval of 99.95%, only rare hits met the criteria of t>8.610 (Figure 2.8A and B).

We also considered genes at the other end of the spectrum of hits, with certain genes resulting in increased survival ratio relative to control cells when knocked down. These genes would therefore represent potential promoters of *anoikis*. One such gene identified in both the screens of TC-71 and TC-32 cells was Syk (Figure 2.7), with survival ratios of 1.576 and 1.937, respectively, arising from the screen. This corresponded to t-scores of 9.150 and 7.224 (Figure 2.8A and B, Table 2.3A and B). Importantly, this result did not appear to be due to a prominent effect on survival in monolayer conditions prior to detachment; for example, in TC-71 cells, Syk knockdown had a minimal effect in monolayer culture, with an assay readout of 0.910 versus control wells, but resulted in a relatively prominent effect in suspension culture with an suspension assay readout of 1.435 (Table 2.3A and B).

Screen for novel suppressors of *anoikis* using a cell cycle regulator library. As mentioned, previous studies have shown that cell cycle inhibitors such as p27/KIP1 (CDKN2B) actually act to promote survival following detachment. We were therefore interested in the role of various cell cycle regulators in modulating *anoikis*. When we applied the siRNA library of cell cycle regulators, we showed a similar distribution of effects on *anoikis* across the various genes in the library, although the magnitude of effect of the siRNAs with the maximal effect (at either end of the list of hits) was less pronounced, resulting in a less prominent “S” shape in the survival ratio curve (Figure 2.9). While few siRNAs demonstrated statistical

significance in their effect on the survival ratio following correction for multiple comparisons (Figure 2.10), some trends did emerge from this data. For example, knockdown of various genes in the retinoblastoma family (particularly RBL2 and Rb1) resulted in a reduced survival ratio, suggesting that members of this family may all contribute to *anoikis* resistance (Table 2.4). However, a consistent trend for cell cycle inhibitors versus promoters as positive suppressors of *anoikis* did not emerge from the results of this screen, as a number of cell cycle promoters such as cyclins and cyclin-dependent kinases were also seen in the top hits. Overall, while the results of this screen raise the possibility of a role for retinoblastoma family members in *anoikis* suppression, a clear role for specific cell cycle regulators was not identified in this screen.

Attempted validation of hits identified in siRNA screens. We then attempted to validate these hits using alternative assays of *anoikis* resistance. We also wished to validate these results in more usual suspension culture conditions, particularly in larger well formats (e.g. 6- or 12-well plates) rather than in a 96-well format. Firstly, we wished to validate PTK9L (also known as twinfilin-2, or Twf2) as a putative suppressor of *anoikis*. Using the pooled siRNA against Twf2/PTK9L from the screen, as well as the individual four siRNAs from the pool, we first established the ability of these siRNAs to knockdown Twf2/PTK9L levels. We demonstrated that the siRNA pool and individual siRNAs #1 and #2 were able to effectively knockdown Twf2/PTK9L protein levels (Figure 2.11A), while siRNAs #3 and #4 were unable to (data not shown). When we then assayed the effect of these siRNAs on cell survival again using the luminescence-based assay, we did establish that the PTK9L siRNA

pool did indeed reduce cell survival in suspension (Figure 2.11B). However, siRNAs #1 and #2 did not show any significant effect on survival. This suggested that the positive result from the screen using the PTK9L siRNA pool was not correlated with levels of the Twf2/PTK9L protein, and likely relates to a non-specific effect of the other siRNAs that did not have an effect on Twf2/PTK9L protein levels.

We then attempted to validate Syk as a potential promoter of *anoikis*, by determining if Syk knockdown does indeed increase cell survival following detachment. However, when we attempted to determine the baseline expression levels of Syk in Ewing sarcoma cells, we were unable to establish any significant expression of this protein by Western blot (data not shown). Furthermore, when we analyzed expression profiling data of the TC32 and TC71 Ewing sarcoma cell lines, we found that *Syk* mRNA expression levels in these two cell lines were in fact very low. Therefore, we concluded that this hit related to Syk was again due to non-specific effects of the Syk siRNA pool on cell survival in these cells.

We also tried to determine whether the retinoblastoma family of proteins had a significant effect on *anoikis*. The cell cycle restrictive functions of these proteins would support the hypothesis that cell cycle inhibition would help support survival during transient periods such as cellular detachment. However, using siRNA pools against Rb1, RBL1 and RBL2, we were unable to establish any significant effect on *anoikis* either when used individually, or when simultaneously used (Figure 2.11C).

Overall, the attempts to validate the hits arising from the siRNA screen were unsuccessful, and appeared to relate to non-specific effects of the siRNAs used, as

the effects observed did not correlate with knockdown of levels of the targeted protein.

2.4 DISCUSSION

In this chapter, we summarize the results of our attempt to utilize an RNAi-based functional screen to identify novel suppressors of *anoikis*. While the screen using various siRNA libraries led to the identification of a number of putative hits, the significance of these hits was inconclusive, as the screen results were of only marginal statistical significance, and the subsequent validation studies also did not yield conclusive results. However, while modulation of these individual hits did not result in prominent modulation of *anoikis* susceptibility, the overall screen results do suggest some biological properties underlying *anoikis* resistance.

A multitude of reasons may explain why this screen did not result in the identification of individual hits that could be subsequently validated. Most importantly, the overall format of this screen may not be amenable to identifying such suppressors of *anoikis*. In particular, one problem is the reliance on normalizing the effect of siRNA knockdown in suspension cultures to the effect of knockdown in monolayer cultures. However, it is apparent that many modulators of *anoikis* also modulate proliferation or survival in suspension cultures, and therefore knockdown of such modulators of *anoikis* may already have significantly impaired the cells prior to detachment, skewing the readout following normalization. One possible way around this would be to subject the cells to detachment after only a short incubation following siRNA transfection (e.g. 24 hours). However, this may result in inconsistent protein knockdown across individual genes in the library

following siRNA delivery, therefore biasing the screen towards less stable proteins more susceptible to RNA interference. Furthermore, incomplete protein knockdown would be seen for many genes (as compared to the usual 48 to 72 hour incubation usually accepted as reliable sufficient for knockdown of any protein), and cells therefore would be subject to detachment and *anoikis* stress under conditions where the gene in question will likely be incompletely knocked down. In the end, the current format was felt to be the most appropriate protocol for this screen.

The poor dynamic range of the screening results also hindered the ability to identify reliable hits. The luciferase-based assay itself demonstrated a broad dynamic range proportional to the viable cell numbers, and does not appear to be the main contributor to this poor dynamic range. Rather, the range is limited by the baseline in each individual screen well, as represented by the total cell numbers following siRNA transfection and subsequent 72-hour culturing. As survival following detachment was very much affected by the *a priori* survival in monolayer conditions following siRNA knockdown, the hits of greatest interest (i.e. with the lowest survival ratio) often showed a low baseline cell number prior to suspension culture (as demonstrated by low monolayer assay readouts), which consequently reduced the overall dynamic range of those assay wells.

Another issue relates to the use of small 96-well format plates, and whether this is reflective of the *anoikis* process usually studied in larger 6- or 12-well plates. Specifically, suspension cultures in the 96-well format commonly resulted in the formation of a few larger cellular spheroids at the center of the well, rather than multiple smaller cell clusters seen in 6- or 12-well formats. Such differences in the

sizes of the cellular clusters certainly may contribute to survive under conditions, due to differences in the proportion of cells at the periphery versus the center of such clusters, leading to variability in the proportion of cells directly exposed to media and serum as well as oxygen. Therefore, it is possible that suppressors of *anoikis* hits identified in our screen may not correlate entirely with the ability to suppress *anoikis* in larger-well conditions.

One other problematic factor related to the absence of a reliable positive control for the screen. Although a number of previously identified suppressors of *anoikis* were used as controls in the screen runs, such as E-cadherin and ErbB4, knockdown of these genes did not display as significant a result using our screening protocol. In the absence of a positive control, we did not have reliable readout of the technical success of each screening protocol run.

Other technical issues may also be contributory. Firstly, it may relate to the actual effectiveness of the RNA interference and subsequent protein knockdown. However, in addition to the demonstration of effective knockdown using siRNA controls such as siRNA against lamin-A/C, knockdown of other modulators of cell survival and proliferation in Ewing sarcoma cell lines previously demonstrated in our lab also resulted in reduced cell numbers in monolayer culture prior to the detachment step, including RPS6. Similarly, knockdown of known suppressors of proliferation, such as TSC1 and TSC2, resulted in increased cell numbers in monolayer culture. These results are supportive of the effectiveness of the siRNA protocol and of the siRNA library itself. However, it is possible that expression of various genes within the library may have recovered following the prolonged

culture period following siRNA transfection (72-hour monolayer culture followed by 48-hour suspension culture), and the amount of residual gene expression may vary between genes depending on the kinetics of expression versus degradation, and the effectiveness of the siRNA used. Another important technical issue relates to the format of the siRNA libraries, which uses a pool of four siRNAs for each target gene. While this format is purported to reduce the chance of off-target RNA interference, through the use of reduced concentrations of multiple siRNAs targeting the same gene, it is arguable that this may in fact result in greater off-target effect due to the four-fold increase in the chance of binding to non-specific, partially-complimentary gene targets. In fact, our validation studies of the PTK9L target suggests this is a valid concern, as only two of four siRNAs in the pool resulted in PTK9L/Twf2 knockdown, and neither of these siRNAs resulted in a phenotypic effect in the validation *anoikis* assay.

Of course, the use of restricted siRNA libraries rather than a genome-wide library may also limit the ability of the screen to identify hits. While cost and time limitations prevented the use of a broader or genome-wide library for this screen, it was also hoped that results from these limited library screen would demonstrate sufficiently promising data to justify broader screens. However, in the absence of promising results from these small screens, it was decided that such broader screens were not justified.

In addition to these issues specific to the design and execution of our screening protocol, one other pertinent general limitation of siRNA-based screens relates to the ability to only knockdown a single gene at a time in each test well. While

identifying single "Achilles heel" genes that regulate *anoikis* suppression is the ideal outcome of this screen, it seems apparent that a wide network of mechanisms contributes to regulating *anoikis*. In particular, multiple homologous genes within an important gene family may all contribute, and knockdown of only individual genes within a family would be insufficient to elicit a prominent phenotypic difference. Therefore, if such partial phenotypic changes do in fact occur, the resulting assay readout may be statistically insignificant, limiting the ability of the screen to identify such hits.

While we were not able to identify a promising and validatable hit, the screen did highlight some interesting trends based on the hits demonstrating statistically-marginal significance. A number of the top hits in the insulin signaling library screen included various promoters of IGF-1R pathway activation, including IRS-1 and Akt1, supporting a role for these proteins in *anoikis* resistance as we previously showed (117). Screening using the cell cycle library also demonstrated that a number of negative regulators of the cell cycle, including various members of the Rb-family of proteins, may have a seemingly paradoxical role for suppressing *anoikis*. Similar to p27/KIP1, which appears to promote *anoikis* resistance through cell cycle arrest, activation of retinoblastoma family members such as RBL2/p130 may also help to promote survival under transient states of stress such as cellular detachment; corollary findings have been demonstrated in ovarian cancer cell lines subjected to growth inhibitory (serum free) conditions, which relied on RBL2/p130- and Mirk-dependent cell cycle arrest to maintain survival, interestingly through up-regulation of p27/KIP1 (235). Similarly, cancer cells have been shown to rely on proficiency of

the retinoblastoma pathway, including the presence of functional Rb1/pRb, to promote survival during conditions such as treatment with cytotoxic agents, tamoxifen or ionizing radiation (236, 237). Therefore, these data lend some vague support for the role of cell cycle inhibition and quiescence to promote survival following a transient stress state such as cellular detachment.

In summary, the results of this suppression of *anoikis* screen were inconclusive, and highlight the difficulties of designing an RNA interference-based functional screen for identifying modulators of *anoikis*. While it is possible that the screening protocol could be further optimized, we felt that even such optimization would be unlikely to resolve the major issues relating to this screen, particularly in relation to the need for normalization of the suspension assay readouts to monolayer cultures, and the resulting compromise in dynamic range. Furthermore, the excessive cost of extending such a screen to a genome-wide level was prohibitory. Therefore, we felt that pursuing other screening approaches to identifying candidate *anoikis* resistance genes would be the best direction from here forward.

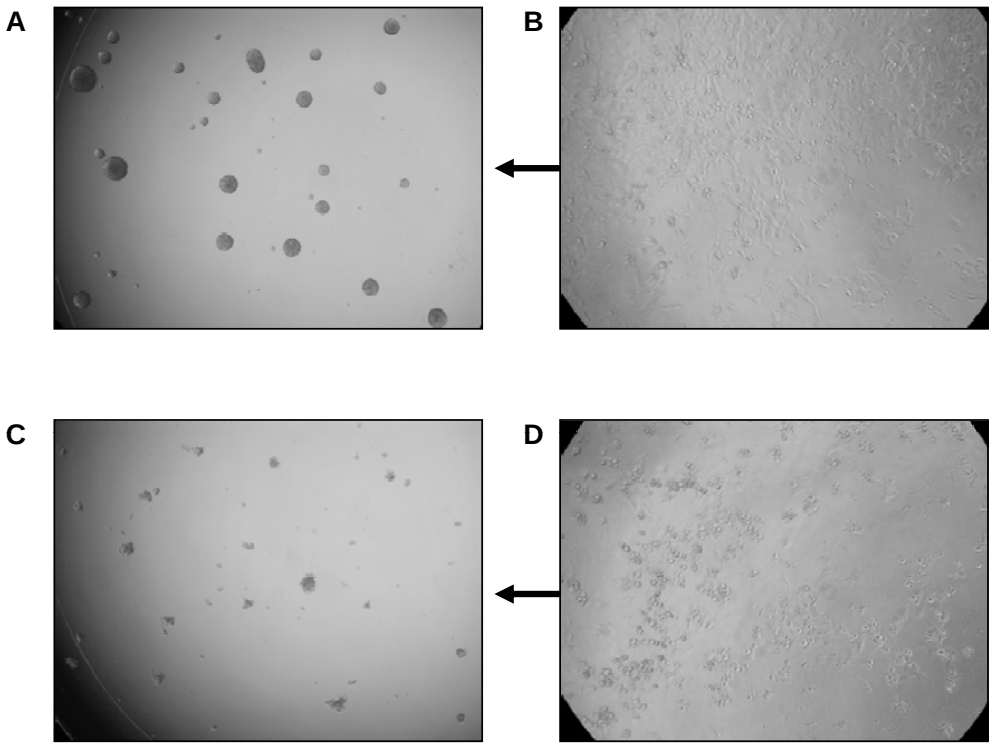

Figure 2.1. Validation of high-throughput 96-well system for suspension culture of Ewing sarcoma cell lines. (A) Phase contrast microscopy images of Ewing sarcoma TC-71 cells cultured for 48 hours in coated 96-well Non-Binding Surface plates. (B) Prior monolayer cultures of same TC-71 cells prior to trypsinization and plating into suspension conditions in coated plates.

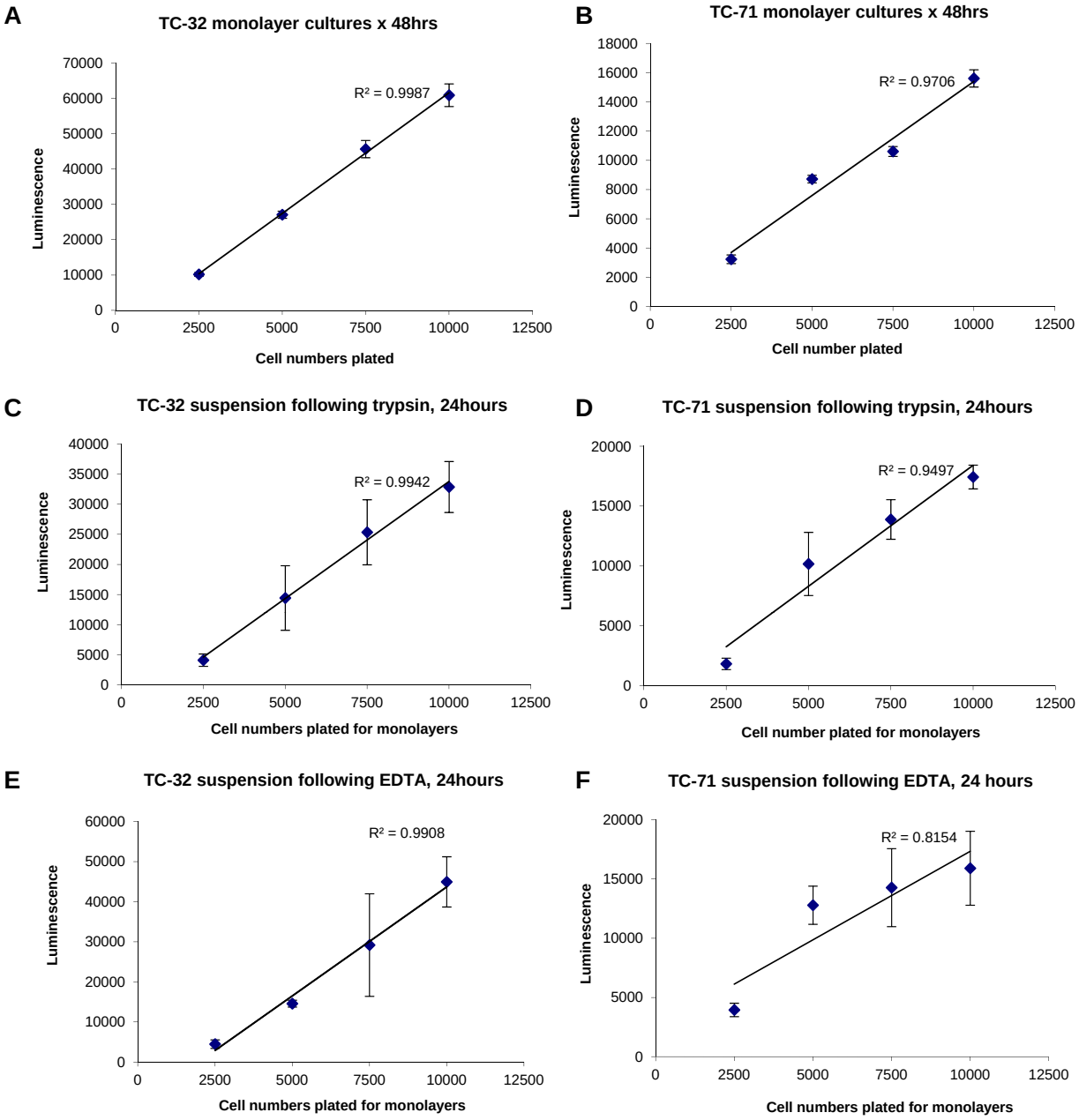

Figure 2.2. Validation of luminscence assay in monolayer and suspension cultures. Correlation between initial cell numbers plated versus final luminescence assay readout, cultured as (A and B) monolayer cultures only for 48 hours, (C and D) monolayer culture for 48 hours followed by cellular detachment using trypsin and subsequent suspension culture for 24 hours, and (E and F) monolayer culture for 48 hours followed by cellular detachment using EDTA and subsequent suspension culture for 24 hour. Luminescence values represent arbitrary values derived from the luminescence plate reader following application of firefly luciferin on the luciferase-overexpressing TC-32 and TC-71 cells. All data are shown as mean ± SEM (n=3) .

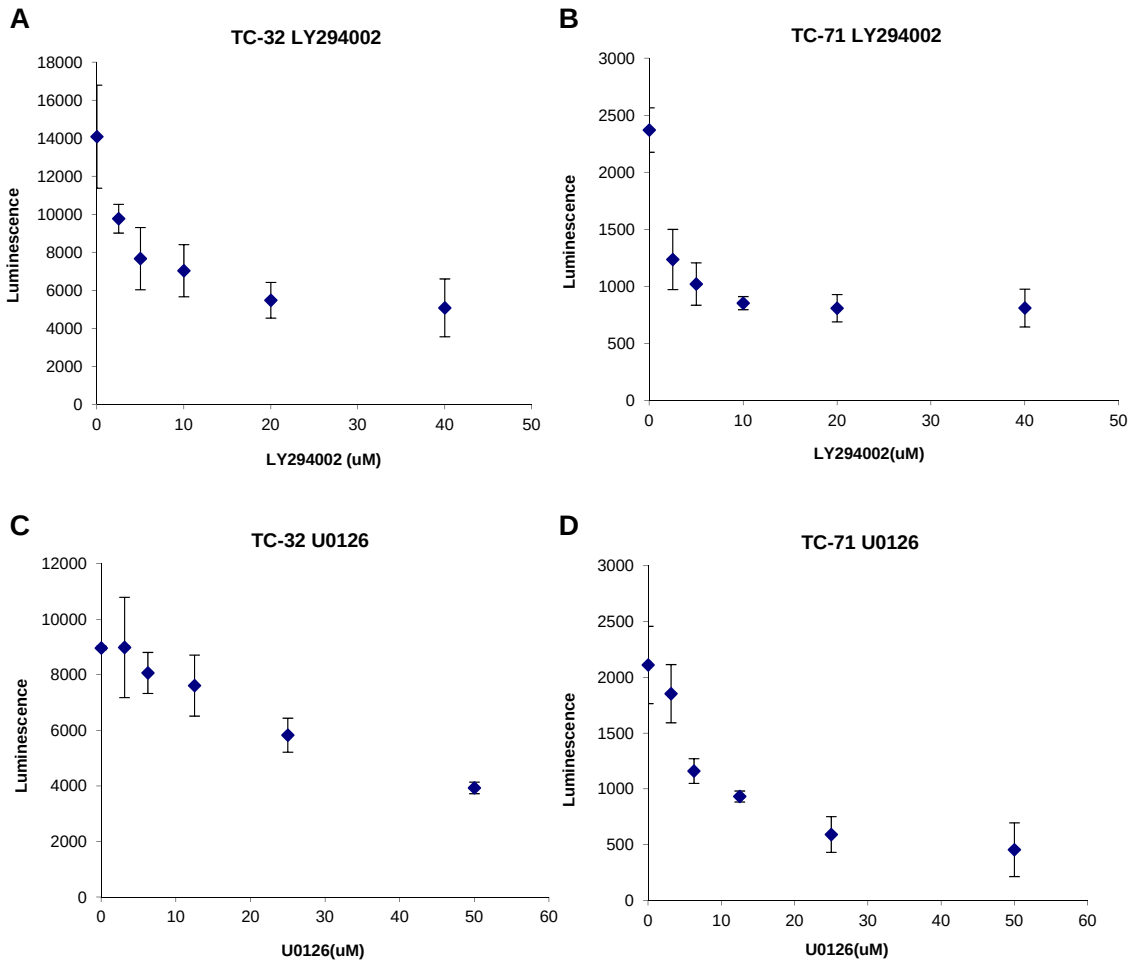

Figure 2.3. Validation of luminescence assay in suspension culture following treatment with known chemical promoters of *anoikis*. Correlation between initial cell numbers plated versus final luminescence assay readout, cultured in suspension for 48 hours, followed by treatment with (A and B) the PI3K inhibitor LY294002 and (C and D) the MEK/ERK pathway inhibitor U0126. Luminescence values represent arbitrary values derived from the luminescence plate reader following application of firefly luciferin on the luciferase-overexpressing TC-32 and TC-71 cells. All data are shown as mean ± SEM (n=3).

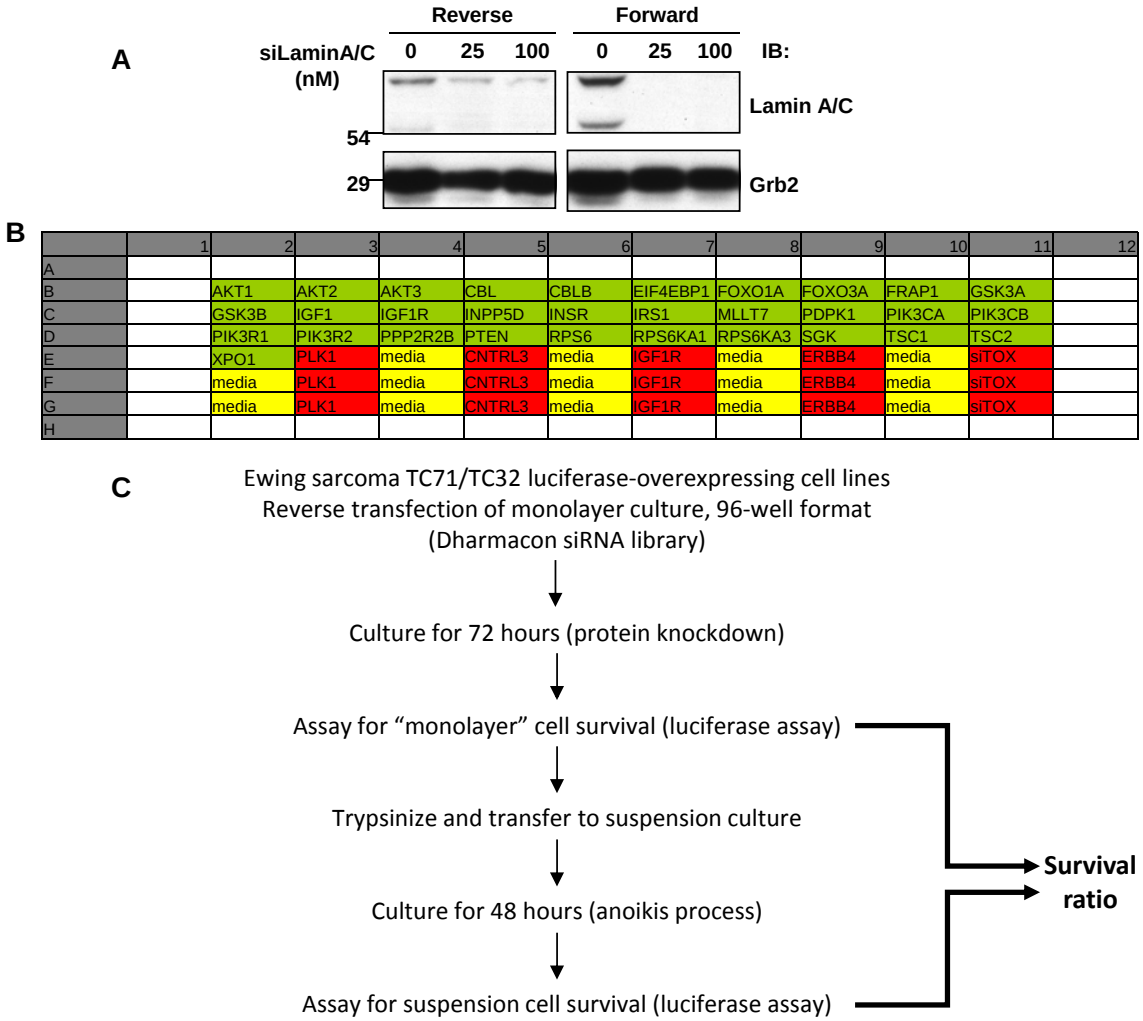

Figure 2.4: High-throughput assay for functional screening for novel suppressors of anoikis. (A) Validation of siRNA knockdown efficiency using a control siRNA against LaminA/C, using either a standard “forward” transfection protocol (transfection into cells cultured as monolayers, followed by cellular detachment and subsequent suspension culture for 48 hours), or a “reverse” transfection protocol (application of cells directly onto siRNA/transfection reagent admixture, and continuation of culture in suspension conditions for 48 hours), using various concentrations of siRNA. Grb2 is used as a loading control. (B) Schematic of the arrangement of siRNAs used from the initial library tested (“insulin signaling pathway”), as arranged in a 96-well format. Green squares represent the library siRNAs, while the red squares represent siRNA controls used, including positive controls siTOX and siPLK1 (both known to result in marked cell death following transfection across a variety of cell types), siIGF1R and siERBB4 (both previously demonstrated to have a role in anoikis suppression in Ewing sarcoma cells) and negative controls siCNTRL3 and media-only controls (yellow wells). Media-only wells were averaged and used as a denominator for normalization. (C) Outline of the screening protocol, with the primary readout being the “survival ratio”, calculated as the ratio of the luciferase assay readout following 48 hours in suspension culture, to the luciferase assay readout in monolayer culture 72 hours after siRNA transfection, immediately prior cellular detachment.

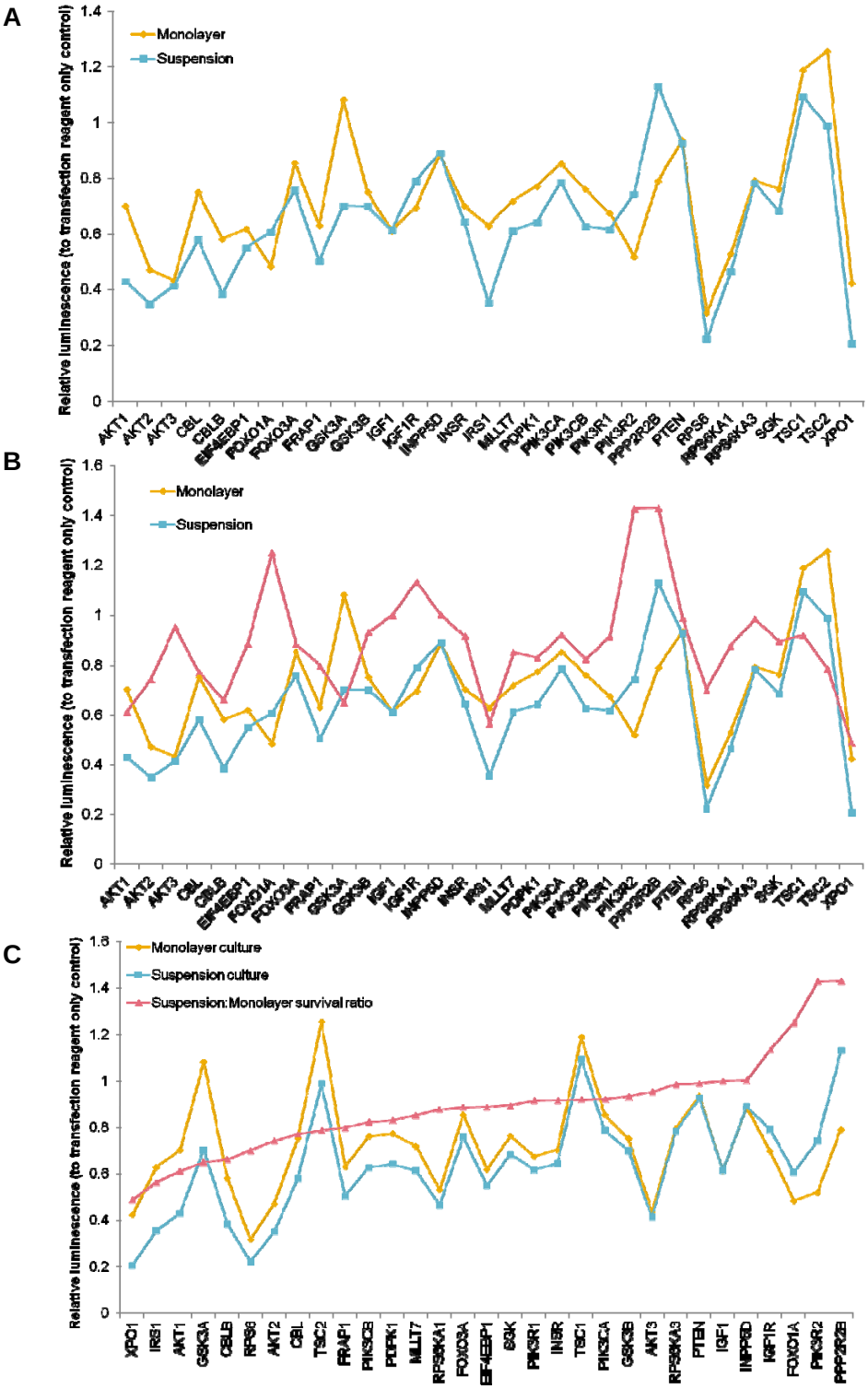

Figure 2.5. Suppression of *anoikis* screen using siRNA library targeting the insulin signaling pathway. (A) Screening results sorted in arbitrary (alphabetical) order of genes following initial monolayer culture (yellow) and subsequent suspension culture (blue), with readout representing luminescence value normalized against media-only (no siRNA) controls. (B) Results with survival ratio calculation (suspension:monolayer ratio). (C) Results sorted by increasing survival ratio.

Gene	Monolayer @ 72 hours	Suspension @ 48 hours	Survival ratio
XPO1	0.424	0.207	0.488
IRS1	0.630	0.355	0.563
AKT1	0.703	0.430	0.612
GSK3A	1.083	0.703	0.649
CBLB	0.583	0.385	0.661
RPS6	0.318	0.223	0.701
AKT2	0.472	0.350	0.742
CBL	0.752	0.580	0.772
TSC2	1.257	0.990	0.787
FRAP1	0.631	0.504	0.799
PIK3CB	0.762	0.628	0.823
PDPK1	0.774	0.643	0.831
MLLT7	0.720	0.614	0.853
RPS6KA1	0.531	0.466	0.878
FOXO3A	0.855	0.759	0.887
EIF4EBP1	0.620	0.550	0.888
SGK	0.763	0.684	0.896
PIK3R1	0.675	0.618	0.916
INSR	0.703	0.645	0.917
TSC1	1.190	1.094	0.920
PIK3CA	0.854	0.787	0.922
GSK3B	0.751	0.701	0.934
AKT3	0.434	0.415	0.954
RPS6KA3	0.794	0.783	0.986
PTEN	0.936	0.927	0.990
IGF1	0.613	0.614	1.002
INPP5D	0.887	0.890	1.004
IGF1R	0.697	0.791	1.135
FOXO1A	0.485	0.607	1.252
PIK3R2	0.520	0.743	1.428
PPP2R2B	0.791	1.132	1.430

Table 2.1. Insulin signaling pathway screening results. Results are sorted by increasing survival ratio.

	media	PLK1	ABL1	ABL2	ALK	AXL	BLK	BMX	BTK	CSF1R	
	CNTRL3	media	DDR2	EGFR	EPHA1	EPHA10	EPHA2	EPHA3	EPHA4	EPHA5	
	media	IGF1R	EPHA8	EPHB1	EPHB2	EPHB3	EPHB4	EPHB6	ERBB2	ERBB3	
	CNTRL2	media	FES	FGFR1	FGFR2	FGFR3	FGFR4	FGR	FLT1	FLT3	
	media	ERBB4	FYN	HCK	IGF1R	INSR	ITK	JAK1	JAK2	JAK3	
	siTOX	media	LCK	LMTK2	LTK	LYN	MATK	MERTK	MET	MST1R	

	media	PLK1	NTRK2	NTRK3	PDGFRA	PDGFRB	PTK2	PTK2B	PTK6	PTK7	
	CNTRL3	media	RET	ROR1	ROR2	ROS1	RYK	SRC	STYK1	SYK	
	media	IGF1R	TIE	TNK1	TNK2	TP53RK	TXK	TYK2	TYRO3	YES1	
	CNTRL2	media	CSK	EPHA6	ERBB4	FLT4	KDR	MUSK	PTK9	TEC	
	media	ERBB4	DDR1	EPHA7	FER	FRK	KIT	NTRK1	PTK9L	TEK	
	siTOX	media	TXNIP	media	ARRDC3	media	media	media	media	media	

Figure 2.6. Tyrosine kinase library screening protocol. Schematic of the arrangement of siRNAs used from the initial library tested ("insulin signaling pathway"), as arranged in a 96 well format. Green squares represent the library siRNAs, while the red squares represent siRNA controls used, including positive controls siTOX and siPLK1 (both known to result in marked cell death following transfection across a variety of cell types), siIGF1R and siERBB4 (both previously demonstrated to have a role in anoikis suppression in Ewing sarcoma cells) and negative controls siCNTRL3 and media-only controls (yellow wells). Media-only wells were averaged and used as a denominator for normalization.

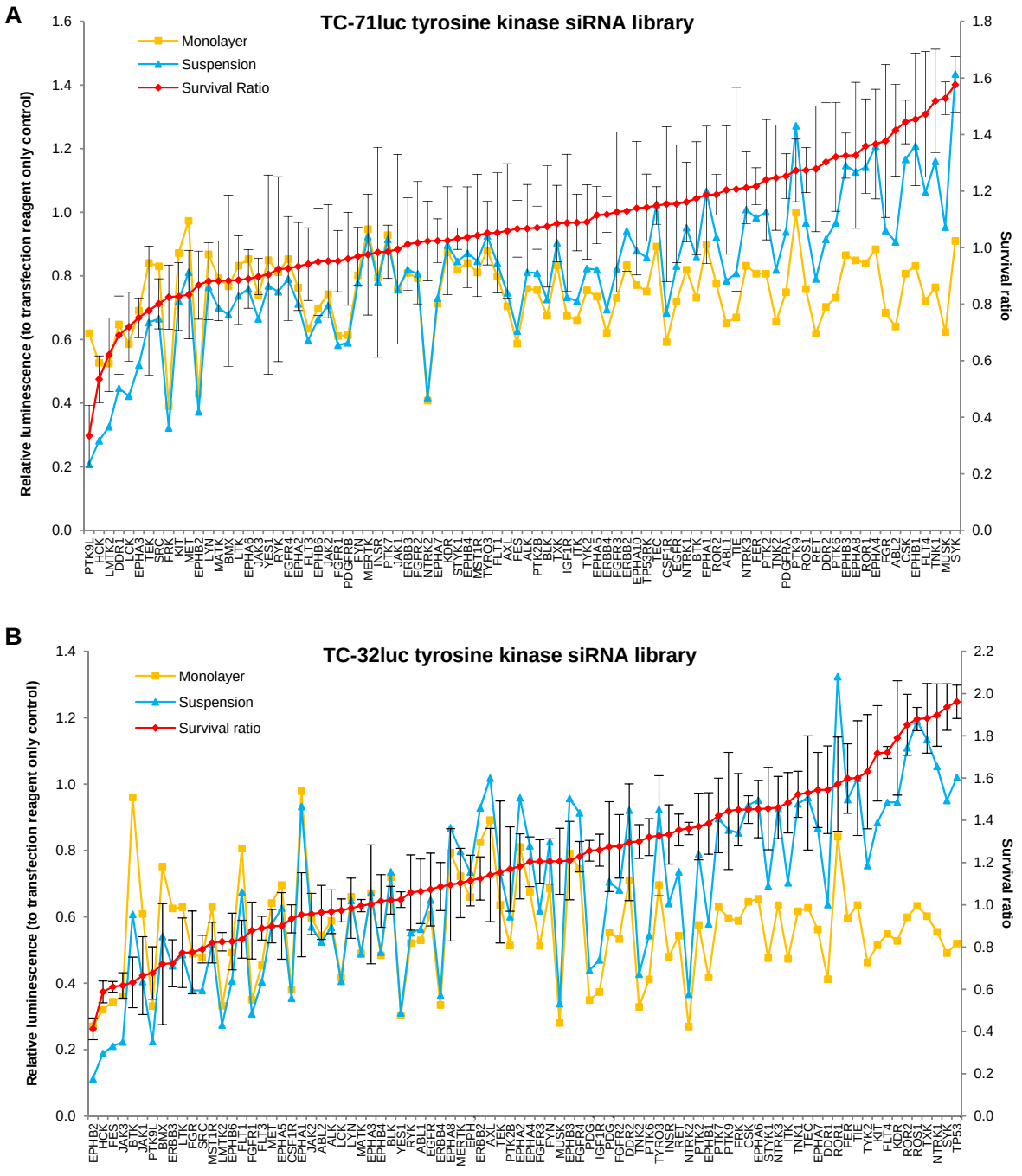

Figure 2.7. Suppression of *anoikis* screening results using an siRNA library against tyrosine kinases. (A) TC-71 and (B) TC-32 cell lines subjected to the screening protocol as previously described, with results sorted by increasing survival ratio. The survival ratio is shown as mean ± SEM (n=3).

A

Gene	Monolayer	Monolayer standard deviation
FRK	0.390	0.054
NTRK2	0.408	0.026
EPHB2	0.430	0.018
LMTK2	0.525	0.093
HCK	0.527	0.046
LCK	0.586	0.019
FES	0.587	0.074
CSF1R	0.592	0.152
FGFR1	0.611	0.017
PDGFRB	0.614	0.006

B

Gene	Monolayer	Monolayer Standard Deviation
NTRK2	0.270	0.020
EPHB2	0.271	0.029
MUSK	0.281	0.049
YES1	0.303	0.023
HCK	0.321	0.025
TNK2	0.329	0.049
PTK9L	0.331	0.038
LMTK2	0.332	0.004
ERBB4	0.335	0.039
FES	0.344	0.020

C

Gene	Survival Ratio	Ratio standard deviation	T Score	Monolayer	Monolayer standard deviation	Suspension	Suspension standard deviation
PTK9L	0.335	0.108	6.596	0.620	0.018	0.207	0.107
HCK	0.535	0.083	5.121	0.527	0.046	0.282	0.069
LMTK2	0.621	0.130	2.652	0.525	0.093	0.326	0.090
DDR1	0.690	0.138	2.506	0.647	0.024	0.447	0.136
LCK	0.720	0.122	2.326	0.586	0.019	0.422	0.120
EPHA3	0.752	0.070	4.223	0.690	0.017	0.519	0.068
TEK	0.778	0.228	1.422	0.841	0.128	0.654	0.188
SRC	0.802	0.089	3.216	0.830	0.055	0.666	0.069
FRK	0.825	0.113	1.042	0.390	0.054	0.322	0.100
KIT	0.827	0.120	2.176	0.872	0.047	0.721	0.110

D

Gene	Survival ratio	Ratio standard deviation	T score	Monolayer	Monolayer standard deviation	Suspension	Suspension standard deviation
EPHB2	0.413	0.051	5.354	0.271	0.029	0.112	0.043
HCK	0.588	0.052	4.420	0.321	0.025	0.189	0.046
FES	0.612	0.025	9.115	0.344	0.020	0.211	0.015
JAK3	0.619	0.060	3.946	0.361	0.025	0.223	0.055
BTK	0.633	0.120	5.096	0.960	0.111	0.608	0.045
JAK1	0.665	0.184	1.918	0.609	0.046	0.405	0.178
PTK9L	0.678	0.124	1.488	0.331	0.038	0.224	0.118
BMX	0.720	0.286	1.274	0.752	0.064	0.541	0.279
ERBB3	0.724	0.111	2.693	0.626	0.082	0.453	0.075
LTK	0.773	0.165	1.502	0.629	0.077	0.487	0.145

Table 2.2. Tyrosine kinase screening results. The top 10 siRNAs resulting in greatest suppression of cell numbers following monolayer cultures of (A) TC-71 and (B) TC-32 cells are shown, sorted by increasing luminescence assay readout values normalized to control wells ("Monolayer"). The top 10 siRNAs resulting in the lowest survival ratio in suspension culture of (C) TC-71 and (D) TC-32 cells are shown, sorted by increasing survival ratio. T-score denotes the Student's t significance value.

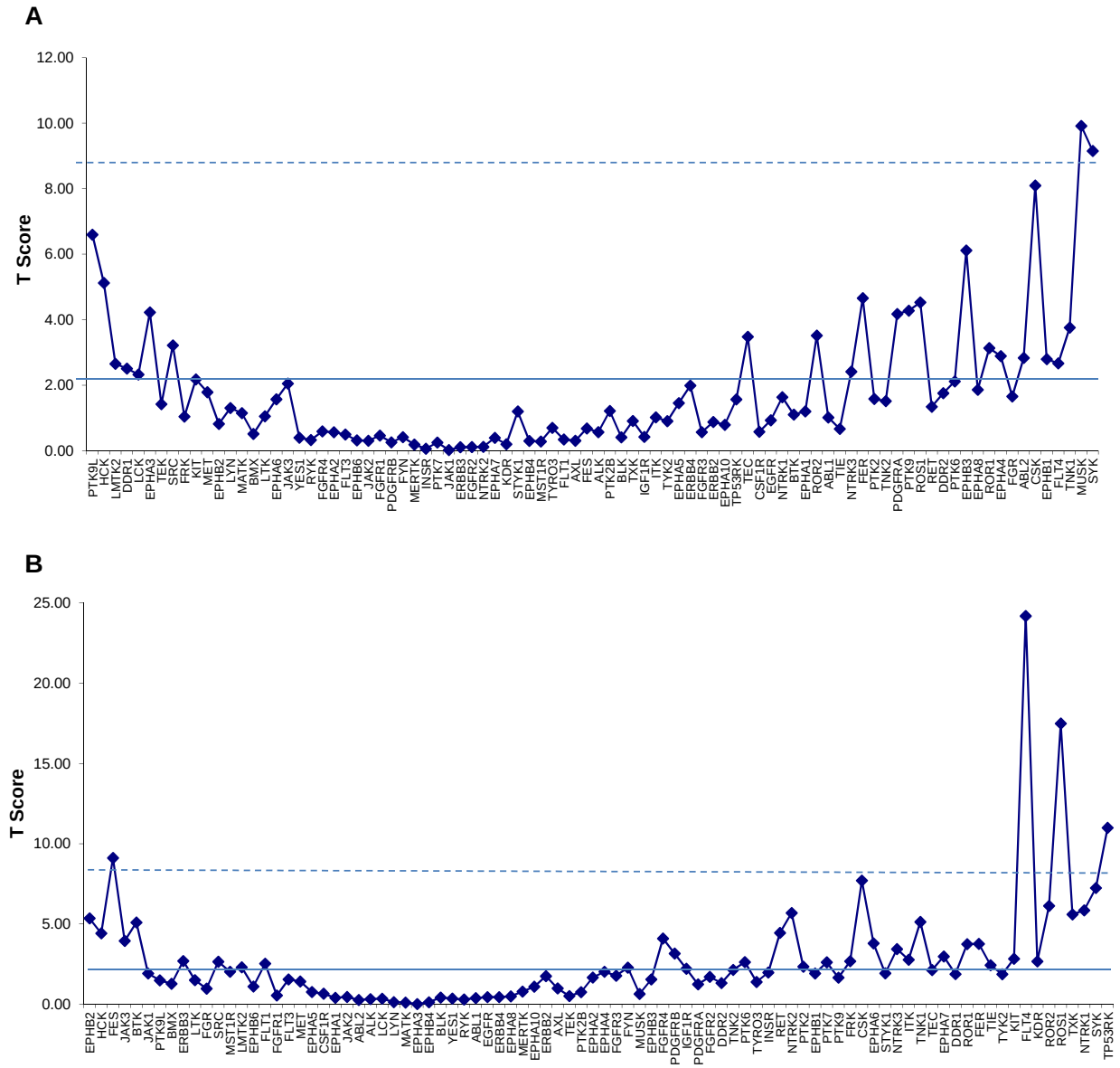

Figure 2.8. Significance values of hits from the tyrosine kinase library screen. Student's t-score significance values for the survival ratio readouts in the tyrosine kinase library screen, for (A) TC-71 and (B) TC-32 cell lines. The solid horizontal line denotes the 95% confidence interval for individual hits (t=2.132), while the upper hashed line denotes the 95% confidence interval as corrected for multiple observations (t=8.610).

A

Gene	Survival Ratio	Ratio standard deviation	T Score	Monolayer	Monolayer standard deviation	Suspension	Suspension standard deviation
SYK	1.576	0.099	9.150	0.910	0.096	1.435	0.024
MUSK	1.528	0.058	9.914	0.624	0.003	0.953	0.058
TNK1	1.519	0.183	3.758	0.764	0.049	1.160	0.176
FLT4	1.472	0.221	2.666	0.721	0.077	1.062	0.207
EPHB1	1.454	0.234	2.795	0.831	0.025	1.209	0.232
CSK	1.445	0.077	8.095	0.807	0.052	1.166	0.056
ABL2	1.415	0.163	2.833	0.641	0.067	0.907	0.148
FGR	1.377	0.270	1.656	0.684	0.112	0.942	0.246
EPHA4	1.366	0.194	2.889	0.884	0.038	1.208	0.190
ROR1	1.360	0.167	3.133	0.840	0.037	1.142	0.163

B

Gene	Survival Ratio	Ratio standard deviation	T Score	Monolayer	Monolayer standard deviation	Suspension	Suspension standard deviation
TP53RK	1.962	0.079	10.995	0.520	0.044	1.020	0.066
SYK	1.937	0.110	7.244	0.491	0.085	0.951	0.070
NTRK1	1.899	0.148	5.851	0.555	0.076	1.054	0.127
TXK	1.883	0.165	5.597	0.602	0.106	1.134	0.126
ROS1	1.880	0.055	17.494	0.633	0.028	1.191	0.047
ROR2	1.853	0.144	6.128	0.599	0.086	1.109	0.116
KDR	1.790	0.271	2.669	0.528	0.135	0.946	0.235
FLT4	1.722	0.028	24.191	0.549	0.012	0.945	0.025
KIT	1.718	0.226	2.832	0.515	0.090	0.884	0.207
TYK2	1.631	0.270	1.869	0.463	0.034	0.755	0.268

Table 2.3. Tyrosine kinase screening results. The top 10 siRNAs resulting in the greatest survival ratio in suspension culture of (A) TC-71 and (B) TC-32 cells are shown, sorted by increasing survival ratio. T-score denotes the Student's t significance value.

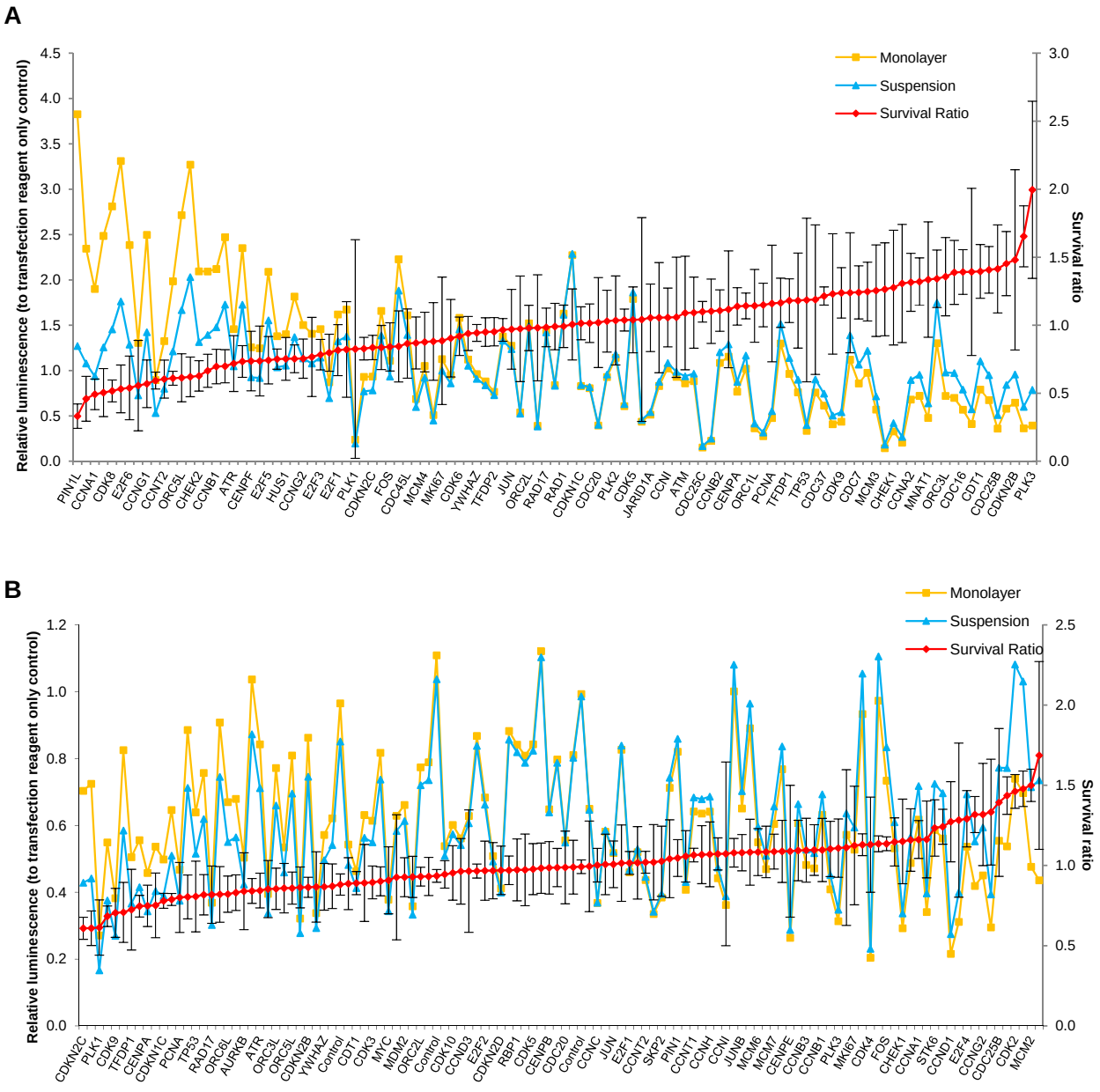

Figure 2.9. Suppression of *anoikis* screening results using an siRNA library against cell cycle regulators. (A) TC-71 and (B) TC-32 cell lines subjected to the screening protocol as previously described, with results sorted by increasing survival ratio. The survival ratio is shown as mean ± SEM (n=3) .

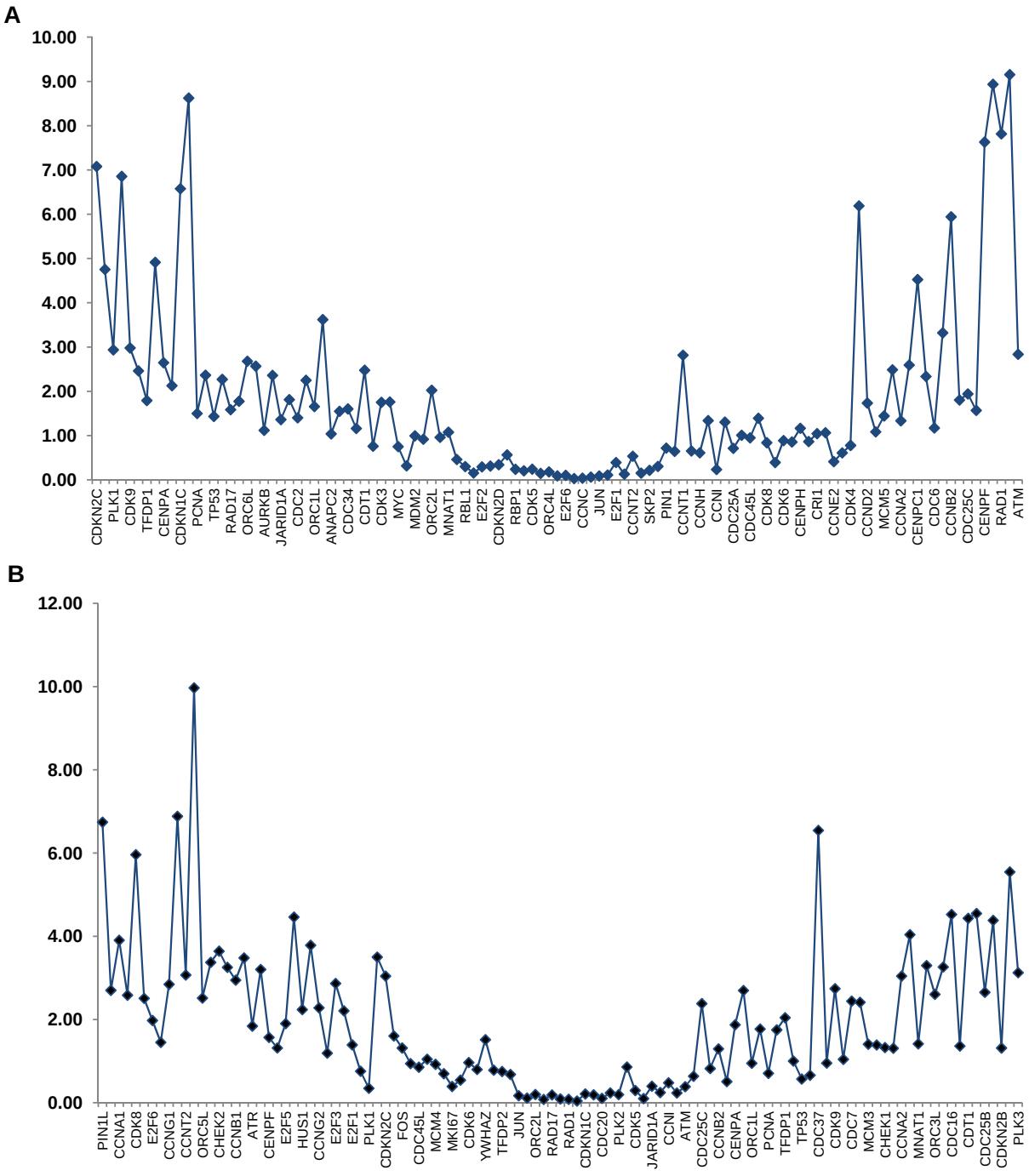

Figure 2.10. Significance values of hits from the cell cycle library screen. Student's t-score significance values for the survival ratio readouts in the cell cycle library screen, for (A) TC-71 and (B) TC-32 cell lines. The solid horizontal line denotes the 95% confidence interval for individual hits (t=2.132), while the upper hashed line denotes the 95% confidence interval as corrected for multiple observations (t=8.610).

A

Gene	Survival Ratio	Ratio standard deviation	T Score	Monolayer	Monolayer standard deviation	Suspension	Suspension standard deviation
PIN1L	0.332	0.090	6.743	3.828	0.593	1.272	0.282
CCNB3	0.460	0.165	2.702	2.345	0.804	1.079	0.116
CCNA1	0.493	0.113	3.905	1.901	0.426	0.937	0.043
ORC4L	0.505	0.176	2.585	2.486	0.808	1.256	0.159
CDK8	0.518	0.080	5.962	2.811	0.378	1.455	0.112
RB1	0.533	0.176	2.509	3.311	1.059	1.763	0.141
E2F6	0.540	0.234	1.977	2.385	0.930	1.287	0.244
RBL2	0.557	0.332	1.451	1.306	0.647	0.727	0.242
CCNG1	0.570	0.175	2.846	2.497	0.591	1.423	0.279
SKP1A	0.594	0.062	6.883	0.897	0.090	0.532	0.015

B

Gene	Survival Ratio	Ratio standard deviation	T Score	Monolayer	Monolayer standard deviation	Suspension	Suspension standard deviation
CDKN2C	0.609	0.069	7.079	0.704	0.059	0.428	0.032
RBL2	0.609	0.108	4.753	0.724	0.085	0.441	0.058
PLK1	0.614	0.172	2.936	0.271	0.051	0.166	0.035
TP73L	0.684	0.064	6.855	0.549	0.036	0.376	0.025
CDK9	0.705	0.152	2.979	0.382	0.042	0.270	0.050
PIN1L	0.708	0.187	2.462	0.825	0.099	0.585	0.138
TFDP1	0.725	0.252	1.793	0.505	0.063	0.366	0.119
SKP1A	0.747	0.067	4.914	0.556	0.049	0.415	0.008
CENPA	0.749	0.129	2.647	0.458	0.070	0.343	0.027
CDC27	0.752	0.202	2.128	0.537	0.009	0.403	0.108

Table 2.4. Cell cycle screening results. The top 10 siRNAs resulting in the greatest survival ratio in suspension culture of (A) TC-71 and (B) TC-32 cells are shown, sorted by increasing survival ratio. T-score denotes the Student's t significance value.

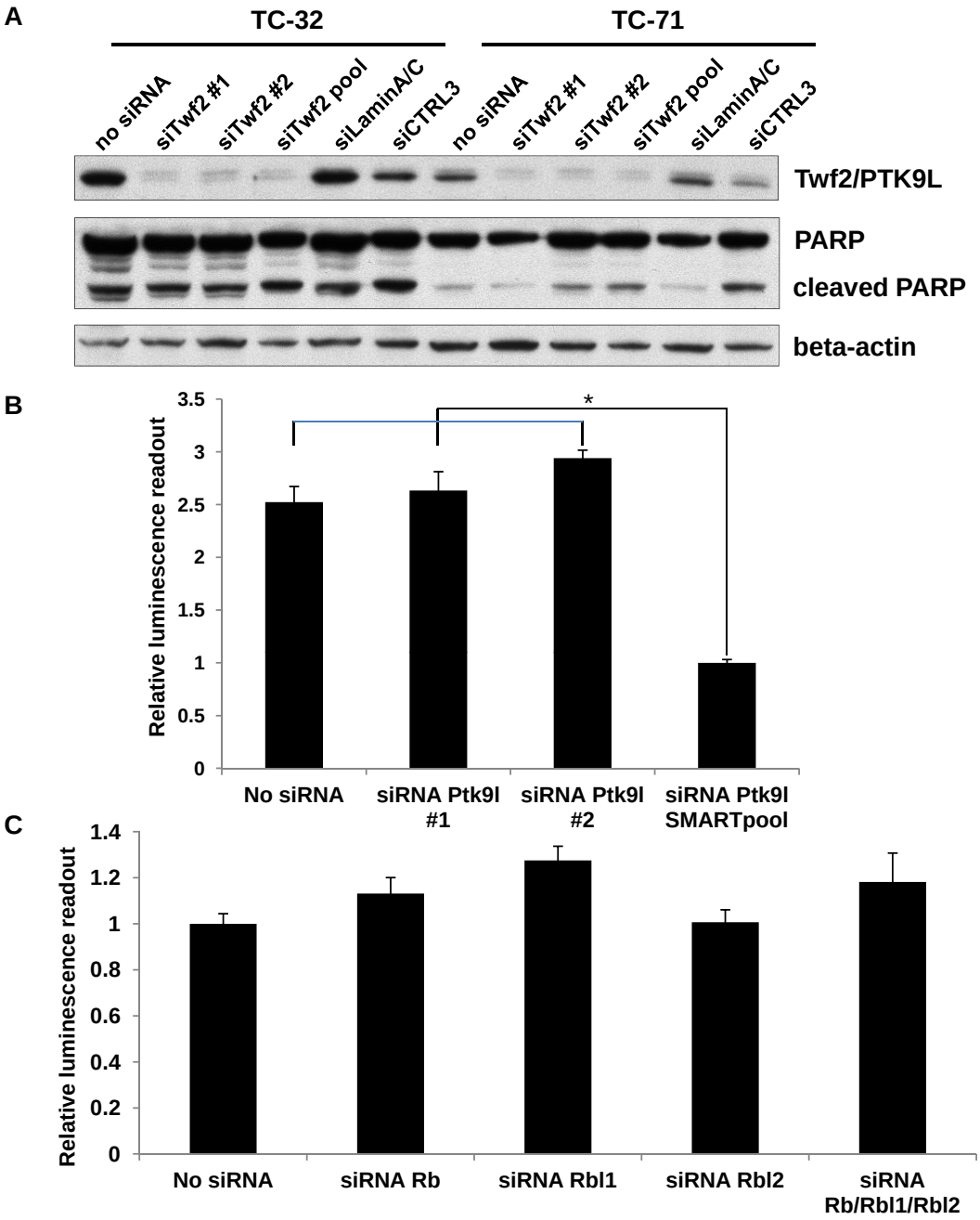

Figure 2.11. Validation studies of positive hits arising from suppression of *anoikis* screen are unable to validate screening results. (A) Western blot demonstrating Twf2/PTK9L protein levels in TC-32 and TC-71 cells following transfection with individual and SMARTpool siRNAs against *Twf2/Ptk9l*, and control siRNAs, with subsequent suspension culture for 48 hours. PARP cleavage is used to analyze levels of apoptosis. Beta-actin is used as loading control. (B and C) Validation studies in TC-71 cells using individual and SMARTpool siRNAs against *Twf2/Ptk9l* (B), or against retinoblastoma family members *Rb, Rbl1* and *Rbl2* (C), with subsequent culture in suspension conditions for 48 hours, and survival assay using the same luminescence readout assay as in the screen. The survival ratio is shown as mean ± SEM (n=3). An asterisk denotes statistical significance as determined by the Student's t-test (* $p<0.05$).

Chapter 3 GENE EXPRESSION PROFILING IDENTIFIES THIOREDOXIN-INTERACTING PROTEIN AS A NOVEL MODULATOR OF *ANOIKIS*

3.1 INTRODUCTION

Gene expression profiling remains a powerful technique for identifying novel genes and pathways functionally involved in cellular processes and disease states such as cancer. While the advent of next-generation-based modalities for investigating such processes have revolutionized our ability to identify alterations at the genomic level, gene expression profiling allows for characterization at the transcriptomic level. This is particularly useful in the analysis of rapid functional alterations that occur during fluctuating cellular conditions such as cellular stress states, where stress conditions lead to global changes in mRNA levels within minutes of onset of the stress state. From the analysis of these transcriptomic changes, one can identify specific genes that show the most prominent changes, as measured by either the fold-change of the mRNA, or the level of statistical significance. However, it is highly unusual that a single gene will be identified that plays a dominant biological role in a cellular or disease process. Alternatively, and arguably more importantly, mRNA level alterations can be analyzed at a systemic level, where changes in multiple genes, known to be altered by certain signaling pathways, can be used as a surrogate marker of activation or repression of these pathways. By identifying a role for such functionally-important pathways, a more

global understanding of the biological implications can be elucidated rather than that identified by single gene alterations alone.

While various techniques are available currently for gene expression profiling, oligonucleotide-based microarrays remain a useful modality (238). Next-generation sequencing-based transcriptome studies have recently become a feasible method for expression profiling by correlating the number of sequencing "reads" of RNA species with the expression level of the corresponding gene (239). However, this remains a cost-intensive modality, particularly when whole-transcriptome level RNA sequencing is used. As a result, when gene expression studies are required in the experimental biology setting where analysis of numerous samples is required, the cost can become prohibitive.

Prior investigations have used gene expression profiling to characterize the response to *anoikis* in normal and cancer cells, but generally have utilized it to a limited extent. Schmelzle and colleagues utilized microarray analysis to identify genes up-regulated following the detachment of anoikis-susceptible MCF-10A human breast epithelial cells, and identified up-regulation of the pro-apoptotic Bmf protein as contributing to anoikis death in these cells (153). Other studies have used expression profiling to compare non-isogenic cells, with one group identifying a number of genes showing increased expression in *anoikis*-resistant cell lines compared to *anoikis*-susceptible lines (240). Another group used a model pancreatic tumor cells to compare clones prone to perineural invasion versus clones demonstrating minimal perineural invasion, and found KIF14 and ARHGDIβ to be overexpressed and functionally important during perineural invasion (241). More

recently, a study used microarray profiling to identify genes up-regulated in cells that were able to survive prolonged cellular detachment in an otherwise *anoikis*-susceptible line, and identified various genes related to the hypoxia response, and metabolic pathways such as glycolysis and gluconeogenesis (242).

Thioredoxin-interacting protein (TXNIP) is a member of the arrestin-domain containing family of proteins, and was initially identified as an interactor with the antioxidant protein thioredoxin; through direct interaction with the redox-active site of thioredoxin, TXNIP was shown to inhibit thioredoxin activity and thus increase intracellular ROS levels (243). Elevated ROS secondary to increased TXNIP level consequently results in increased apoptosis and reduced proliferation levels. This ROS-mediated mechanism has been implicated in a number of disease phenotypes associated with dysregulated TXNIP levels, such as cardiac hypertrophy and cancer (244, 245).

In addition, a role for TXNIP in glucose homeostasis has been elucidated. Its role in metabolic regulation was first identified as the gene responsible for the hyperlipidemia and hypoglycemia phenotype in *hyplip* mice (246). A similar phenotype was demonstrated in mice with an engineered TXNIP knockout (247). Further evidence was shown in the *in vitro* setting. In response to high glucose levels, multiple cell line models have shown a rapid transcriptional up-regulation of TXNIP. Conversely, elevated TXNIP levels repress glucose uptake and increase glucose flux through the citric acid cycle, resulting in increased glucose consumption and reduced intracellular glucose levels. Ultimately, this TXNIP-mediated reduction

in cellular glucose results in reduced cell growth, and perhaps also in increased cell death in association with TXNIP-mediated elevation of ROS levels.

TXNIP has also been shown to play an important role in promoting cell death as a result of ER stress and prolonged activation of the unfolded protein response (UPR) (248, 249). TXNIP mRNA becomes rapidly stabilized following UPR-mediated activation of IRE1alpha and destabilization of miR-17 that normally targets the TXNIP transcript (249). TXNIP transcription is also up-regulated following UPR-mediated phosphorylation of PERK, which results in increased translation of the transcription factor ATF5 (248). Irremediable ER stress results in prolonged elevation of TXNIP, which then increases levels of the pro-apoptotic IL-1beta through its ability to bind and directly activate the NLRP3 inflammasome, as previously shown (250).

Most recently, TXNIP has been shown to be modulated directly downstream of energy stress through a mechanism mediated by AMP-dependent protein kinase (AMPK), a central regulator of the energy stress response pathway (251). Wu and colleagues demonstrated that under energy-rich states, TXNIP reduces glucose uptake by suppressing levels of the glucose transporter GLUT1. TXNIP directly binds and promotes the internalization of clathrin-coated pits that contain GLUT1, resulting in its degradation. Under energy stress conditions such as treatment with 2-deoxyglucose (2-DG), AMPK directly phosphorylates TXNIP on residue Ser308, resulting in rapid degradation of TXNIP in a proteasomal-dependent manner. Consequently, this allows for increased surface GLUT1 levels, and therefore increased glucose uptake levels. This suggests that TXNIP plays a role in a negative

feedback mechanism that helps restore cellular energy conditions during starvation conditions.

Here, we investigated the expression profile response of Ewing sarcoma cells, oncogenically-transformed and non-transformed NIH3T3 cells, subjected to cellular detachment, and show that the expression response mimics that of various cellular stress response pathways. We also identify TXNIP as a significant response gene. Previously, we have shown that the highly metastatic Ewing sarcoma cells utilize a number of mechanisms to suppress anoikis, including activation of pro-survival kinases such as ErbB4, but little more is known about the more broad mechanisms regulating anoikis in these cells. We demonstrate that TXNIP is highly and rapidly up-regulated following cellular detachment, and this is seen in association with a change in expression profile reflective of ER stress and activation of the UPR. We also show that the highly-related arrestin domain-containing genes ARRDC3 and ARRDC4 are also rapidly up-regulated. We further demonstrate that knockdown of TXNIP up-regulation is associated with increase cell survival, consistent with the pro-apoptotic role for TXNIP in other stress types such as ER stress. Overall, we show evidence that TXNIP promotes anoikis-related cell death.

3.2 MATERIALS AND METHODS

Cell culture and DNA transfection. Early passage NIH3T3 and HeLa were obtained from ATCC (Rockville, MD). *IGF1R-/-* MEFs (R-) and *IGF1R-/-* MEFs re-expressing IGF1-R (R+) were kindly provided by Renato Baserga (Kimmel Cancer Centre, Philadelphia, PA). Ewing sarcoma cell lines TC-32 and TC-71 were obtained as previously described (231) and maintained in RPMI 1640 media supplemented

with 10% fetal bovine serum. Retroviral expression vectors pMSCVpuro-ETV6-NTRK3 and pMSCVpuro-ETV6-NTRK3myr were used for generation of stable cell lines as previously described (117). The pMSCVpuro-K-Ras(V12) vector was constructed by subcloning the BamHI-SalI fragment from the pBabe-puro-K-Ras(V12) vector obtained from Addgene (courtesy of William Hahn) containing the K-Ras(V12) open reading frame into the BglII-XhoI sites of pMSCVpuro. The pMSCVneo-DN-AMPK vector was constructed by subcloning the EcoRI fragment from pBabe-GFP-DN AMPK (gift from Nissim Hay) into the pMSCVneo vector. Infections of the NIH3T3 cells and MEFs were performed using retrovirus generated following introduction of the retroviral vectors into PhoenixA cells. For suspension cultures, cells at subconfluence were detached by trypsinization and diluted to a concentration of 250,000 cells/mL, plated on polyHEMA-coated 10cm dishes or 6-/12-well plates and incubated for the indicated timecourses. Chemical inhibitors were added to suspension cultures immediately following detachment and plating onto polyHEMA-coated plates to determine their effects on the early stages of the *anoikis* response.

Antibodies and chemicals. The anti-TXNIP antibody was purchased from MBL International (Woburn, MA). Anti-BiP/GRP78, anti-p27/KIP1 and anti-Grb2 antibodies were obtained from BD Biosciences (San Jose, CA). Anti-phospho-eIF2alpha, anti-cyclin D1, anti-cyclin E1, anti-cleaved caspase-3, anti-p-Akt (S473) and anti-Akt were purchased from Cell Signaling (Danvers, MA). Anti-cyclin E was purchased from Upstate (Millipore, Billerica, MA). Anti-beta-actin antibody was

purchased from Santa Cruz Biotechnologies (Santa Cruz, CA). Thapsigargin, tunicamycin, MG132 and H_2O_2 were obtained from Sigma Aldrich (St. Louis, MO).

siRNA and RNA transfection. All siRNAs were obtained from Dharmacon, Thermo Fisher Scientific (Pittsburgh, PA) against human and mouse targets, with the ON-TARGETplus modification. Control siRNAs used were siCNTRL2 and siCNTRL3 (scrambled controls) and siLaminA/C. Individual siRNAs against human and mouse TXNIP, ARRDC3 and ARRDC4 were obtained as a SMARTpools and sets of four individual siRNAs. Transfection was performed using the Dharmafect 3 reagent (Thermo Fisher Scientific), with siRNA delivered at a concentration of 25 nM.

Gene expression profiling. Biotin-labeled cRNA was prepared from total RNA and hybridized to Affymetrix GeneChip Mouse 430A Expression Arrays according to the manufacturer's protocol (Affymetrix Inc, Santa Clara, CA). Array data was normalized using the Robust Multi-Array Average module in the Genetrix software package (Epicenter Software; Pasadena, CA), which was used for subsequent gene expression analysis. The normalized expression values were log transformed and genes were selected as differentially expressed based on at least 2-fold mean difference in expression between monolayer (R+EN/R-EN/R-ENmyr) and suspension (SPHR+EN/SPHR-EN/SPHR-ENmyr) groups, each cultured in their respective conditions for 24h, and t-tests were used to determine significance ($p<0.05$). Functional annotation was performed using the DAVID online tool for overrepresentation analysis of functional gene categories and Gene Ontology terms. Gene Set Enrichment Analysis between the monolayer and suspension phenotypes

was performed as previously described (252), using the Broad Institute software (v. 2.07), with the analysis performed using permutations of gene sets (1000) and Signal2Noise metric for ranking of genes.

For the exon-level microarray analysis using the Affymetrix Exon 1.0 ST platform, total RNA was isolated using the TRIzol reagent (Life Technologies, Grand Island, NY). Biotin-labeled cRNA was prepared from total RNA was hybridized to Human Exon 1.0 ST (HuEx 1.0) GeneChips (Affymetrix, Santa Clara, CA) following manufacturer's recommendations. Human Exon GeneChips profile coding and non-coding regions of the transcriptome using approximately 1.4 million probe selection regions (PSRs) were analyzed, but only coding core PSRs were used in the analysis (corresponding to exonic regions). Array data was normalized using the Robust Multi-Array Average module in the Genetrix software package (Epicenter Software; Pasadena, CA). All statistical analyses were performed with the Genetrix software.

Caspase-3 activity assay. Cells were lysed in caspase-3 lysis buffer (10mM HEPES pH 7.5, 50mM NaCl, 2mM $MgCl_2$, 5mM EGTA, 0.2% CHAPS), and assayed for protein concentration using the D_C protein assay (BioRad). Lysates were mixed at a 1:1 ratio with caspase-3 reaction buffer (40mM PIPES pH 7.2, 200mM NaCl, 20% sucrose, 0.2% CHAPS, 20mM DTT), caspase-3 substrate was added to a concentration of 0.5μM (Caspase-3 Substrate IX fluorogenic, Calbiochem), and incubated for 1 hour at 37^{o}C. Fluorescence intensity was measured and normalized to protein concentration.

Reverse transcriptase PCR. Total RNA was obtained from cell culture timepoints using the TRIzol reagent. For semi-quantitative RT-PCR analysis, RNA

samples were reverse transcribed using random hexamer primers, and the resulting cDNA was amplified by PCR in the linear range for each transcript (25 cycles) using Taq polymerase (Invitrogen). Quantitative RT-PCR was performed in the iCycler real time PCR machine (BioRad) using the SYBR green/fluorescein PCR Master Mix (SuperArray). All values were normalized to an endogenous human beta-actin. Relative mRNA expression was calculated using the comparative ΔΔCt method.

3.3 RESULTS

Transformed fibroblasts activate multiple stress responses during detachment-induced stress. To model *anoikis* suppression we used NIH3T3 and MEF cell lines stably expressing the oncogenes ETV6-NTRK3 (EN) and K-Ras(V12), each previously shown to suppress *anoikis* (73, 117). We have previously generated expression profile datasets of NIH3T3 cells cultured in suspension (detached) versus monolayer cultures for 24 hours each, and performed microarray analysis using the Affymetrix MOE430 platform. We then also performed gene expression profiling to compare suspension cultures of EN-transformed MEFs versus corresponding monolayer cultures, using the same microarray platform. Three cell line models were used to avoid cell line-specific effects, including R- cells expressing ENmyr and R+ cells expressing either EN or ENmyr. As mentioned, EN cannot transform R- cells unless IGF1R is re-expressed, while ENmyr transforms R- or R+ cells and suppresses *anoikis* in both (117). Principal component analysis of the resulting gene expression profiles (GEPs) demonstrated detachment as a major source of variation in gene expression (Figures 3.1A). Contribution of either cell line type or specific EN construct did not feature prominently in any of the first three

principal components (Figure 3.1A). A large number of genes were differentially expressed in suspension versus monolayer cultures (Figure 3.1B). Overall, we detected more differentially expressed genes with higher fold-change in suspension ('up-regulated') than in monolayer cultures ('down-regulated'). When the three different cell lines were analyzed individually, there was considerable overlap in up-regulated genes for each cell line in suspension, with a core of 212 probesets (corresponding to 170 genes) that were significantly up-regulated >2-fold in all three cell lines (Figure 3.1C & Table A1.1; equivalently >2-fold down-regulated genes in Table A1.2).

Gene ontology (GO) over-representation analysis of these 170 genes showed significant enrichment for functional categories relating to cell death (Figure 3.1D). In addition, there was enrichment for diverse categories relating to cellular stress; for example, under the GO category of "response to stress", many up-regulated genes were prototypical stress response genes such as *Gadd45a*, *Bnip3*, *Cdkn1* and *Ddit3.* Importantly, several enriched categories were specifically related to negative regulation of cellular processes such as "gene expression" and "metabolic process." We therefore hypothesized that detachment of transformed cells triggers a significant stress response associated with attenuation of bioenergetically-rich processes. To better characterize the observed stress responses, we used a publicly-available dataset of annotated microarray experiments ("Chemical and Genetic Perturbations" dataset, Broad Institute) to analyze detachment-induced GEPs of EN-transformed cells by Gene Set Enrichment Analysis (GSEA). Amongst the most significantly enriched gene sets in detached cells were signatures previously linked

to stress conditions such as hypoxia, nutrient and amino acid deprivation, and epithelial-to-mesenchymal transition (Table A1.3 and A1.4). Similar specific stress categories were observed amongst down-regulated genes (e.g. see "peng_leucine_up" versus "peng_leucine_dn"; and "manalo_hypoxia_up" versus "manalo_hypoxia_dn"). Overall, the transcriptional profiles observed following detachment mimic diverse forms of cellular stress, suggesting that detachment induces multiple stress responses.

To further establish a role for stress response pathways following cellular detachment, we generated our own expression profile datasets to represent various prototypical stress responses. Using HEK293 cells, we subjected subconfluent monolayer cultures of these cells to 1.5 hour period of various stresses, including ER stress (treatment with 5 uM thapsigargin), nutrient starvation (change of cell culture media to HBSS-HEPES buffer only), hypoxia (culture in 1% O2) and irradiation (treatment of cells with gamma-irradiation). RNA from these cells were analyzed using the Affymetrix Human Exon 1.0 microarray platform, and this was compared to RNA from control HEK293 cells lines grown in control 10% serum culture conditions. For each stress type, a list of approximately 100 up-regulated genes was generated, using a >1.5-fold increase and $p<0.01$ cutoff parameter (Figure 3.2A). GSEA using these datasets was applied to the expression profiles of EN-transformed NIH3T3 cells subjected to suspension versus monolayer culture conditions. Interestingly, genes up-regulated following detachment were highly enriched in genes found to be up-regulated in each of the comparator stress response types (Figure 3.2B). Again, genes well-known in the literature to be

associated with these stress types were found in the up-regulated gene sets, such as the ER stress-related genes *Gadd45a*, *Xbp1* and *Edem1* (Figure 3.2C) and nutrient starvation-related genes *Paip2* and *Gla* (Figure 3.2D). Overall, these data demonstrate that cellular detachment alters the gene expression profile in a manner resembling a multi-faceted stress response.

***Anoikis*-resistant Ewing sarcoma cells demonstrate rapid and sustained changes in expression profile in response to cellular detachment.** To investigate *anoikis* resistance in a more clinically-relevant model, we performed expression profiling on Ewing sarcoma cells that we have previously demonstrated to show robust *anoikis* resistance. Using two different Ewing sarcoma cell lines, TC-32 and TC-71, we have previously generated expression profile data of suspension versus monolayer cultures of these cell lines grown for 24 hours, and analyzed using the Affymetrix human U133B platform. We subsequently performed a more extensive experiment, where we cultured the cells as either monolayer and suspension cultures under various conditions, including normal serum conditions (10% FBS) and low serum conditions (1% FBS), for various timepoints (1 hour, 6 hours, 24 hours), for a total of 24 culture conditions. These samples were subjected to analysis using the Affymetrix Human Exon 1.0 array. Principal component analysis demonstrated that the suspension versus monolayer condition was the first (dominant) principal component compared to the other conditions, with the cell line type representing the second principal component (Figure 3.3A). Surprisingly, when we analyzed different culture conditions in isolation for differentially-expressed genes, neither serum percentage or timepoint of culturing significantly altered the

differentially expressed genes. In fact, a very large set of genes showed significant up-regulation even at 1 hour following detachment, and showed sustained up-regulation at 6 and 24 hours (Figure 3.3E). Even the two cell line types, despite the significant differences in gene expression between the two cell lines when analyzed in isolation, show significant overlap in the genes up-regulated in suspension conditions (Figure 3.3B).

Due to the significant overlap in genes up-regulated following cellular detachment under various conditions, we were able to isolate a set of 1531 genes that showed at least 2-fold up-regulation in suspension versus monolayer conditions, regardless of cell line type, serum conditions and timepoint. Using this 1531 set of genes as a whole, we utilized GSEA in comparison with the gene lists of HEK293 cells under various stress conditions, and we again demonstrated that this gene set showed significantly enrichment for a broad range of stress-related genes (Figure 3.4A). Prototypical genes again showed differential expression, including ER stress-related genes *Edem1* and *Dnajb9,* hypoxia-related genes *Hif1a* and *Bnip3*, starvation-related genes *Paip2* and *Hace1*, and DNA damage-related genes *Mdm2* and *Rb1.*

In addition, by clustering analysis of this set of genes, we showed a subset of genes that demonstrated particularly prominent differences in gene expression (Figure 3.5A). In particular, when the set of 103 genes showing 5-fold regulation in at least one of the timepoints was analyzed, this set clustered into 3 smaller subsets. We designated these sets as either showing an early response (>5-fold up-regulation at either 1 or 6 hours, with reduced up-regulation at 24 hours), late

response (>5-fold up-regulation at 6 or 24 hours but not at 1 hour), or fixed response (>5-fold up-regulation at all time points). Interestingly, the small subset of late response genes showed certain genes suggestive of the hypoxia and ER stress response, including *Pdk1* and *Ddit3* (Figure 3.5B), while the fixed response gene set showed up-regulation of genes not typically associated with any classic stress response (Figure 3.5C). The large set of early response genes showed no specific association with a cellular stress response type, but was overrepresented for cell cycle-related genes. When we further investigated a role for ER stress in the response to cellular detachment, we were able to biochemically validate that the various arms of the ER stress pathway were activated following detachment, including phosphorylation of eIF2-alpha and elevation of BiP (Figure 3.4B). Highly elevated transcript levels of *Ddit3/Chop* and *Atf6* in suspension also supported a role for ER stress (Figure 3.4C).

TXNIP and related arrestin domain-containing family members show rapid and sustained up-regulation following cellular detachment in multiple cell line models, in association with cell cycle inhibition. In the analysis for a candidate outlier gene showing consistent up-regulation following detachment, we compared the expression profile between multiple experimental datasets. Using our expression profile data from NIH3T3 cells and EN-transformed MEFs analyzed using the Affymetrix MOE430 platform, and Ewing sarcoma cells analyzed using the U133B platform, and comparing genes found to be up-regulated at least 3-fold in suspension versus monolayer cultures ($p<0.05$), we identified a single gene, thioredoxin-interacting protein (*TXNIP*) to be commonly up-regulated in all three

cell lines (Figure 3.6A). We were also able to identify *Txnip* as highly up-regulated in the expression profile data of Ewing sarcoma cells analyzed using the Affymetrix Human Exon 1.0 microarray, showing a "fixed-response" pattern with 3.5-fold up-regulation by 1 hour in suspension versus monolayer cultures, and sustained elevation at 6 and 24 hours (Figure 3.6C). Therefore, *Txnip* is prominently up-regulated in response to cellular detachment in multiple cell types.

Two proteins demonstrating the greatest homology with TXNIP are arrestin domain-containing protein 3 (ARRDC3) and arrest domain-containing protein 4 (ARRDC4) (253). When we analyzed the levels of transcripts for *Arrdc3* and *Arrdc4,* we also found consistent up-regulation of these genes following cellular detachment in multiple cell types, whenever probes for these genes were present on the microarray platform (Figure 3.6B). In the Ewing sarcoma cells analyzed with the Human Exon 1.0 array, we found a very significant 9-fold elevation of *Arrdc3*, while probes for exons of *Arrdc4* showed an approximate 2-fold elevation (Figure 3.6B). We confirmed the elevation of *Txnip* and *Arrdc3* by RT-PCR in the TC-32 cell line, showing fluctuating but consistent elevation of both transcripts in suspension versus monolayer cultures across various timepoints (Figure 3.6D).

Biochemically, we were also able to demonstrate pronounced up-regulation of TXNIP across timepoints in both TC-32 and TC-71 cells in suspension versus monolayer conditions (Figure 3.7A). Interestingly, as it is known that TXNIP regulates p27/KIP1 (254), we analyzed various cell cycle markers at multiple timepoints in relation to TXNIP levels. We showed that in conjunction with elevated TXNIP levels, there is evidence of cell cycle suppression, with elevation of p27/KIP1,

and reduced levels of the cell cycle promoter cyclin D1. We were able to reproduce these findings in other transformed cell line models, including EN-transformed NIH3T3 cells, and HeLa cervical adenocarcinoma cells (Figure 3.7B). Overall, these findings show rapid and sustained up-regulation of TXNIP and related arrestin domain-containing proteins in response to cellular detachment.

When we reanalyzed the gene sets of cellular stress response pathways, we found that *Txnip* and *Arrdc3* were most prominently up-regulated in the ER stress response. In support of this, we demonstrated that TXNIP is also up-regulated in response to typical triggers of ER stress, including treatment with thapsigargin and tunicamycin, in both non-transformed and ER-transformed NIH3T3 cells (Figure 3.7C). This again was associated with reduced levels of cyclin D1, but surprisingly was not associated with increased levels of p27/KIP1. Importantly, we did not observe elevation of TXNIP in the manner of a general stress response protein, as we did not see changes in TXNIP levels following proteasomal stress through MG132 treatment, or oxidative stress through H2O2 treatment (Figure 3.7D). Therefore, the observed up-regulation of TXNIP may be due to the activation of the ER stress response pathway following cellular detachment.

We then investigated the effect of TXNIP loss-of-function. Using TC-71 cells, we compared the effects of siRNA knockdown of TXNIP versus no siRNA and control siRNA. In these cells, TXNIP knockdown did not show a significant effect on apoptotic cell death as measured by PARP cleavage and caspase-3 activity assay (Figure 3.8A and B). However, we did show an association with reduced p27/KIP1 levels, as predicted by previous literature (254) (Figure 3.8A). These data therefore

suggest that TXNIP levels do not significantly affect *anoikis*-related cell death in Ewing sarcoma cells. In addition, the data also suggests that TXNIP-mediated alterations in p27/KIP1 levels, and potentially alterations in cell cycle status, are not linked with survival under detachment conditions.

We then investigated the role of TXNIP in NIH3T3 cells. In particular, we were interested in the relative role of TXNIP knockdown in transformed versus non-transformed cells, particularly due to the possibility that TXNIP may have a role in promoting rather than suppressing *anoikis*, in line with the pro-apoptotic role of TXNIP in ER stress (248, 249). Using NIH3T3 cells transformed with ETV6-NTRK3 versus MSCV vector control, we analyzed the effects of TXNIP knockdown on *anoikis*-related death. Consistent with the role in ER stress, we showed that non-transformed NIH3T3 cells show significantly reduced cell death with TXNIP knockdown as compared to an siRNA control, as measured by levels of cleaved caspase-3 by Western blot (Figure 3.9A). Interestingly, we also showed that knockdown of the related ARRDC3 and ARRDC4 was not associated with the same degree of reduction in cell death. When all three proteins were simultaneously knocked-down, the reduction in cell death was similar to that seen with TXNIP knockdown alone, supporting a more dominant role of TXNIP versus the other arrestin domain-containing proteins in regulating this cell death. In ETV6-NTRK3-transformed cells, cleaved caspase-3 levels were lower in siRNA control-transfected cells as compared to siRNA control, confirming the suppression of *anoikis* associated with transformation. Interestingly, while a similar reduction in cell death was seen with TXNIP knockdown, the proportional decrease in cell death was lesser in

transformed cells compared to non-transformed cells. Similar trends were seen with ARRDC3, ARRDC4 and combined TXNIP/ARRDC3/ARRDC4 knockdown. In support of these Western blot results, a fluorogenic caspase-3 activity assay also showed a similar trend in relative cell death in these knockdown conditions (Figure 3.9B). In summary, these data suggest that TXNIP may in fact promote *anoikis*-related cell death. In addition, these data suggest that within the arrestin domain-containing family of proteins, TXNIP specifically appears to play a role in *anoikis*, despite similar up-regulation of related members ARRDC3 and ARRDC4.

3.4 DISCUSSION

In this chapter, we demonstrated that cellular detachment induces changes in gene expression profile reminiscent of a broad cellular stress response. We showed similar findings in multiple transformed cell line models, and demonstrated that the transcriptional response is rapid and sustained, with up-regulation of numerous genes within 1 hour of cellular detachment. We also showed that the profile of the up-regulated genes is broad, but demonstrated a strong enrichment for many genes associated with numerous prototypical stress responses. In particular, genes related to the ER stress response were found as an early response, while hypoxia-related genes were seen in the late response. We also identified TXNIP and other highly homologous members of the arrestin domain-containing protein family to be consistently up-regulated in response to cellular detachment. Consistent with previous literature in other stress types such as ER stress, we showed that TXNIP knockdown in fact appears to promote cell death under detachment conditions,

since knockdown of TXNIP, unlike knockdown of the related ARRDC3 and ARRDC4, was associated with reduced *anoikis*-related cell death.

As previously described, the role of various individual cellular stress responses in *anoikis* has recently been described by a number of groups. However, it has not been well-recognized that cellular detachment results in such a rapid and diverse switch in the transcriptional profile, appearing to simultaneously activate multiple stress response pathways. Previous expression profile studies have focused on identifying single gene candidates rather than analyzing the data in a broader manner using techniques such as GSEA, and therefore concentrated their follow-up studies on outlier genes (153, 240). As such, our study appears to be one of the first descriptions in the literature correlating cellular detachment to activation of a broad transcriptional program mimicking various stress response types. However, it remains unclear whether such stress responses help to promote or suppress *anoikis*, although we would hypothesize that their function would be to mitigate stress to promote survival following detachment. However, it is clear that certain stress responses, best illustrated by the ER stress response, can have a pro-death role if they become hyperactivated or unchecked (255).

In support of literature data showing a role for ER stress in *anoikis,* we also showed that multiple branches of the ER stress response are activated following cellular detachment, including phosphorylation of eIF2alpha by PERK, and up-regulation of BiP downstream of IRE1alpha. Interestingly, we also identify TXNIP as rapidly up-regulated in response to both cellular detachment as well as more typical pharmacologic triggers of ER stress. Recently, TXNIP has been shown to be rapidly

induced as a result of ER stress-induced hyperactivation of IRE1alpha, which reduces levels of miR-17 that normally suppresses levels of *Txnip* mRNA (248, 249). TXNIP consequently promotes apoptotic cell death in these cells by activating the NLRP3 inflammasome and resulting in downstream production and secretion of the pro-apoptotic interleukin IL-1beta. Therefore, while such rapid up-regulation following detachment of transformed cells was suggestive of an *anoikis* suppressive role for TXNIP, this literature data suggests that TXNIP may in fact be a promoter of *anoikis*. Therefore, we believe future studies into the role of TXNIP in modulating *anoikis* in non-transformed cells is warranted, with the hypothesis that TXNIP promotes *anoikis* downstream of ER stress activation, while transformed cells are capable of resisting *anoikis* despite such up-regulation of TXNIP.

Another recent literature report raises the possibility of a role for TXNIP in *anoikis*. Wu, Cantley and colleagues demonstrated that TXNIP binds to the glucose transporter GLUT1 and promotes its degradation by inducing its internalization through clathrin-coated pits (251), leading to reduced glucose uptake. Such a mechanism may help explain the phenomenon described by Schafer and colleagues where cellular detachment triggers a reduction in cellular ATP levels due to suppressed glucose uptake (216). Detachment-induced ER stress and subsequent up-regulation of TXNIP may therefore help explain this reduced glucose uptake. Other studies have demonstrated reduced glucose uptake associated with reduced cell surface GLUT1 levels following tunicamycin-induced ER stress in non-transformed cells, and this suppressed GLUT1 levels is rescued by constitutive activation of Akt (24). Therefore, TXNIP may again help to promote *anoikis* through

its ability to suppress GLUT1-mediated glucose uptake, thus promoting energy stress in the cells. Furthermore, oncogene-mediated hyperactivation of Akt may help counteract this energy stress by restoring glucose uptake in an Akt-dependent manner.

Moreover, a very recent report has shown a prominent role for TXNIP during oxidative stress (256). ROS levels were found to be significantly elevated in the hematopoietic stem and progenitor cell pool of TXNIP knockout versus wild type mice, associated with reduced a hematopoietic cell population. Therefore, TXNIP was found to be associated with increased survival under oxidative stress. This group also described a novel mechanism whereby TXNIP promotes the stability and function of p53 by directly interacting with p53 and interfering with the ability of the E3 ligase MDM2 to destabilize p53. They propose that, in the absence of TXNIP, there is reduced p53 transcriptional activity, which is normally has a pro-antioxidant effect. Overall, while TXNIP may promote levels of ROS through its inhibitory action on thioredoxin, it appears to also promote levels of compensatory antioxidant activity through p53. Therefore, since cellular detachment appears to result in elevated ROS levels based on various studies, these recent literature data demonstrate both a pro- and anti-survival effect of TXNIP.

In summary, we show that cellular detachment induces a broad switch in gene expression that mimics various types of cellular stress response pathways, and particularly shows resemblance to the ER stress response. We also demonstrate that TXNIP, a known ER stress response gene, is a rapid response gene that is highly up-regulated following cellular detachment. We show that TXNIP levels are positively

associated with p27/KIP1 levels, a known suppressor of *anoikis* through its ability to suppress proliferation, although this is not directly associated with differences in detachment-induced cell death in Ewing sarcoma cells. Rather, we demonstrate that in the NIH3T3 cell line model, TXNIP levels are positively associated with *anoikis*-related cell death, in both transformed and non-transformed cells, consistent with the pro-death role of TXNIP in other stress types. Our data raise a possible role for TXNIP as a promoter of the *anoikis* process, potentially through its recognized ability to suppress glucose uptake through reduction of GLUT1 levels, a known proximal metabolic alteration following cellular detachment.

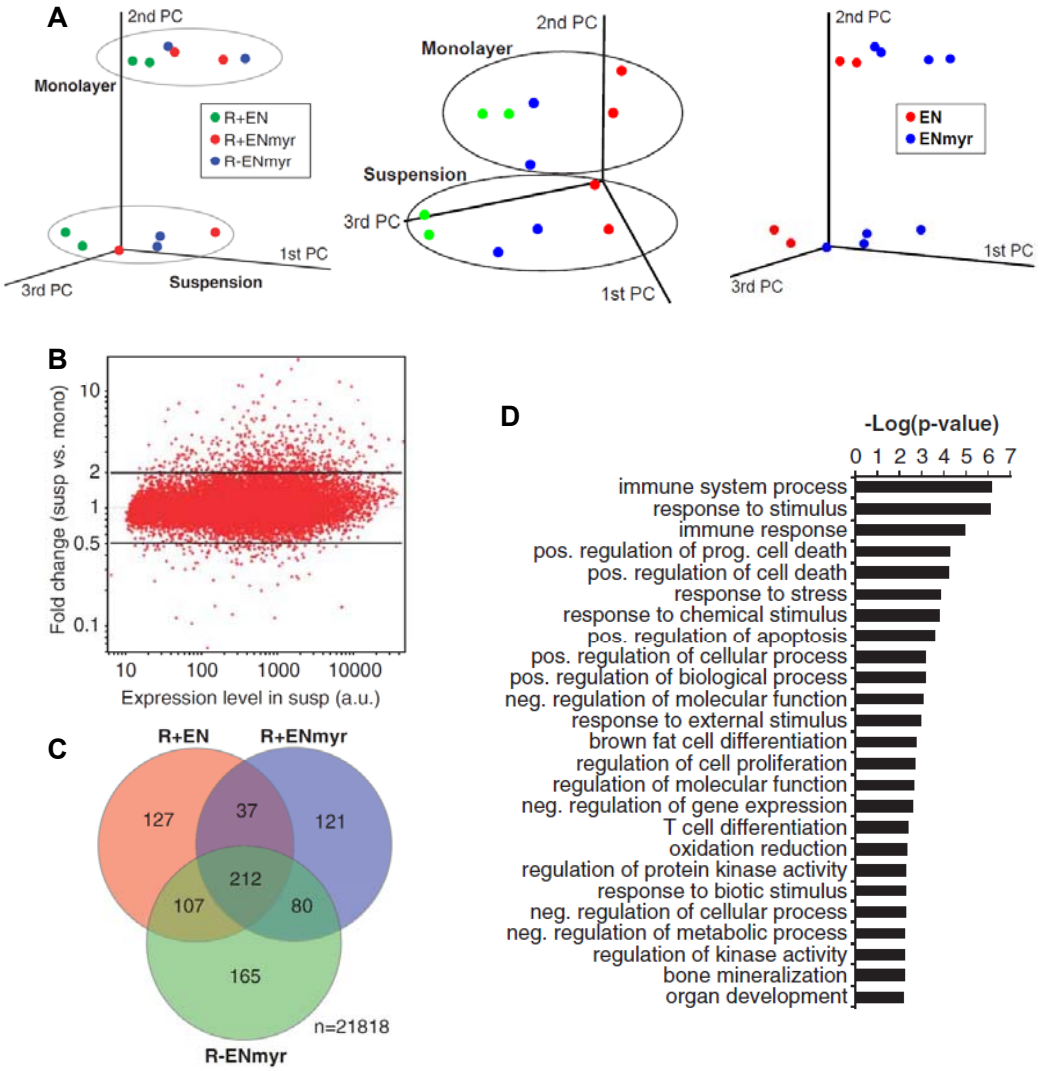

Figure 3.1. Cellular detachment induces a multi-faceted transcriptional pattern resembling other bioenergetic stress responses. (A) Principal component analysis depicting global differences in gene expression profile of the indicated ETV6-NTRK3 (EN) transformed MEF cell lines, with samples grouped as either monolayer or suspension. (B) Scatterplot summarizing the expression fold-changes of individual genes in all three EN-transformed cell lines grown in suspension (susp) versus monolayer (mono) cultures (C) Venn diagram depicting the overlap of up-regulated genes in suspension for the indicated EN-transformed cell lines used in the microarray analysis of Fig. 3.1B. (D) Gene ontology (GO) analysis of over-represented categories in the genes commonly up-regulated following cellular detachment in all three EN-transformed cell lines (Table A1), for all biological process categories with FDR<0.10.

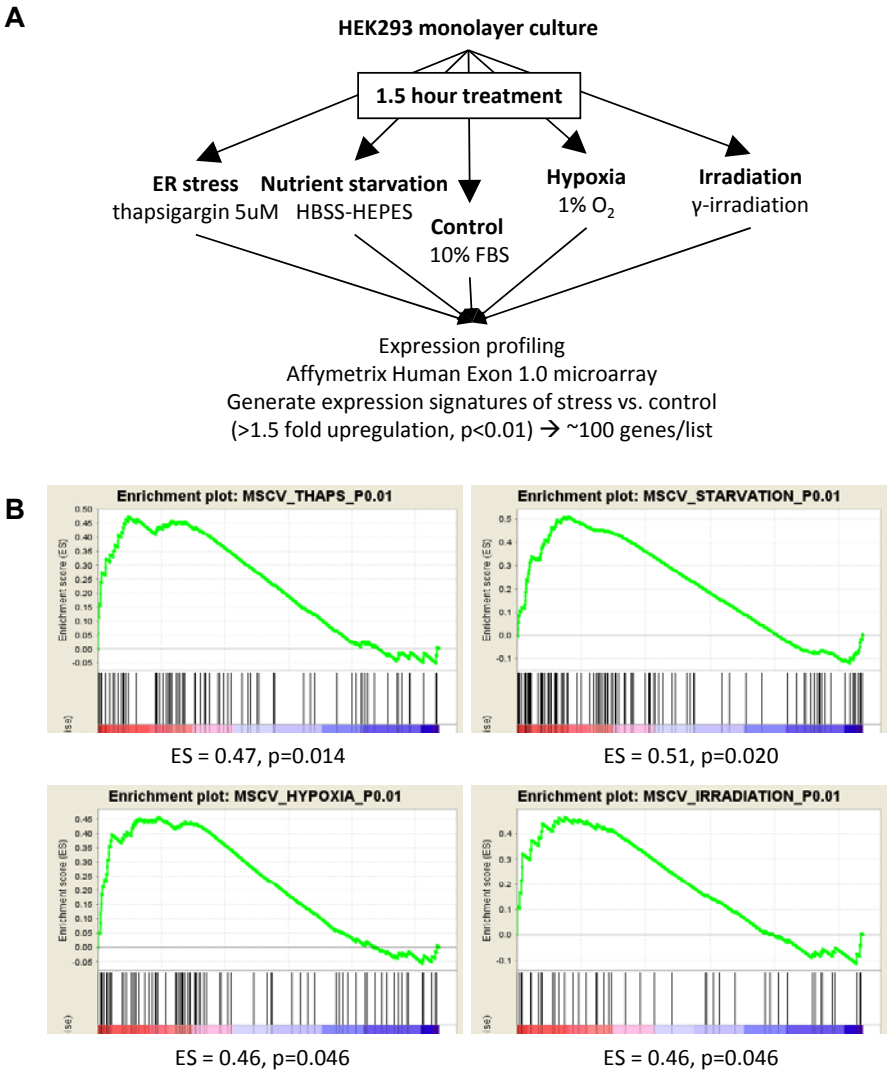

Figure 3.2. Genes up-regulated following cellular detachment shows significant enrichment with genes up-regulated during other prototypical cellular stress responses. (A) Expression profile datasets generated using HEK293 cell lines subjected to prototypical cellular stress types, resulting in a gene list of approximately 100 genes for each stress type. (B) Gene Set Enrichment Analysis (GSEA) of expression profiles of ETV6-NTRK3-transformed NIH/3T3 cells in suspension versus monolayer conditions, analyzed against the expression profiles generated as described in Figure 3.2A. ES denotes the Enrichment Score, while the p-value denotes the significance of the ES.

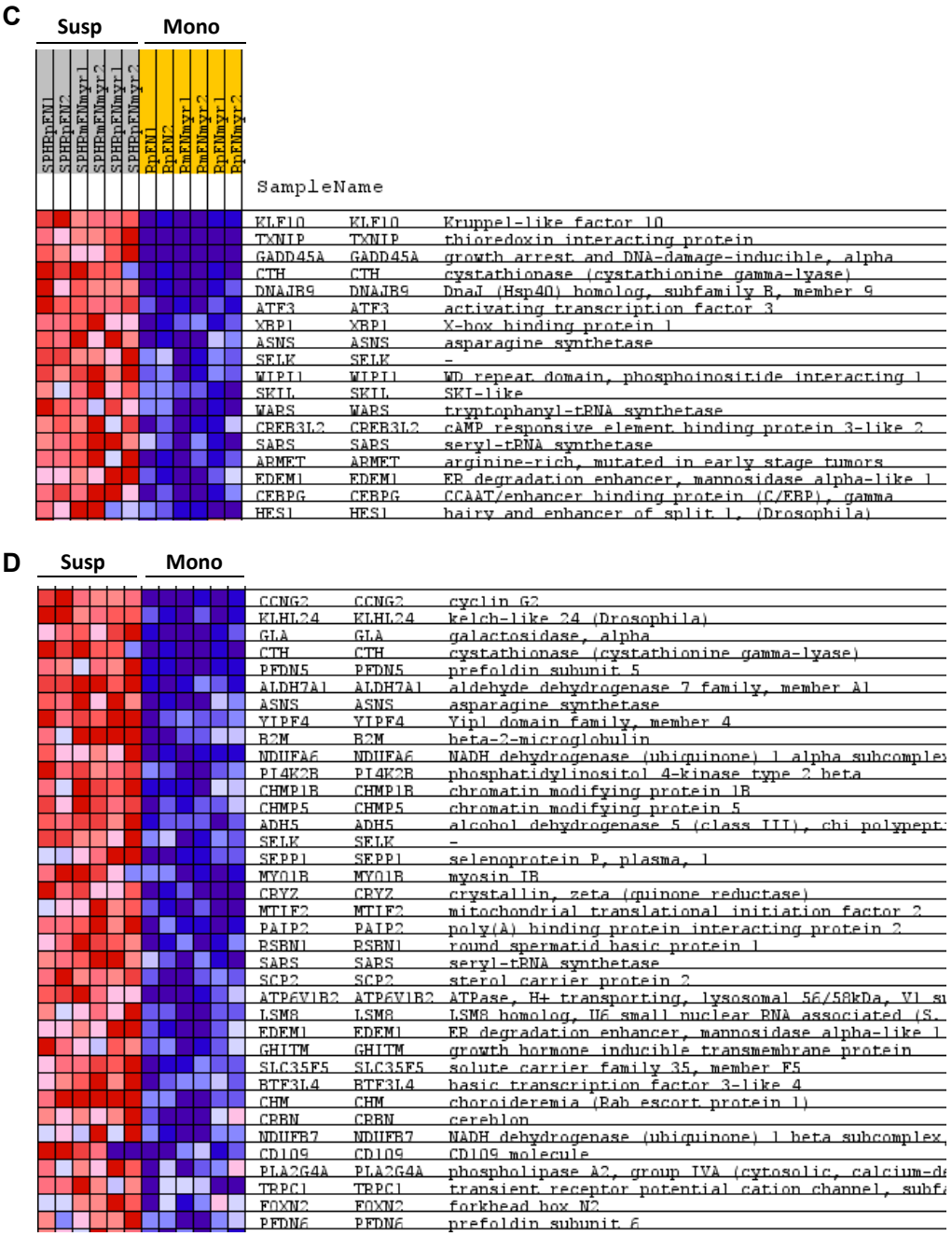

Figure 3.2 (cont'd). Genes related to (C) ER stress and (D) nutrient starvation are up-regulated following cellular detachment. Heat maps and gene lists of stress-related genes, comparing suspension cultures of EN-transformed fibroblasts (SPH=spheroid/suspension culture, RpEN=R+EN, RmENmyr=R-ENmyr, RpENmyr=R+ENmyr) with monolayer cultures. Red represents elevated expression, blue represents suppressed expression.

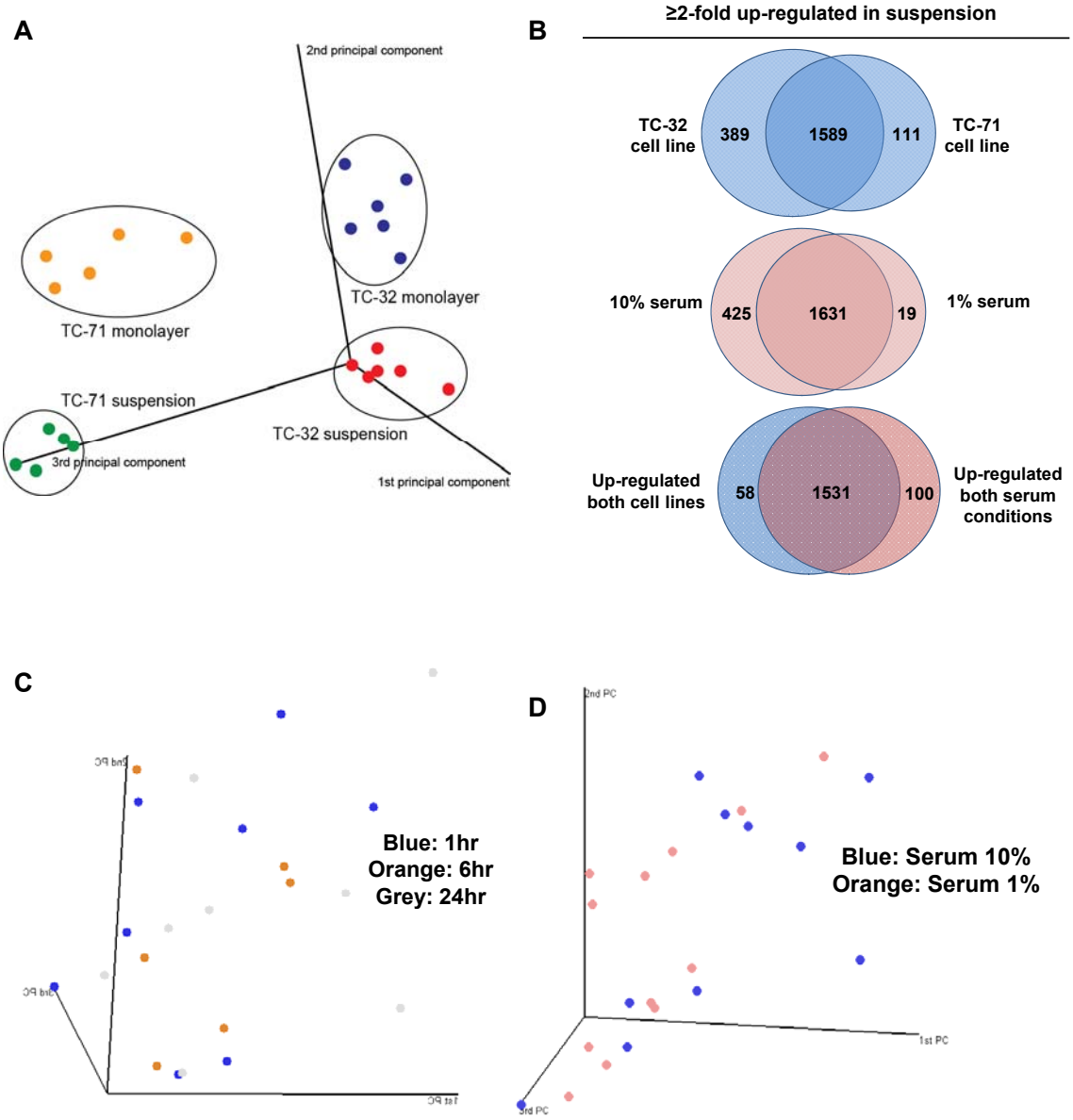

Figure 3.3 Cellular detachment in Ewing sarcoma cell lines induces a rapid and sustained change in gene expression profile. (A) Principal component analysis of the expression profile results, grouped by suspension versus monolayer condition and cell line type. (B) Venn diagram of gene numbers up-regulated ≥2-fold in suspension versus monolayer conditions, grouped by cell line type or serum conditions. (C) Principal component analysis of expression profile results grouped by timepoint or (D) serum conditions.

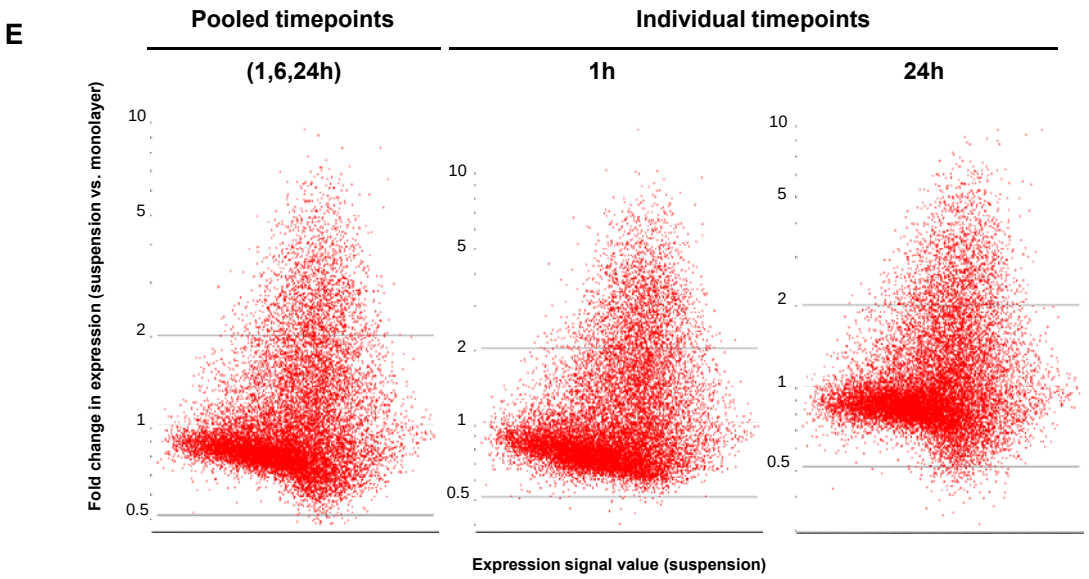

Figure 3.3 Cellular detachment in Ewing sarcoma cell lines induces a rapid and sustained change in gene expression profile (cont'd). (E) Dot plots comparing fold-change differences in expression of genes in suspension versus monolayer, versus arbitrary expression levels in suspension culture. Plots are either for individual timepoints (1h, 24h) following cellular detachment, or for averaged/pooled expression across all timepoints.

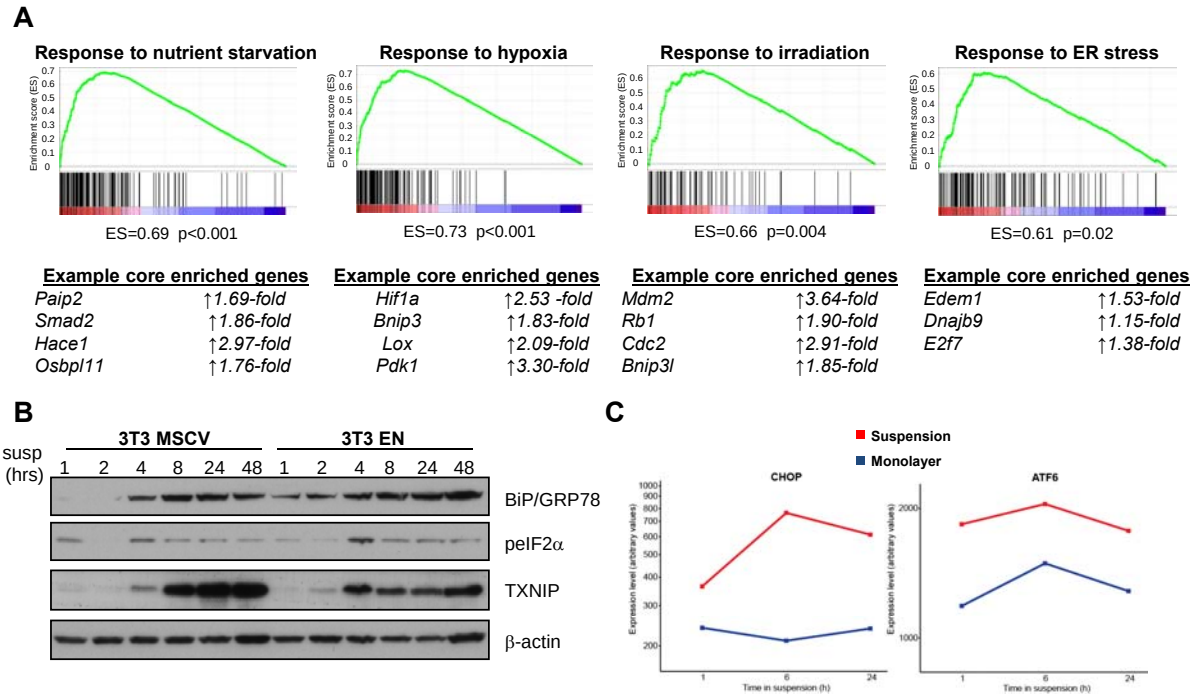

Figure 3.4. Cellular detachment in Ewing sarcoma cells trigger multiple stress response pathways. (A) Gene Set Enrichment Analysis (GSEA) of expression profiles Ewing sarcoma cells in suspension versus monolayer conditions (pooled across timepoints and serum conditions), analyzed against the expression profiles generated as described in Figure 3.2A. ES denotes the Enrichment Score, while the p-value denotes the significance of the ES. (B) Non-transformed and ETV6-NTRK3-transformed NIH/3T3 cells subjected to cellular detachment, analyzed for protein levels of various ER stress-related markers. Beta-actin is used a loading control. (C) Transcript levels of the ER stress markers CHOP and ATF6 as determined in the expression profiling of Ewing sarcoma cells subjected to cellular detachment.

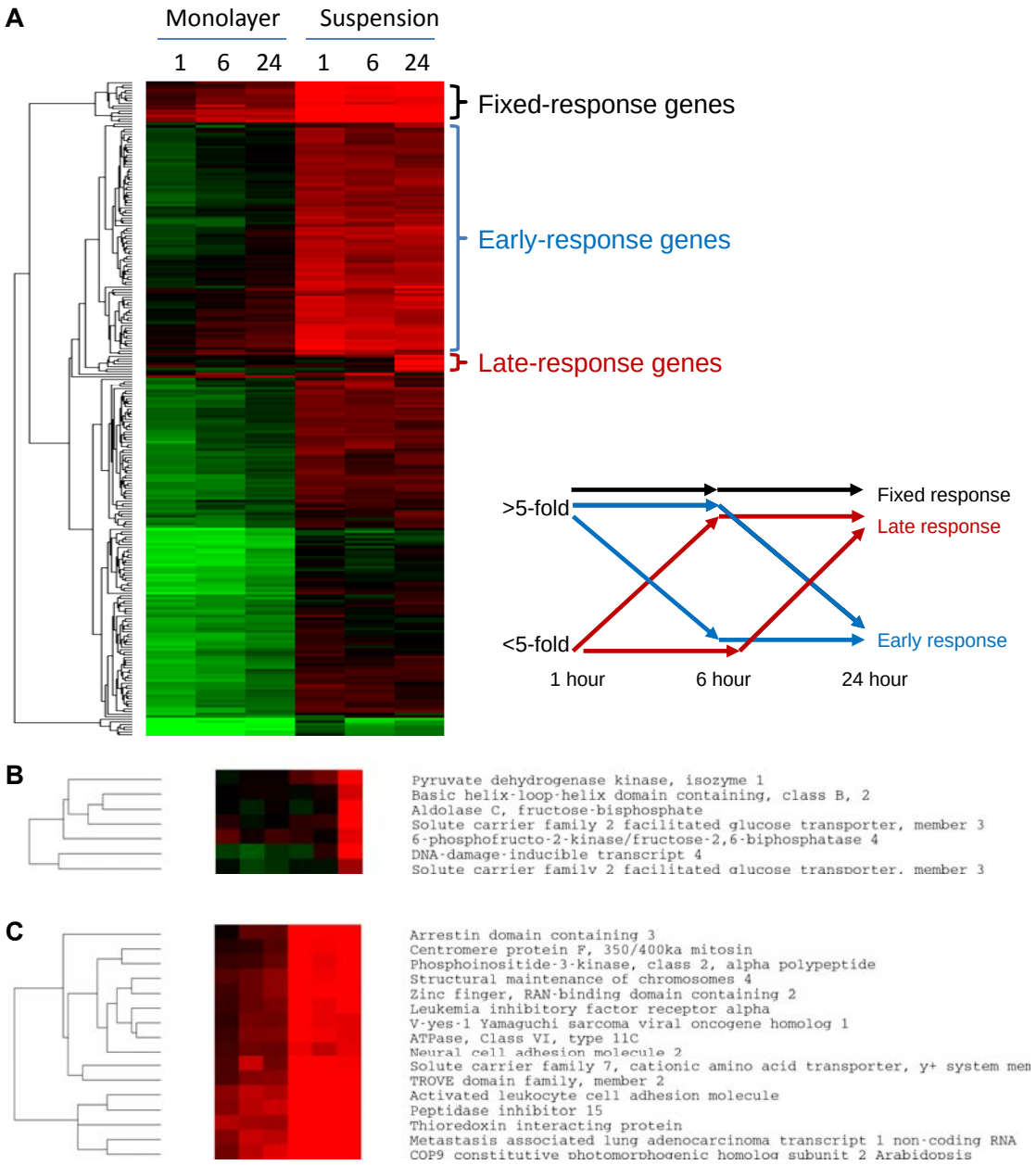

Figure 3.5. Patterns of gene expression clustered based on kinetics of expression. (A) Supervised clustering of genes showing at least 5-fold difference in gene expression in at least one timepoint in suspension versus monolayer. Three patterns of kinetics of gene expression were identified, including "fixed response" (>5-fold up-regulation in suspension versus monolayer, across all timepoints), "late response" (<5-fold up-regulation at 1 hour, followed by >5-fold up-regulation at 6 and 24 hours) and "early response" (>5-fold up-regulation at 1 and 6 hours, followed by <5-fold up-regulation at 24 hours). (B) "Late response" genes. (C) "Fixed response" genes.

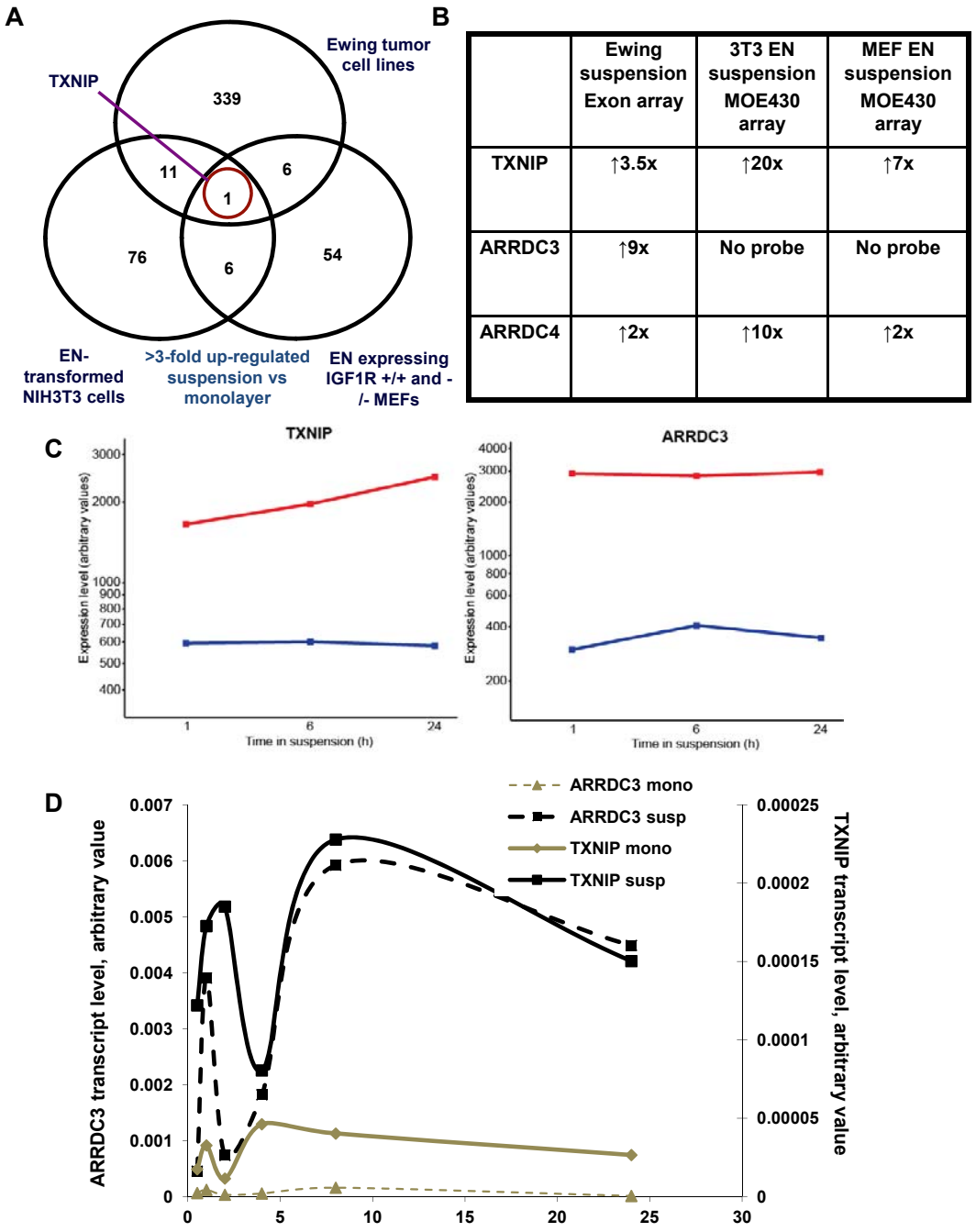

	Ewing suspension Exon array	3T3 EN suspension MOE430 array	MEF EN suspension MOE430 array
TXNIP	↑3.5x	↑20x	↑7x
ARRDC3	↑9x	No probe	No probe
ARRDC4	↑2x	↑10x	↑2x

Figure 3.6. TXNIP is up-regulated following cellular detachment in multiple cell types. (A) Venn diagram quantifying genes up-regulated >3-fold in various cell line models. (B) Expression levels of TXNIP and related arrestin domain-containing across multiple cell line types, as derived from expression profiling data from the various microarray experiments. "No probe" indicates that a probe was unavailable for that gene in the microarray platform. (C and D) Transcript levels of TXNIP and ARRDC3 across various timepoints for Ewing sarcoma cells following cellular detachment. (D) RT-PCR for *Txnip* and *Arrdc3* transcripts across various timepoints of Ewing sarcoma cells in either suspension or monolayer cultures.

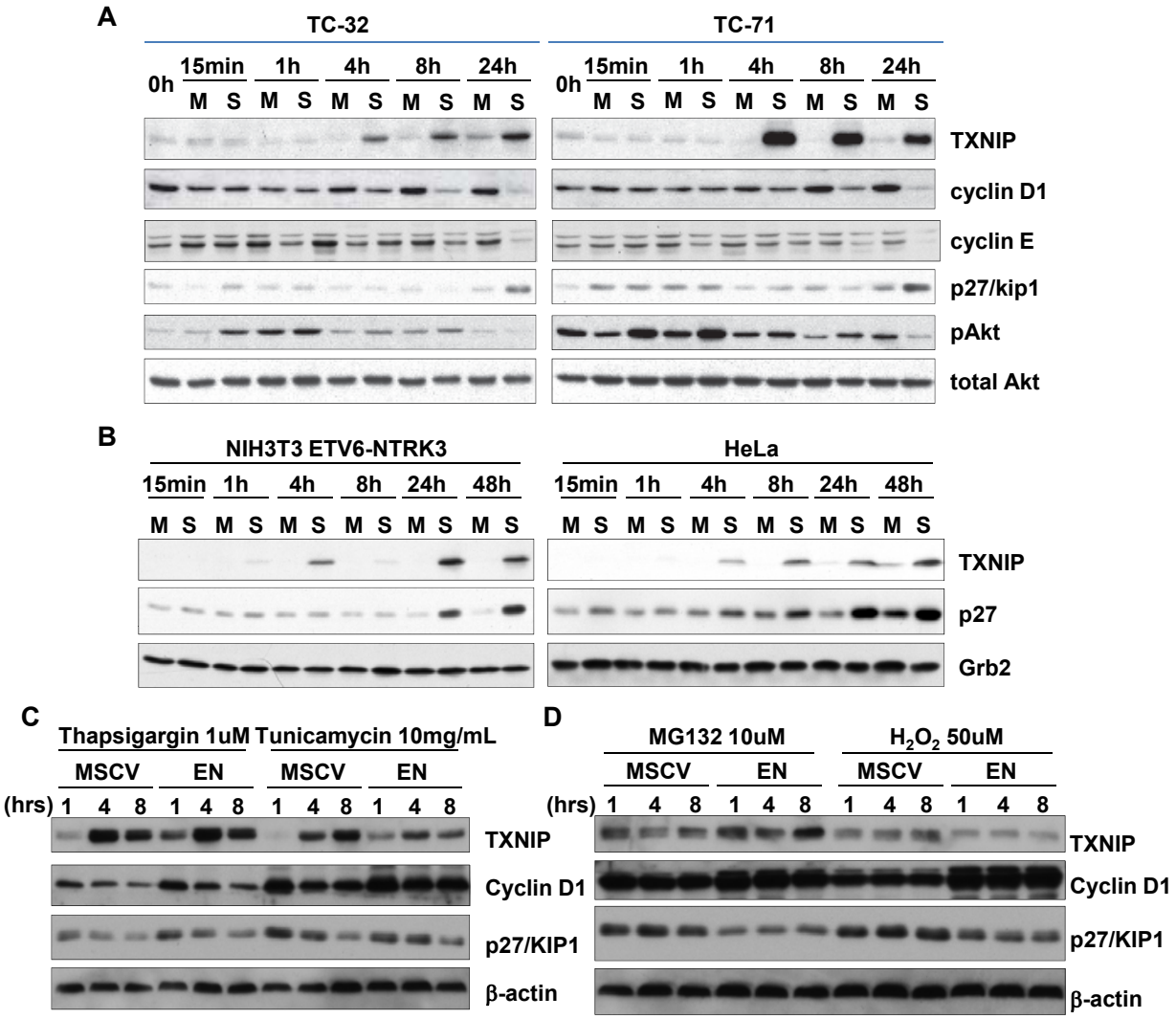

Figure 3.7. TXNIP is a response gene to cellular detachment and ER stress. (A) Western blot of TXNIP and related cell cycle genes, including p27, following cellular detachment of Ewing sarcoma cells (time in monolayer (M) or suspension (S)). Total Akt is used as loading control (B) Western blot of TXNIP and p27 following cellular detachment of ETV6-NTRK3 (EN)-transformed NIH/3T3 cells and HeLa cells (time in monolayer (M) or suspension (S)). Grb2 is used as loading control. (C) Western blot of EN transformed and non-transformed MSCV control NIH/3T3 cells subjected to ER stress following treatment with thapsigargin or tunicamycin. Beta-actin is used as loading control. (D) Western blot of EN transformed and non-transformed MSCV control NIH/3T3 cells subjected to proteasomal stress (following treatment with MG132) or oxidative stress (following treatment with H2O2). Beta-actin is used as loading control.

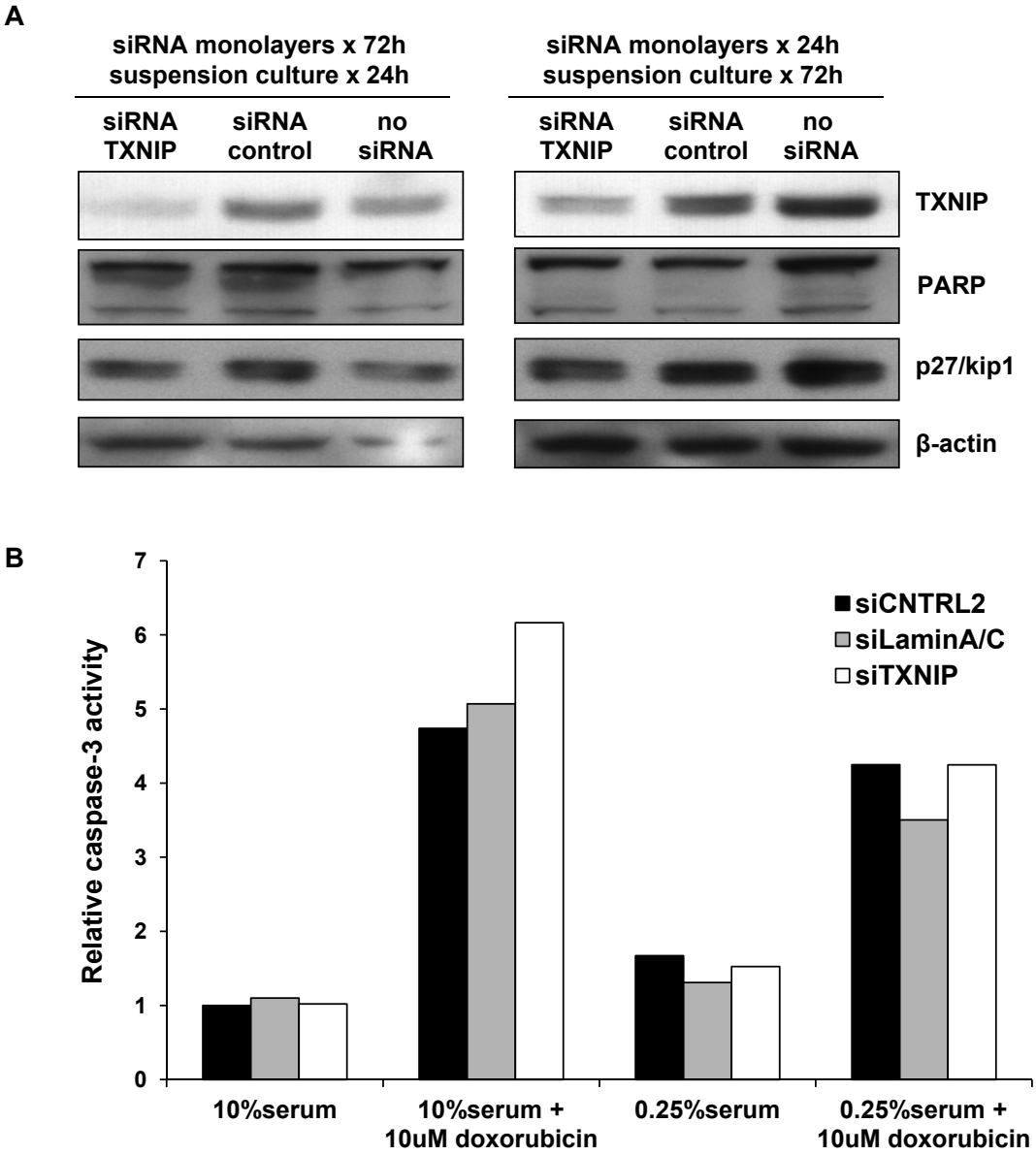

Figure 3.8. TXNIP knockdown suppresses p27/kip1 levels in suspension conditions. (A) TXNIP and p27 protein levels in Ewing sarcoma cells following TXNIP knockdown by two different protocols. Either scrambled siRNA control or no siRNA control were used. PARP cleavage (bottom band indicating cleaved PARP) was analyzed for levels of apoptosis. Beta-actin was used as loading control. (B) Levels of apoptosis as analyzed by relative caspase-3 activity in Ewing sarcoma cells in suspension following TXNIP knockdown versus control. Normal (10%) or low (0.25%) serum conditions were used, with or without concomitant treatment with the cytotoxic agent doxorubicin.

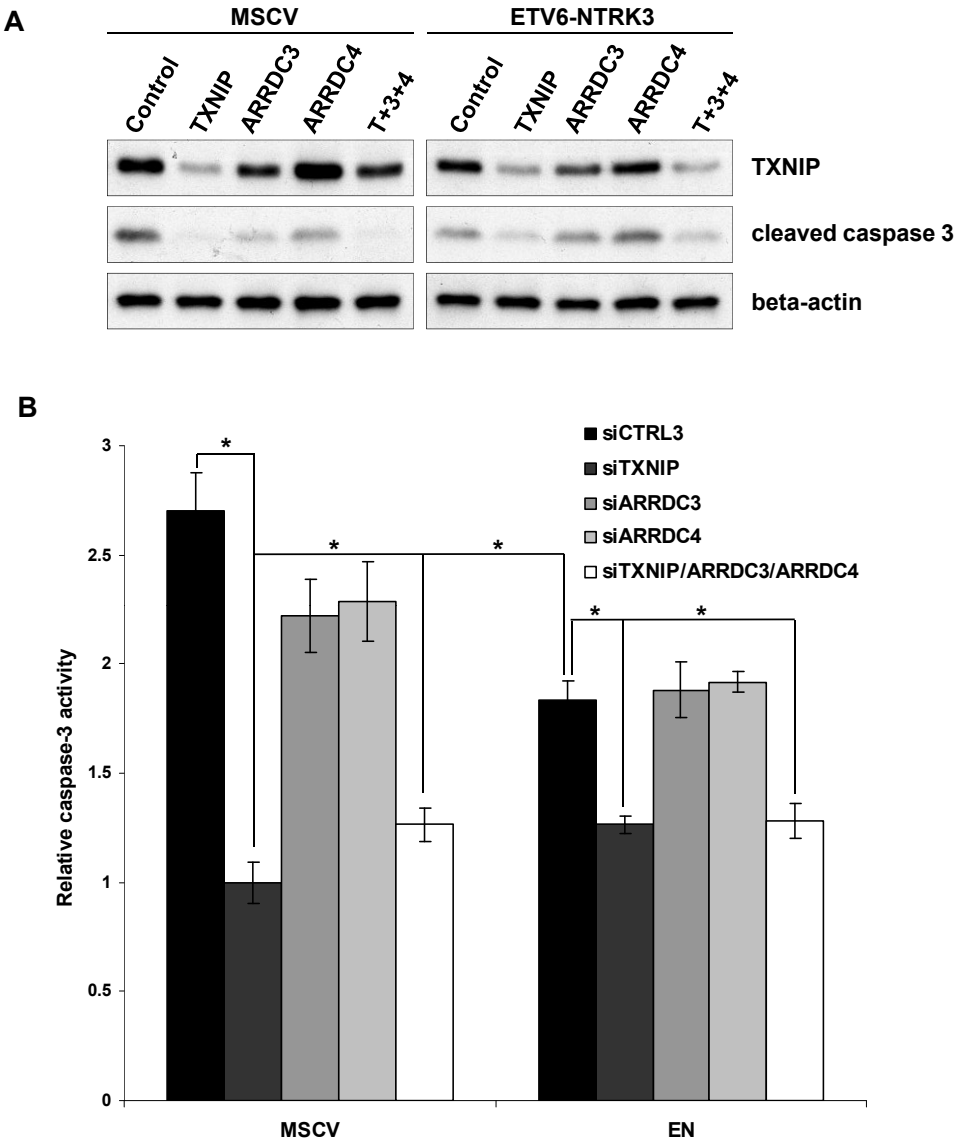

Figure 3.9. TXNIP knockdown in transformed and non-transformed NIH3T3 cells is associated with suppression of anoikis. (A) NIH3T3 cells transformed with either ETV6-NTRK3 or MSCV control were subjected to siRNA knockdown for TXNIP or related proteins ARRDC3 and ARRDC4, as well as pooled knockdown of all three proteins, and then subjected to suspension conditions for 48 hours. Cleaved caspase-3 levels were analyzed by western blot. Beta-actin was used as loading control. (B) Same experimental conditions, with cell lysates analyzed by caspase-3 activity assay. All data are shown as mean ± SEM (n=3). An asterisk indicates statistical significance as determined by Student's t test (*$p < 0.05$).

Chapter 4 THE AMPK STRESS RESPONSE PATHWAY MEDIATES *ANOIKIS* RESISTANCE THROUGH INHIBITION OF mTOR AND SUPPRESSION OF PROTEIN SYNTHESIS

4.1 INTRODUCTION

While the majority of signal transduction pathways modulate cellular metabolism to some degree, certain pathways have particularly critical and specific role in modulating metabolic activity. During periods of cellular energetic stress, such pathways play a central role in energy homeostasis and maintaining survival. One such pathway is mediated by the AMP-activated protein kinase (AMPK), representing a highly-conserved pathway in all eukaryotes, including a well-established pathway regulated by the AMPK autologue SNF1 kinase in *Saccharomyces cerevisiae* (257). In mammals, AMPK consists of a multimeric protein, with a catalytic alpha1 or alpha2 subunit, a regulatory beta subunit and a regulatory gamma subunit. In response to a decrease in the ATP-to-AMP ratio, AMP binding to the gamma subunit results in a conformational change in the alpha subunit, exposing the Thr-172 phosphorylation site (257). This allows the constitutively-active upstream LKB1 kinase to promote phosphorylation at this site, activating the kinase function of AMPK (258). An alternative pathway to AMPK activation is through the calmodulin-dependent protein kinase kinase 2 (CaMKK2), which phosphorylates and activates AMPK as a result of increased intracellular Ca2+, independent of the ATP-to-AMP ratio (259). ROS has also been recognized to

promote AMPK activation in association with phosphorylation at Thr-172, but it is unclear whether ROS activates AMPK through one of these upstream kinases, or if it acts directly on AMPK or indirectly through modulating levels of AMP or calcium (259).

The proximal stressors that lead to reduced ATP levels and AMPK activation are diverse, but the best recognized are nutrient starvation and hypoxia, which deprive cells of the substrates for catabolic processes, including glucose, fatty acids, amino acids and oxygen (258). Other stressors such as ROS are also known to activate AMPK despite the lack of an apparent link with substrate availability. Many pharmacologic activators of AMPK are also known, and utilized both in experimental and clinical settings. In the experimental setting, 5-amino-1-beta-Dffff-ribofuranosyl-imidazole-4-carboxamide (AICAR) is often used, and functions as a mimic of AMP, capable of activating AMPK without altering the ATP-to-AMP ratio (260). Metformin, a drug frequently utilized to treat diabetes, is also known to activate AMPK, through an unclear mechanism that alters mitochondrial function to increase cellular AMP levels (261).

The consequences of AMPK activation are also extremely diverse, but share the common objective of restoring cellular energy status by suppressing anabolic processes and promoting catabolic processes. The first known targets were described by Carling, Hardie and colleagues, who demonstrated that an AMP-dependent protein kinase, subsequent termed AMPK, was responsible for phosphorylating and inactivating two enzymes that control metabolic processes, namely acetyl-CoA carboxylase and HMG-CoA reductase (262). Subsequent studies

showed that such inhibition of acetyl CoA carboxylase 1 and 2 (ACC1 and ACC2) resulted in reduced fatty acid synthesis (FAS), as ACC1/2 normally converts acetyl CoA into malonyl CoA as a substrate for FAS, as well as increased fatty acid oxidation (257). Similarly, AMPK mediated inhibition of HMG-CoA reductase leads to reduced cholesterol synthesis. Since these early studies on AMPK, numerous other downstream targets have been identified. FAS is also inhibited through AMPK-mediated suppression of the FAS genes HNF4alpha and SREBP1c at the transcript level (257). Another key target of AMPK is FOXO3a (263). While AMPK-mediated phosphorylation and activation of FOXO3a triggers a transcriptional program that promotes cell cycle arrest and autophagy (264), this axis may have a critical pro-survival role in stress conditions, particularly in the context of oncogenic transformation and Akt hyperactivity (265). Other actions of AMPK include phosphorylation of eEF2K at serine 366, which leads to inhibition protein translation elongation through increased eEF2K-mediated phosphorylation of eEF2, and activation of p53 and downstream p21 to promote cell cycle arrest (25).

One of the most characterized downstream targets of AMPK is the mTOR pathway. Specifically, AMPK is able to phosphorylate and activate the intermediary GTPase-activating protein (GAP) tuberous sclerosis complex 2 (TSC2), which acts in a multi-protein complex to inhibit the mTOR-containing protein complex mTORC1 (233). AMPK also inhibits mTORC1 more directly through phosphorylation of Raptor (266). Such inhibition of mTORC1 leads to the suppression of a multitude of cellular functions, including reduced cell growth and proliferation and reduced protein synthesis (258). This is as a result of reduced mTORC1-mediated

phosphorylation and activation of p70 ribosomal S6 kinase (p70S6K), which then results in reduced phosphorylation of ribosomal protein S6 and reduced protein translation (267). AMPK-mediated inhibition of mTORC1 also results in reduced phosphorylation of eIF4E binding protein 1 (4E-BP1), allowing it to remain bound to the protein translation initiation complex protein eIF4E, thus inhibiting translation initiation (268). Therefore, AMPK-mediated mTORC1 inhibition represents a critical branch of this energy homeostasis pathway by suppressing the highly energy-rich processes of proliferation and protein synthesis.

Since AMPK activation leads to the inhibition of cellular growth and proliferation, AMPK has generally been considered tumor suppressive in nature. Indeed, there has been evidence over the years that AMPK overall has a tumor suppressive role. In primary tumors of breast cancer, there appears to be reduced AMPK pathway activity compared to normal breast epithelium, as demonstrated using phospho-specific antibodies for ACC1 (269). Such reduced staining also correlated with poor prognosis and increased histological grade. Loss of AMPK alpha1 subunit also appears to promote tumor progression in a mouse model of Myc-driven lymphomas (270), while loss of the AMPK alpha2 subunit (but not loss of the alpha1 subunit) appears to increased the transforming ability of oncogenic H-Ras(V12) in a murine fibroblast model (271). As a result of this interpretation of the role of AMPK, pharmacologic activators such as metformin have been evaluated extensively as a potential therapeutic, currently being evaluated in phase III trials following biochemical and biomarker evidence of therapeutic effect in phase II trials. In a similar manner, mTOR inhibition has also been used as an approach to

cancer therapy, as numerous agents have been developed to treat cancer through mTOR inhibition, such as rapamycin/sirolimus and other "rapalogues" such as temsirolimus and everolimus (272). In fact, such therapies have shown some degree of efficacy in various cancer types (273-275). Furthermore, genetic events found in relation to familial cancer syndromes do lend some support to this notion, as various familial tumor syndromes are associated with reduced activation of AMPK, including Peutz-Jehgers syndrome (with inactivating mutations in the LKB1 kinase upstream of AMPK) and tuberous sclerosis syndrome (with inactivating mutations in the TSC1/2 proteins, resulting in hyperactivation of the mTOR pathway) .

While there is evidence that hyperactivation of the AMPK pathway has anti-tumorigenic effects such as inhibition of proliferation, there is little evidence that AMPK is a *bona fide* tumor suppressor, as inactivating AMPK mutations or deletions are not a frequent event in cancers (276). Although inactivating mutations in the upstream kinase LKB1 are recognized to be pro-oncogenic, particularly in the clinical context of the Peutz-Jehgers syndrome, and in sporadic non-small cell lung cancers and cervical cancers, AMPK represents only one of many known targets of LKB1, and there is no conclusive evidence that AMPK represents the critical downstream kinase in the Peutz-Jehgers syndrome setting (259). Furthermore, AMPK knockout mice do not appear to have an increased propensity for tumors (277). Overall, there is no conclusive evidence that AMPK activation is sufficient to prevent tumor progression. In fact, there is growing data demonstrating a pro-tumorigenic role for AMPK. An interesting study by Bardeesy and colleagues showed that loss of *LKB1* in a transgenic mouse model showed significantly

increased rates of benign intestinal polyps, comparable to the polyposis seen in Peutz-Jehgers syndrome, but MEFs derived from these mice are highly resistant to transformation by H-Ras(V12) (278). In a carcinogen-induced model of gliomas in rats, hyperactivity of the AMPK pathway is seen in all stages of tumor development (279). An RNAi-based screen also identified a pro-survival role for the beta subunit of AMPK in prostate cancer cells, and increased AMPKbeta expression is seen in metastatic prostate cancers compared to primary tumors (280). A very interesting study identified AMPK and AMPK-related kinase 5 (ARK5, an upstream kinase activator of AMPK) in an shRNA-based screen for kinases critical for survival in Myc-regulated osteosarcoma cells (281). Although ARK5 and AMPK depletion resulted in increased proliferation in conjunction with increased mTOR pathway activity, such cells showed markedly increased cell death in the context of MYC-deregulation, which could be rescued by rapamycin treatment.

A role for AMPK in promoting anchorage independent growth has also been demonstrated in a number of cell line models. Laderoute and colleagues showed that mouse embryonic fibroblasts (MEFs) derived from AMPKalpha1/alpha2 double-knockout mice, as compared to wild type MEFs, are resistant to *in vitro* colony formation in soft agar as well as *in vivo* subcutaneous xenograft formation in immunodeficient mice (282). Knockdown of AMPK in pancreatic cancer cell lines also suppresses anchorage independent growth both *in vitro* and *in vivo* (283). In addition, AMPK knockdown in these same cells showed increased cell death in glucose starvation, demonstrating that AMPK is necessary for survival during such stress conditions. A further study showed that depletion of kinase suppressor of

Ras-2 (KSR2), another upstream activator of AMPK, reduced the *in vitro* transformation phenotype of H-Ras(V12)-expressing MEFs as well as various cancer cell lines (284).

A pro-survival role for AMPK in various cancer cell models under cellular stress conditions has also been consistently demonstrated. Laderoute and colleagues have shown that AMPK is important for survival under hypoxic conditions (282). In a glioma cell line model, LKB1-dependent AMPK activity is supportive of survival under conditions of glucose deprivation (285). Interestingly, while LKB1/AMPK activity remains low in the primary tumor, it appears reactivated in alternate conditions such as during migration away from the primary tumor to allow for their survival. In prostate cancer cells, particularly androgen-independent cells that show an exaggerated response to metabolic stress, blockade of AMPK resulted in increased cell death following glucose deprivation. Overall, these data support an important role for AMPK in the adaptive response of cancer cells to various forms of stress, and suggests that cancers show dependence on AMPK for survival under various metabolic stresses to support the transformation phenotype. This is in contrast to the previously mentioned studies showing an anti-tumorigenic role for AMPK, but those studies focused on cell line models grown under non-stressed conditions, as well as on rapidly-growing primary tumors and xenografts that presumably are not in a nutrient-deprived state.

Here we investigated *anoikis* resistance in transformed cells driven by oncoproteins known to suppress *anoikis*, namely ETV6-NTRK3 and oncogenic K-Ras. Based on our analysis of the detachment-induced changes in gene expression

profiling, one specific pathway that we identified to be activated was AMPK pathway. We show that *anoikis* resistance in transformed cells strongly correlates with and is dependent on AMPK activation. Moreover, AMPK-dependent mTORC1 blockade and inhibition of energy-demanding protein synthesis are critical for *anoikis* suppression, through mitigation of the metabolic defects induced by detachment. We show that detachment represents a form of cellular stress, and that subsequent survival is dependent on stress response processes typically considered tumor suppressive, namely AMPK activation and mTOR inhibition. We propose that this represents a further example of "non-oncogene addiction," whereby cancer cells require a robust stress response to survive transient stresses such as cellular detachment (286).

4.2 MATERIALS AND METHODS

Cell culture and DNA transfection. Early passage NIH3T3 were obtained from ATCC (Rockville, MD). *AMPK+/+* and *-/-* MEFs were obtained as previously described (282). *TSC1+/+* and *-/-* MEFs were kindly provided by David Kwiatkowski (Harvard Medical School, Boston, MA). *4E-BP* E1A/Ras *wt* and double knockout (DKO) MEFs were kindly provided by Nahum Sonenberg (McGill University, Montreal, QC). *ATG5+/+* and *-/-* MEFs were kindly provided by Noboru Mizushima (National Institute for Basic Biology, Okazaki, Japan). *IGF1R-/-* MEFs (R-) and *IGF1R-/-* MEFs re-expressing IGF1-R (R+) were kindly provided by Renato Baserga (Kimmel Cancer Centre, Philadelphia, PA). Retroviral expression vectors pMSCVpuro-ETV6-NTRK3 and pMSCVpuro-ETV6-NTRK3myr were used for generation of stable cell lines as previously described (117). The pMSCVpuro-K-

Ras(V12) vector was constructed by subcloning the BamHI-SalI fragment from the pBabe-puro-K-Ras(V12) vector obtained from Addgene (courtesy of William Hahn) containing the K-Ras(V12) open reading frame into the BglII-XhoI sites of pMSCVpuro. The pMSCVneo-DN-AMPK vector was constructed by subcloning the EcoRI fragment from pBabe-GFP-DN AMPK (gift from Nissim Hay) into the pMSCVneo vector. Infections of the NIH3T3 cells and MEFs were performed using retrovirus generated following introduction of the retroviral vectors into PhoenixA cells. For suspension cultures, cells at subconfluence were detached by trypsinization and diluted to a concentration of 250,000 cells/mL, plated on polyHEMA-coated 10cm dishes or 6-/12-well plates, or precoated 96-well plates (Non-Binding Surface coated microplates, Corning, Lowell, MA) and incubated for the indicated timecourses. Chemical inhibitors were added to suspension cultures immediately following detachment and plating onto polyHEMA-coated plates to determine their effects on the early stages of the *anoikis* response.

Antibodies and chemicals. Anti-p-ACC (S79), anti-ACC, anti-p-Raptor (S792), anti-p-AMPKalpha (T172), anti-cleaved caspase-3, anti-p-p70 S6 kinase (T389), anti-4E-BP1, anti-p-Akt (S473), anti-p-MEK1/2 (S217/221), anti-GAPDH and anti-LC3B antibodies were purchased from Cell Signaling (Danvers, MA). Anti-TrkC, to detect ETV6-NTRK3 expression, and anti-beta-actin antibodies were purchased from Santa Cruz Biotechnologies (Santa Cruz, CA). Anti-K-Ras antibody was purchased from Calbiochem. Compound C was obtained from Calbiochem/EMD Biosciences (Darmstadt, Germany). Rapamycin was obtained from Cayman

Chemical Co. (Ann Arbor, MI). Cycloheximide was obtained from Sigma-Aldrich (Oakville, ON). Bafilomycin A was obtained from A.G. Scientific (San Diego, CA).

Caspase-3 activity assay. Cells were lysed in caspase-3 lysis buffer (10mM HEPES pH 7.5, 50mM NaCl, 2mM $MgCl_2$, 5mM EGTA, 0.2% CHAPS), and assayed for protein concentration using the D_C protein assay (BioRad). Lysates were mixed at a 1:1 ratio with caspase-3 reaction buffer (40mM PIPES pH 7.2, 200mM NaCl, 20% sucrose, 0.2% CHAPS, 20mM DTT), caspase-3 substrate was added to a concentration of 0.5μM (Caspase-3 Substrate IX fluorogenic, Calbiochem), and incubated for 1 hour at 37^{o}C. Fluorescence intensity was measured and normalized to protein concentration.

Annexin V/7-aminoactinomycin D (7-AAD) fluorescence assisted cell-sorting (FACS) assay. Transformed and non-transformed *AMPK* MEFs were cultured in suspension for 48 hours, harvested by centrifugation, washed and trypsinized for 10min. These dispersed cells were washed, centrifuged and filtered (0.45 μm) to obtain a single cell suspension. Annexin V-FITC and 7-AAD were added with the cells in binding buffer according to the manufacturer's protocol (BD Pharmingen, Mississauga, ON), incubated at room temperature for 15min and subjected to FACS analysis.

Cell survival and cytotoxicity assays. Cell survival was measured using the AlamarBlue assay (Invitrogen), according to the manufacturer's instructions. Briefly, cells were detached and cultured for 48h in suspension on a 96-well coated plate. The AlamarBlue reagent was added at a 1:10 ratio, incubated for 4h at 37^{o}C, and absorbance was read and corrected for background. The LDH release Cytotoxicity

Detection Kit (Roche, Indianapolis, IN) was performed according to the manufacturer's instructions. Briefly, cells were detached and cultured for 48h in suspension on a 6-well coated plate. Cleared supernatant media was collected, combined with the LDH assay reaction mixture, incubated for 0.5h and absorbance was read, corrected for background, and normalized to the total cell count. The Cytotox-Glo cytotoxicity assay (Promega, Madison, WI) was performed according to the manufacturer's protocol. Briefly, cells were detached and cultured for 24h in suspension on a 96-well coated plate. The assay reagent was added at room temperature, incubated for 15min, and total luminescence was measured, corresponding to protease levels released by dead cells. This value was normalized to total cell protease activity after reincubation for 15min with additional assay reagent combined with digitonin for complete cell lysis, as supplied by the assay kit.

ATP assay. Cells were lysed in ATP assay lysis buffer (10mM Tris pH 7.5, 40mM NaCl, 1% Triton X-100, 20mM EDTA) supplemented with a protease inhibitor cocktail (Complete Mini tablets, Roche), and assayed for protein concentration. Lysates were mixed at a 1:1 ratio with ATP reaction buffer from the ATP Bioluminescent Assay kit (Sigma) at room temperature, and luminescence was measured immediately. Luminescence values were normalized to protein concentration.

Total protein synthesis assay. Cells were cultured in suspension conditions and pulsed with 10 μCi [^{35}S]-methionine/cysteine mix (EasyTag EXPRESS Protein Labeling Mix, Perkin Elmer) for 30min. Cells were washed then lysed using buffer containing 50mM HEPES pH 7.4, 150mM NaCl, 2mM EDTA, 10% glycerol, 1% NP-40

and protease inhibitors (Roche). Using 10μg of lysate, total protein was precipitated using 10% trichloroacetic acid (TCA), vacuum-filtered using glass microfiber filters (GF/C, Whatman), washed with TCA and ethanol, and total [^{35}S] activity was measured to reflect methionine incorporation and global protein synthesis.

4.3 RESULTS

Cellular detachment induces expression profile changes resembling that seen with AMPK activation. Given the gene expression profile results from the previous chapter, we wondered whether a specific signaling pathway might underlie this broad stress response. One pathway known to negatively modulate diverse cellular functions under stress conditions is the AMP-activated protein kinase (AMPK) cascade, which suppresses multiple energy-demanding functions such as proliferation and protein translation in response to reduced ATP/AMP ratios (287). To explore this possibility, we cross-compared detachment-induced gene expression profiles with published transcriptional responses observed following modulation of the AMPK pathway (Table A1.5-1.7) (263, 288, 289). By GSEA, detachment-induced GEPs showed marked enrichment for genes known to be down-regulated after AMPK inhibition and up-regulated after AMPK activation (263, 288, 289) (Figure 4.1A). Prominent were genes previously ascribed to AMPK activation, including down-regulation of *FASN* and *G6Pase*, and up-regulation of *p21/Cip1* and *cyclin G* (Table A1.1 and A1.2) (287, 290). These data support the notion that the transcriptional response to detachment mirrors AMPK activation.

AMPK is activated during detachment-induced stress and promotes resistance to anoikis. We next investigated whether the AMPK pathway is biochemically activated in response to detachment. Using NIH3T3 fibroblasts transformed with EN or K-Ras versus MSCV vector alone, the known AMPK targets ACC1 and Raptor, as well as AMPK itself, showed rapid and sustained phosphorylation following detachment (Figure 4.1B). Since this was observed in both transformed and non-transformed cells, AMPK activation alone is likely insufficient for survival of detached cells. To specifically test whether AMPK activation is critical for *anoikis* resistance in transformed cells, we expressed EN, K-Ras, or vector alone in *wt* (*AMPK+/+*) versus *AMPKα1* and *AMPKα2* double knockout (*AMPK-/-*) MEFs and subjected the cells to detachment. Cell death was significantly increased in all *AMPK-/-* compared to *AMPK+/+* cells despite EN or K-Ras transformation, measured by caspase-3 cleavage (Figure 4.1C). This corresponded closely to apoptosis as measured by annexinV/7-AAD FACS, with increased annexinV-positivity in *AMPK-/-* versus *AMPK+/+* cells, in both EN-transformed (24.81% versus 8.57%) and K-Ras-transformed (27.41% versus 14.81%) MEFs (Figure 4.1D). Similar findings were obtained using the AlamarBlue cell survival assay (Figure 4.2A) and in two different cytotoxicity assays, namely LDH release (Figure 4.2B) and Cytotox-Glo dead cell protease release (Figure 4.2C). Results were validated in EN or K-Ras transformed NIH3T3 cells by chemical inhibition of AMPK using compound C (Figure 4.1E), or by molecular inhibition using dominant-negative AMPK (Figure 4.2D), each of which partially restored *anoikis*.

Since AMPK is activated by reduced ATP/AMP ratios (287), we next compared ATP levels of transformed cell lines following detachment. EN- or K-Ras-transformed *AMPK+/+* and *AMPK-/-* MEFs both showed reduced ATP levels after detachment (Figure 4.1F). Therefore the drop in ATP appears proximal to AMPK activation in transformed cells subjected to detachment (216). However, the ATP drop was significantly more pronounced in AMPK-deficient cells compared to corresponding *wt* cells, suggesting that AMPK activation functions to maintain ATP levels following detachment. Together, these data demonstrate that AMPK activation promotes survival during detachment-induced stress, possibly by mitigating ATP reduction after detachment.

AMPK activation following detachment inhibits mTORC1 to promote *anoikis* resistance in transformed cells. AMPK modulates numerous downstream targets to maintain survival during energy stress, including ACC1, eEF2K, mTORC1 and p53 (287). We next wished to determine which pathways downstream of AMPK activation act to suppress *anoikis*. Consistent with NIH3T3 cells, ACC1 and Raptor show increased phosphorylation in suspension versus monolayer cultures of *AMPK+/+* MEFs, while as expected no phosphorylation was seen in *AMPK-/-* MEFs (Figure 4.3A). Again, no significant difference in the phosphorylation status of these two proteins was seen between transformed and non-transformed cells. However, we found that survival after detachment in transformed *AMPK+/+*/EN or *AMPK+/+*/K-Ras MEFs strongly correlated with mTORC1 inhibition, as demonstrated by hypophosphorylation of p70S6K and 4E-BP1 (Figure 4.3A). In contrast, all *AMPK-/-* MEF lines showed sustained mTORC1 activity in suspension. A

causative role for AMPK activation was corroborated using either dominant-negative AMPK expression (Figure 4.4A) or compound C treatment of NIH3T3 cells (Figure 4.4B), each of which prevented mTORC1 suppression following detachment (Figure 4.4B). In addition, *anoikis* sensitive *AMPK+/+*/MSCV MEFs also maintained mTORC1 activation, suggesting that, paradoxically, AMPK-mediated mTORC1 suppression is dependent on oncogenic transformation by EN or K-Ras. Hence, under detachment-induced stress, mTORC1 activity is uncoupled from hyperactivation of PI3K-Akt and Ras-ERK normally driven by EN or K-Ras. Transformed NIH3T3 cells similarly suppressed mTORC1 activity, in contrast to NIH3T3-MSCV cells that maintained mTORC1 activity following detachment, again demonstrating that *anoikis* resistance correlates with mTORC1 suppression (Figure 4.3B). The latter was again uncoupled from PI3K-Akt and Ras-ERK hyperactivation in transformed cells, as high p-Akt and p-MEK levels were sustained even after 48 hours in suspension. This further supports the notion that AMPK-mediated mTORC1 inhibition is somehow dependent on oncogenic transformation.

We then wished to establish a direct role for mTORC1 inhibition in *anoikis* resistance. Firstly, *AMPK-/-*/EN and *AMPK-/-*/K-Ras MEFs, neither of which suppresses mTORC1 activity under detachment, were treated with rapamycin immediately following detachment. Rapamycin reduced cell death in transformed *AMPK-/-* cells in a dose-dependent manner (Figure 4.3C), validated in Cytotox-Glo cytotoxicity assays (Figure 4.4D). Rapamycin also restored ATP levels (Figure 4.3D), which were otherwise significantly reduced following detachment (Figure 4.1F). To support these findings, we used *TSC1-/-* MEFs, which show constitutive mTORC1

activation (291). Detached EN and K-Ras transformed *TSC1-/-* MEFs indeed showed increased mTORC1 activity following detachment compared to corresponding *TSC1+/+* MEFs (Figure 4.4C). Like *AMPK-/-* MEFs, *TSC1-/-* MEFs showed dramatically increased cell death relative to corresponding *wt* MEFs (Figure 4.3E), as well as reduced cell survival (Figure 4.4E) and increased cytotoxicity (Figures 4.4F & 4.4G). Furthermore, rapamycin again partially suppressed *anoikis* in *TSC1-/-*/EN and *TSC1-/-*/K-Ras MEFs (Figure 4.3F & 4.4H). Similar experiments were then performed using MEFs deficient in both 4E-BP1 and 4E-BP2 (downstream of mTORC1/p70S6K) transformed with E1A and H-Ras (*4E-BP* DKO E1A/Ras MEFs), which lack inhibitory control of protein translation (292). Indeed, by 72 hours in suspension, *4E-BP* DKO E1A/Ras MEFs were markedly more susceptible to *anoikis* compared to corresponding *wt* MEFs (Figure 4.3G). Altogether, these data establish a critical role for AMPK-mediated mTORC1 inhibition in *anoikis* resistance of transformed cells.

Loss of ATG5-dependent autophagy is insufficient to restore *anoikis* susceptibility to transformed cells. Inhibition of mTORC1 induces multiple other processes that could contribute to *anoikis* resistance, including induction of macroautophagy. It was previously reported that macroautophagy is induced following detachment and has a pro-survival role in detached non-transformed or Bcl-2-transformed breast cells (95). Consistent with this, both transformed and non-transformed *AMPK+/+* MEFs show increased macroautophagy in suspension cultures, with increased LC3B-II levels following bafilomycin A-mediated lysosomal inhibition to monitor autophagic flux (Figure 4.5A). Interestingly, while bafilomycin

A treated *AMPK-/-* MEFs also accumulate LC3B-II after detachment, transformed *AMPK-/-* MEFs accumulate less LC3B-II compared to corresponding transformed *AMPK+/+* MEFs (Figure 4.5B). Although mTORC1 is known to block proximal steps of macroautophagy (293), the inability of transformed *AMPK-/-* MEFs to induce autophagic flux compared to non-transformed *AMPK-/-* control cells is unlikely due to differences in mTORC1 activity, as mTORC1 is re-activated in both transformed and non-transformed *AMPK-/-* MEFs in suspension (Figure 4.3A). Therefore our results are inconsistent with macroautophagy alone as the basis of *anoikis* resistance, as both transformed and non-transformed *AMPK-/-* MEFs undergo *anoikis* in suspension (Figure 4.5A). To more directly demonstrate this, we tested whether defective autophagy restores *anoikis* to transformed cells. Under detachment, we observed a significant increase in cell death of autophagy-deficient non-transformed *ATG5-/-* versus *ATG5+/+* MEFs (Figure 4.5C), consistent with previous reports (95). In contrast, EN or K-Ras expression almost completely abrogated *anoikis* in both *ATG5+/+* and *ATG5-/-* MEFs following 72h in suspension (Figure 4.5C). Similarly, there was no significant difference in cell death in EN- or K-Ras-transformed *ATG5+/+* versus *ATG5-/-* MEFs at 12h and 24h of suspension, while at these time points there were significant differences in cell death in transformed *AMPK+/+* versus *AMPK-/-* MEFs (Figure 4.6). Therefore, defective macroautophagy is insufficient to restore *anoikis* to transformed cells at either early or prolonged time-points, arguing against a major role for this process in AMPK-mediated *anoikis* resistance.

Inhibition of protein synthesis reduces energy stress following cellular detachment and promotes *anoikis* resistance. We next investigated whether mTORC1-mediated inhibition of protein synthesis promotes *anoikis* resistance in transformed cells, since protein synthesis is highly demanding bioenergetically (294). Firstly, using transformed *AMPK-/-* or *TSC1-/-* MEFs, we observed increased global protein synthesis rates in comparison with their *wt* counterparts (Figures 4.7A & 4.7B), suggesting that *anoikis* susceptibility is linked to their inability to suppress protein synthesis. To directly determine whether reduced protein synthesis promotes survival, *AMPK-/-*/EN and *AMPK-/-*/K-Ras MEFs were treated with cycloheximide (CHX) immediately following detachment. For these experiments we used considerably lower concentrations than for standard translation inhibition assays (i.e. 50-200 ng/ml vs. 10-20 μg/ml) and in the range where its effects on translation are linear and dose-dependent (295). Low-dose CHX indeed partially restored survival in transformed *AMPK-/-* cells under detachment conditions (Figures 4.7C and 4.4D). Interestingly, CHX had little effect on survival in transformed *AMPK+/+* MEFs under detachment, and in fact showed a trend towards reducing survival. This is consistent with its pro-survival effects being limited to cells that fail to suppress detachment-induced mTORC1 and protein synthesis. Similar effects were observed in transformed *TSC1-/-* MEFs (Figure 4.7D and 4.4H). Finally, as seen with rapamycin, CHX restored ATP levels in *AMPK-/-*/EN and *AMPK-/-*/K-Ras MEFs under detachment (Figure 4.7E). The ability of rapamycin and CHX to promote *anoikis* resistance was not via suppression of p53 translation (Figure 4.8), as was previously reported in adherent cells under glucose deprivation (296).

Therefore *anoikis* resistance mediated by translation inhibition may be due in part to mitigation of the metabolic defects occurring after loss of attachment. Overall, these data point to a model whereby detachment stress leads to AMPK-mediated mTORC1 inhibition in transformed cells, thus suppressing *anoikis* by preserving bioenergetic levels through a block in protein translation.

AMPK activation contributes to *anoikis* resistance in breast carcinoma cell lines. It is reported that fibroblasts are relatively more resistant to *anoikis* than epithelial cells (297). We have observed that mesenchymal cell lines such as murine fibroblasts and human sarcoma cell lines demonstrate robust *anoikis* under detachment conditions when key *anoikis* suppressors such as IGF1R or ERBB4 are inhibited (109, 117). Nevertheless, we wished to extend our current findings to an epithelial cancer model. Using two metastatic breast carcinoma cell lines, MDA-MB231 and MDA-MB435, both demonstrated previously to be *anoikis* resistant (298), we analyzed the activity of AMPK and mTOR pathways following detachment. Consistent with results in fibroblasts, both cell lines activate AMPK and suppress mTORC1 following detachment (Figure 4.9A). Furthermore, *anoikis* was restored following compound C inhibition of AMPK activation under detachment conditions (Figure 4.9B). Therefore, our finding that AMPK activation contributes to *anoikis* resistance is applicable to transformed epithelial cells as well.

4.4 DISCUSSION

Cancer cells face diverse forms of stress during the metastatic process as they traverse harsh microenvironments and energy-depleted conditions. Many such stresses, including nutrient depletion and hypoxia, may be transient and cancer cells

must rapidly respond to these conditions in order to survive. Various stress response pathways are critical for such survival, and reliance of cancer cells on these pathways has been termed "non-oncogene addiction." Here we have shown that cellular detachment elicits a broad stress response in cancer cells, which is likely critical for *anoikis* resistance. In particular, we show that AMPK activation promotes survival in detached cells by mitigating drops in ATP levels, and that this is linked to a block in mTORC1 signaling and global protein synthesis. Paradoxically, mTORC1 inhibition relies on expression of oncogenes such as activated K-Ras or EN to suppress mTORC1 activity following detachment. These oncogenes typically hyperactivate mTORC1 through sustained Akt activity during proliferative conditions (73). Therefore, activation of this AMPK-mTORC1 cascade appears to be dominant over pro-growth and metabolically-demanding pathways such as those driven by Akt, demonstrating the emphasis cancer cells place on stress response pathways to maintain survival during episodes of bioenergetic compromise.

Despite the functional diversity of AMPK- and mTOR-regulated pathways (Figure 4.10), their relative roles in *anoikis* resistance have not been well studied. AMPK activation was previously demonstrated following detachment in breast epithelial cells, and was associated with induction of autophagy (95). However, the relative contribution of AMPK activation to survival and/or autophagy was not determined. Over-expression of mTOR in non-transformed *wt* fibroblasts promoted *anoikis* resistance, and mTOR knockdown in MEFs deficient in all retinoblastoma family members restored *anoikis* (299). However, whether mTOR overexpression correlates with gain-of-function of downstream pathways, particularly in relation to

mTORC1 versus mTORC2 complex function, was not determined. Interestingly, in thyroid epithelial cells, inhibition of protein synthesis using low-dose cycloheximide also promoted survival in suspension but showed no effect on survival of monolayer cells (300), supporting our finding that translation inhibition promotes *anoikis* resistance.

Recently, a pro-survival role for macroautophagy in anchorage-independent growth was reported (301). Consistent with our data, these authors demonstrated that detachment of H-Ras(V12)-transformed cells led to activation of autophagy in association with mTORC1 inhibition. However, *ATG5* deficiency in H-Ras(V12)-transformed MEFs led to increased apoptosis under anchorage-independent conditions, contrary to our findings in which EN- and K-Ras(V12)-transformed MEFs, whether deficient or *wt* for *ATG5*, were able to suppress *anoikis*. Several recent studies demonstrated a key role for macroautophagy in proliferation and metabolism during Ras-mediated transformation (302, 303). In these studies, while macroautophagy was critically important to maintain a metabolic phenotype permissive for sustained proliferation during transformation, a function for autophagy in suppressing *anoikis* after cellular detachment was not required for Ras transformation. In fact, direct suppression of apoptosis through Bcl-2 overexpression was insufficient to restore prolonged anchorage-independent growth in Ras-transformed autophagy-deficient cells (301). Our data suggests that AMPK is important for both prolonged anchorage-independent growth as previously demonstrated (282), and for survival at early periods following detachment. Therefore, while autophagy is required for certain essential

components of Ras-mediated transformation such as proliferation and altered metabolism, *anoikis* resistance appears to represent a divergent oncogenic property potentially dependent on other processes such as activation of the AMPK pathway.

Consistent with our results, a pro-survival role for AMPK activation and mTORC1 inhibition has been documented under other stress conditions. AMPK activation promotes survival during nutrient deprivation, which appears to be dependent on an AMPK-mediated cell cycle checkpoint (25). Under starvation and DNA damage, constitutive mTORC1 activity in the context of TSC-deficiency compromises survival through modulation of p53 levels (296). Inhibition of mTORC1 also promotes survival in TSC-deficient cells during glucose starvation by maintaining energy levels (304). Interestingly, TSC2 over-expression has been associated with increased tumor invasion and metastasis (305), contrary to its well-studied tumor suppressive role. 4E-BP levels also correlate with metastatic potential, allowing cells to better tolerate hypoxic stress, possibly through its ability to promote a switch to cap-independent translation of pro-survival factors such as VEGF-A and Bcl-2 (306, 307).

In summary, our data indicate that cellular detachment generates significant energy stress, and that bioenergetic homeostasis following detachment is necessary for survival. We demonstrate a novel *anoikis* resistance pathway mediated by an AMPK-mTORC1 axis that suppresses protein synthesis. This axis appears to be specifically important for oncogene-transformed cells. The AMPK pathway is broadly considered to be tumor suppressive in nature, and pharmacologic activation of AMPK or inhibition of mTOR are currently under investigation as components of

cancer therapy. However, consideration of how these pathways may alter survival and potentially metastatic potential through their ability to suppress *anoikis* will be important in the development of cancer therapeutics and in our understanding of cancer progression.

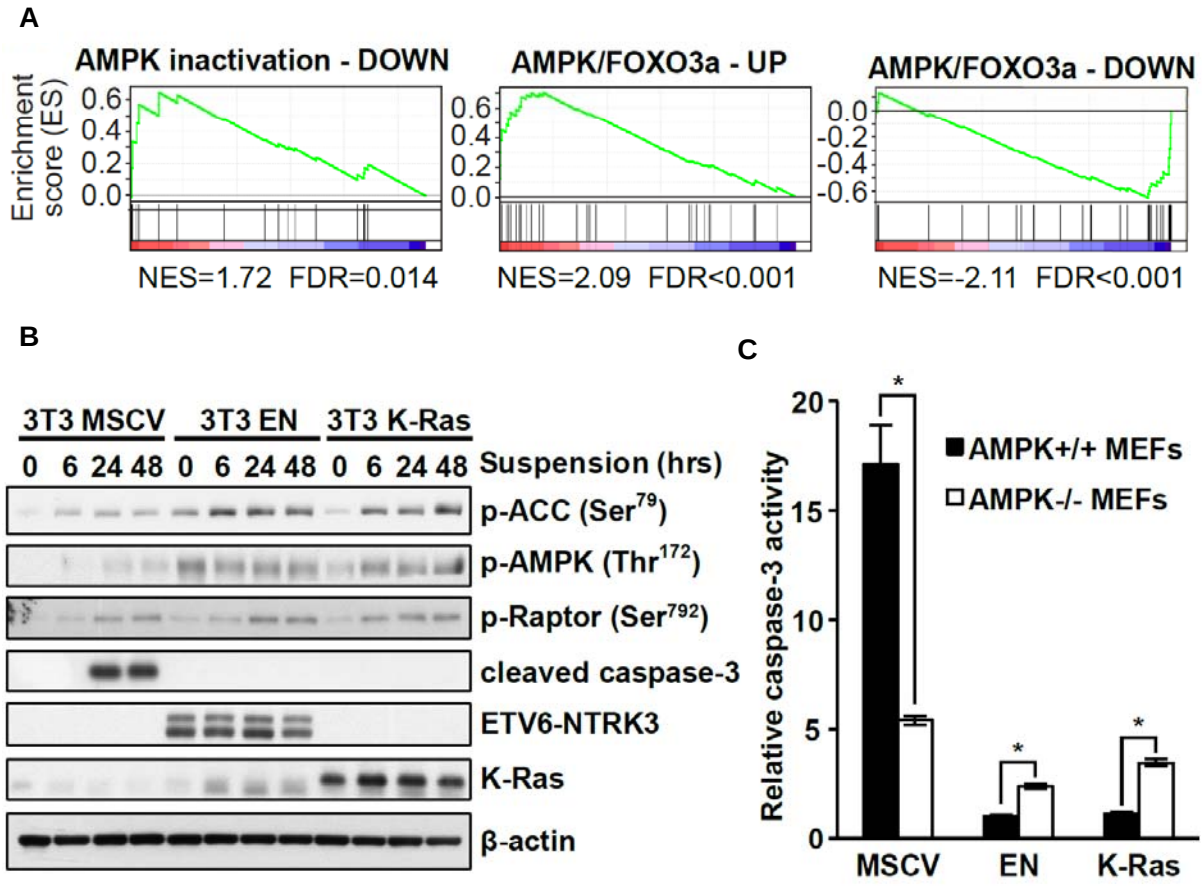

Figure 4.1. The AMPK pathway is activated following cellular detachment and promotes anoikis resistance. (A) GSEA analysis of detachment-induced gene expression profiles using annotated sets from the literature of genes known to be altered following AMPK pathway modulation. (B) Western blot demonstrating levels of p-ACC, p-Raptor and p-AMPK as readouts of AMPK pathway activation at various time-points following detachment of transformed and non-transformed NIH3T3 cells. EN and K-Ras(V12) levels are shown by NTRK3 and K-Ras immunoblotting, respectively. Cleaved caspase-3 immunoblotting demonstrates levels of apoptosis in transformed versus non-transformed cells. β-actin is used as a loading control. (C) Caspase-3 activity assay of MSCV vector-alone, EN or K-Ras transformed *AMPK+/+* versus *AMPK-/-* MEFs after 48 hours in suspension. All data are shown as mean ± SEM (n=3). An asterisk indicates statistical significance as determined by Student's t-test (*$p < 0.05$).

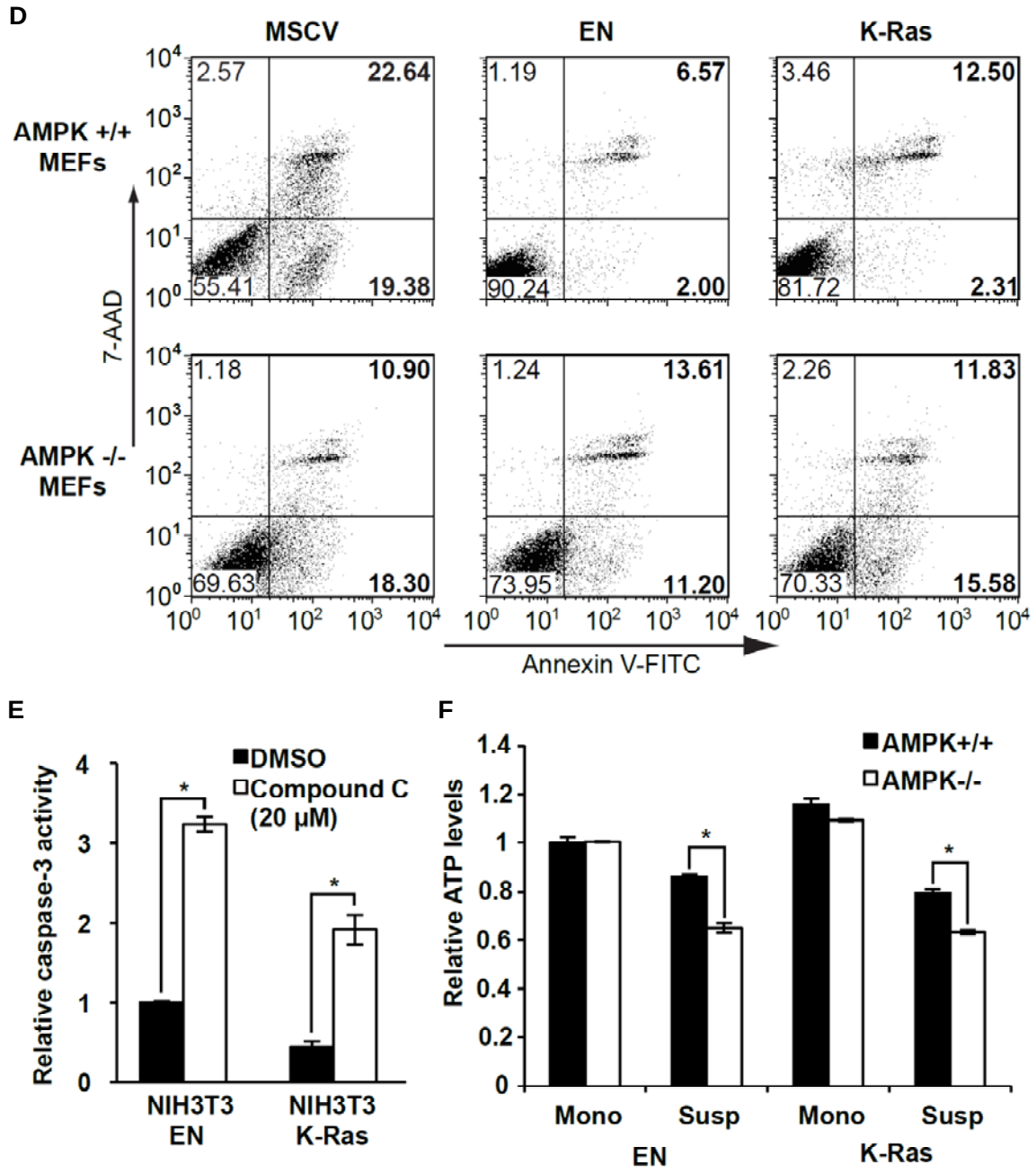

Figure 4.1 (cont'd). The AMPK pathway is activated following cellular detachment and promotes anoikis resistance. (D) AnnexinV/7-aminoactinomycin D (AAD) FACS analysis of MSCV vector-alone, EN or K-Ras transformed *AMPK+/+* versus *AMPK-/-* MEFs after 48 hours in suspension. (E) Caspase-3 activity assay of EN or K-Ras transformed NIH3T3 cells treated with compound C immediately following detachment and cultured in suspension for 48 hours. (F) ATP assay of EN or K-Ras transformed *AMPK+/+* versus -/- MEFs following 24 hours in suspension. All data are shown as mean ± SEM (n=3). An asterisk indicates statistical significance as determined by Student's t-test (*$p < 0.05$).

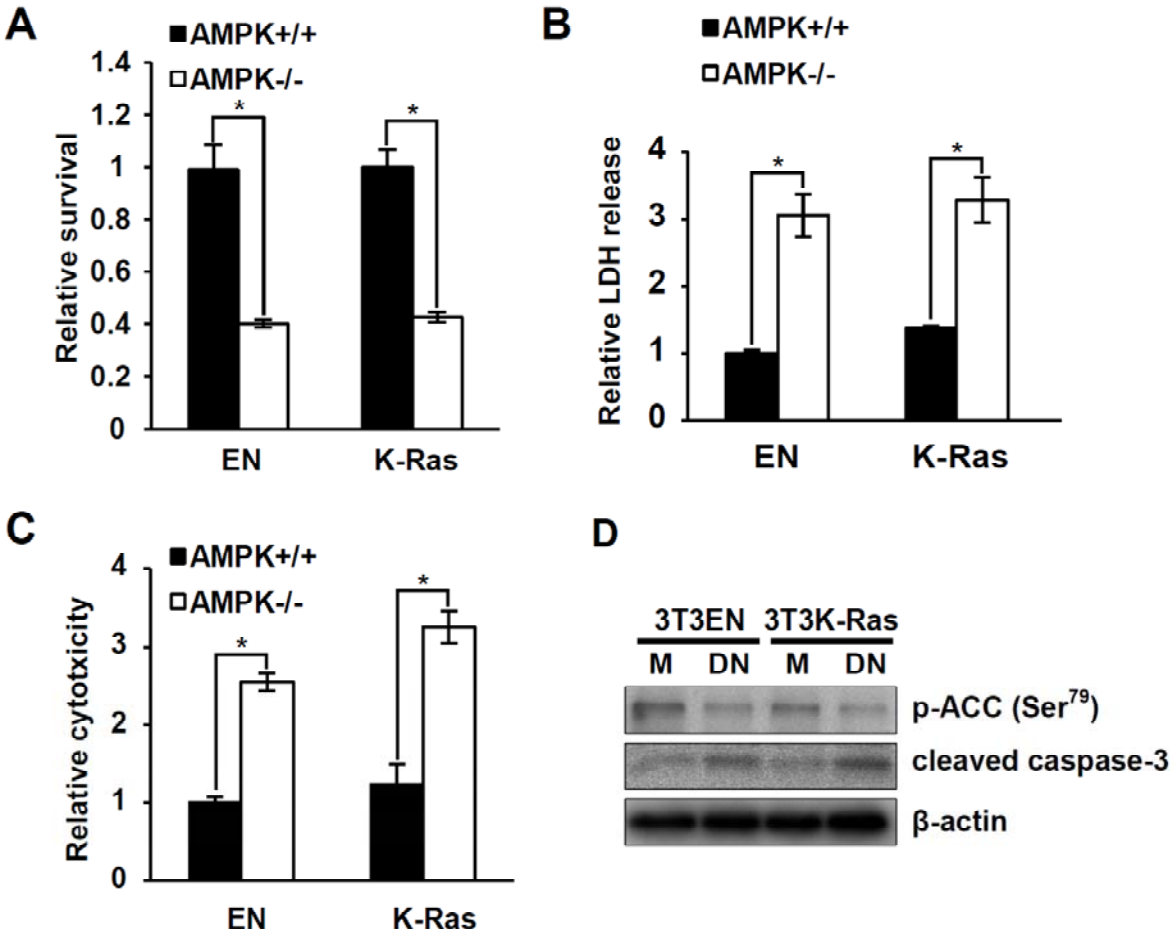

Figure 4.2. AMPK inhibition promotes sustained mTOR activity following detachment, and AMPK deficiency is associated with reduced *anoikis* resistance. (A) Alamar Blue cell survival assay of EN or K-Ras transformed *AMPK+/+* versus *AMPK-/-* MEFs after 48 hours in suspension. (B) LDH release cytotoxicity assay of EN or K-Ras transformed *AMPK+/+* versus *AMPK-/-* MEFs after 48 hours in suspension. (C) Cytotox-Glo cytotoxicity assay of EN or K-Ras transformed *AMPK+/+* versus *AMPK-/-* MEFs after 24 hours in suspension. (D) Western blots of EN or K-Ras transformed NIH3T3 cell lines expressing a dominant negative (DN) AMPK construct or MSCV vector alone, cultured in suspension for 72 hours. AMPK pathway inhibition was determined by p-ACC blotting, and cleaved caspase-3 was used to determine relative apoptosis levels. All data are shown as mean ± SEM (n=3). An asterisk indicates statistical significance as determined by Student's t test (*$p < 0.05$).

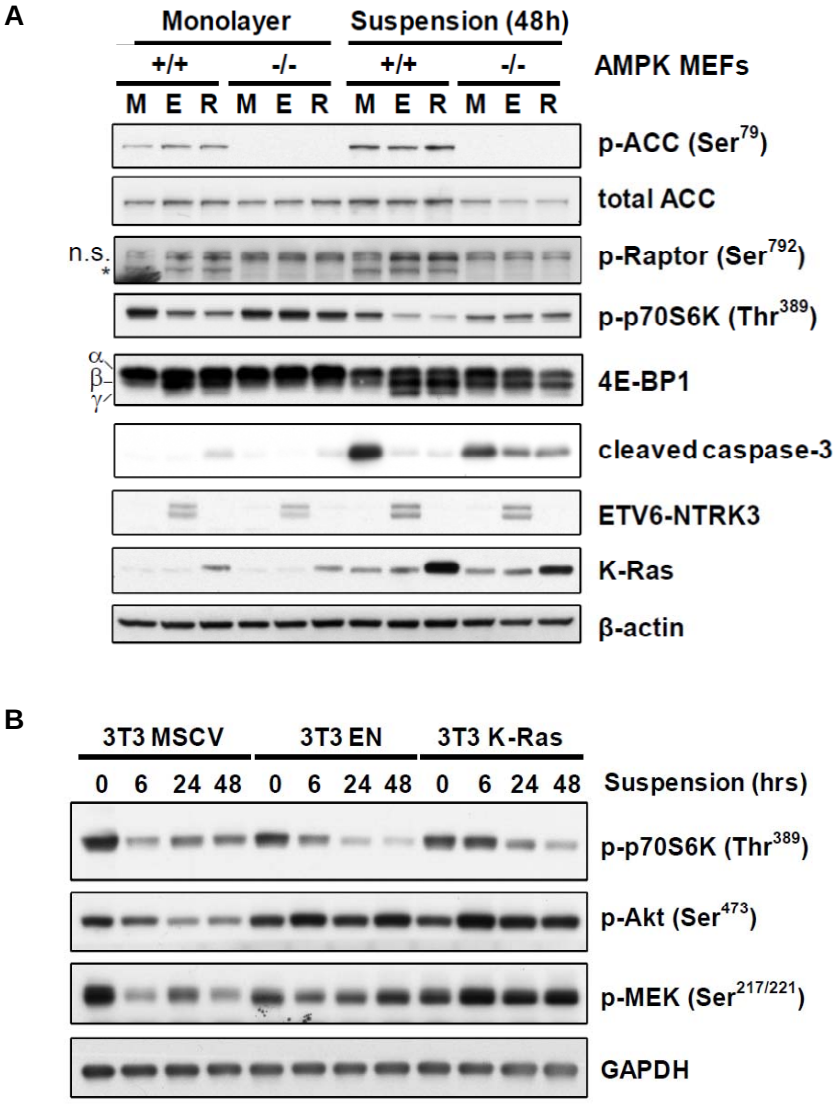

Figure 4.3. mTORC1 pathway inhibition is dependent on both AMPK activation and oncogenic transformation and promotes anoikis resistance. (A) Western blot of transformed and non-transformed *AMPK+/+* versus *-/-* MEFs 48 hours following plating as monolayer or suspension cultures, using antibodies to the indicated proteins as pathway readouts for AMPK (p-ACC and p-Raptor) and mTORC1 (p-p70S6K and 4E-BP1). EN and K-Ras(V12) levels are demonstrated as in Fig. 2B, cleaved caspase-3 levels are shown to reflect levels of apoptosis, and β-actin is used as a loading control. (B) Western blot of NIH3T3 cells expressing MSCV vector alone versus EN or K-Ras(V12) demonstrating the indicated readouts of mTORC1 (p-p70S6K), PI3K-Akt (p-Akt), and Ras-ERK (p-MEK) pathway activities at various time-points after detachment. GAPDH is used as a loading control.

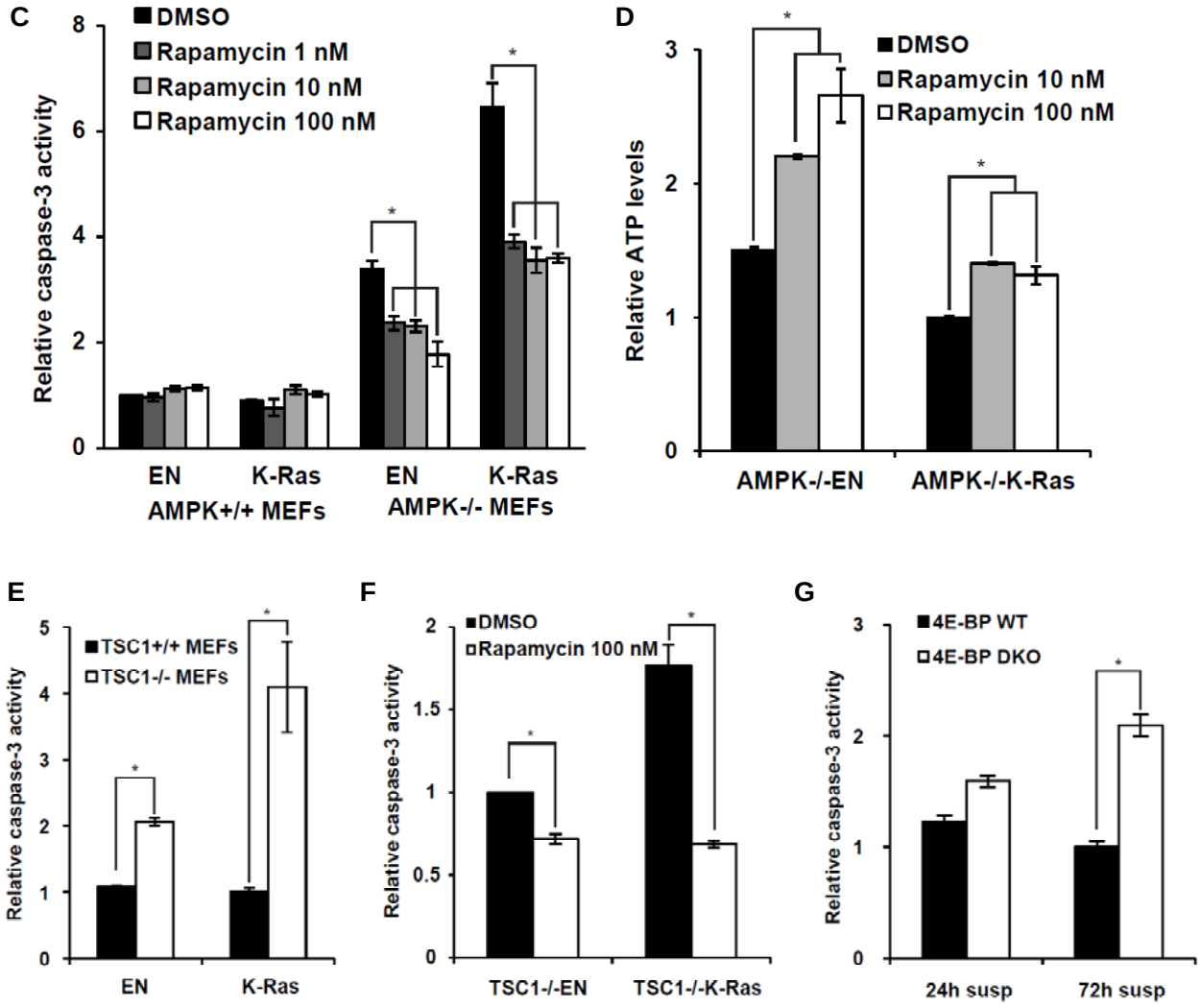

Figure 4.3 (cont'd). mTORC1 pathway inhibition is dependent on both AMPK activation and oncogenic transformation and promotes anoikis resistance. (C) Caspase-3 activity assay of EN or K-Ras transformed *AMPK+/+* versus *-/-* MEFs treated with a dose response curve of rapamycin immediately following detachment, and cultured in suspension for 48 hours. (D) ATP assay of rapamycin-treated EN or K-Ras expressing *AMPK-/-* MEFs after 24 hours in suspension. (E) Caspase-3 activity assay of EN or K-Ras transformed *TSC1+/+* versus *TSC1-/-* MEFs subjected to 48 hours in suspension. (F) Caspase-3 activity assay of EN or K-Ras expressing *TSC1-/-* MEFs treated with rapamycin and subjected to 48 hours in suspension. (G) Caspase-3 activity assay of 4E-BP1 *wt* versus double knockout (DKO) MEFs expressing E1A/Ras at 24 hours and 72 hours following detachment. All data are shown as mean ± SEM (n=3). An asterisk indicates statistical significance as determined by Student's t test (*$p < 0.05$).

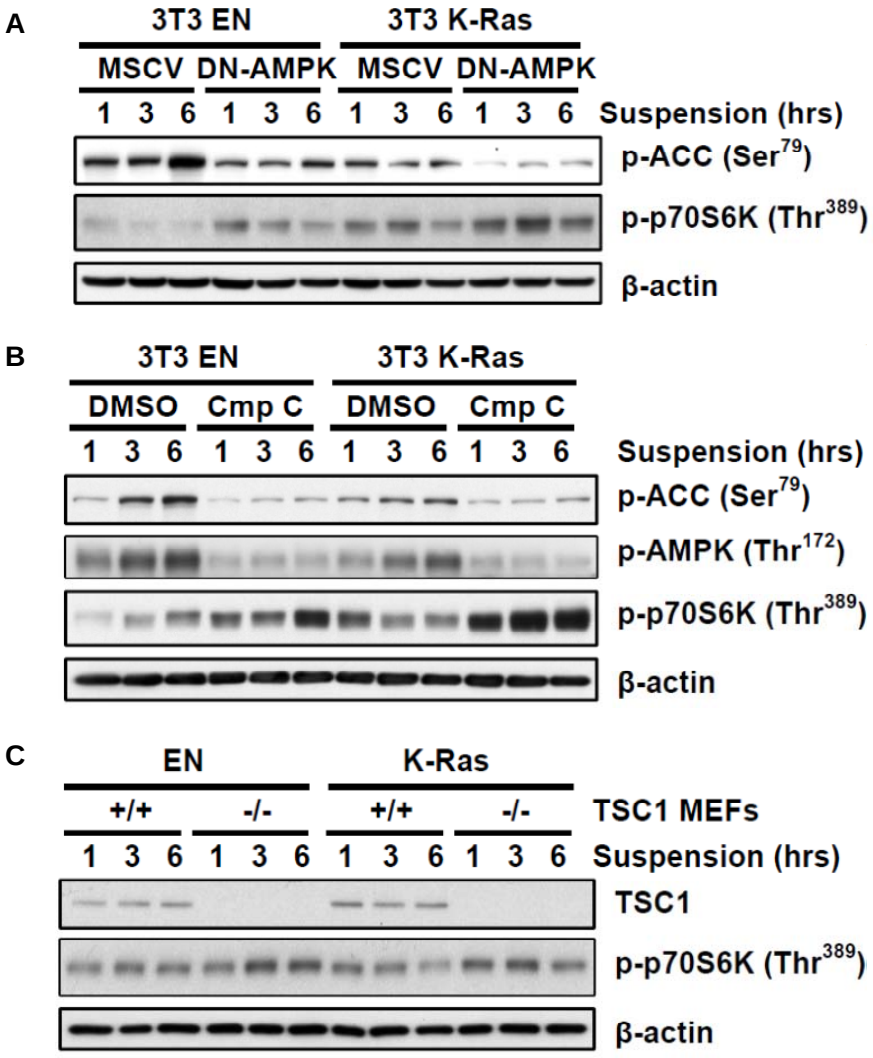

Figure 4.4. AMPK inhibition or *TSC1* deficiency is sufficient to restore mTORC1 activity in detachment conditions, and sustained mTORC1 activity is associated with reduced *anoikis.* (A) Western blots of EN or K-Ras transformed NIH3T3 cell lines expressing DN-AMPK versus vector alone, and cultured in suspension for the indicated times. AMPK pathway inhibition was determined using p-ACC, and relative mTORC1 activity was determined using p-p70S6K as readout. (B) Western blots of EN or K-Ras transformed NIH3T3 cell lines treated with the AMPK inhibitor compound C (20 μM) versus DMSO vehicle control, and cultured in suspension for the indicated times. AMPK pathway inhibition was determined using p-ACC and p-AMPK, and relative mTORC1 activity was determined using p-p70S6K as readout. (C) Western blots of EN or K-Ras transformed *TSC1+/+* versus *TSC1-/-* MEFs cultured in suspension for the indicated times. Levels of p-p70S6K were used as readout of mTORC1 activity. β-actin was used as a loading control.

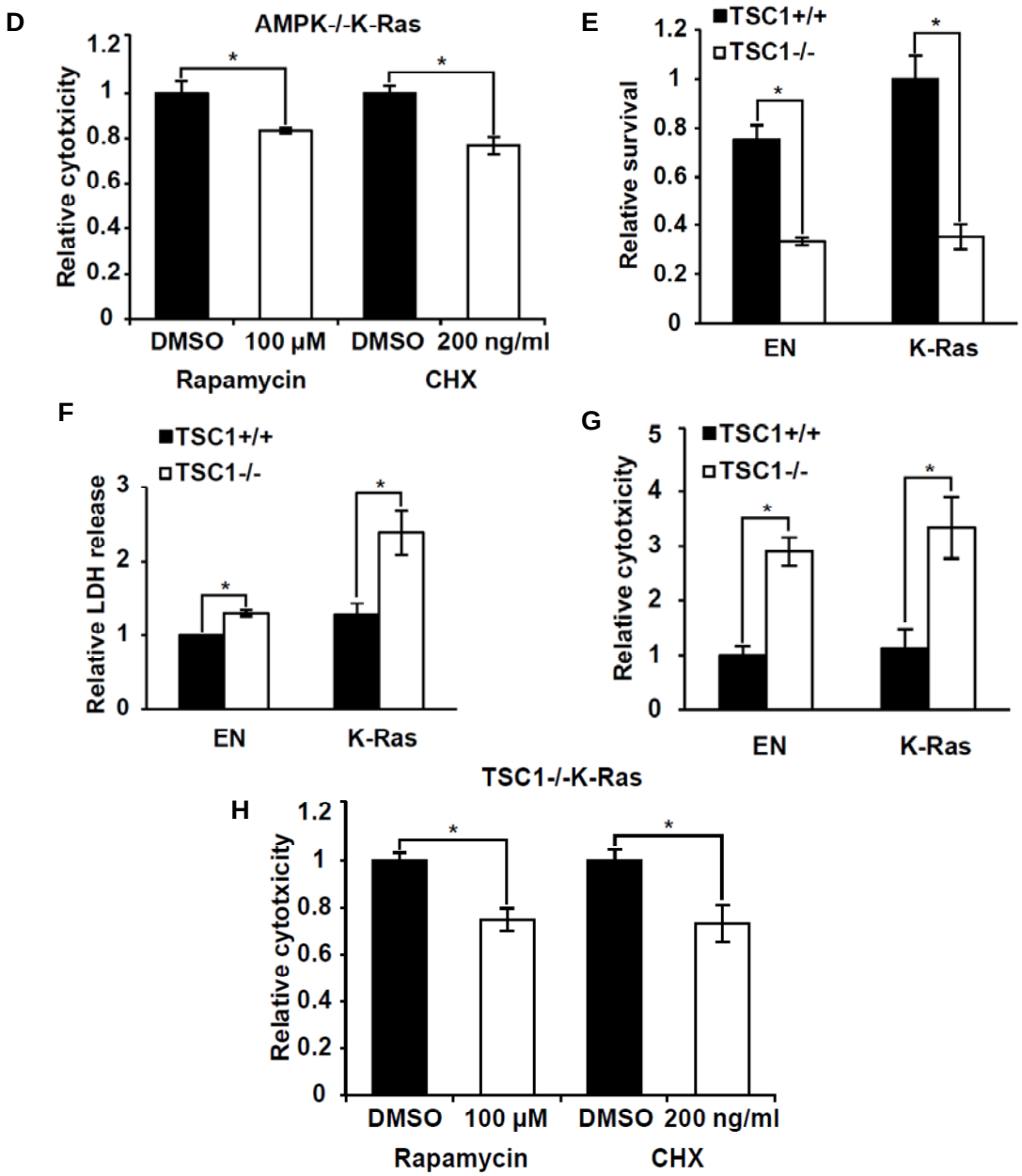

Figure 4.4. AMPK inhibition or TSC1 deficiency is sufficient to restore mTORC1 activity in detachment conditions, and sustained mTORC1 activity is associated with reduced anoikis (cont'd). (D) Cytotox-Glo cytotoxicity assay of rapamycin-treated EN or K-Ras expressing *AMPK-/-* MEFs after 24 hours in suspension. (E) Alamar Blue cell survival assay of EN or K-Ras transformed *TSC1+/+* versus *TSC1-/-* MEFs after 48 hours in suspension. (F) LDH release cytotoxicity assay of EN or K-Ras transformed *TSC1+/+* versus *TSC1-/-* MEFs after 48 hours in suspension. (G) Cytotox-Glo cytotoxicity assay of EN or K-Ras transformed *TSC1+/+* versus *TSC1-/-* MEFs after 48 hours in suspension. (H) Cytotox-Glo cytotoxicity assay of rapamycin-treated EN or K-Ras expressing *TSC1-/-* MEFs after 24 hours in suspension. All data are shown as mean ± SEM (n=3). An asterisk indicates statistical significance as determined by Student's t test (*$p < 0.05$).

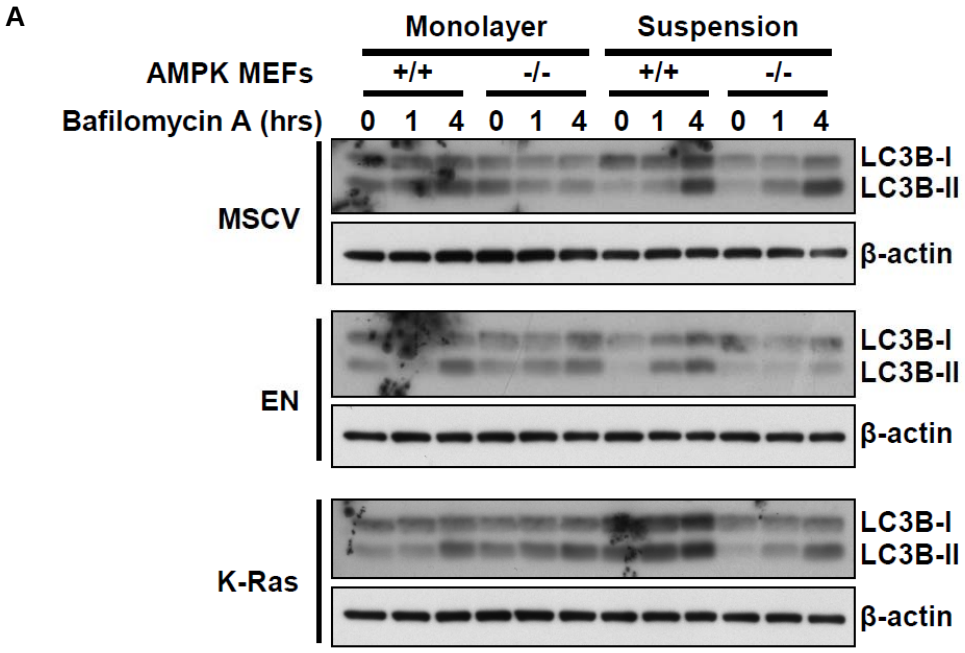

Figure 4.5. Autophagic flux is increased following cellular detachment, but loss of autophagy is insufficient to restore *anoikis* in EN or K-Ras transformed cells. (A) Western blot of LC3B-II levels in *AMPK+/+* versus *AMPK-/-* MEFs expressing EN or K-Ras versus MSCV vector alone following bafilomycin A inhibition to assay for autophagic flux in monolayer versus 24-hour suspension cultures. β-actin is used as a loading control.

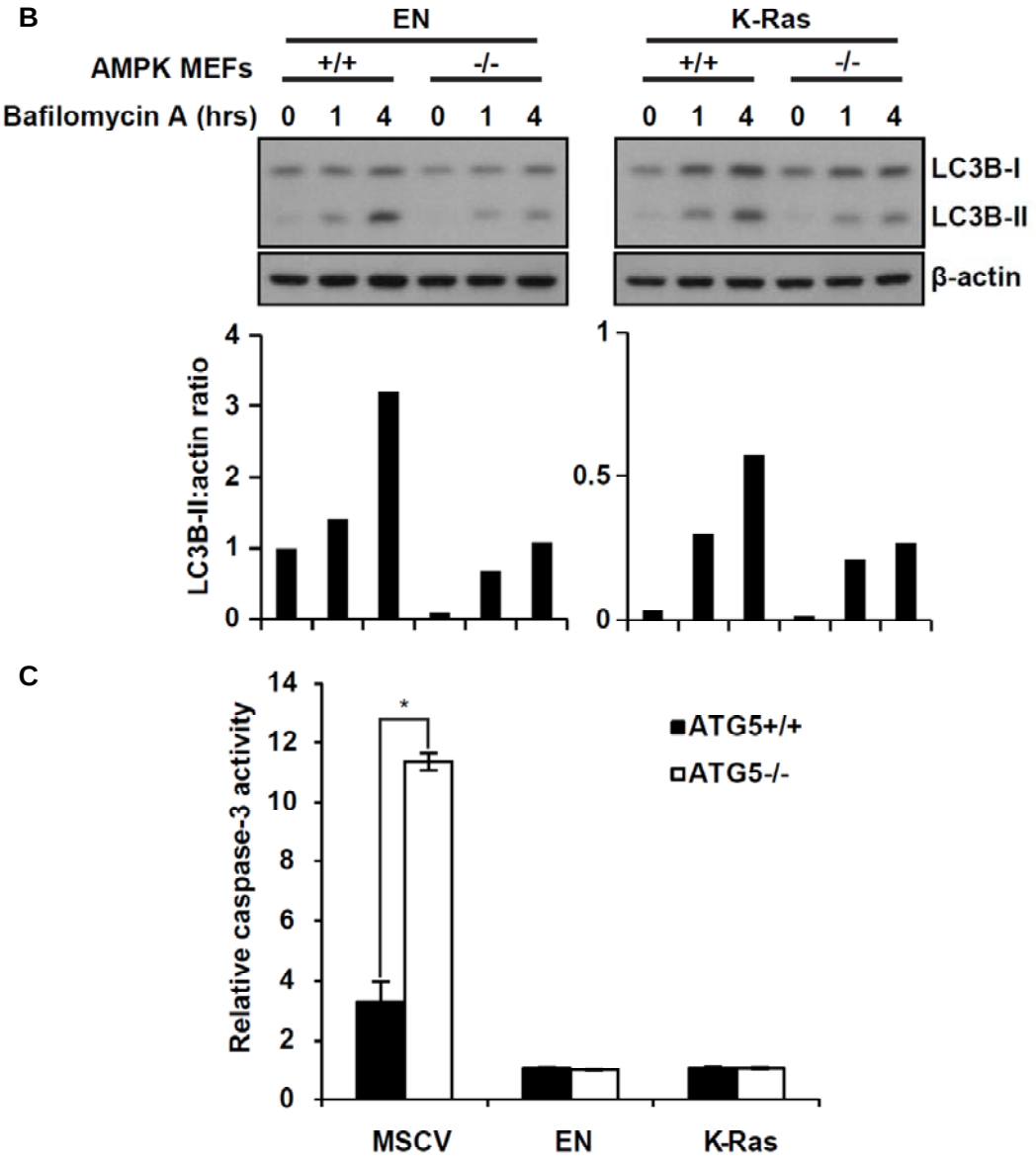

Figure 4.5 (cont'd). Autophagic flux is increased following cellular detachment, but loss of autophagy is insufficient to restore *anoikis* in EN or K-Ras transformed cells. (B) Densitometric quantification of the ratios of LC3B-II/β-actin immunoblot levels in EN or K-Ras transformed *AMPK+/+* versus *AMPK-/-* MEFs. (C) Caspase-3 activity in EN or K-Ras or MSCV vector-alone expressing *ATG5+/+* versus *ATG5-/-* MEFs following 72 hours in suspension. All data are shown as mean ± SEM (n=3). An asterisk indicates statistical significance as determined by Student's t test (*$p < 0.05$).

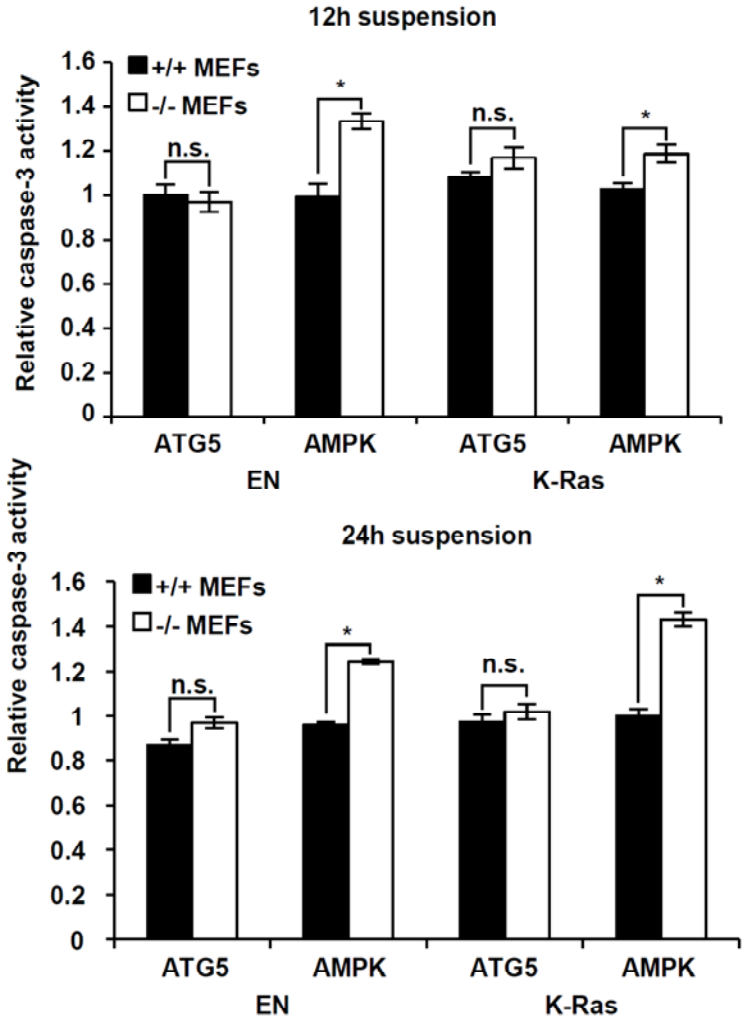

Figure 4.6. *ATG5* deficiency is insufficient to restore *anoikis* in EN- and K-Ras transformed MEFs at early time-points following detachment. Caspase-3 activity in EN/K-Ras expressing *AMPK* or *ATG5* +/+ and -/- MEFs, following 12 and 24 hours in suspension. For each time-point and MEF cell line, *AMPK* and *ATG5* +/+ and -/- cells are compared side-by-side. All data are shown as means ± SEM (n=3). An asterisk indicates statistical significance as determined by Student's t test (*$p < 0.05$).

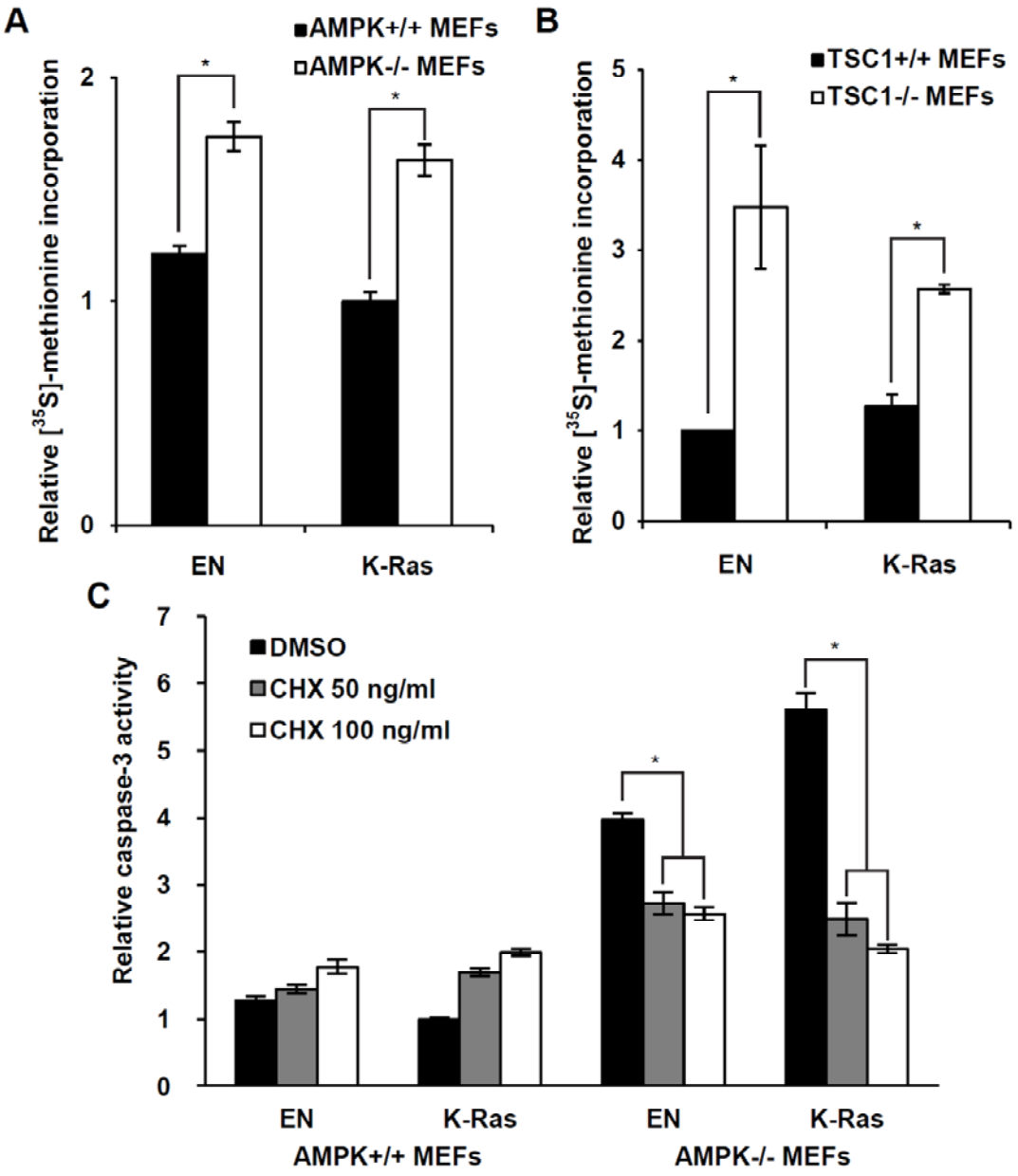

Figure 4.7. Inhibition of protein synthesis partially restores ATP levels and promotes anoikis resistance in cells with sustained mTORC1 activity following cellular detachment. (A, B) Assay of global protein synthesis rates as measured by levels of 35S-methionine/cysteine incorporation into newly synthesized proteins in *AMPK+/+/TSC1+/+* versus *AMPK-/-/TSC1-/-* MEFs expressing EN or K-Ras 48 hours after detachment. (C) Caspase-3 activity in *AMPK+/+* versus *AMPK-/-* EN or K-Ras-transformed MEFs treated with low-dose cycloheximide and assayed after 48 hours in suspension.

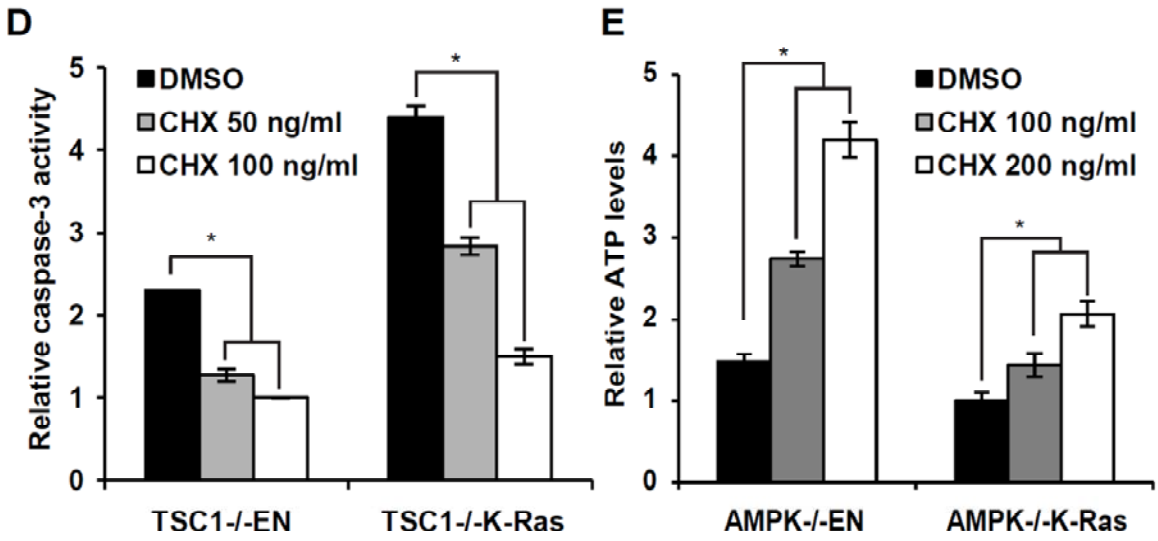

Figure 4.7 (cont'd). Inhibition of protein synthesis partially restores ATP levels and promotes anoikis resistance in cells with sustained mTORC1 activity following cellular detachment. (D) Caspase-3 activity in cycloheximide-treated *TSC1-/-* MEFs transformed with EN or K-Ras after 48 hours in suspension. (E) ATP levels in cycloheximide-treated *AMPK-/-* MEFs transformed with EN or K-Ras after 24 hours in suspension. All data are shown as mean ± SEM (n=3). An asterisk indicates statistical significance as determined by Student's t test (*p < 0.05).

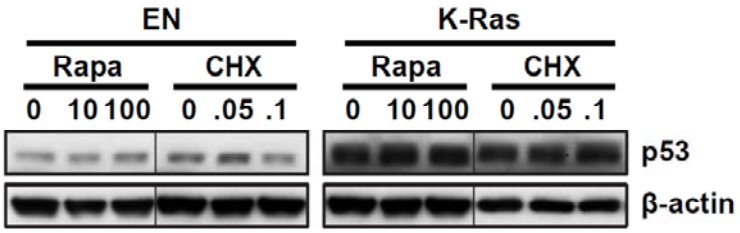

Figure 4.8. Increased *anoikis* resistance seen following inhibition of protein synthesis is not associated with reduced p53 levels. Western blots of EN or K-Ras expressing *AMPK-/-* MEFs treated with rapamycin (Rapa) or cycloheximide (CHX) at the indicated doses, and cultured in suspension for 24 hours. Total p53 protein levels were analyzed, and β-actin was used as a loading control.

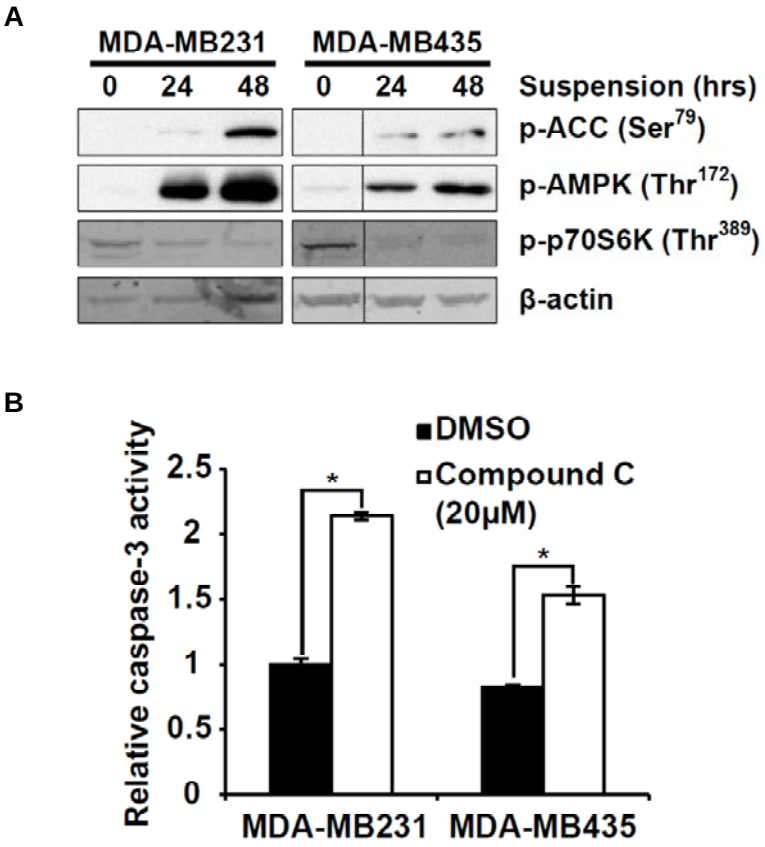

Figure 4.9. *Anoikis*-resistant breast carcinoma cell lines activate AMPK and suppress mTORC1 following detachment, and AMPK inhibition partially restores *anoikis*. (A) Western blot demonstrating levels of p-ACC, p-AMPK and p-p70S6K as readouts of AMPK and mTORC1 pathway activity in MDA-MB-231 and MDA-MB-435 breast cancer cell lines at the indicated time-points following detachment. β-actin is used as a loading control. (B) Caspase-3 activity assays of MDA-MB-231 and MDA-MB-435 cell lines treated with compound C immediately following detachment and cultured in suspension for a further 48 hours. All data are shown as mean ± SEM (n=3). An asterisk indicates statistical significance as determined by Student's t test (*$p < 0.05$).

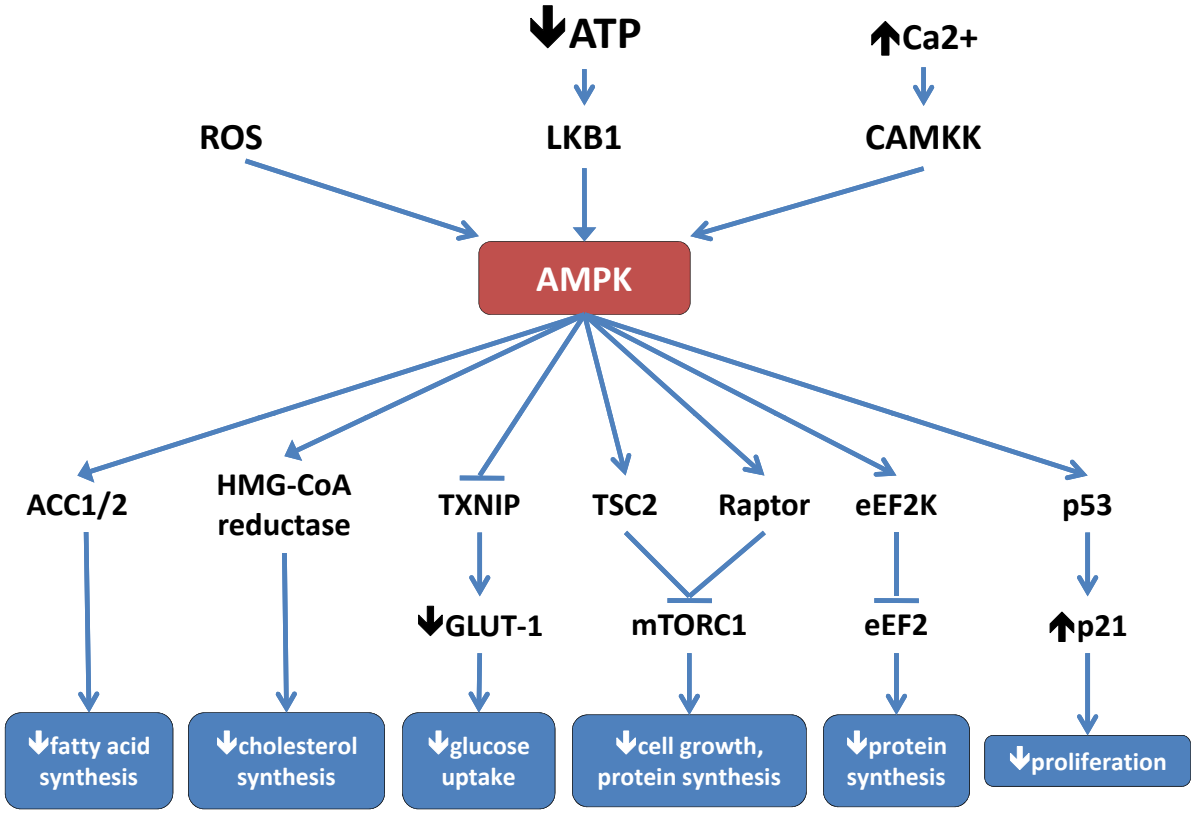

Figure 4.10. Schematic summarizing the upstream activators, downstream phosphorylation targets and metabolic processes regulated by AMPK.

Chapter 5 CONCLUSIONS AND FUTURE STUDIES

In this thesis, we detail the results of the various approaches we used to elucidate novel mechanisms of suppression of *anoikis* in cancer cells, with the major finding in our studies demonstrating a pro-survival role for cellular stress response mechanisms in promoting *anoikis* resistance. In congruence with prior studies in other cellular stress types, our studies show that anti-metabolic pathways such as the AMPK/mTOR axis have an important pro-survival role for cancer cells during transient states of stress, despite such pathways being conventionally accepted as "tumor suppressive." Such metabolic stress may in part be mediated by ER stress-related elevation of TXNIP levels, a known metabolic modulator that suppresses glucose uptake, thus acting as a promoter of *anoikis* cell death. The findings therefore suggest a model in which tumor cells undergoing metastasis, initially subjected to the metabolic stress associated with *anoikis*, requires transient activation of AMPK or other pathways to maintain survival during these initial stages of metastasis (Figure 5.1). Ultimately, such cells would then need to restore their proliferative and metabolically-active pathways to allow growth at secondary organ sites. While these results illustrate an intriguing link between bioenergetic cellular stress, *anoikis* and metastasis, they also raise novel avenues for future studies.

One of the most intriguing but unanswered questions arising from our studies and from *anoikis* studies in general relates to the biological relevance of the *anoikis* phenomenon. One biological phenomenon that cellular detachment is thought to

closely mimic is that of lymphovascular invasion of tumor cells, and the development of lymphovascular tumor emboli. As mentioned, this represents a well-recognized histologic predictor of tumor aggressivity in a number of tumor types, and is proposed to represent a critical initial step in the development of metastases. As multiple mechanisms have been identified that promote both *anoikis* resistance and the development of lymphovascular emboli, such as E-cadherin (which both promotes *anoikis* resistance and survival of lymphovascular emboli) (50, 109), and transdifferentiation into a stem cell-like phenotype (49, 308), this suggests a relationships between *anoikis* resistance and the ability to develop lymphovascular emboli. However, it has not yet been shown whether there is evidence of cellular or metabolic stress in such lymphovascular emboli, or whether corresponding stress response mechanisms are activated. We have demonstrated preliminarily that lymphovascular emboli also show activation of AMPK using phospho-eEF2 immunohistochemistry, comparing primary breast tumor invasive carcinoma cells with corresponding tumor cells in lymphovascular spaces within the same slide (Figure 5.2). Such studies were limited to a few cases, but further exploration by immunohistochemistry may help further establish a link between our *in vitro* model of cellular detachment and *anoikis* resistance, and the clinically-established phenomenon of lymphovascular invasion.

At a more clinically relevant level, an important line of investigation would be to study the expression profile as well as the proliferative and metabolic status of circulating tumor cells (CTCs). If detached tumor cells *in vitro* do in fact reflect metastatic cells in transit *in vivo*, we would hypothesize that such circulating tumor

cells would demonstrate reduced proliferation and metabolic activity as compared to cells from the primary tumor. As mentioned, such circulating tumor cells have been found to exist as both single tumor cells as well as circulating tumor microemboli (CTM), which in particular show reduced cellular proliferation and apoptotic activity (8). Due to their resemblance to the tumor spheroids that we observe in suspension cultures following cellular detachment, a key question that arises is whether such CTMs show phenotypic evidence of cellular stress, in particular activation of the AMPK pathway, suppression of the mTORC1 pathway and elevation of TXNIP levels. It would also be intriguing to determine whether there is activation of other stress response pathways in these CTMs, such as the ER stress or hypoxic response. As such CTCs and CTMs are rare in numbers, even patients with widely metastatic disease (309), such phenotypic characterization may be technically difficult; alternatively, a genomic approach would be feasible, through next-generation-based sequencing and expression profiling of these CTCs/CTMs, particularly with the advent of single cell-based genomic technologies (310).

Mechanistically, one of the most intriguing questions arising from our studies of AMPK in *anoikis* resistance relates to our unexpected finding of a paradoxical reliance of detached cells on oncogenes such as activated K-Ras and EN to suppress mTORC1, despite concurrent hyperactivation of Akt, in contrast to non-transformed cells which appear unable to suppress the mTORC1 pathway during detachment-induced stress. One possible explanation for this apparent uncoupling of Akt activation from mTORC1 signaling is the maintenance of a stress-specific

transcriptional program mediated by FoxO transcription factors (265). Under many stress conditions FoxO proteins become activated, presumably through AMPK-mediated phosphorylation (263), and suppress mTORC1 activity through up-regulation of Sestrin3 and Rictor (265). Importantly, FoxO activity appears to be maintained under stress conditions regardless of Akt activity, which otherwise suppresses FoxO levels under normal conditions. In our model systems, where PI3K-Akt is constitutively activated through oncogene expression, we propose that Akt-mediated inhibitory phosphorylation of FoxO factors may somehow be blocked or ineffective under detachment. The ability of FoxO3A to remain activated despite Akt activity might therefore allow cells to maintain both the pro-survival functions of FoxO factors and the anti-apoptotic effects of Akt activation.

Another important mechanistic question is the role of other pathways downstream of AMPK that can also modulate protein synthesis that may contribute in a similar fashion to *anoikis* resistance as seen with mTORC1 inhibition. Importantly, the role of the eEF2K/eEF2 axis has been shown recently to play an important role in mediating cell survival during metabolic stress states, particular under nutrient deprivation conditions (23). Similar to our findings, this paper illustrates a pro-survival role for inhibition of protein translation during such stress conditions, through inhibition of translation elongation rather than translation initiation as would be expected under mTORC1-inhibited conditions. While we also see phosphorylation of eEF2 following cellular detachment (data not shown), as would be expected under conditions of AMPK activation, we would also predict a role for translation elongation inhibition in helping to promote *anoikis* resistance.

Multiple reports in the recent literature describe a very interesting link between the AMPK and TXNIP pathways that have clear relevance to our findings. Wu, Cantley and colleagues demonstrate that TXNIP is a direct phosphorylation target of AMPK, with such phosphorylation triggering a rapid degradation of TXNIP (251). As mentioned, such regulation of TXNIP modulates glucose uptake, and we propose that this may partially explain the mechanism by which AMPK activation helps to restore the bioenergetic status of cells during detachment-induced stress. We have shown in preliminary studies that TXNIP may be hyperphosphorylated in AMPK wild-type cells as compared to AMPK knockdown cells following cellular detachment, as demonstrated by the slight apparent increase in molecular weight of the TXNIP band by Western blot in *AMPK+/+* cells as compared to *AMPK-/-* cells, in both EN-transformed cells and MSCV vector control cells (Figure 5.3). Interestingly, in the EN-transformed cells, levels of TXNIP are increased in the setting of AMPK knockout, supportive of a role for AMPK in the degradation of TXNIP as previously described. However, the converse is observed in MSCV control cells, and it is unclear why TXNIP is not also highly elevated in *AMPK-/-* MSCV control cells. Critical future studies would include look into the effect of the observed TXNIP up-regulation on glucose uptake, as well as GLUT-1 levels, under cellular detachment conditions; we hypothesize that such experiments would confirm an inhibitory role for TXNIP on GLUT-1 levels and glucose uptake. In addition, such studies would ideally show a role for such AMPK phosphorylation of TXNIP in promoting its degradation, and that forced re-expression of TXNIP under such conditions, particularly in transformed cells, would restore the normal suppression of glucose uptake, decreased ATP levels,

and therefore *anoikis* in these otherwise *anoikis*-resistant cells. Further studies would ideally show a direct role for this phosphorylation event in mediating *anoikis* through the use of TXNIP constructs mutated at the phosphorylation site, as well as explore the role of ER stress in this initial modulation of TXNIP levels.

In summary, our findings add to the growing evidence that metabolic regulation represents a critical arm in *anoikis* resistance (Figure 5.4). In addition to directly mitigating the cellular stress experienced by cancer cells following cellular detachment, these metabolic regulatory pathways counteract the energy-intensive processes driven by the other critical arm in *anoikis* resistance, namely the inhibition of apoptosis by PI3K/Akt and MAPK/Erk downstream of oncogenic kinases and receptor tyrosine kinases. In particular, our data supports an important role for AMPK in the cross-talk between these two arms of *anoikis* resistance, suppressing anabolic processes such as proliferation, cell growth and protein synthesis that are unnecessary during the process of cellular detachment and metastasis (Figure 5.4). Although cellular detachment and metastasis represent biomechanical processes involving the physical movement of tumor cells into the circulatory system, our studies and others show a role for such cell-autonomous cellular stress response pathways in modulating *anoikis*. Such cell-autonomous dependency on these stress response pathways therefore represents a unique target for therapy to suppress tumor metastasis, and offers insight into a role for normally "tumor-suppressive" anti-metabolic and anti-proliferative pathways in promoting tumor progression.

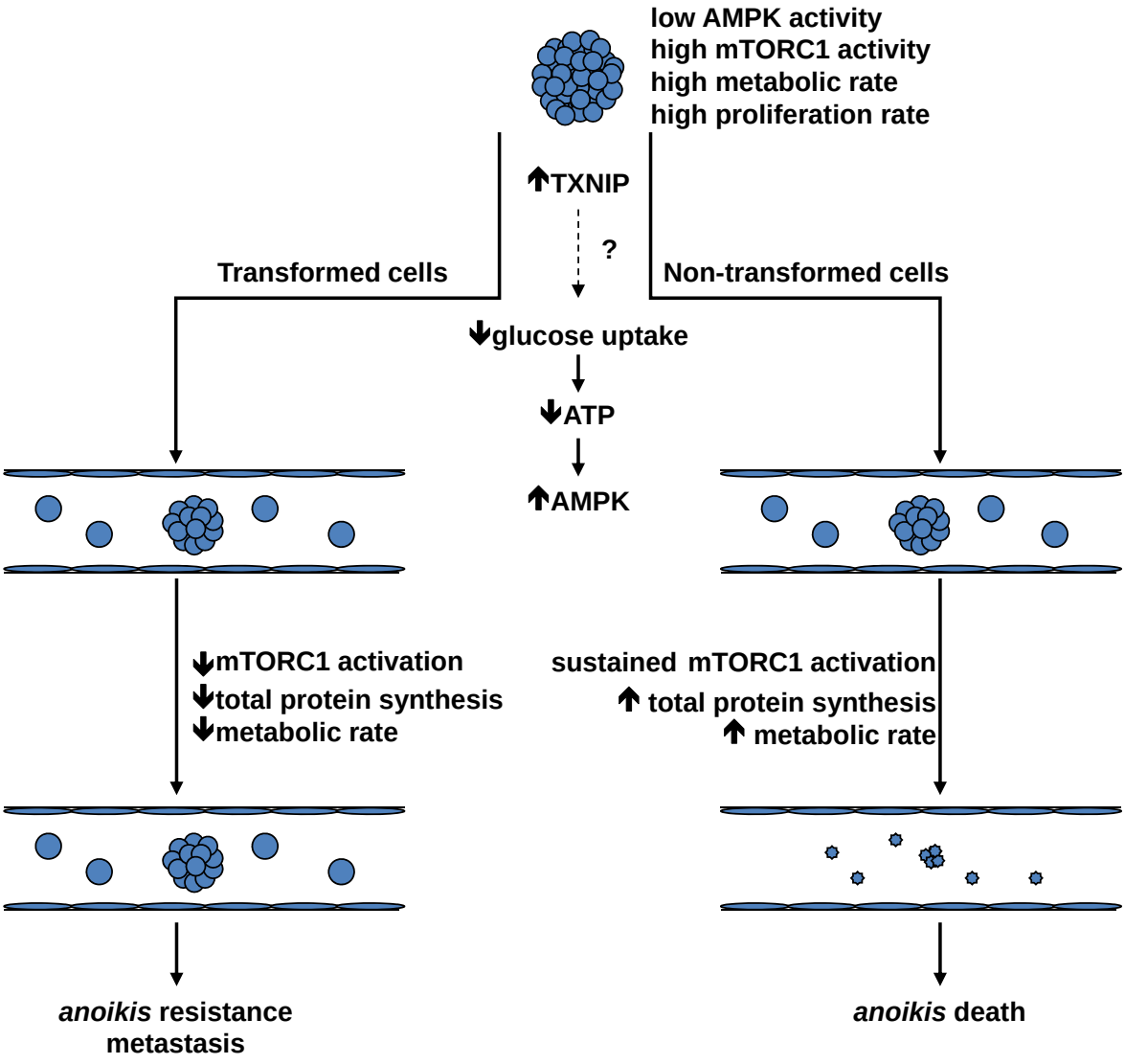

Figure 5.1. Proposed model for the role of cellular stress response pathways in *anoikis* resistance and tumor metastasis

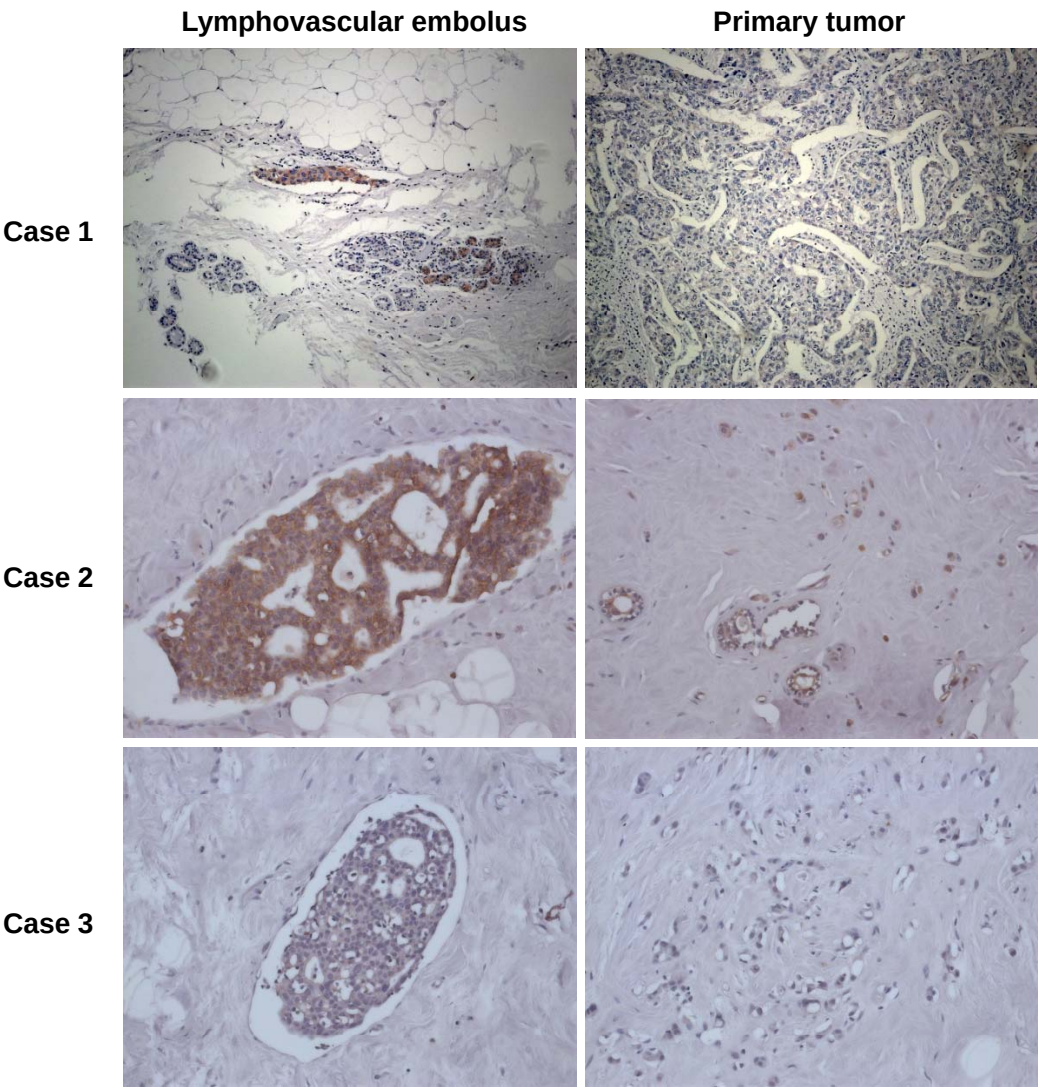

Figure 5.2. Breast cancer lymphovascular tumor emboli show evidence of AMPK pathway activation. Immunohistochemistry for phospho-eEF2 performed on cases of breast ductal carcinoma showing conspicuous lymphovascular invasion. Images demonstrate areas with either the lymphovascular tumor emboli versus a slide-matched area of the primary tumor.

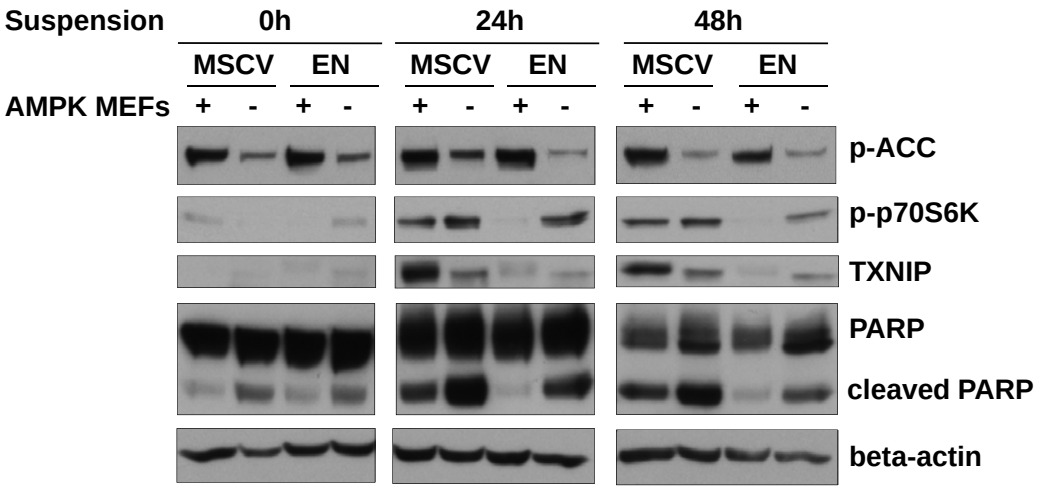

Figure 5.3. AMPK activation following cellular detachment is associated with possible hyperphosphorylation of TXNIP. Western blot of *AMPK+/+* and *AMPK-/-* MEFs transformed with either EN or MSCV vector control, following 0h, 24h or 48h in suspension. Phospho-ACC and phospho-p70S6K are used as readouts of AMPK activity, while PARP cleavage is used as a readout of apoptotic cell death. Beta-actin is used as a loading control.

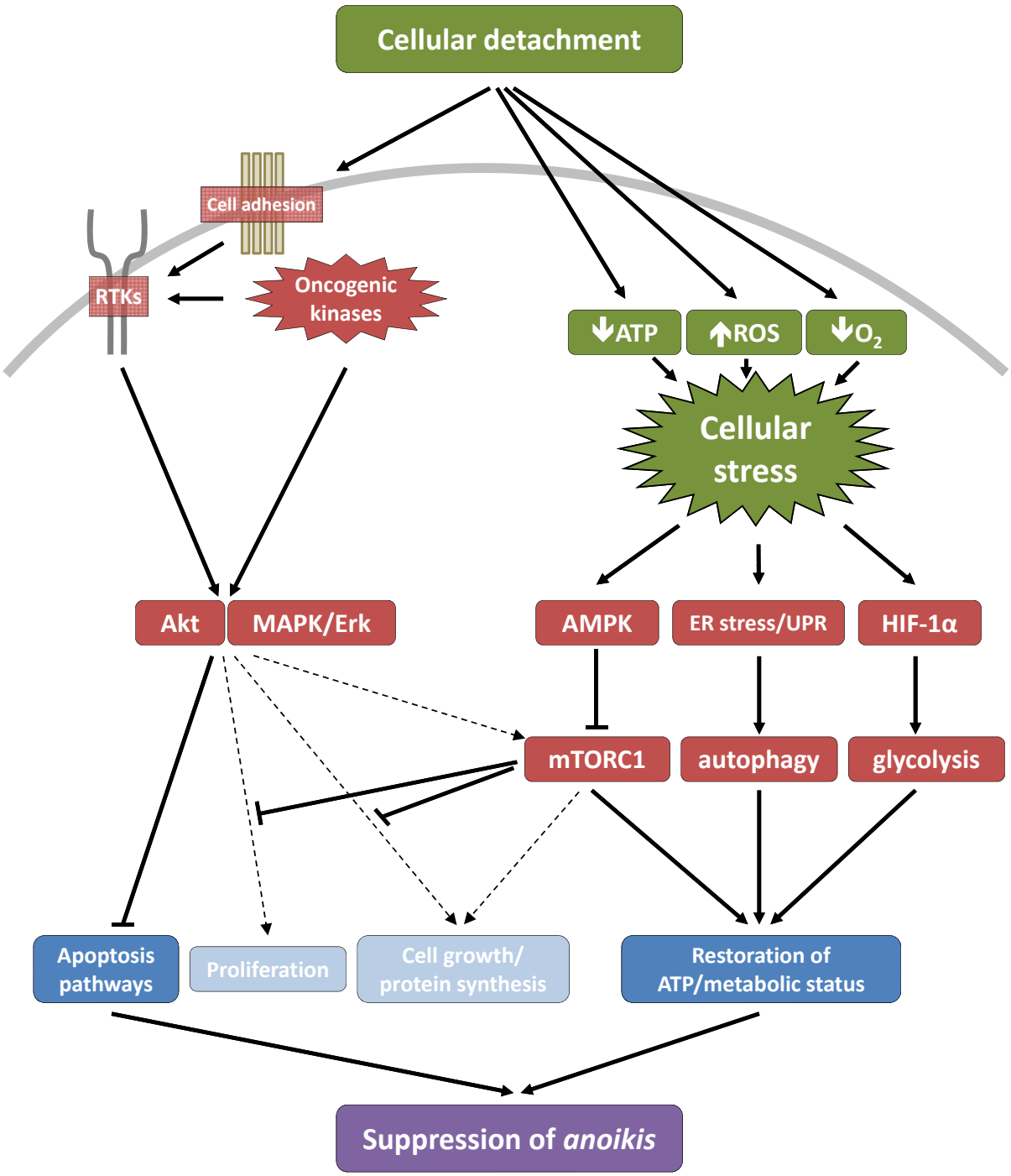

Figure 5.4. Schematic model of two major arms of *anoikis* resistance. One arm, mediated primarily by the Akt and MAPK/Erk pathways, is critical in suppressing the apoptotic mechanisms underlying *anoikis,* while the second arm represents the metabolic regulation mediated by various cellular stress response pathways. AMPK plays a particularly interesting role within this model, mediating crosstalk between these two mechanistic arms, in part through the mTORC1 pathway.

REFERENCES

1. Valastyan S, Weinberg RA. Tumor metastasis: molecular insights and evolving paradigms. *Cell* 2011 Oct 14; **147**(2)**:** 275-292.

2. Simpson CD, Anyiwe K, Schimmer AD. Anoikis resistance and tumor metastasis. *Cancer Lett* 2008 Dec 18; **272**(2)**:** 177-185.

3. Frisch SM, Francis H. Disruption of epithelial cell-matrix interactions induces apoptosis. *J Cell Biol* 1994 Feb; **124**(4)**:** 619-626.

4. Paoli P, Giannoni E, Chiarugi P. Anoikis molecular pathways and its role in cancer progression. *Biochim Biophys Acta* 2013 Dec; **1833**(12)**:** 3481-3498.

5. Buchheit CL, Rayavarapu RR, Schafer ZT. The regulation of cancer cell death and metabolism by extracellular matrix attachment. *Semin Cell Dev Biol* 2012 Jun; **23**(4)**:** 402-411.

6. American Cancer Society. Cancer Facts & Figures 2013. Atlanta: American Cancer Society; 2013.

7. Nguyen DX, Massague J. Genetic determinants of cancer metastasis. *Nat Rev Genet* 2007 May; **8**(5)**:** 341-352.

8. Hou JM, Krebs MG, Lancashire L, Sloane R, Backen A, Swain RK*, et al.* Clinical significance and molecular characteristics of circulating tumor cells and circulating tumor microemboli in patients with small-cell lung cancer. *J Clin Oncol* 2012 Feb 10; **30**(5)**:** 525-532.

9. Aguirre-Ghiso JA. Models, mechanisms and clinical evidence for cancer dormancy. *Nat Rev Cancer* 2007 Nov; **7**(11)**:** 834-846.

10. Holohan C, Van Schaeybroeck S, Longley DB, Johnston PG. Cancer drug resistance: an evolving paradigm. *Nat Rev Cancer* 2013 Oct; **13**(10)**:** 714-726.

11. Cleeland CS, Allen JD, Roberts SA, Brell JM, Giralt SA, Khakoo AY*, et al.* Reducing the toxicity of cancer therapy: recognizing needs, taking action. *Nat Rev Clin Oncol* 2012 Aug; **9**(8)**:** 471-478.

12. Malhotra V, Perry MC. Classical chemotherapy: mechanisms, toxicities and the therapeutic window. *Cancer Biol Ther* 2003 Jul-Aug; **2**(4 Suppl 1)**:** S2-4.

13. Taub JW. Factors in improved survival from paediatric cancer. *Drugs* 1998 Nov; **56**(5)**:** 757-765.

14. Hanahan D, Weinberg RA. The hallmarks of cancer. *Cell* 2000 Jan 7; **100**(1)**:** 57-70.

15. Zhang J, Hochwald SN. Targeting receptor tyrosine kinases in solid tumors. *Surg Oncol Clin N Am* 2013 Oct; **22**(4)**:** 685-703.

16. Levitzki A. Tyrosine kinase inhibitors: views of selectivity, sensitivity, and clinical performance. *Annu Rev Pharmacol Toxicol* 2013; **53:** 161-185.

17. Weil MK, Chen AP. PARP inhibitor treatment in ovarian and breast cancer. *Curr Probl Cancer* 2011 Jan-Feb; **35**(1)**:** 7-50.

18. Hanahan D, Weinberg RA. Hallmarks of cancer: the next generation. *Cell* 2011 Mar 4; **144**(5)**:** 646-674.

19. Kim JW, Gao P, Dang CV. Effects of hypoxia on tumor metabolism. *Cancer Metastasis Rev* 2007 Jun; **26**(2)**:** 291-298.

20. Luo J, Solimini NL, Elledge SJ. Principles of cancer therapy: oncogene and non-oncogene addiction. *Cell* 2009 Mar 6; **136**(5)**:** 823-837.

21. Freed-Pastor WA, Prives C. Mutant p53: one name, many proteins. *Genes Dev* 2012 Jun 15; **26**(12)**:** 1268-1286.

22. Dang CV. Links between metabolism and cancer. *Genes Dev* 2012 May 1; **26**(9)**:** 877-890.

23. Leprivier G, Remke M, Rotblat B, Dubuc A, Mateo AR, Kool M*, et al.* The eEF2 kinase confers resistance to nutrient deprivation by blocking translation elongation. *Cell* 2013 May 23; **153**(5)**:** 1064-1079.

24. Wang X, Eno CO, Altman BJ, Zhu Y, Zhao G, Olberding KE*, et al.* ER stress modulates cellular metabolism. *Biochem J* 2011 Apr 1; **435**(1)**:** 285-296.

25. Jones RG, Plas DR, Kubek S, Buzzai M, Mu J, Xu Y*, et al.* AMP-activated protein kinase induces a p53-dependent metabolic checkpoint. *Mol Cell* 2005 Apr 29; **18**(3)**:** 283-293.

26. Gupta GP, Massague J. Cancer metastasis: building a framework. *Cell* 2006 Nov 17; **127**(4)**:** 679-695.

27. Hoda SA, Hoda RS, Merlin S, Shamonki J, Rivera M. Issues relating to lymphovascular invasion in breast carcinoma. *Adv Anat Pathol* 2006 Nov; **13**(6)**:** 308-315.

28. Tomlinson JS, Alpaugh ML, Barsky SH. An intact overexpressed E-cadherin/alpha,beta-catenin axis characterizes the lymphovascular emboli of inflammatory breast carcinoma. *Cancer Res* 2001 Jul 1; **61**(13)**:** 5231-5241.

29. Nassar H. Carcinomas with micropapillary morphology: clinical significance and current concepts. *Adv Anat Pathol* 2004 Nov; **11**(6)**:** 297-303.

30. Mohammed RA, Martin SG, Gill MS, Green AR, Paish EC, Ellis IO. Improved methods of detection of lymphovascular invasion demonstrate that it is the predominant method of vascular invasion in breast cancer and has important clinical consequences. *Am J Surg Pathol* 2007 Dec; **31**(12)**:** 1825-1833.

31. Kikuchi E, Margulis V, Karakiewicz PI, Roscigno M, Mikami S, Lotan Y*, et al.* Lymphovascular invasion predicts clinical outcomes in patients with node-negative upper tract urothelial carcinoma. *J Clin Oncol* 2009 Feb 1; **27**(4)**:** 612-618.

32. Mohammed RA, Martin SG, Mahmmod AM, Macmillan RD, Green AR, Paish EC*, et al.* Objective assessment of lymphatic and blood vascular invasion in lymph node-negative breast carcinoma: findings from a large case series with long-term follow-up. *J Pathol* 2011 Feb; **223**(3)**:** 358-365.

33. Ejlertsen B, Jensen MB, Rank F, Rasmussen BB, Christiansen P, Kroman N*, et al.* Population-based study of peritumoral lymphovascular invasion and outcome among patients with operable breast cancer. *J Natl Cancer Inst* 2009 May 20; **101**(10)**:** 729-735.

34. Sonoshita M, Aoki M, Fuwa H, Aoki K, Hosogi H, Sakai Y*, et al.* Suppression of colon cancer metastasis by Aes through inhibition of Notch signaling. *Cancer Cell* 2011 Jan 18; **19**(1)**:** 125-137.

35. Giampieri S, Manning C, Hooper S, Jones L, Hill CS, Sahai E. Localized and reversible TGFbeta signalling switches breast cancer cells from cohesive to single cell motility. *Nat Cell Biol* 2009 Nov; **11**(11)**:** 1287-1296.

36. Yang J, Mani SA, Donaher JL, Ramaswamy S, Itzykson RA, Come C*, et al.* Twist, a master regulator of morphogenesis, plays an essential role in tumor metastasis. *Cell* 2004 Jun 25; **117**(7)**:** 927-939.

37. Wyckoff JB, Wang Y, Lin EY, Li JF, Goswami S, Stanley ER*, et al.* Direct visualization of macrophage-assisted tumor cell intravasation in mammary tumors. *Cancer Res* 2007 Mar 15; **67**(6)**:** 2649-2656.

38. Carmeliet P, Jain RK. Molecular mechanisms and clinical applications of angiogenesis. *Nature* 2011 May 19; **473**(7347)**:** 298-307.

39. Hoshimoto S, Shingai T, Morton DL, Kuo C, Faries MB, Chong K*, et al.* Association Between Circulating Tumor Cells and Prognosis in Patients With Stage III Melanoma With Sentinel Lymph Node Metastasis in a Phase III International Multicenter Trial. *J Clin Oncol* 2012 Nov 1; **30**(31)**:** 3819-3826.

40. Yu M, Ting DT, Stott SL, Wittner BS, Ozsolak F, Paul S*, et al.* RNA sequencing of pancreatic circulating tumour cells implicates WNT signalling in metastasis. *Nature* 2012 Jul 26; **487**(7408)**:** 510-513.

41. Magbanua MJ, Sosa EV, Roy R, Eisenbud LE, Scott JH, Olshen A*, et al.* Genomic profiling of isolated circulating tumor cells from metastatic breast cancer patients. *Cancer Res* 2012 Nov 7.

42. Helzer KT, Barnes HE, Day L, Harvey J, Billings PR, Forsyth A. Circulating tumor cells are transcriptionally similar to the primary tumor in a murine prostate model. *Cancer Res* 2009 Oct 1; **69**(19)**:** 7860-7866.

43. Meng S, Tripathy D, Shete S, Ashfaq R, Haley B, Perkins S*, et al.* HER-2 gene amplification can be acquired as breast cancer progresses. *Proc Natl Acad Sci U S A* 2004 Jun 22; **101**(25)**:** 9393-9398.

44. Schardt JA, Meyer M, Hartmann CH, Schubert F, Schmidt-Kittler O, Fuhrmann C*, et al.* Genomic analysis of single cytokeratin-positive cells from bone marrow reveals early mutational events in breast cancer. *Cancer Cell* 2005 Sep; **8**(3)**:** 227-239.

45. Kallergi G, Agelaki S, Kalykaki A, Stournaras C, Mavroudis D, Georgoulias V. Phosphorylated EGFR and PI3K/Akt signaling kinases are expressed in circulating tumor cells of breast cancer patients. *Breast Cancer Res* 2008; **10**(5)**:** R80.

46. Stott SL, Lee RJ, Nagrath S, Yu M, Miyamoto DT, Ulkus L*, et al.* Isolation and characterization of circulating tumor cells from patients with localized and metastatic prostate cancer. *Sci Transl Med* 2010 Mar 31; **2**(25)**:** 25ra23.

47. Stott SL, Hsu CH, Tsukrov DI, Yu M, Miyamoto DT, Waltman BA*, et al.* Isolation of circulating tumor cells using a microvortex-generating herringbone-chip. *Proc Natl Acad Sci U S A* 2010 Oct 26; **107**(43)**:** 18392-18397.

48. Maheswaran S, Sequist LV, Nagrath S, Ulkus L, Brannigan B, Collura CV*, et al.* Detection of mutations in EGFR in circulating lung-cancer cells. *N Engl J Med* 2008 Jul 24; **359**(4)**:** 366-377.

49. Xiao Y, Ye Y, Yearsley K, Jones S, Barsky SH. The lymphovascular embolus of inflammatory breast cancer expresses a stem cell-like phenotype. *Am J Pathol* 2008 Aug; **173**(2)**:** 561-574.

50. Alpaugh ML, Tomlinson JS, Ye Y, Barsky SH. Relationship of sialyl-Lewis(x/a) underexpression and E-cadherin overexpression in the lymphovascular embolus of inflammatory breast carcinoma. *Am J Pathol* 2002 Aug; **161**(2)**:** 619-628.

51. Alpaugh ML, Tomlinson JS, Kasraeian S, Barsky SH. Cooperative role of E-cadherin and sialyl-Lewis X/A-deficient MUC1 in the passive dissemination of tumor emboli in inflammatory breast carcinoma. *Oncogene* 2002 May 16; **21**(22)**:** 3631-3643.

52. Ye Y, Tian H, Lange AR, Yearsley K, Robertson FM, Barsky SH. The genesis and unique properties of the lymphovascular tumor embolus are because of calpain-regulated proteolysis of E-cadherin. *Oncogene* 2013 Mar 28; **32**(13)**:** 1702-1713.

53. Xiao Y, Ye Y, Zou X, Jones S, Yearsley K, Shetuni B*, et al.* The lymphovascular embolus of inflammatory breast cancer exhibits a Notch 3 addiction. *Oncogene* 2011 Jan 20; **30**(3)**:** 287-300.

54. Fidler IJ. The pathogenesis of cancer metastasis: the 'seed and soil' hypothesis revisited. *Nat Rev Cancer* 2003 Jun; **3**(6)**:** 453-458.

55. Wikman H, Vessella R, Pantel K. Cancer micrometastasis and tumour dormancy. *APMIS* 2008 Jul-Aug; **116**(7-8)**:** 754-770.

56. Braun S, Vogl FD, Naume B, Janni W, Osborne MP, Coombes RC*, et al.* A pooled analysis of bone marrow micrometastasis in breast cancer. *N Engl J Med* 2005 Aug 25; **353**(8)**:** 793-802.

57. Braun S, Kentenich C, Janni W, Hepp F, de Waal J, Willgeroth F*, et al.* Lack of effect of adjuvant chemotherapy on the elimination of single dormant tumor cells in bone marrow of high-risk breast cancer patients. *J Clin Oncol* 2000 Jan; **18**(1)**:** 80-86.

58. Al-Mehdi AB, Tozawa K, Fisher AB, Shientag L, Lee A, Muschel RJ. Intravascular origin of metastasis from the proliferation of endothelium-attached tumor cells: a new model for metastasis. *Nat Med* 2000 Jan; **6**(1)**:** 100-102.

59. Gupta GP, Nguyen DX, Chiang AC, Bos PD, Kim JY, Nadal C*, et al.* Mediators of vascular remodelling co-opted for sequential steps in lung metastasis. *Nature* 2007 Apr 12; **446**(7137)**:** 765-770.

60. Qian BZ, Li J, Zhang H, Kitamura T, Zhang J, Campion LR*, et al.* CCL2 recruits inflammatory monocytes to facilitate breast-tumour metastasis. *Nature* 2011 Jul 14; **475**(7355)**:** 222-225.

61. Padua D, Zhang XH, Wang Q, Nadal C, Gerald WL, Gomis RR*, et al.* TGFbeta primes breast tumors for lung metastasis seeding through angiopoietin-like 4. *Cell* 2008 Apr 4; **133**(1)**:** 66-77.

62. Koop S, Schmidt EE, MacDonald IC, Morris VL, Khokha R, Grattan M*, et al.* Independence of metastatic ability and extravasation: metastatic ras-transformed and control fibroblasts extravasate equally well. *Proc Natl Acad Sci U S A* 1996 Oct 1; **93**(20)**:** 11080-11084.

63. Zhang XH, Wang Q, Gerald W, Hudis CA, Norton L, Smid M*, et al.* Latent bone metastasis in breast cancer tied to Src-dependent survival signals. *Cancer Cell* 2009 Jul 7; **16**(1)**:** 67-78.

64. Muller A, Homey B, Soto H, Ge N, Catron D, Buchanan ME*, et al.* Involvement of chemokine receptors in breast cancer metastasis. *Nature* 2001 Mar 1; **410**(6824)**:** 50-56.

65. Luzzi KJ, MacDonald IC, Schmidt EE, Kerkvliet N, Morris VL, Chambers AF*, et al.* Multistep nature of metastatic inefficiency: dormancy of solitary cells after successful extravasation and limited survival of early micrometastases. *Am J Pathol* 1998 Sep; **153**(3)**:** 865-873.

66. Shibue T, Weinberg RA. Integrin beta1-focal adhesion kinase signaling directs the proliferation of metastatic cancer cells disseminated in the lungs. *Proc Natl Acad Sci U S A* 2009 Jun 23; **106**(25)**:** 10290-10295.

67. McAllister SS, Gifford AM, Greiner AL, Kelleher SP, Saelzler MP, Ince TA*, et al.* Systemic endocrine instigation of indolent tumor growth requires osteopontin. *Cell* 2008 Jun 13; **133**(6)**:** 994-1005.

68. Kang SY, Halvorsen OJ, Gravdal K, Bhattacharya N, Lee JM, Liu NW*, et al.* Prosaposin inhibits tumor metastasis via paracrine and endocrine stimulation of stromal p53 and Tsp-1. *Proc Natl Acad Sci U S A* 2009 Jul 21; **106**(29)**:** 12115-12120.

69. Mazzieri R, Pucci F, Moi D, Zonari E, Ranghetti A, Berti A*, et al.* Targeting the ANG2/TIE2 axis inhibits tumor growth and metastasis by impairing angiogenesis and disabling rebounds of proangiogenic myeloid cells. *Cancer Cell* 2011 Apr 12; **19**(4)**:** 512-526.

70. Sotiriou C, Lacroix M, Lespagnard L, Larsimont D, Paesmans M, Body JJ. Interleukins-6 and -11 expression in primary breast cancer and subsequent development of bone metastases. *Cancer Lett* 2001 Aug 10; **169**(1)**:** 87-95.

71. Freedman VH, Shin SI. Cellular tumorigenicity in nude mice: correlation with cell growth in semi-solid medium. *Cell* 1974 Dec; **3**(4)**:** 355-359.

72. Stevens CW, Manoharan TH, Fahl WE. Characterization of mutagen-activated cellular oncogenes that confer anchorage independence to human fibroblasts and tumorigenicity to NIH 3T3 cells: sequence analysis of an enzymatically amplified mutant HRAS allele. *Proc Natl Acad Sci U S A* 1988 Jun; **85**(11)**:** 3875-3879.

73. Khwaja A, Rodriguez-Viciana P, Wennstrom S, Warne PH, Downward J. Matrix adhesion and Ras transformation both activate a phosphoinositide 3-OH kinase and protein kinase B/Akt cellular survival pathway. *EMBO J* 1997 May 15; **16**(10)**:** 2783-2793.

74. Frisch SM, Ruoslahti E. Integrins and anoikis. *Curr Opin Cell Biol* 1997 Oct; **9**(5)**:** 701-706.

75. Sodek KL, Murphy KJ, Brown TJ, Ringuette MJ. Cell-cell and cell-matrix dynamics in intraperitoneal cancer metastasis. *Cancer Metastasis Rev* 2012 Jun; **31**(1-2)**:** 397-414.

76. Boudreau N, Sympson CJ, Werb Z, Bissell MJ. Suppression of ICE and apoptosis in mammary epithelial cells by extracellular matrix. *Science* 1995 Feb 10; **267**(5199)**:** 891-893.

77. Hungerford JE, Compton MT, Matter ML, Hoffstrom BG, Otey CA. Inhibition of pp125FAK in cultured fibroblasts results in apoptosis. *J Cell Biol* 1996 Dec; **135**(5)**:** 1383-1390.

78. Yawata A, Adachi M, Okuda H, Naishiro Y, Takamura T, Hareyama M*, et al.* Prolonged cell survival enhances peritoneal dissemination of gastric cancer cells. *Oncogene* 1998 May; **16**(20)**:** 2681-2686.

79. Nishimura S, Adachi M, Ishida T, Matsunaga T, Uchida H, Hamada H*, et al.* Adenovirus-mediated transfection of caspase-8 augments anoikis and inhibits peritoneal dissemination of human gastric carcinoma cells. *Cancer Res* 2001 Oct 1; **61**(19)**:** 7009-7014.

80. Duxbury MS, Ito H, Zinner MJ, Ashley SW, Whang EE. Focal adhesion kinase gene silencing promotes anoikis and suppresses metastasis of human pancreatic adenocarcinoma cells. *Surgery* 2004 May; **135**(5)**:** 555-562.

81. Wei L, Yang Y, Yu Q. Tyrosine kinase-dependent, phosphatidylinositol 3'-kinase, and mitogen-activated protein kinase-independent signaling pathways prevent lung adenocarcinoma cells from anoikis. *Cancer Res* 2001 Mar 15; **61**(6)**:** 2439-2444.

82. Streuli CH, Gilmore AP. Adhesion-mediated signaling in the regulation of mammary epithelial cell survival. *J Mammary Gland Biol Neoplasia* 1999 Apr; **4**(2)**:** 183-191.

83. Zhu Z, Sanchez-Sweatman O, Huang X, Wiltrout R, Khokha R, Zhao Q*, et al.* Anoikis and metastatic potential of cloudman S91 melanoma cells. *Cancer Res* 2001 Feb 15; **61**(4)**:** 1707-1716.

84. Bonfoco E, Chen W, Paul R, Cheresh DA, Cooper NR. beta1 integrin antagonism on adherent, differentiated human neuroblastoma cells triggers an apoptotic signaling pathway. *Neuroscience* 2000; **101**(4)**:** 1145-1152.

85. Douma S, Van Laar T, Zevenhoven J, Meuwissen R, Van Garderen E, Peeper DS. Suppression of anoikis and induction of metastasis by the neurotrophic receptor TrkB. *Nature* 2004 Aug 26; **430**(7003)**:** 1034-1039.

86. Geiger TR, Peeper DS. Critical role for TrkB kinase function in anoikis suppression, tumorigenesis, and metastasis. *Cancer Res* 2007 Jul 1; **67**(13)**:** 6221-6229.

87. Jiang K, Sun J, Cheng J, Djeu JY, Wei S, Sebti S. Akt mediates Ras downregulation of RhoB, a suppressor of transformation, invasion, and metastasis. *Mol Cell Biol* 2004 Jun; **24**(12)**:** 5565-5576.

88. Scotlandi K, Maini C, Manara MC, Benini S, Serra M, Cerisano V*, et al.* Effectiveness of insulin-like growth factor I receptor antisense strategy against Ewing's sarcoma cells. *Cancer Gene Ther* 2002 Mar; **9**(3)**:** 296-307.

89. Leong KG, Niessen K, Kulic I, Raouf A, Eaves C, Pollet I*, et al.* Jagged1-mediated Notch activation induces epithelial-to-mesenchymal transition through Slug-induced repression of E-cadherin. *J Exp Med* 2007 Nov 26; **204**(12)**:** 2935-2948.

90. Derksen PW, Liu X, Saridin F, van der Gulden H, Zevenhoven J, Evers B*, et al.* Somatic inactivation of E-cadherin and p53 in mice leads to metastatic lobular mammary carcinoma through induction of anoikis resistance and angiogenesis. *Cancer Cell* 2006 Nov; **10**(5)**:** 437-449.

91. Debnath J, Muthuswamy SK, Brugge JS. Morphogenesis and oncogenesis of MCF-10A mammary epithelial acini grown in three-dimensional basement membrane cultures. *Methods* 2003 Jul; **30**(3)**:** 256-268.

92. Debnath J, Mills KR, Collins NL, Reginato MJ, Muthuswamy SK, Brugge JS. The role of apoptosis in creating and maintaining luminal space within normal and oncogene-expressing mammary acini. *Cell* 2002 Oct 4; **111**(1)**:** 29-40.

93. Haenssen KK, Caldwell SA, Shahriari KS, Jackson SR, Whelan KA, Klein-Szanto AJ*, et al.* ErbB2 requires integrin alpha5 for anoikis resistance via Src regulation of receptor activity in human mammary epithelial cells. *J Cell Sci* 2010 Apr 15; **123**(Pt 8)**:** 1373-1382.

94. Wen HC, Avivar-Valderas A, Sosa MS, Girnius N, Farias EF, Davis RJ*, et al.* p38alpha Signaling Induces Anoikis and Lumen Formation During Mammary Morphogenesis. *Sci Signal* 2011; **4**(174)**:** ra34.

95. Fung C, Lock R, Gao S, Salas E, Debnath J. Induction of autophagy during extracellular matrix detachment promotes cell survival. *Mol Biol Cell* 2008 Mar; **19**(3)**:** 797-806.

96. Michel JB. Anoikis in the cardiovascular system: known and unknown extracellular mediators. *Arterioscler Thromb Vasc Biol* 2003 Dec; **23**(12)**:** 2146-2154.

97. Lee HY, You HJ, Won JY, Youn SW, Cho HJ, Park KW*, et al.* Forkhead factor, FOXO3a, induces apoptosis of endothelial cells through activation of matrix metalloproteinases. *Arterioscler Thromb Vasc Biol* 2008 Feb; **28**(2)**:** 302-308.

98. Liu W, Ahmad SA, Reinmuth N, Shaheen RM, Jung YD, Fan F*, et al.* Endothelial cell survival and apoptosis in the tumor vasculature. *Apoptosis* 2000 Oct; **5**(4)**:** 323-328.

99. Efklidou S, Bailey R, Field N, Noursadeghi M, Collins MK. vFLIP from KSHV inhibits anoikis of primary endothelial cells. *J Cell Sci* 2008 Feb 15; **121**(Pt 4)**:** 450-457.

100. Frisch SM, Vuori K, Kelaita D, Sicks S. A role for Jun-N-terminal kinase in anoikis; suppression by bcl-2 and crmA. *J Cell Biol* 1996 Dec; **135**(5)**:** 1377-1382.

101. Cardone MH, Salvesen GS, Widmann C, Johnson G, Frisch SM. The regulation of anoikis: MEKK-1 activation requires cleavage by caspases. *Cell* 1997 Jul 25; **90**(2)**:** 315-323.

102. Khwaja A, Downward J. Lack of correlation between activation of Jun-NH2-terminal kinase and induction of apoptosis after detachment of epithelial cells. *J Cell Biol* 1997 Nov 17; **139**(4)**:** 1017-1023.

103. Frisch SM, Vuori K, Ruoslahti E, Chan-Hui PY. Control of adhesion-dependent cell survival by focal adhesion kinase. *J Cell Biol* 1996 Aug; **134**(3)**:** 793-799.

104. Delcommenne M, Tan C, Gray V, Rue L, Woodgett J, Dedhar S. Phosphoinositide-3-OH kinase-dependent regulation of glycogen synthase kinase 3 and protein kinase B/AKT by the integrin-linked kinase. *Proc Natl Acad Sci U S A* 1998 Sep 15; **95**(19)**:** 11211-11216.

105. Jost M, Huggett TM, Kari C, Rodeck U. Matrix-independent survival of human keratinocytes through an EGF receptor/MAPK-kinase-dependent pathway. *Mol Biol Cell* 2001 May; **12**(5)**:** 1519-1527.

106. Demers MJ, Thibodeau S, Noel D, Fujita N, Tsuruo T, Gauthier R*, et al.* Intestinal epithelial cancer cell anoikis resistance: EGFR-mediated sustained activation of Src overrides Fak-dependent signaling to MEK/Erk and/or PI3-K/Akt-1. *J Cell Biochem* 2009 Jul 1; **107**(4)**:** 639-654.

107. Zoppi N, Barlati S, Colombi M. FAK-independent alphavbeta3 integrin-EGFR complexes rescue from anoikis matrix-defective fibroblasts. *Biochim Biophys Acta* 2008 Jun; **1783**(6)**:** 1177-1188.

108. Shen X, Kramer RH. Adhesion-mediated squamous cell carcinoma survival through ligand-independent activation of epidermal growth factor receptor. *Am J Pathol* 2004 Oct; **165**(4)**:** 1315-1329.

109. Kang HG, Jenabi JM, Zhang J, Keshelava N, Shimada H, May WA*, et al.* E-cadherin cell-cell adhesion in ewing tumor cells mediates suppression of anoikis through activation of the ErbB4 tyrosine kinase. *Cancer Res* 2007 Apr 1; **67**(7)**:** 3094-3105.

110. Jin W, Kim GM, Kim MS, Lim MH, Yun C, Jeong J*, et al.* TrkC plays an essential role in breast tumor growth and metastasis. *Carcinogenesis* 2010 Nov; **31**(11)**:** 1939-1947.

111. Geiger TR, Peeper DS. The neurotrophic receptor TrkB in anoikis resistance and metastasis: a perspective. *Cancer Res* 2005 Aug 15; **65**(16)**:** 7033-7036.

112. Lagadec C, Meignan S, Adriaenssens E, Foveau B, Vanhecke E, Romon R*, et al.* TrkA overexpression enhances growth and metastasis of breast cancer cells. *Oncogene* 2009 May 7; **28**(18)**:** 1960-1970.

113. Valentinis B, Reiss K, Baserga R. Insulin-like growth factor-I-mediated survival from anoikis: role of cell aggregation and focal adhesion kinase. *J Cell Physiol* 1998 Sep; **176**(3)**:** 648-657.

114. Prisco M, Romano G, Peruzzi F, Valentinis B, Baserga R. Insulin and IGF-I receptors signaling in protection from apoptosis. *Horm Metab Res* 1999 Feb-Mar; **31**(2-3)**:** 80-89.

115. Valentinis B, Morrione A, Peruzzi F, Prisco M, Reiss K, Baserga R. Anti-apoptotic signaling of the IGF-I receptor in fibroblasts following loss of matrix adhesion. *Oncogene* 1999 Mar 11; **18**(10)**:** 1827-1836.

116. Scotlandi K, Avnet S, Benini S, Manara MC, Serra M, Cerisano V*, et al.* Expression of an IGF-I receptor dominant negative mutant induces apoptosis, inhibits tumorigenesis and enhances chemosensitivity in Ewing's sarcoma cells. *Int J Cancer* 2002 Sep 1; **101**(1)**:** 11-16.

117. Martin MJ, Melnyk N, Pollard M, Bowden M, Leong H, Podor TJ*, et al.* The insulin-like growth factor I receptor is required for Akt activation and suppression of anoikis in cells transformed by the ETV6-NTRK3 chimeric tyrosine kinase. *Mol Cell Biol* 2006 Mar; **26**(5)**:** 1754-1769.

118. Morrison KB, Tognon CE, Garnett MJ, Deal C, Sorensen PH. ETV6-NTRK3 transformation requires insulin-like growth factor 1 receptor signaling and is associated with constitutive IRS-1 tyrosine phosphorylation. *Oncogene* 2002 Aug 22; **21**(37)**:** 5684-5695.

119. Tognon CE, Mackereth CD, Somasiri AM, McIntosh LP, Sorensen PH. Mutations in the SAM domain of the ETV6-NTRK3 chimeric tyrosine kinase block polymerization and transformation activity. *Mol Cell Biol* 2004 Jun; **24**(11)**:** 4636-4650.

120. Li Z, Tognon CE, Godinho FJ, Yasaitis L, Hock H, Herschkowitz JI*, et al.* ETV6-NTRK3 fusion oncogene initiates breast cancer from committed mammary progenitors via activation of AP1 complex. *Cancer Cell* 2007 Dec; **12**(6)**:** 542-558.

121. Tognon CE, Somasiri AM, Evdokimova VE, Trigo G, Uy EE, Melnyk N*, et al.* ETV6-NTRK3-mediated breast epithelial cell transformation is blocked by targeting the IGF1R signaling pathway. *Cancer Res* 2011 Feb 1; **71**(3)**:** 1060-1070.

122. Sachdev D, Zhang X, Matise I, Gaillard-Kelly M, Yee D. The type I insulin-like growth factor receptor regulates cancer metastasis independently of primary tumor growth by promoting invasion and survival. *Oncogene* 2010 Jan 14; **29**(2)**:** 251-262.

123. Li H, Baldwin BR, Zahnow CA. LIP expression is regulated by IGF-1R signaling and participates in suppression of anoikis. *Mol Cancer* 2011; **10:** 100.

124. Boisvert-Adamo K, Aplin AE. B-RAF and PI-3 kinase signaling protect melanoma cells from anoikis. *Oncogene* 2006 Aug 10; **25**(35)**:** 4848-4856.

125. Horowitz JC, Rogers DS, Sharma V, Vittal R, White ES, Cui Z*, et al.* Combinatorial activation of FAK and AKT by transforming growth factor-beta1 confers an anoikis-resistant phenotype to myofibroblasts. *Cell Signal* 2007 Apr; **19**(4)**:** 761-771.

126. Liu XW, Bernardo MM, Fridman R, Kim HR. Tissue inhibitor of metalloproteinase-1 protects human breast epithelial cells against intrinsic apoptotic cell death via the focal adhesion kinase/phosphatidylinositol 3-kinase and MAPK signaling pathway. *J Biol Chem* 2003 Oct 10; **278**(41)**:** 40364-40372.

127. Schmidt M, Hovelmann S, Beckers TL. A novel form of constitutively active farnesylated Akt1 prevents mammary epithelial cells from anoikis and suppresses chemotherapy-induced apoptosis. *Br J Cancer* 2002 Oct 7; **87**(8)**:** 924-932.

128. Vitolo MI, Weiss MB, Szmacinski M, Tahir K, Waldman T, Park BH*, et al.* Deletion of PTEN promotes tumorigenic signaling, resistance to anoikis, and altered response to chemotherapeutic agents in human mammary epithelial cells. *Cancer Res* 2009 Nov 1; **69**(21)**:** 8275-8283.

129. Skurk C, Maatz H, Kim HS, Yang J, Abid MR, Aird WC*, et al.* The Akt-regulated forkhead transcription factor FOXO3a controls endothelial cell viability through modulation of the caspase-8 inhibitor FLIP. *J Biol Chem* 2004 Jan 9; **279**(2)**:** 1513-1525.

130. Zugasti O, Rul W, Roux P, Peyssonnaux C, Eychene A, Franke TF*, et al.* Raf-MEK-Erk cascade in anoikis is controlled by Rac1 and Cdc42 via Akt. *Mol Cell Biol* 2001 Oct; **21**(19)**:** 6706-6717.

131. Eckert LB, Repasky GA, Ulku AS, McFall A, Zhou H, Sartor CI*, et al.* Involvement of Ras activation in human breast cancer cell signaling, invasion, and anoikis. *Cancer Res* 2004 Jul 1; **64**(13)**:** 4585-4592.

132. Galante JM, Mortenson MM, Bowles TL, Virudachalam S, Bold RJ. ERK/BCL-2 pathway in the resistance of pancreatic cancer to anoikis. *J Surg Res* 2009 Mar; **152**(1)**:** 18-25.

133. Windham TC, Parikh NU, Siwak DR, Summy JM, McConkey DJ, Kraker AJ*, et al.* Src activation regulates anoikis in human colon tumor cell lines. *Oncogene* 2002 Nov 7; **21**(51)**:** 7797-7807.

134. Wei L, Yang Y, Zhang X, Yu Q. Altered regulation of Src upon cell detachment protects human lung adenocarcinoma cells from anoikis. *Oncogene* 2004 Dec 2; **23**(56)**:** 9052-9061.

135. Diaz-Montero CM, Wygant JN, McIntyre BW. PI3-K/Akt-mediated anoikis resistance of human osteosarcoma cells requires Src activation. *Eur J Cancer* 2006 Jul; **42**(10)**:** 1491-1500.

136. Yamaguchi H, Woods NT, Dorsey JF, Takahashi Y, Gjertsen NR, Yeatman T*, et al.* SRC directly phosphorylates Bif-1 and prevents its interaction with Bax and the initiation of anoikis. *J Biol Chem* 2008 Jul 4; **283**(27)**:** 19112-19118.

137. Loza-Coll MA, Perera S, Shi W, Filmus J. A transient increase in the activity of Src-family kinases induced by cell detachment delays anoikis of intestinal epithelial cells. *Oncogene* 2005 Mar 3; **24**(10)**:** 1727-1737.

138. Cheng H, Liu P, Wang ZC, Zou L, Santiago S, Garbitt V*, et al.* SIK1 couples LKB1 to p53-dependent anoikis and suppresses metastasis. *Sci Signal* 2009; **2**(80)**:** ra35.

139. Shaw RJ. Tumor suppression by LKB1: SIK-ness prevents metastasis. *Sci Signal* 2009; **2**(86)**:** pe55.

140. Rosen K, Rak J, Jin J, Kerbel RS, Newman MJ, Filmus J. Downregulation of the pro-apoptotic protein Bak is required for the ras-induced transformation of intestinal epithelial cells. *Curr Biol* 1998 Dec 3; **8**(24)**:** 1331-1334.

141. Liu Z, Li H, Derouet M, Berezkin A, Sasazuki T, Shirasawa S*, et al.* Oncogenic Ras inhibits anoikis of intestinal epithelial cells by preventing the release of a mitochondrial pro-apoptotic protein Omi/HtrA2 into the cytoplasm. *J Biol Chem* 2006 May 26; **281**(21)**:** 14738-14747.

142. Rosen K, Rak J, Leung T, Dean NM, Kerbel RS, Filmus J. Activated Ras prevents downregulation of Bcl-X(L) triggered by detachment from the extracellular matrix. A mechanism of Ras-induced resistance to anoikis in intestinal epithelial cells. *J Cell Biol* 2000 Apr 17; **149**(2)**:** 447-456.

143. Coll ML, Rosen K, Ladeda V, Filmus J. Increased Bcl-xL expression mediates v-Src-induced resistance to anoikis in intestinal epithelial cells. *Oncogene* 2002 Apr 25; **21**(18)**:** 2908-2913.

144. Reginato MJ, Mills KR, Paulus JK, Lynch DK, Sgroi DC, Debnath J*, et al.* Integrins and EGFR coordinately regulate the pro-apoptotic protein Bim to prevent anoikis. *Nat Cell Biol* 2003 Aug; **5**(8)**:** 733-740.

145. Mailleux AA, Overholtzer M, Schmelzle T, Bouillet P, Strasser A, Brugge JS. BIM regulates apoptosis during mammary ductal morphogenesis, and its absence reveals alternative cell death mechanisms. *Dev Cell* 2007 Feb; **12**(2)**:** 221-234.

146. Marani M, Hancock D, Lopes R, Tenev T, Downward J, Lemoine NR. Role of Bim in the survival pathway induced by Raf in epithelial cells. *Oncogene* 2004 Apr 1; **23**(14)**:** 2431-2441.

147. Boisvert-Adamo K, Aplin AE. Mutant B-RAF mediates resistance to anoikis via Bad and Bim. *Oncogene* 2008 May 22; **27**(23)**:** 3301-3312.

148. Valentijn AJ, Gilmore AP. Translocation of full-length Bid to mitochondria during anoikis. *J Biol Chem* 2004 Jul 30; **279**(31)**:** 32848-32857.

149. Valentijn AJ, Metcalfe AD, Kott J, Streuli CH, Gilmore AP. Spatial and temporal changes in Bax subcellular localization during anoikis. *J Cell Biol* 2003 Aug 18; **162**(4)**:** 599-612.

150. Jan Y, Matter M, Pai JT, Chen YL, Pilch J, Komatsu M*, et al.* A mitochondrial protein, Bit1, mediates apoptosis regulated by integrins and Groucho/TLE corepressors. *Cell* 2004 Mar 5; **116**(5)**:** 751-762.

151. Kairouz-Wahbe R, Biliran H, Luo X, Khor I, Wankell M, Besch-Williford C*, et al.* Anoikis effector Bit1 negatively regulates Erk activity. *Proc Natl Acad Sci U S A* 2008 Feb 5; **105**(5)**:** 1528-1532.

152. Puthalakath H, Villunger A, O'Reilly LA, Beaumont JG, Coultas L, Cheney RE*, et al.* Bmf: a proapoptotic BH3-only protein regulated by interaction with the myosin V actin motor complex, activated by anoikis. *Science* 2001 Sep 7; **293**(5536)**:** 1829-1832.

153. Schmelzle T, Mailleux AA, Overholtzer M, Carroll JS, Solimini NL, Lightcap ES*, et al.* Functional role and oncogene-regulated expression of the BH3-only factor Bmf in mammary epithelial anoikis and morphogenesis. *Proc Natl Acad Sci U S A* 2007 Mar 6; **104**(10)**:** 3787-3792.

154. Berezovskaya O, Schimmer AD, Glinskii AB, Pinilla C, Hoffman RM, Reed JC*, et al.* Increased expression of apoptosis inhibitor protein XIAP contributes to anoikis resistance of circulating human prostate cancer metastasis precursor cells. *Cancer Res* 2005 Mar 15; **65**(6)**:** 2378-2386.

155. Liu Z, Li H, Derouet M, Filmus J, LaCasse EC, Korneluk RG*, et al.* ras Oncogene triggers up-regulation of cIAP2 and XIAP in intestinal epithelial cells: epidermal growth factor receptor-dependent and -independent mechanisms

of ras-induced transformation. *J Biol Chem* 2005 Nov 11; **280**(45)**:** 37383-37392.

156. Liu Z, Li H, Wu X, Yoo BH, Yan SR, Stadnyk AW*, et al.* Detachment-induced upregulation of XIAP and cIAP2 delays anoikis of intestinal epithelial cells. *Oncogene* 2006 Dec 14; **25**(59)**:** 7680-7690.

157. Woods NT, Yamaguchi H, Lee FY, Bhalla KN, Wang HG. Anoikis, initiated by Mcl-1 degradation and Bim induction, is deregulated during oncogenesis. *Cancer Res* 2007 Nov 15; **67**(22)**:** 10744-10752.

158. Boisvert-Adamo K, Longmate W, Abel EV, Aplin AE. Mcl-1 is required for melanoma cell resistance to anoikis. *Mol Cancer Res* 2009 Apr; **7**(4)**:** 549-556.

159. Chunhacha P, Pongrakhananon V, Rojanasakul Y, Chanvorachote P. Caveolin-1 regulates Mcl-1 stability and anoikis in lung carcinoma cells. *Am J Physiol Cell Physiol* 2012 May 1; **302**(9)**:** C1284-1292.

160. Frisch SM. Evidence for a function of death-receptor-related, death-domain-containing proteins in anoikis. *Curr Biol* 1999 Sep 23; **9**(18)**:** 1047-1049.

161. Mawji IA, Simpson CD, Gronda M, Williams MA, Hurren R, Henderson CJ*, et al.* A chemical screen identifies anisomycin as an anoikis sensitizer that functions by decreasing FLIP protein synthesis. *Cancer Res* 2007 Sep 1; **67**(17)**:** 8307-8315.

162. Mawji IA, Simpson CD, Hurren R, Gronda M, Williams MA, Filmus J*, et al.* Critical role for Fas-associated death domain-like interleukin-1-converting enzyme-like inhibitory protein in anoikis resistance and distant tumor formation. *J Natl Cancer Inst* 2007 May 16; **99**(10)**:** 811-822.

163. Laguinge LM, Samara RN, Wang W, El-Deiry WS, Corner G, Augenlicht L*, et al.* DR5 receptor mediates anoikis in human colorectal carcinoma cell lines. *Cancer Res* 2008 Feb 1; **68**(3)**:** 909-917.

164. Li HM, Fujikura D, Harada T, Uehara J, Kawai T, Akira S*, et al.* IPS-1 is crucial for DAP3-mediated anoikis induction by caspase-8 activation. *Cell Death Differ* 2009 Dec; **16**(12)**:** 1615-1621.

165. Miyazaki T, Shen M, Fujikura D, Tosa N, Kim HR, Kon S*, et al.* Functional role of death-associated protein 3 (DAP3) in anoikis. *J Biol Chem* 2004 Oct 22; **279**(43)**:** 44667-44672.

166. Overholtzer M, Mailleux AA, Mouneimne G, Normand G, Schnitt SJ, King RW*, et al.* A nonapoptotic cell death process, entosis, that occurs by cell-in-cell invasion. *Cell* 2007 Nov 30; **131**(5)**:** 966-979.

167. Janes SM, Watt FM. Switch from alphavbeta5 to alphavbeta6 integrin expression protects squamous cell carcinomas from anoikis. *J Cell Biol* 2004 Aug 2; **166**(3)**:** 419-431.

168. Shen W, Chen D, Fu H, Liu S, Sun K, Sun X. S100A4 protects gastric cancer cells from anoikis through regulation of alphav and alpha5 integrin. *Cancer Sci* 2011 May; **102**(5)**:** 1014-1018.

169. Zhang Y, Yang M, Ji Q, Fan D, Peng H, Yang C*, et al.* Anoikis induction and metastasis suppression by a new integrin alphavbeta3 inhibitor in human melanoma cell line M21. *Invest New Drugs* 2011 Aug; **29**(4)**:** 666-673.

170. Marco RA, Diaz-Montero CM, Wygant JN, Kleinerman ES, McIntyre BW. Alpha 4 integrin increases anoikis of human osteosarcoma cells. *J Cell Biochem* 2003 Apr 1; **88**(5)**:** 1038-1047.

171. Fouquet S, Lugo-Martinez VH, Faussat AM, Renaud F, Cardot P, Chambaz J*, et al.* Early loss of E-cadherin from cell-cell contacts is involved in the onset of Anoikis in enterocytes. *J Biol Chem* 2004 Oct 8; **279**(41)**:** 43061-43069.

172. Ko H, Kim S, Jin CH, Lee E, Ham S, Yook JI*, et al.* Protein kinase casein kinase 2-mediated upregulation of N-cadherin confers anoikis resistance on esophageal carcinoma cells. *Mol Cancer Res* 2012 Aug; **10**(8)**:** 1032-1038.

173. Sullivan R, Graham CH. Hypoxia-driven selection of the metastatic phenotype. *Cancer Metastasis Rev* 2007 Jun; **26**(2)**:** 319-331.

174. Onder TT, Gupta PB, Mani SA, Yang J, Lander ES, Weinberg RA. Loss of E-cadherin promotes metastasis via multiple downstream transcriptional pathways. *Cancer Res* 2008 May 15; **68**(10)**:** 3645-3654.

175. Kumar S, Park SH, Cieply B, Schupp J, Killiam E, Zhang F*, et al.* A pathway for the control of anoikis sensitivity by E-cadherin and epithelial-to-mesenchymal transition. *Mol Cell Biol* 2011 Oct; **31**(19)**:** 4036-4051.

176. Smit MA, Peeper DS. Zeb1 is required for TrkB-induced epithelial-mesenchymal transition, anoikis resistance and metastasis. *Oncogene* 2011 Sep 1; **30**(35)**:** 3735-3744.

177. Cieply B, Riley Pt, Pifer PM, Widmeyer J, Addison JB, Ivanov AV*, et al.* Suppression of the epithelial-mesenchymal transition by Grainyhead-like-2. *Cancer Res* 2012 May 1; **72**(9)**:** 2440-2453.

178. Frisch SM. E1a induces the expression of epithelial characteristics. *J Cell Biol* 1994 Nov; **127**(4)**:** 1085-1096.

179. Nagafuchi A, Shirayoshi Y, Okazaki K, Yasuda K, Takeichi M. Transformation of cell adhesion properties by exogenously introduced E-cadherin cDNA. *Nature* 1987 Sep 24-30; **329**(6137)**:** 341-343.

180. Islam S, Carey TE, Wolf GT, Wheelock MJ, Johnson KR. Expression of N-cadherin by human squamous carcinoma cells induces a scattered fibroblastic phenotype with disrupted cell-cell adhesion. *J Cell Biol* 1996 Dec; **135**(6 Pt 1)**:** 1643-1654.

181. Tannock I. Cell kinetics and chemotherapy: a critical review. *Cancer Treat Rep* 1978 Aug; **62**(8)**:** 1117-1133.

182. Kerbel RS, Rak J, Kobayashi H, Man MS, St Croix B, Graham CH. Multicellular resistance: a new paradigm to explain aspects of acquired drug resistance of solid tumors. *Cold Spring Harb Symp Quant Biol* 1994; **59:** 661-672.

183. St Croix B, Florenes VA, Rak JW, Flanagan M, Bhattacharya N, Slingerland JM*, et al.* Impact of the cyclin-dependent kinase inhibitor p27Kip1 on resistance of tumor cells to anticancer agents. *Nat Med* 1996 Nov; **2**(11)**:** 1204-1210.

184. St Croix B, Sheehan C, Rak JW, Florenes VA, Slingerland JM, Kerbel RS. E-Cadherin-dependent growth suppression is mediated by the cyclin-dependent kinase inhibitor p27(KIP1). *J Cell Biol* 1998 Jul 27; **142**(2)**:** 557-571.

185. Kim HR, Lin HM, Biliran H, Raz A. Cell cycle arrest and inhibition of anoikis by galectin-3 in human breast epithelial cells. *Cancer Res* 1999 Aug 15; **59**(16)**:** 4148-4154.

186. Collins NL, Reginato MJ, Paulus JK, Sgroi DC, Labaer J, Brugge JS. G1/S cell cycle arrest provides anoikis resistance through Erk-mediated Bim suppression. *Mol Cell Biol* 2005 Jun; **25**(12)**:** 5282-5291.

187. Taube ME, Liu XW, Fridman R, Kim HR. TIMP-1 regulation of cell cycle in human breast epithelial cells via stabilization of p27(KIP1) protein. *Oncogene* 2006 May 18; **25**(21)**:** 3041-3048.

188. Li AE, Ito H, Rovira, II, Kim KS, Takeda K, Yu ZY*, et al.* A role for reactive oxygen species in endothelial cell anoikis. *Circ Res* 1999 Aug 20; **85**(4)**:** 304-310.

189. Khan AU, Wilson T. Reactive oxygen species as cellular messengers. *Chem Biol* 1995 Jul; **2**(7)**:** 437-445.

190. Cai J, Niu X, Chen Y, Hu Q, Shi G, Wu H*, et al.* Emodin-induced generation of reactive oxygen species inhibits RhoA activation to sensitize gastric carcinoma cells to anoikis. *Neoplasia* 2008 Jan; **10**(1)**:** 41-51.

191. Laguinge LM, Lin S, Samara RN, Salesiotis AN, Jessup JM. Nitrosative stress in rotated three-dimensional colorectal carcinoma cell cultures induces microtubule depolymerization and apoptosis. *Cancer Res* 2004 Apr 15; **64**(8)**:** 2643-2648.

192. Giannoni E, Buricchi F, Grimaldi G, Parri M, Cialdai F, Taddei ML*, et al.* Redox regulation of anoikis: reactive oxygen species as essential mediators of cell survival. *Cell Death Differ* 2008 May; **15**(5)**:** 867-878.

193. Giannoni E, Fiaschi T, Ramponi G, Chiarugi P. Redox regulation of anoikis resistance of metastatic prostate cancer cells: key role for Src and EGFR-mediated pro-survival signals. *Oncogene* 2009 May 21; **28**(20)**:** 2074-2086.

194. Chanvorachote P, Nimmannit U, Lu Y, Talbott S, Jiang BH, Rojanasakul Y. Nitric oxide regulates lung carcinoma cell anoikis through inhibition of ubiquitin-proteasomal degradation of caveolin-1. *J Biol Chem* 2009 Oct 9; **284**(41)**:** 28476-28484.

195. Rungtabnapa P, Nimmannit U, Halim H, Rojanasakul Y, Chanvorachote P. Hydrogen peroxide inhibits non-small cell lung cancer cell anoikis through the inhibition of caveolin-1 degradation. *Am J Physiol Cell Physiol* 2011 Feb; **300**(2)**:** C235-245.

196. Zhu P, Tan MJ, Huang RL, Tan CK, Chong HC, Pal M*, et al.* Angiopoietin-like 4 protein elevates the prosurvival intracellular O2(-):H2O2 ratio and confers anoikis resistance to tumors. *Cancer Cell* 2011 Mar 8; **19**(3)**:** 401-415.

197. Klionsky DJ. Autophagy: from phenomenology to molecular understanding in less than a decade. *Nat Rev Mol Cell Biol* 2007 Nov; **8**(11)**:** 931-937.

198. Yorimitsu T, Nair U, Yang Z, Klionsky DJ. Endoplasmic reticulum stress triggers autophagy. *J Biol Chem* 2006 Oct 6; **281**(40)**:** 30299-30304.

199. Ogata M, Hino S, Saito A, Morikawa K, Kondo S, Kanemoto S*, et al.* Autophagy is activated for cell survival after endoplasmic reticulum stress. *Mol Cell Biol* 2006 Dec; **26**(24)**:** 9220-9231.

200. Tracy K, Dibling BC, Spike BT, Knabb JR, Schumacker P, Macleod KF. BNIP3 is an RB/E2F target gene required for hypoxia-induced autophagy. *Mol Cell Biol* 2007 Sep; **27**(17)**:** 6229-6242.

201. Azad MB, Chen Y, Henson ES, Cizeau J, McMillan-Ward E, Israels SJ*, et al.* Hypoxia induces autophagic cell death in apoptosis-competent cells through a mechanism involving BNIP3. *Autophagy* 2008 Feb; **4**(2)**:** 195-204.

202. Galluzzi L, Vicencio JM, Kepp O, Tasdemir E, Maiuri MC, Kroemer G. To die or not to die: that is the autophagic question. *Curr Mol Med* 2008 Mar; **8**(2)**:** 78-91.

203. Rosenfeldt MT, O'Prey J, Morton JP, Nixon C, MacKay G, Mrowinska A*, et al.* p53 status determines the role of autophagy in pancreatic tumour development. *Nature* 2013 Dec 12; **504**(7479)**:** 296-300.

204. Debnath J. Detachment-induced autophagy during anoikis and lumen formation in epithelial acini. *Autophagy* 2008 Apr; **4**(3)**:** 351-353.

205. Lock R, Roy S, Kenific CM, Su JS, Salas E, Ronen SM*, et al.* Autophagy facilitates glycolysis during Ras-mediated oncogenic transformation. *Mol Biol Cell* 2011 Jan 15; **22**(2)**:** 165-178.

206. Chen N, Eritja N, Lock R, Debnath J. Autophagy restricts proliferation driven by oncogenic phosphatidylinositol 3-kinase in three-dimensional culture. *Oncogene* 2012 Jul 9.

207. Rohwer N, Welzel M, Daskalow K, Pfander D, Wiedenmann B, Detjen K*, et al.* Hypoxia-inducible factor 1alpha mediates anoikis resistance via suppression of alpha5 integrin. *Cancer Res* 2008 Dec 15; **68**(24)**:** 10113-10120.

208. Lee SH, Koo KH, Park JW, Kim HJ, Ye SK, Park JB*, et al.* HIF-1 is induced via EGFR activation and mediates resistance to anoikis-like cell death under lipid rafts/caveolae-disrupting stress. *Carcinogenesis* 2009 Dec; **30**(12)**:** 1997-2004.

209. Whelan KA, Caldwell SA, Shahriari KS, Jackson SR, Franchetti LD, Johannes GJ*, et al.* Hypoxia suppression of Bim and Bmf blocks anoikis and luminal clearing during mammary morphogenesis. *Mol Biol Cell* 2010 Nov 15; **21**(22)**:** 3829-3837.

210. Woelfle U, Cloos J, Sauter G, Riethdorf L, Janicke F, van Diest P*, et al.* Molecular signature associated with bone marrow micrometastasis in human breast cancer. *Cancer Res* 2003 Sep 15; **63**(18)**:** 5679-5684.

211. Bartkowiak K, Riethdorf S, Pantel K. The interrelating dynamics of hypoxic tumor microenvironments and cancer cell phenotypes in cancer metastasis. *Cancer Microenviron* 2012 Apr; **5**(1)**:** 59-72.

212. Kim I, Xu W, Reed JC. Cell death and endoplasmic reticulum stress: disease relevance and therapeutic opportunities. *Nat Rev Drug Discov* 2008 Dec; **7**(12)**:** 1013-1030.

213. Sano R, Reed JC. ER stress-induced cell death mechanisms. *Biochim Biophys Acta* 2013 Jul 10.

214. Sequeira SJ, Ranganathan AC, Adam AP, Iglesias BV, Farias EF, Aguirre-Ghiso JA. Inhibition of proliferation by PERK regulates mammary acinar morphogenesis and tumor formation. *PLoS One* 2007; **2**(7)**:** e615.

215. Avivar-Valderas A, Salas E, Bobrovnikova-Marjon E, Diehl JA, Nagi C, Debnath J*, et al.* PERK integrates autophagy and oxidative stress responses to promote survival during extracellular matrix detachment. *Mol Cell Biol* 2011 Sep; **31**(17)**:** 3616-3629.

216. Schafer ZT, Grassian AR, Song L, Jiang Z, Gerhart-Hines Z, Irie HY*, et al.* Antioxidant and oncogene rescue of metabolic defects caused by loss of matrix attachment. *Nature* 2009 Sep 3; **461**(7260)**:** 109-113.

217. Carracedo A, Weiss D, Leliaert AK, Bhasin M, de Boer VC, Laurent G*, et al.* A metabolic prosurvival role for PML in breast cancer. *J Clin Invest* 2012 Sep 4; **122**(9)**:** 3088-3100.

218. Caneba CA, Bellance N, Yang L, Pabst L, Nagrath D. Pyruvate uptake is increased in highly invasive ovarian cancer cells under anoikis conditions for anaplerosis, mitochondrial function, and migration. *Am J Physiol Endocrinol Metab* 2012 Oct; **303**(8)**:** E1036-1052.

219. Kamarajugadda S, Stemboroski L, Cai Q, Simpson NE, Nayak S, Tan M*, et al.* Glucose oxidation modulates anoikis and tumor metastasis. *Mol Cell Biol* 2012 May; **32**(10)**:** 1893-1907.

220. Koh EY, Chen T, Daley GQ. Novel retroviral vectors to facilitate expression screens in mammalian cells. *Nucleic Acids Res* 2002 Dec 15; **30**(24)**:** e142.

221. Demir K, Boutros M. Cell perturbation screens for target identification by RNAi. *Methods Mol Biol* 2012; **910:** 1-13.

222. Lydon NB, Druker BJ. Lessons learned from the development of imatinib. *Leuk Res* 2004 May; **28 Suppl 1:** S29-38.

223. Djuranovic S, Nahvi A, Green R. A parsimonious model for gene regulation by miRNAs. *Science* 2011 Feb 4; **331**(6017)**:** 550-553.

224. Vasudevan S, Tong Y, Steitz JA. Switching from repression to activation: microRNAs can up-regulate translation. *Science* 2007 Dec 21; **318**(5858)**:** 1931-1934.

225. Kaelin WG, Jr. Molecular biology. Use and abuse of RNAi to study mammalian gene function. *Science* 2012 Jul 27; **337**(6093)**:** 421-422.

226. Cully M, Genevet A, Warne P, Treins C, Liu T, Bastien J*, et al.* A role for p38 stress-activated protein kinase in regulation of cell growth via TORC1. *Mol Cell Biol* 2010 Jan; **30**(2)**:** 481-495.

227. Kukushkin AN, Svetlikova SB, Amanzholov RA, Pospelov VA. Anisomycin abrogates repression of protooncogene c-fos transcription in E1A + cHa-ras-transformed cells through activation of MEK/ERK kinase cascade. *J Cell Biochem* 2008 Feb 15; **103**(3)**:** 1005-1012.

228. Abayasiriwardana KS, Barbone D, Kim KU, Vivo C, Lee KK, Dansen TB*, et al.* Malignant mesothelioma cells are rapidly sensitized to TRAIL-induced apoptosis by low-dose anisomycin via Bim. *Mol Cancer Ther* 2007 Oct; **6**(10)**:** 2766-2776.

229. Irie HY, Shrestha Y, Selfors LM, Frye F, Iida N, Wang Z*, et al.* PTK6 regulates IGF-1-induced anchorage-independent survival. *PLoS One* 2010; **5**(7)**:** e11729.

230. Simpson CD, Hurren R, Kasimer D, MacLean N, Eberhard Y, Ketela T*, et al.* A genome wide shRNA screen identifies alpha/beta hydrolase domain containing 4 (ABHD4) as a novel regulator of anoikis resistance. *Apoptosis* 2012 Jul; **17**(7)**:** 666-678.

231. Sorensen PH, Liu XF, Delattre O, Rowland JM, Biggs CA, Thomas G*, et al.* Reverse transcriptase PCR amplification of EWS/FLI-1 fusion transcripts as a diagnostic test for peripheral primitive neuroectodermal tumors of childhood. *Diagn Mol Pathol* 1993 Sep; **2**(3)**:** 147-157.

232. Hu-Lieskovan S, Heidel JD, Bartlett DW, Davis ME, Triche TJ. Sequence-specific knockdown of EWS-FLI1 by targeted, nonviral delivery of small interfering RNA inhibits tumor growth in a murine model of metastatic Ewing's sarcoma. *Cancer Res* 2005 Oct 1; **65**(19)**:** 8984-8992.

233. Kwiatkowski DJ. Rhebbing up mTOR: new insights on TSC1 and TSC2, and the pathogenesis of tuberous sclerosis. *Cancer Biol Ther* 2003 Sep-Oct; **2**(5)**:** 471-476.

234. Cheng WT, Guo ZX, Lin CA, Lin MY, Tung LC, Fang K. Oxidative stress promotes autophagic cell death in human neuroblastoma cells with ectopic transfer of mitochondrial PPP2R2B (Bbeta2). *BMC Cell Biol* 2009; **10:** 91.

235. Hu J, Nakhla H, Friedman E. Transient arrest in a quiescent state allows ovarian cancer cells to survive suboptimal growth conditions and is mediated by both Mirk/dyrk1b and p130/RB2. *Int J Cancer* 2011 Jul 15; **129**(2)**:** 307-318.

236. Bosco EE, Wang Y, Xu H, Zilfou JT, Knudsen KE, Aronow BJ*, et al.* The retinoblastoma tumor suppressor modifies the therapeutic response of breast cancer. *J Clin Invest* 2007 Jan; **117**(1)**:** 218-228.

237. Sharma A, Comstock CE, Knudsen ES, Cao KH, Hess-Wilson JK, Morey LM*, et al.* Retinoblastoma tumor suppressor status is a critical determinant of therapeutic response in prostate cancer cells. *Cancer Res* 2007 Jul 1; **67**(13)**:** 6192-6203.

238. Schena M, Shalon D, Davis RW, Brown PO. Quantitative monitoring of gene expression patterns with a complementary DNA microarray. *Science* 1995 Oct 20; **270**(5235)**:** 467-470.

239. Oshlack A, Robinson MD, Young MD. From RNA-seq reads to differential expression results. *Genome Biol* 2010; **11**(12)**:** 220.

240. Kupferman ME, Patel V, Sriuranpong V, Amornphimoltham P, Jasser SA, Mandal M*, et al.* Molecular analysis of anoikis resistance in oral cavity squamous cell carcinoma. *Oral Oncol* 2007 May; **43**(5)**:** 440-454.

241. Abiatari I, DeOliveira T, Kerkadze V, Schwager C, Esposito I, Giese NA*, et al.* Consensus transcriptome signature of perineural invasion in pancreatic carcinoma. *Mol Cancer Ther* 2009 Jun; **8**(6)**:** 1494-1504.

242. Jinka R, Kapoor R, Pavuluri S, Raj AT, Kumar MJ, Rao L*, et al.* Differential gene expression and clonal selection during cellular transformation induced by adhesion deprivation. *BMC Cell Biol* 2010; **11:** 93.

243. Junn E, Han SH, Im JY, Yang Y, Cho EW, Um HD*, et al.* Vitamin D3 up-regulated protein 1 mediates oxidative stress via suppressing the thioredoxin function. *J Immunol* 2000 Jun 15; **164**(12)**:** 6287-6295.

244. Yoshioka J, Schulze PC, Cupesi M, Sylvan JD, MacGillivray C, Gannon J*, et al.* Thioredoxin-interacting protein controls cardiac hypertrophy through regulation of thioredoxin activity. *Circulation* 2004 Jun 1; **109**(21)**:** 2581-2586.

245. Sheth SS, Bodnar JS, Ghazalpour A, Thipphavong CK, Tsutsumi S, Tward AD*, et al.* Hepatocellular carcinoma in Txnip-deficient mice. *Oncogene* 2006 Jun 15; **25**(25)**:** 3528-3536.

246. Bodnar JS, Chatterjee A, Castellani LW, Ross DA, Ohmen J, Cavalcoli J*, et al.* Positional cloning of the combined hyperlipidemia gene Hyplip1. *Nat Genet* 2002 Jan; **30**(1)**:** 110-116.

247. Chutkow WA, Patwari P, Yoshioka J, Lee RT. Thioredoxin-interacting protein (Txnip) is a critical regulator of hepatic glucose production. *J Biol Chem* 2008 Jan 25; **283**(4)**:** 2397-2406.

248. Oslowski CM, Hara T, O'Sullivan-Murphy B, Kanekura K, Lu S, Hara M*, et al.* Thioredoxin-interacting protein mediates ER stress-induced beta cell death through initiation of the inflammasome. *Cell Metab* 2012 Aug 8; **16**(2)**:** 265-273.

249. Lerner AG, Upton JP, Praveen PV, Ghosh R, Nakagawa Y, Igbaria A*, et al.* IRE1alpha induces thioredoxin-interacting protein to activate the NLRP3 inflammasome and promote programmed cell death under irremediable ER stress. *Cell Metab* 2012 Aug 8; **16**(2)**:** 250-264.

250. Zhou R, Tardivel A, Thorens B, Choi I, Tschopp J. Thioredoxin-interacting protein links oxidative stress to inflammasome activation. *Nat Immunol* 2010 Feb; **11**(2)**:** 136-140.

251. Wu N, Zheng B, Shaywitz A, Dagon Y, Tower C, Bellinger G*, et al.* AMPK-dependent degradation of TXNIP upon energy stress leads to enhanced glucose uptake via GLUT1. *Mol Cell* 2013 Mar 28; **49**(6)**:** 1167-1175.

252. Subramanian A, Tamayo P, Mootha VK, Mukherjee S, Ebert BL, Gillette MA*, et al.* Gene set enrichment analysis: a knowledge-based approach for interpreting genome-wide expression profiles. *Proc Natl Acad Sci U S A* 2005 Oct 25; **102**(43)**:** 15545-15550.

253. Spindel ON, World C, Berk BC. Thioredoxin interacting protein: redox dependent and independent regulatory mechanisms. *Antioxid Redox Signal* 2012 Mar 15; **16**(6)**:** 587-596.

254. Jeon JH, Lee KN, Hwang CY, Kwon KS, You KH, Choi I. Tumor suppressor VDUP1 increases p27(kip1) stability by inhibiting JAB1. *Cancer Res* 2005 Jun 1; **65**(11)**:** 4485-4489.

255. Hetz C. The unfolded protein response: controlling cell fate decisions under ER stress and beyond. *Nat Rev Mol Cell Biol* 2012 Feb; **13**(2)**:** 89-102.

256. Jung H, Kim MJ, Kim DO, Kim WS, Yoon SJ, Park YJ*, et al.* TXNIP maintains the hematopoietic cell pool by switching the function of p53 under oxidative stress. *Cell Metab* 2013 Jul 2; **18**(1)**:** 75-85.

257. Hardie DG. AMP-activated/SNF1 protein kinases: conserved guardians of cellular energy. *Nat Rev Mol Cell Biol* 2007 Oct; **8**(10)**:** 774-785.

258. Towler MC, Hardie DG. AMP-activated protein kinase in metabolic control and insulin signaling. *Circ Res* 2007 Feb 16; **100**(3)**:** 328-341.

259. Jeon SM, Hay N. The dark face of AMPK as an essential tumor promoter. *Cell Logist* 2012 Oct 1; **2**(4)**:** 197-202.

260. Nielsen JN, Jorgensen SB, Frosig C, Viollet B, Andreelli F, Vaulont S*, et al.* A possible role for AMP-activated protein kinase in exercise-induced glucose utilization: insights from humans and transgenic animals. *Biochem Soc Trans* 2003 Feb; **31**(Pt 1)**:** 186-190.

261. Leone A, Di Gennaro E, Bruzzese F, Avallone A, Budillon A. New perspective for an old antidiabetic drug: metformin as anticancer agent. *Cancer Treat Res* 2014; **159:** 355-376.

262. Carling D, Zammit VA, Hardie DG. A common bicyclic protein kinase cascade inactivates the regulatory enzymes of fatty acid and cholesterol biosynthesis. *FEBS Lett* 1987 Nov 2; **223**(2)**:** 217-222.

263. Greer EL, Oskoui PR, Banko MR, Maniar JM, Gygi MP, Gygi SP*, et al.* The energy sensor AMP-activated protein kinase directly regulates the mammalian FOXO3 transcription factor. *J Biol Chem* 2007 Oct 12; **282**(41)**:** 30107-30119.

264. Chiacchiera F, Simone C. The AMPK-FoxO3A axis as a target for cancer treatment. *Cell Cycle* 2010 Mar 15; **9**(6)**:** 1091-1096.

265. Chen CC, Jeon SM, Bhaskar PT, Nogueira V, Sundararajan D, Tonic I*, et al.* FoxOs inhibit mTORC1 and activate Akt by inducing the expression of Sestrin3 and Rictor. *Dev Cell* 2010 Apr 20; **18**(4)**:** 592-604.

266. Gwinn DM, Shackelford DB, Egan DF, Mihaylova MM, Mery A, Vasquez DS*, et al.* AMPK phosphorylation of raptor mediates a metabolic checkpoint. *Mol Cell* 2008 Apr 25; **30**(2)**:** 214-226.

267. Hayashi AA, Proud CG. The rapid activation of protein synthesis by growth hormone requires signaling through mTOR. *Am J Physiol Endocrinol Metab* 2007 Jun; **292**(6)**:** E1647-1655.

268. Fingar DC, Salama S, Tsou C, Harlow E, Blenis J. Mammalian cell size is controlled by mTOR and its downstream targets S6K1 and 4EBP1/eIF4E. *Genes Dev* 2002 Jun 15; **16**(12)**:** 1472-1487.

269. Hadad SM, Baker L, Quinlan PR, Robertson KE, Bray SE, Thomson G*, et al.* Histological evaluation of AMPK signalling in primary breast cancer. *BMC Cancer* 2009; **9:** 307.

270. Faubert B, Boily G, Izreig S, Griss T, Samborska B, Dong Z*, et al.* AMPK is a negative regulator of the Warburg effect and suppresses tumor growth in vivo. *Cell Metab* 2013 Jan 8; **17**(1)**:** 113-124.

271. Phoenix KN, Devarakonda CV, Fox MM, Stevens LE, Claffey KP. AMPKalpha2 Suppresses Murine Embryonic Fibroblast Transformation and Tumorigenesis. *Genes Cancer* 2012 Jan; **3**(1)**:** 51-62.

272. Benjamin D, Colombi M, Moroni C, Hall MN. Rapamycin passes the torch: a new generation of mTOR inhibitors. *Nat Rev Drug Discov* 2011 Nov; **10**(11)**:** 868-880.

273. Hudes G, Carducci M, Tomczak P, Dutcher J, Figlin R, Kapoor A*, et al.* Temsirolimus, interferon alfa, or both for advanced renal-cell carcinoma. *N Engl J Med* 2007 May 31; **356**(22)**:** 2271-2281.

274. Yao JC, Shah MH, Ito T, Bohas CL, Wolin EM, Van Cutsem E*, et al.* Everolimus for advanced pancreatic neuroendocrine tumors. *N Engl J Med* 2011 Feb 10; **364**(6)**:** 514-523.

275. Baselga J, Campone M, Piccart M, Burris HA, 3rd, Rugo HS, Sahmoud T*, et al.* Everolimus in postmenopausal hormone-receptor-positive advanced breast cancer. *N Engl J Med* 2012 Feb 9; **366**(6)**:** 520-529.

276. Liang J, Mills GB. AMPK: a contextual oncogene or tumor suppressor? *Cancer Res* 2013 May 15; **73**(10)**:** 2929-2935.

277. Viollet B, Athea Y, Mounier R, Guigas B, Zarrinpashneh E, Horman S*, et al.* AMPK: Lessons from transgenic and knockout animals. *Front Biosci (Landmark Ed)* 2009; **14:** 19-44.

278. Bardeesy N, Sinha M, Hezel AF, Signoretti S, Hathaway NA, Sharpless NE*, et al.* Loss of the Lkb1 tumour suppressor provokes intestinal polyposis but resistance to transformation. *Nature* 2002 Sep 12; **419**(6903)**:** 162-167.

279. Jang T, Calaoagan JM, Kwon E, Samuelsson S, Recht L, Laderoute KR. 5'-AMP-activated protein kinase activity is elevated early during primary brain tumor development in the rat. *Int J Cancer* 2011 May 1; **128**(9)**:** 2230-2239.

280. Ros S, Santos CR, Moco S, Baenke F, Kelly G, Howell M*, et al.* Functional metabolic screen identifies 6-phosphofructo-2-kinase/fructose-2,6-biphosphatase 4 as an important regulator of prostate cancer cell survival. *Cancer Discov* 2012 Apr; **2**(4)**:** 328-343.

281. Liu L, Ulbrich J, Muller J, Wustefeld T, Aeberhard L, Kress TR*, et al.* Deregulated MYC expression induces dependence upon AMPK-related kinase 5. *Nature* 2012 Mar 29; **483**(7391)**:** 608-612.

282. Laderoute KR, Amin K, Calaoagan JM, Knapp M, Le T, Orduna J*, et al.* 5'-AMP-activated protein kinase (AMPK) is induced by low-oxygen and glucose deprivation conditions found in solid-tumor microenvironments. *Mol Cell Biol* 2006 Jul; **26**(14)**:** 5336-5347.

283. Kato K, Ogura T, Kishimoto A, Minegishi Y, Nakajima N, Miyazaki M*, et al.* Critical roles of AMP-activated protein kinase in constitutive tolerance of cancer cells to nutrient deprivation and tumor formation. *Oncogene* 2002 Sep 5; **21**(39)**:** 6082-6090.

284. Fernandez MR, Henry MD, Lewis RE. Kinase suppressor of Ras 2 (KSR2) regulates tumor cell transformation via AMPK. *Mol Cell Biol* 2012 Sep; **32**(18)**:** 3718-3731.

285. Godlewski J, Nowicki MO, Bronisz A, Nuovo G, Palatini J, De Lay M*, et al.* MicroRNA-451 regulates LKB1/AMPK signaling and allows adaptation to metabolic stress in glioma cells. *Mol Cell* 2010 Mar 12; **37**(5)**:** 620-632.

286. Solimini NL, Luo J, Elledge SJ. Non-oncogene addiction and the stress phenotype of cancer cells. *Cell* 2007 Sep 21; **130**(6)**:** 986-988.

287. McGee SL, Hargreaves M. AMPK and transcriptional regulation. *Front Biosci* 2008; **13:** 3022-3033.

288. Narkar VA, Downes M, Yu RT, Embler E, Wang YX, Banayo E*, et al.* AMPK and PPARdelta agonists are exercise mimetics. *Cell* 2008 Aug 8; **134**(3)**:** 405-415.

289. Zhou J, Huang W, Tao R, Ibaragi S, Lan F, Ido Y*, et al.* Inactivation of AMPK alters gene expression and promotes growth of prostate cancer cells. *Oncogene* 2009 May 7; **28**(18)**:** 1993-2002.

290. Bungard D, Fuerth BJ, Zeng PY, Faubert B, Maas NL, Viollet B*, et al.* Signaling kinase AMPK activates stress-promoted transcription via histone H2B phosphorylation. *Science* 2010 Sep 3; **329**(5996)**:** 1201-1205.

291. Kwiatkowski DJ, Zhang H, Bandura JL, Heiberger KM, Glogauer M, el-Hashemite N*, et al.* A mouse model of TSC1 reveals sex-dependent lethality from liver hemangiomas, and up-regulation of p70S6 kinase activity in Tsc1 null cells. *Hum Mol Genet* 2002 Mar 1; **11**(5)**:** 525-534.

292. Petroulakis E, Parsyan A, Dowling RJ, LeBacquer O, Martineau Y, Bidinosti M*, et al.* p53-dependent translational control of senescence and transformation via 4E-BPs. *Cancer Cell* 2009 Nov 6; **16**(5)**:** 439-446.

293. Sarbassov DD, Ali SM, Sabatini DM. Growing roles for the mTOR pathway. *Curr Opin Cell Biol* 2005 Dec; **17**(6)**:** 596-603.

294. Buttgereit F, Brand MD. A hierarchy of ATP-consuming processes in mammalian cells. *Biochem J* 1995 Nov 15; **312 (Pt 1):** 163-167.

295. Schneider-Poetsch T, Ju J, Eyler DE, Dang Y, Bhat S, Merrick WC*, et al.* Inhibition of eukaryotic translation elongation by cycloheximide and lactimidomycin. *Nat Chem Biol* 2010; **6**(3)**:** 209-217.

296. Lee CH, Inoki K, Karbowniczek M, Petroulakis E, Sonenberg N, Henske EP*, et al.* Constitutive mTOR activation in TSC mutants sensitizes cells to energy starvation and genomic damage via p53. *EMBO J* 2007 Nov 28; **26**(23)**:** 4812-4823.

297. Gilmore AP. Anoikis. *Cell Death Differ* 2005 Nov; **12 Suppl 2:** 1473-1477.

298. Phadke PA, Vaidya KS, Nash KT, Hurst DR, Welch DR. BRMS1 suppresses breast cancer experimental metastasis to multiple organs by inhibiting several steps of the metastatic process. *Am J Pathol* 2008 Mar; **172**(3)**:** 809-817.

299. El-Naggar S, Liu Y, Dean DC. Mutation of the Rb1 pathway leads to overexpression of mTor, constitutive phosphorylation of Akt on serine 473, resistance to anoikis, and a block in c-Raf activation. *Mol Cell Biol* 2009 Nov; **29**(21)**:** 5710-5717.

300. Vitale M, Di Matola T, Bifulco M, Casamassima A, Fenzi G, Rossi G. Apoptosis induced by denied adhesion to extracellular matrix (anoikis) in thyroid epithelial cells is p53 dependent but fails to correlate with modulation of p53 expression. *FEBS Lett* 1999 Nov 26; **462**(1-2)**:** 57-60.

301. Lock R, Roy S, Kenific CM, Su JS, Salas E, Ronen SM*, et al.* Autophagy Facilitates Glycolysis During Ras Mediated Oncogenic Transformation. *Mol Biol Cell* 2010 Dec 14.

302. Guo JY, Chen HY, Mathew R, Fan J, Strohecker AM, Karsli-Uzunbas G*, et al.* Activated Ras requires autophagy to maintain oxidative metabolism and tumorigenesis. *Genes Dev* 2011 Mar 1; **25**(5)**:** 460-470.

303. Kim MJ, Woo SJ, Yoon CH, Lee JS, An S, Choi YH*, et al.* Involvement of autophagy in oncogenic K-Ras-induced malignant cell transformation. *J Biol Chem* 2011 Apr 15; **286**(15)**:** 12924-12932.

304. Choo AY, Kim SG, Vander Heiden MG, Mahoney SJ, Vu H, Yoon SO*, et al.* Glucose addiction of TSC null cells is caused by failed mTORC1-dependent balancing of metabolic demand with supply. *Mol Cell* 2010 May 28; **38**(4)**:** 487-499.

305. Liu H, Radisky DC, Nelson CM, Zhang H, Fata JE, Roth RA*, et al.* Mechanism of Akt1 inhibition of breast cancer cell invasion reveals a protumorigenic role for TSC2. *Proc Natl Acad Sci U S A* 2006 Mar 14; **103**(11)**:** 4134-4139.

306. Dubois L, Magagnin MG, Cleven AH, Weppler SA, Grenacher B, Landuyt W*, et al.* Inhibition of 4E-BP1 sensitizes U87 glioblastoma xenograft tumors to irradiation by decreasing hypoxia tolerance. *Int J Radiat Oncol Biol Phys* 2009 Mar 15; **73**(4)**:** 1219-1227.

307. Braunstein S, Karpisheva K, Pola C, Goldberg J, Hochman T, Yee H*, et al.* A hypoxia-controlled cap-dependent to cap-independent translation switch in breast cancer. *Mol Cell* 2007 Nov 9; **28**(3)**:** 501-512.

308. Frisch SM, Schaller M, Cieply B. Mechanisms that link the oncogenic epithelial-mesenchymal transition to suppression of anoikis. *J Cell Sci* 2013 Jan 1; **126**(Pt 1)**:** 21-29.

309. Plaks V, Koopman CD, Werb Z. Cancer. Circulating tumor cells. *Science* 2013 Sep 13; **341**(6151)**:** 1186-1188.

310. Wang D, Bodovitz S. Single cell analysis: the new frontier in 'omics'. *Trends Biotechnol* 2010 Jun; **28**(6)**:** 281-290.

APPENDIX 1: SUPPLEMENTARY TABLES

Table A1.1. Genes up-regulated greater than 2-fold following cellular detachment of EN-transformed MEFs (>2-fold, p-value <0.05 in all cell lines when analyzed individually).

Gene Name	Symbol	Fold Change Susp vs. Mono	p-value
Lipocalin 2	Lcn2	13.14	0.0013
RIKEN cDNA 1810011O10 gene	1810011O10Rik	9.37	<0.00001
Aldehyde dehydrogenase family 3, subfamily A1	Aldh3a1	9.3	0.00002
Matrix metallopeptidase 13	Mmp13	9.22	0.00061
CCAAT/enhancer binding protein (C/EBP), delta	Cebpd	8.67	<0.00001
N-myc downstream regulated gene 1	Ndrg1	8.57	<0.00001
Interleukin 33	Il33	8.48	0.00003
Chemokine (C-C motif) ligand 5	Ccl5	8.29	<0.00001
Very low density lipoprotein receptor	Vldlr	7.44	<0.00001
Growth arrest and DNA-damage-inducible 45 alpha	Gadd45a	7.43	<0.00001
Scavenger receptor class A, member 5 (putative)	Scara5	7.23	0.00006
Insulin-like growth factor binding protein 4	Igfbp4	6.66	<0.00001
Very low density lipoprotein receptor	Vldlr	6.49	<0.00001
Thioredoxin interacting protein	Txnip	6.21	<0.00001
Histone cluster 1, H2bc	Hist1h2bc	5.97	<0.00001
N-myc downstream regulated gene 1	Ndrg1	5.97	<0.00001
Early growth response 2	Egr2	5.75	<0.00001
Interferon activated gene 203	Ifi203	5.71	<0.00001
N-myc downstream regulated gene 1	Ndrg1	5.51	<0.00001
Early growth response 1	Egr1	5.49	<0.00001
N-myc downstream regulated gene 1	Ndrg1	5.44	<0.00001
Histone cluster 1, H1c	Hist1h1c	5.2	0.00001
Thioredoxin interacting protein	Txnip	4.94	<0.00001
ERO1-like (S. cerevisiae)	Ero1l	4.88	0.00002
Histocompatibility 2, T region locus 23	C920025E04Rik	4.83	<0.00001
Cold inducible RNA binding protein	Cirbp	4.77	<0.00001
Tumor necrosis factor receptor superfamily, member 9	Tnfrsf9	4.77	0.00008
Nuclear protein 1	Nupr1	4.75	<0.00001
Interferon activated gene 203	Ifi203	4.7	<0.00001
Chemokine (C-X-C motif) ligand 1	Cxcl1	4.68	0.00012
DNA-damage inducible transcript 3	Ddit3	4.53	<0.00001
ERO1-like (S. cerevisiae)	Ero1l	4.48	<0.00001
ERO1-like (S. cerevisiae)	Ero1l	4.45	0.00001

Gene Name	Symbol	Fold Change Susp vs. Mono	p-value
RIKEN cDNA 2900042B11 gene	2900042B11Rik	4.39	<0.00001
Unconventional SNARE in the ER 1 homolog (S. cerevisiae)	Use1	4.32	<0.00001
N-myc downstream regulated gene 1	Ndrg1	4.31	<0.00001
Interferon activated gene 203	Ifi203	4.28	<0.00001
Amphiregulin	Areg	4.27	<0.00001
Uridine phosphorylase 1	Upp1	4.25	<0.00001
Nuclear factor of kappa light polypeptide gene enhancer in B-cells inhibitor, zeta	Nfkbiz	4.24	<0.00001
Ribosomal protein L22	Rpl22	4.2	<0.00001
UDP glucuronosyltransferase 1 family, polypeptide A2	Ugt1a1	4.16	0.0053
Basic helix-loop-helix domain containing, class B2	Bhlhb2	4.09	<0.00001
Cyclin-dependent kinase inhibitor 1A (P21)	Cdkn1a	4.09	<0.00001
Casein kappa	Csn3	4.08	0.00046
UDP glucuronosyltransferase 1 family, polypeptide A2	Ugt1a1	4.07	0.0066
Adenylosuccinate synthetase like 1	Adssl1	3.98	<0.00001
RIKEN cDNA 2310002J21 gene	2310002J21Rik	3.91	<0.00001
Teashirt zinc finger family member 1	Tshz1	3.9	<0.00001
Early growth response 2	Egr2	3.89	<0.00001
Nuclear protein 1	Nupr1	3.87	<0.00001
RIKEN cDNA 1110003E01 gene	1110003E01Rik	3.81	<0.00001
Cyclin G2	Ccng2	3.75	<0.00001
Transforming growth factor, beta induced	Tgfbi	3.75	<0.00001
Annexin A8	Anxa8	3.73	0.00019
Guanylate nucleotide binding protein 2	Gbp2	3.69	0.0019
G protein-coupled receptor 137B		3.67	<0.00001
DNA-damage-inducible transcript 4	Ddit4	3.64	<0.00001
Aldehyde dehydrogenase family 6, subfamily A1	Aldh6a1	3.6	<0.00001
Collagen, type VI, alpha 1	Col6a1	3.6	<0.00001
Tribbles homolog 3 (Drosophila)	Trib3	3.6	<0.00001
Selenoprotein P, plasma, 1	Sepp1	3.59	0.00052
Guanylate nucleotide binding protein 1	Gbp1	3.58	0.00042
Trafficking protein particle complex 6A	Trappc6a	3.57	<0.00001
Glutaminyl-peptide cyclotransferase (glutaminyl cyclase)	Qpct	3.53	<0.00001
Arrestin domain containing 4	Arrdc4	3.52	<0.00001
Biliverdin reductase B (flavin reductase (NADPH))	Blvrb	3.52	<0.00001
Tripartite motif protein 30	Trim30	3.51	0.0017
Microsomal glutathione S-transferase 1	Mgst1	3.46	0.089
Transforming growth factor, beta induced	Tgfbi	3.43	0.00002
Insulin-like growth factor binding protein 4	Igfbp4	3.37	<0.00001
Kruppel-like factor 10	Klf10	3.34	<0.00001

Gene Name	Symbol	Fold Change Susp vs. Mono	p-value
SRY-box containing gene 4	Sox4	3.34	<0.00001
Harvey rat sarcoma oncogene, subgroup R	Rras	3.33	<0.00001
Phytanoyl-CoA dioxygenase domain containing 1	Lrrc8a	3.32	<0.00001
BCL2/adenovirus E1B interacting protein 1, NIP3	Bnip3	3.31	<0.00001
Hydroxy-delta-5-steroid dehydrogenase, 3 beta- and steroid delta-isomerase 7	Hsd3b7	3.31	<0.00001
Nephroblastoma overexpressed gene	Nov	3.29	0.00004
Glypican 1	Gpc1	3.27	<0.00001
Kruppel-like factor 4 (gut)	Klf4	3.24	<0.00001
Unconventional SNARE in the ER 1 homolog (S. cerevisiae)	Use1	3.23	<0.00001
UDP glucuronosyltransferase 1 family, polypeptide A2	Ugt1a1	3.22	0.0048
LYR motif containing 5	Lyrm5	3.2	<0.00001
RIKEN cDNA 2310043N10 gene	2310043N10Rik	3.2	<0.00001
Pyrroline-5-carboxylate reductase 1	Pycr1	3.19	<0.00001
Plasma glutamate carboxypeptidase	Pgcp	3.16	<0.00001
Vesicle-associated membrane protein 4	Vamp4	3.16	<0.00001
Sulfatase 2	Sulf2	3.14	0.00008
CD99 antigen	Cd99	3.13	0.00005
Interferon, alpha-inducible protein 27	Ifi27	3.13	0.0008
RIKEN cDNA 0610010K14 gene	0610010K14Rik	3.13	<0.00001
RIKEN cDNA 5830443L24 gene	5830443L24Rik	3.13	0.00006
Cathepsin B	Ctsb	3.1	<0.00001
Metallothionein 2	Mt2	3.08	<0.00001
Proline-rich nuclear receptor coactivator 1	Pnrc1	3.08	<0.00001
Syndecan 4	Sdc4	3.06	<0.00001
Tetraspanin 17	Tspan17	3.05	0.00001
Cathepsin B	Ctsb	3.02	<0.00001
D site albumin promoter binding protein	Dbp	3.01	0.0002
RIKEN cDNA 1200015M12 gene	1200015M12Rik	3.01	<0.00001
Programmed cell death 4	Pdcd4	2.99	<0.00001
Interferon activated gene 203	Ifi203	2.98	<0.00001
Yippee-like 5 (Drosophila)	Ypel5	2.98	<0.00001
Interferon activated gene 205	Ifi205	2.97	0.00011
Nephroblastoma overexpressed gene	Nov	2.97	0.00001
Aryl-hydrocarbon receptor	Ahr	2.96	<0.00001
Sulfide quinone reductase-like (yeast)	Sqrdl	2.93	0.00003
G protein-coupled receptor 137B	Gpr137b	2.9	<0.00001
Tumor necrosis factor (ligand) superfamily, member 13	Tnfsf12-tnfsf13	2.88	<0.00001
Cyclin-dependent kinase inhibitor 1A (P21)	Cdkn1a	2.86	<0.00001
Collagen, type XVIII, alpha 1	Col18a1	2.85	<0.00001
Cytochrome b5 reductase 1	Cyb5r1	2.84	<0.00001

Gene Name	Symbol	Fold Change Susp vs. Mono	p-value
Leukemia inhibitory factor	Lif	2.84	<0.00001
Transglutaminase 2, C polypeptide	Tgm2	2.82	<0.00001
G protein-coupled receptor 137B		2.81	<0.00001
C1q domain containing 2	C1qdc2	2.78	0.00003
Ectonucleotide pyrophosphatase/phosphodiesterase 2	Enpp2	2.77	<0.00001
Galactosidase, alpha	Gla	2.77	<0.00001
Crystallin, zeta	Cryz	2.76	<0.00001
Immediate early response 3	Ier3	2.76	<0.00001
Max interacting protein 1	Mxi1	2.76	<0.00001
Transforming growth factor, beta 1	Tgfb1	2.76	<0.00001
Neuron derived neurotrophic factor	Nenf	2.75	<0.00001
Androgen-induced 1	Aig1	2.74	0.0032
Tribbles homolog 3 (Drosophila)	Trib3	2.74	<0.00001
Citrate lyase beta like	Clybl	2.73	<0.00001
CD99 antigen	Cd99	2.72	0.00001
Cyclin G2	Ccng2	2.71	<0.00001
Histone cluster 3, H2a	Hist3h2a	2.7	0.00002
Tribbles homolog 2 (Drosophila)	Trib2	2.7	<0.00001
RIKEN cDNA 1110003E01 gene	1110003E01Rik	2.69	<0.00001
Tumor necrosis factor receptor superfamily, member 9	Tnfrsf9	2.69	0.00032
Kelch-like 24 (Drosophila)	Klhl24	2.68	<0.00001
CD82 antigen	Cd82	2.67	<0.00001
Preimplantation protein 4	Prei4	2.66	0.00004
Transmembrane protein 140	Tmem140	2.66	0.00001
Niemann Pick type C2	Npc2	2.65	<0.00001
RIKEN cDNA 4930504E06 gene	4930504E06Rik	2.65	<0.00001
cDNA sequence BC004044	BC004044	2.64	<0.00001
MACRO domain containing 1	Macrod1	2.64	0.00003
Plasmalemma vesicle associated protein	Plvap	2.62	<0.00001
Purinergic receptor P2X, ligand-gated ion channel 4	P2rx4	2.62	<0.00001
Component of Sp100-rs		2.6	0.0008
Kruppel-like factor 4 (gut)	Klf4	2.6	0.00009
Epiregulin	Ereg	2.59	<0.00001
Sarcospan	Sspn	2.57	<0.00001
Cellular repressor of E1A-stimulated genes 1	Creg1	2.56	<0.00001
Chromatin modifying protein 1B	Chmp1b	2.55	<0.00001
Histocompatibility 2, D region locus 1	H2-D1	2.55	0.00045
SRY-box containing gene 4	Sox4	2.54	<0.00001
Avian viral (v-rel) oncogene related B	Relb	2.53	<0.00001

Gene Name	Symbol	Fold Change Susp vs. Mono	p-value
SRY-box containing gene 4	Sox4	2.53	<0.00001
Nuclear factor of kappa light chain gene enhancer in B-cells inhibitor, alpha	Nfkbia	2.51	<0.00001
Transmembrane protein 77	Tmem77	2.51	<0.00001
cDNA sequence BC010787	BC010787	2.49	<0.00001
Glucosamine-6-phosphate deaminase 2	Gnpda2	2.49	<0.00001
Phospholipid transfer protein	Pltp	2.49	0.0011
Collagen, type V, alpha 3	Col5a3	2.48	0.00049
CNDP dipeptidase 2 (metallopeptidase M20 family)	Cndp2	2.47	<0.00001
Ecotropic viral integration site 2a	Evi2a	2.45	0.0013
Epithelial membrane protein 2	Emp2	2.43	<0.00001
Growth arrest specific 5	Gas5	2.41	<0.00001
Serine incorporator 3	Serinc3	2.41	<0.00001
RAD52 motif 1	Rdm1	2.4	<0.00001
RIKEN cDNA 1810030N24 gene	1810030N24Rik	2.4	<0.00001
Receptor accessory protein 5	Reep5	2.39	<0.00001
Alpha-N-acetylglucosaminidase (Sanfilippo disease IIIB)	Naglu	2.38	<0.00001
G protein-coupled receptor 137B, pseudogene	Gpr137b	2.38	<0.00001
H2A histone family, member V	H2afv	2.38	<0.00001
Similar to H-2K(d) antigen		2.38	0.00051
Gene rich cluster, C10 gene	Grcc10	2.37	<0.00001
Matrix metallopeptidase 11	Mmp11	2.37	<0.00001
Phosphoglucomutase 2	Pgm2	2.37	0.00009
Teashirt zinc finger family member 1	Tshz1	2.37	<0.00001
Zinc finger, FYVE domain containing 21	Zfyve21	2.37	<0.00001
BCL2-like 11 (apoptosis facilitator)	Bcl2l11	2.34	<0.00001
Calpastatin	Cast	2.34	<0.00001
Interferon (alpha and beta) receptor 2	Ifnar2	2.33	0.00024
Ribonuclease T2B		2.33	0.00025
Serine incorporator 3	Serinc3	2.33	0.00003
Histocompatibility 2, T region locus 10	H2-T18	2.31	0.004
Interferon activated gene 202B	Ifi202b	2.31	<0.00001
Peroxiredoxin 5	Prdx5	2.31	<0.00001
PTEN induced putative kinase 1		2.29	<0.00001
TG interacting factor 1	Tgif1	2.29	<0.00001
CD47 antigen (Rh-related antigen, integrin-associated signal transducer)	Cd47	2.28	<0.00001
Ectonucleotide pyrophosphatase/phosphodiesterase 2	Enpp2	2.27	<0.00001
Nuclear factor of kappa light chain gene enhancer in B-cells inhibitor, alpha	Nfkbia	2.27	<0.00001

Gene Name	Symbol	Fold Change Susp vs. Mono	p-value
Regulator of G-protein signaling 2	Rgs2	2.26	<0.00001
Cytochrome P450, family 2, subfamily c, polypeptide 55	Cyp2c55	2.23	<0.00001
Niemann Pick type C2	Npc2	2.23	<0.00001
Acetyl-Coenzyme A acyltransferase 1A	Acaa1a	2.22	<0.00001
Dehydrogenase/reductase (SDR family) member 7	Dhrs7	2.22	<0.00001
B-cell translocation gene 1, anti-proliferative		2.21	<0.00001
RIKEN cDNA 5730494N06 gene	5730494N06Rik	2.21	<0.00001
Dehydrogenase/reductase (SDR family) member 1	Dhrs1	2.2	<0.00001
Plasmacytoma variant translocation 1	Pvt1	2.2	<0.00001
RIKEN cDNA 5730427N09 gene	EG433230	2.2	<0.00001
Jun-B oncogene	Junb	2.19	<0.00001
Mitochondrial ribosomal protein L24	Mrpl24	2.17	<0.00001
RIO kinase 3 (yeast)	Riok3	2.17	<0.00001
Chemokine (C-X3-C motif) ligand 1	Cx3cl1	2.15	<0.00001
Epithelial membrane protein 2	Emp2	2.13	<0.00001
Meningioma expressed antigen 5 (hyaluronidase)	Mgea5	2.12	<0.00001
BCL2-like 11 (apoptosis facilitator)	Bcl2l11	2.11	0.00005
Poly(A)-specific ribonuclease (deadenylation nuclease)	Parn	2.11	<0.00001
Rab acceptor 1 (prenylated)	Rabac1	2.1	<0.00001
Myristoylated alanine rich protein kinase C substrate	Marcks	2.07	0.0023
Neighbor of Brca1 gene 1	Nbr1	2.07	<0.00001
Transmembrane 7 superfamily member 3	Tm7sf3	2.06	<0.00001
BCL2/adenovirus E1B interacting protein 3-like	Bnip3l	2.04	0.00002
TCDD-inducible poly(ADP-ribose) polymerase	Tiparp	2.04	<0.00001

Table A1.2. Genes down-regulated greater than 2-fold following cellular detachment of EN-transformed MEFs (>2-fold down, p-value <0.05 in all cell lines when analyzed individually)

Gene Name	Symbol	Fold Change Susp vs. Mono	p-value
Connective tissue growth factor	Ctgf	0.09	<0.00001
Carboxylesterase 1	Ces1	0.11	<0.00001
Actin, alpha 2, smooth muscle, aorta	Acta2	0.16	0.00004
Ankyrin repeat domain 1 (cardiac muscle)	Ankrd1	0.17	0.00022
Ankyrin repeat domain 1 (cardiac muscle)	Ankrd1	0.17	0.00022
Thrombospondin 1	LOC640441	0.24	<0.00001
ATPase, Na+/K+ transporting, beta 1 polypeptide	Atp1b1	0.25	<0.00001
Serum deprivation response	Sdpr	0.25	<0.00001
Heat shock protein 110	Hsp110	0.26	<0.00001
Similar to thrombospondin 1	LOC640441	0.27	<0.00001
Heat shock protein 110	Hsp110	0.28	<0.00001
Gap junction protein, beta 3	Gjb3	0.29	<0.00001
Plakophilin 2	Pkp2	0.33	<0.00001
Serum deprivation response	Sdpr	0.34	<0.00001
Aquaporin 5	Aqp5	0.35	0.0015
Fatty acid synthase	Fasn	0.35	<0.00001
Inhibitor of DNA binding 3	Id3	0.36	0.00002
Plakophilin 2	Pkp2	0.37	<0.00001
Fascin homolog 1, actin bundling protein	Fscn1	0.38	0.00003
FUS interacting protein (serine-arginine rich) 1	Fusip1	0.38	<0.00001
Testis-specific kinase 2	Tesk2	0.38	<0.00001
Interferon-related developmental regulator 2	Ifrd2	0.39	<0.00001
Proliferation-associated 2G4	Pa2g4	0.39	<0.00001
Ajuba	Jub	0.41	<0.00001
Fibrillin 1	Fbn1	0.41	<0.00001
Eukaryotic translation elongation factor 1 delta (guanine nucleotide exchange protein)	Eef1d	0.42	<0.00001
PRP31 pre-mRNA processing factor 31 homolog (yeast)	Prpf31	0.42	<0.00001
RIKEN cDNA 1700023A16 gene	1700023A16Rik	0.42	<0.00001
AT hook containing transcription factor 1	Ahctf1	0.43	<0.00001
Carbamoyl-phosphate synthetase 2, aspartate transcarbamylase, and dihydroorotase	Cad	0.43	<0.00001
Paternally expressed 10	Peg10	0.43	<0.00001
Arginine and glutamate rich 1	Arglu1	0.44	<0.00001
Karyopherin (importin) beta 1	Kpnb1	0.44	<0.00001
Osteoglycin	Ogn	0.44	0.0028
Ubiquilin 2	Ubqln2	0.44	<0.00001
Fascin homolog 1, actin bundling protein	Fscn1	0.45	<0.00001

Gene Name	Symbol	Fold Change Susp vs. Mono	p-value
Adiponectin receptor 1	Adipor1	0.46	<0.00001
TAR (HIV) RNA binding protein 2	Tarbp2	0.46	<0.00001
Catenin (cadherin associated protein), alpha-like 1	Ctnnal1	0.47	<0.00001
Integrin alpha 3	Itga3	0.49	0.00016
Myosin XIX	Myo19	0.49	<0.00001

Table A1.3: Annotated experimental gene sets (c2.cgp.2.5.symbols.gmt) significantly enriched in the up-regulated genes following cellular detachment of EN-transformed MEFs, as determined by GSEA (FDR < 0.05)

EXPERIMENT NAME	SIZE	ES	NES	NOMINAL P-VALUE	FDR Q-VALUE
GALINDO_ACT_UP	78	0.682	2.395	0.0000	0.0000
EMT_UP	55	0.724	2.389	0.0000	0.0000
JECHLINGER_EMT_UP	51	0.704	2.306	0.0000	0.0000
MENSE_HYPOXIA_UP	78	0.650	2.294	0.0000	0.0000
ET743_SARCOMA_72HRS_UP	60	0.651	2.199	0.0000	0.0000
ABBUD_LIF_UP	46	0.679	2.181	0.0000	0.0000
BASSO_HCL_DIFF	64	0.645	2.172	0.0000	0.0000
ET743_HELA_UP	49	0.656	2.155	0.0000	0.0000
PENG_LEUCINE_UP	85	0.598	2.144	0.0000	0.0000
HINATA_NFKB_UP	89	0.595	2.128	0.0000	0.0001
SERUM_FIBROBLAST_CORE_DN	142	0.561	2.113	0.0000	0.0001
ET743_SARCOMA_UP	59	0.618	2.091	0.0000	0.0005
LINDSTEDT_DEND_UP	44	0.633	2.078	0.0000	0.0005
CMV_HCMV_TIMECOURSE_12HRS_UP	21	0.750	2.072	0.0000	0.0005
CHANG_SERUM_RESPONSE_DN	96	0.572	2.067	0.0000	0.0004
TNFA_NFKB_DEP_UP	17	0.801	2.056	0.0000	0.0005
APPEL_IMATINIB_UP	30	0.689	2.048	0.0000	0.0006
ZHAN_MM_MOLECULAR_CLASSI_UP	44	0.633	2.030	0.0000	0.0009
IFNA_HCMV_6HRS_UP	39	0.640	2.003	0.0000	0.0016
MANALO_HYPOXIA_UP	90	0.561	2.000	0.0000	0.0016
ZHAN_MM_CD138_CD1_VS_REST	30	0.670	1.996	0.0000	0.0017
IFN_ALPHA_UP	34	0.646	1.995	0.0000	0.0016
ZMPSTE24_KO_UP	30	0.686	1.993	0.0000	0.0016
GERY_CEBP_TARGETS	134	0.525	1.975	0.0000	0.0021
DER_IFNA_UP	53	0.594	1.972	0.0000	0.0021
GOLDRATH_MEMORY	63	0.586	1.969	0.0000	0.0021
SHIPP_FL_VS_DLBCL_UP	25	0.683	1.966	0.0000	0.0021
JNK_DN	30	0.660	1.962	0.0000	0.0023
HYPOXIA_FIBRO_UP	20	0.716	1.955	0.0000	0.0024
LEE_ACOX1_UP	56	0.582	1.952	0.0000	0.0024
LINDSTEDT_DEND_8H_VS_48H_UP	59	0.580	1.946	0.0000	0.0027
RADAEVA_IFNA_UP	40	0.617	1.944	0.0000	0.0027
PASSERINI_INFLAMMATION	23	0.696	1.943	0.0000	0.0027
ET743_SARCOMA_6HRS_UP	27	0.655	1.941	0.0000	0.0027
DSRNA_UP	33	0.633	1.937	0.0000	0.0026
CARIES_PULP_UP	168	0.504	1.936	0.0000	0.0026

EXPERIMENT NAME	SIZE	ES	NES	NOMINAL P-VALUE	FDR Q-VALUE
HOFFMANN_BIVSBII_BI	113	0.530	1.935	0.0000	0.0026
HYPOXIA_REG_UP	34	0.625	1.931	0.0000	0.0028
PARK_RARALPHA_UP	35	0.635	1.911	0.0000	0.0039
CHEN_HOXA5_TARGETS_UP	146	0.499	1.910	0.0000	0.0038
MOOTHA_VOXPHOS	72	0.547	1.905	0.0000	0.0039
MARCINIAK_CHOP_DIFF	25	0.666	1.903	0.0000	0.0038
P53_BRCA1_UP	32	0.632	1.903	0.0000	0.0037
RUTELLA_HEPATGFSNDCS_UP	126	0.513	1.902	0.0000	0.0037
BROCKE_IL6	117	0.508	1.902	0.0000	0.0037
SANA_TNFA_ENDOTHELIAL_UP	64	0.558	1.898	0.0000	0.0039
RUTELLA_HEMATOGFSNDCS_DIFF	495	0.453	1.898	0.0000	0.0039
NEMETH_TNF_UP	91	0.526	1.898	0.0000	0.0038
KRETZSCHMAR_IL6_DIFF	117	0.508	1.898	0.0000	0.0037
CISPLATIN_PROBCELL_UP	16	0.737	1.892	0.0032	0.0038
IFNALPHA_RESIST_DN	18	0.719	1.886	0.0000	0.0041
ROSS_CBF_MYH	40	0.591	1.876	0.0000	0.0046
IGF_VS_PDGF_DN	35	0.607	1.873	0.0000	0.0047
ADDYA_K562_HEMIN_TREATMENT	59	0.564	1.871	0.0000	0.0048
DAC_IFN_BLADDER_UP	16	0.727	1.863	0.0017	0.0052
HYPOXIA_NORMAL_UP	171	0.475	1.863	0.0000	0.0052
FALT_BCLL_DN	41	0.588	1.858	0.0015	0.0055
DAC_BLADDER_UP	23	0.662	1.856	0.0000	0.0056
BRCA_ER_POS	370	0.446	1.850	0.0000	0.0060
NAKAJIMA_MCS_UP	88	0.516	1.849	0.0000	0.0059
BENNETT_SLE_UP	20	0.683	1.849	0.0000	0.0059
IRITANI_ADPROX_VASC	128	0.491	1.849	0.0000	0.0058
BLEO_HUMAN_LYMPH_HIGH_4HRS_UP	21	0.681	1.846	0.0000	0.0059
HYPOXIA_REVIEW	71	0.538	1.835	0.0000	0.0069
LI_FETAL_VS_WT_KIDNEY_UP	149	0.476	1.833	0.0000	0.0070
WIELAND_HEPATITIS_B_INDUCED	74	0.525	1.829	0.0000	0.0073
JISON_SICKLECELL_DIFF	273	0.452	1.829	0.0000	0.0072
UV-CMV_UNIQUE_HCMV_6HRS_UP	87	0.513	1.826	0.0000	0.0073
RIBAVIRIN_RSV_UP	20	0.671	1.824	0.0000	0.0074
CMV-UV_HCMV_6HRS_UP	102	0.505	1.822	0.0000	0.0074
NING_COPD_DN	110	0.497	1.822	0.0000	0.0074
DER_IFNB_UP	77	0.515	1.815	0.0000	0.0079
BRUNO_IL3_DN	66	0.526	1.815	0.0000	0.0078
BYSTRYKH_HSC_CIS_GLOCUS	140	0.474	1.811	0.0000	0.0083
PENG_GLUTAMINE_UP	196	0.458	1.801	0.0000	0.0094
DER_IFNG_UP	55	0.539	1.801	0.0000	0.0094
IFNALPHA_NL_UP	20	0.676	1.799	0.0016	0.0095

EXPERIMENT NAME	SIZE	ES	NES	NOMINAL P-VALUE	FDR Q-VALUE
TNFALPHA_30MIN_UP	38	0.589	1.799	0.0015	0.0094
INNEREAR_UP	35	0.595	1.797	0.0015	0.0097
TAKEDA_NUP8_HOXA9_3D_UP	114	0.484	1.789	0.0000	0.0106
GREENBAUM_E2A_DN	25	0.625	1.784	0.0048	0.0111
STRESS_ARSENIC_SPECIFIC_UP	120	0.480	1.780	0.0000	0.0115
AGED_MOUSE_RETINA_ANY_UP	19	0.663	1.780	0.0032	0.0113
TNFALPHA_ALL_UP	68	0.515	1.777	0.0014	0.0117
LEE_CIP_UP	55	0.531	1.774	0.0000	0.0121
MYOD_NIH3T3_DN	46	0.553	1.772	0.0045	0.0123
GAMMA_ESR_WS_UNREG	24	0.622	1.768	0.0000	0.0128
AGED_MOUSE_HIPPOCAMPUS_ANY_UP	41	0.559	1.759	0.0015	0.0141
SANA_IFNG_ENDOTHELIAL_UP	47	0.549	1.756	0.0029	0.0144
ZHAN_MMPC_SIMAL	42	0.557	1.755	0.0000	0.0144
IDX_TSA_DN_CLUSTER2	61	0.517	1.745	0.0014	0.0163
5FU_RESIST_GASTRIC_UP	19	0.660	1.744	0.0015	0.0164
BLEO_HUMAN_LYMPH_HIGH_24HRS_UP	88	0.481	1.737	0.0000	0.0177
VERHAAK_AML_NPM1_MUT_VS_WT_UP	133	0.457	1.731	0.0000	0.0186
TARTE_PC	67	0.510	1.730	0.0027	0.0187
NADLER_OBESITY_UP	56	0.523	1.728	0.0000	0.0189
ABRAHAM_MM_VS_AL_DN	20	0.643	1.727	0.0080	0.0187
KENNY_WNT_DN	38	0.563	1.723	0.0015	0.0194
ABRAHAM_AL_VS_MM_UP	21	0.623	1.722	0.0032	0.0194
NI2_MOUSE_UP	39	0.553	1.720	0.0015	0.0198
FLOTHO_CASP8AP2_MRD_DIFF	56	0.506	1.716	0.0014	0.0205
CAMPTOTHECIN_PROBCELL_UP	20	0.642	1.716	0.0048	0.0204
UVB_NHEK4_6HRS_UP	24	0.603	1.710	0.0047	0.0214
UVB_NHEK4_6HRS_DN	17	0.640	1.708	0.0082	0.0215
TCELL_ANERGIC_UP	70	0.499	1.708	0.0014	0.0213
FERRARI_4HPR_UP	20	0.620	1.705	0.0049	0.0221
IRITANI_ADPROX_DN	47	0.529	1.702	0.0058	0.0227
IFNALPHA_HCC_UP	25	0.601	1.699	0.0016	0.0232
YANG_OSTECLASTS_SIG	39	0.528	1.699	0.0031	0.0230
IDX_TSA_DN_CLUSTER1	40	0.548	1.695	0.0045	0.0236
DAC_FIBRO_UP	17	0.653	1.692	0.0064	0.0244
TIS7_OVEREXP_DN	17	0.644	1.692	0.0050	0.0242
ICHIBA_GVHD	314	0.409	1.690	0.0000	0.0244
IRS_KO_ADIP_DN	38	0.542	1.690	0.0029	0.0244
NAKAJIMA_MCSMBP_MAST	42	0.539	1.688	0.0030	0.0246
BECKER_TAMOXIFEN_RESISTANT_UP	33	0.550	1.683	0.0046	0.0262
BRCA_BRCA1_NEG	113	0.452	1.681	0.0026	0.0263
CMV_HCMV_TIMECOURSE_6HRS_DN	33	0.558	1.678	0.0103	0.0272

EXPERIMENT NAME	SIZE	ES	NES	NOMINAL P-VALUE	FDR Q-VALUE
IFNA_UV-CMV_COMMON_HCMV_6HRS_UP	21	0.613	1.677	0.0098	0.0271
LIZUKA_L0_SM_L1	16	0.642	1.676	0.0101	0.0274
KNUDSEN_PMNS_UP	64	0.497	1.674	0.0028	0.0274
AS3_FIBRO_DN	28	0.577	1.673	0.0062	0.0275
TAKEDA_NUP8_HOXA9_8D_UP	99	0.463	1.673	0.0000	0.0274
METHOTREXATE_PROBCELL_UP	16	0.647	1.672	0.0116	0.0274
HDACI_COLON_BUT24HRS_UP	53	0.510	1.671	0.0015	0.0275
LEE_MYC_TGFA_UP	53	0.507	1.671	0.0085	0.0273
P53GENES_ALL	15	0.660	1.668	0.0116	0.0279
LEE_DENA_UP	50	0.516	1.667	0.0014	0.0280
RAS_ONCOGENIC_SIGNATURE	186	0.428	1.664	0.0000	0.0288
CHIARETTI_T_ALL_DIFF	214	0.421	1.663	0.0000	0.0288
BASSO_GERMINAL_CENTER_CD40_UP	84	0.473	1.662	0.0014	0.0291
ADIP_DIFF_CLUSTER1	52	0.516	1.661	0.0014	0.0290
CMV_UV-CMV_COMMON_HCMV_6HRS_UP	17	0.637	1.661	0.0066	0.0288
IL6_FIBRO_UP	37	0.541	1.659	0.0091	0.0292
IFN_BETA_UP	56	0.497	1.659	0.0070	0.0290
ADIP_VS_PREADIP_UP	34	0.544	1.656	0.0134	0.0298
ROSS_MLL_FUSION	61	0.482	1.653	0.0053	0.0307
KUMAR_HOXA_DIFF	436	0.394	1.651	0.0000	0.0311
SCHRAETS_MLL_UP	35	0.539	1.648	0.0076	0.0316
IDX_TSA_DN_CLUSTER5	41	0.521	1.646	0.0074	0.0322
HDACI_COLON_BUT30MIN_DN	23	0.594	1.646	0.0080	0.0319
HOUSTIS_ROS	36	0.540	1.643	0.0090	0.0326
AGED_MOUSE_CEREBELLUM_UP	56	0.485	1.643	0.0058	0.0324
UVB_NHEK3_C6	29	0.565	1.641	0.0155	0.0331
VEGF_MMMEC_ALL_UP	86	0.460	1.639	0.0013	0.0332
AGEING_BRAIN_UP	175	0.421	1.639	0.0024	0.0330
HDACI_COLON_TSABUT_DN	16	0.634	1.637	0.0129	0.0335
CARIES_PULP_HIGH_UP	70	0.469	1.636	0.0054	0.0338
CHIARETTI_T_ALL	198	0.417	1.636	0.0024	0.0336
KANNAN_P53_UP	31	0.545	1.635	0.0088	0.0338
TAKEDA_NUP8_HOXA9_10D_DN	96	0.451	1.634	0.0013	0.0337
UVC_HIGH_ALL_UP	15	0.650	1.632	0.0135	0.0347
LEE_TCELLS9_UP	18	0.617	1.631	0.0151	0.0346
CMV_UV-CMV_COMMON_HCMV_6HRS_DN	23	0.577	1.629	0.0108	0.0350
BAF57_BT549_UP	177	0.420	1.627	0.0000	0.0355
IRS1_KO_ADIP_DN	104	0.449	1.626	0.0000	0.0359
ZHAN_MMPC_LATEVS	40	0.519	1.624	0.0151	0.0362
HOHENKIRK_MONOCYTE_DEND_DN	100	0.447	1.623	0.0026	0.0364
IFN_ALL_UP	16	0.634	1.621	0.0162	0.0368

EXPERIMENT NAME	SIZE	ES	NES	NOMINAL P-VALUE	FDR Q-VALUE
UVB_NHEK1_UP	145	0.425	1.621	0.0000	0.0366
HIPPOCAMPUS_DEVELOPMENT_POSTNATAL	43	0.516	1.618	0.0075	0.0376
UVB_NHEK4_24HRS_DN	15	0.632	1.617	0.0238	0.0376
PENG_RAPAMYCIN_UP	128	0.424	1.615	0.0000	0.0380
XPB_TTD-CS_DN	22	0.581	1.613	0.0288	0.0388
CROONQUIST_IL6_RAS_UP	18	0.612	1.612	0.0155	0.0388
AGED_MOUSE_HYPOTH_UP	39	0.513	1.611	0.0087	0.0388
TAVOR_CEBP_UP	43	0.505	1.611	0.0146	0.0387
UVB_NHEK3_C3	15	0.634	1.607	0.0237	0.0401
CANCERDRUGS_PROBCELL_UP	18	0.621	1.606	0.0228	0.0403
BOQUEST_CD31PLUS_VS_CD31MINUS_UP	484	0.385	1.605	0.0000	0.0403
NAB_LUNG_UP	24	0.563	1.604	0.0123	0.0403
LIZUKA_L1_GR_G1	19	0.589	1.599	0.0233	0.0423
AGUIRRE_PANCREAS_CHR8	40	0.506	1.593	0.0134	0.0443
TAKEDA_NUP8_HOXA9_3D_DN	20	0.583	1.593	0.0133	0.0444
AGED_MOUSE_CORTEX_UP	30	0.550	1.592	0.0128	0.0442
HIPPOCAMPUS_DEVELOPMENT_PRENATAL	29	0.543	1.592	0.0185	0.0442
TSADAC_PANC50_UP	33	0.520	1.589	0.0181	0.0450
HEMATOP_STEM_ALL_UP	22	0.574	1.587	0.0274	0.0456
TAKEDA_NUP8_HOXA9_16D_DN	134	0.424	1.586	0.0000	0.0458
ZHAN_MM_CD1_VS_CD2_DN	36	0.512	1.586	0.0060	0.0456
MUNSHI_MM_UP	59	0.475	1.585	0.0112	0.0457
HDACI_COLON_BUT12HRS_UP	33	0.523	1.585	0.0220	0.0456
HSC_MATURE_SHARED	182	0.406	1.584	0.0000	0.0455
BRCA1_OVEREXP_UP	140	0.418	1.576	0.0012	0.0490
IFN_ANY_UP	72	0.460	1.575	0.0027	0.0494
JNK_UP	29	0.541	1.573	0.0233	0.0497

Table A1.4: Annotated experimental gene sets (c2.cgp.2.5.symbols.gmt) significantly enriched in the down-regulated genes following cellular detachment of EN-transformed MEFs, as determined by GSEA (FDR < 0.05)

EXPERIMENT NAME	SIZE	ES	NES	NOMINAL P-VALUE	FDR Q-VALUE
MANALO_HYPOXIA_DN	73	-0.731	-2.992	0.0000	0.0000
SERUM_FIBROBLAST_CELLCYCLE	97	-0.648	-2.779	0.0000	0.0000
PENG_LEUCINE_DN	129	-0.594	-2.603	0.0000	0.0000
IDX_TSA_UP_CLUSTER3	82	-0.597	-2.441	0.0000	0.0000
PENG_GLUTAMINE_DN	223	-0.503	-2.382	0.0000	0.0000
CROONQUIST_IL6_RAS_DN	20	-0.752	-2.278	0.0000	0.0002
BRCA1_OVEREXP_DN	96	-0.530	-2.270	0.0000	0.0001
CMV_IE86_UP	42	-0.606	-2.186	0.0000	0.0002
LI_FETAL_VS_WT_KIDNEY_DN	130	-0.489	-2.181	0.0000	0.0002
LEE_TCELLS3_UP	68	-0.537	-2.166	0.0000	0.0004
PENG_RAPAMYCIN_DN	169	-0.461	-2.133	0.0000	0.0008
FALT_BCLL_UP	36	-0.609	-2.131	0.0000	0.0007
CROONQUIST_IL6_STARVE_UP	32	-0.613	-2.120	0.0000	0.0008
YU_CMYC_UP	41	-0.577	-2.092	0.0000	0.0012
DOX_RESIST_GASTRIC_UP	29	-0.618	-2.048	0.0000	0.0023
CMV_HCMV_TIMECOURSE_20HRS_UP	62	-0.527	-2.046	0.0000	0.0022
GOLDRATH_CELLCYCLE	32	-0.604	-2.033	0.0000	0.0024
SCHUMACHER_MYC_UP	49	-0.536	-2.021	0.0000	0.0025
ADIP_DIFF_CLUSTER4	32	-0.591	-2.020	0.0030	0.0024
ZHAN_MM_CD138_PR_VS_REST	31	-0.615	-2.011	0.0000	0.0026
COLLER_MYC_UP	16	-0.720	-2.002	0.0000	0.0029
PRMT5_KD_UP	167	-0.432	-1.983	0.0000	0.0035
HOFFMANN_BIVSBII_BI_TABLE2	231	-0.409	-1.952	0.0000	0.0052
TARTE_PLASMA_BLASTIC	268	-0.401	-1.947	0.0000	0.0054
RUIZ_TENASCIN_TARGETS	73	-0.465	-1.900	0.0000	0.0079
CHEN_HOXA5_TARGETS_DN	39	-0.529	-1.886	0.0000	0.0087
SERUM_FIBROBLAST_CORE_UP	160	-0.413	-1.885	0.0000	0.0084
P21_ANY_DN	30	-0.565	-1.883	0.0056	0.0083
ZELLER_MYC_UP	23	-0.609	-1.883	0.0054	0.0081
CHANG_SERUM_RESPONSE_UP	129	-0.426	-1.882	0.0000	0.0079
REN_E2F1_TARGETS	36	-0.537	-1.875	0.0000	0.0084
PEART_HISTONE_DN	62	-0.474	-1.849	0.0000	0.0106
OLDAGE_DN	41	-0.510	-1.806	0.0000	0.0161
UVC_HIGH_D5_DN	29	-0.528	-1.794	0.0028	0.0174
INOS_ALL_UP	46	-0.481	-1.793	0.0000	0.0170
GREENBAUM_E2A_UP	31	-0.528	-1.776	0.0000	0.0197

EXPERIMENT NAME	SIZE	ES	NES	NOMINAL P-VALUE	FDR Q-VALUE
HESS_HOXAANMEIS1_UP	70	-0.432	-1.748	0.0000	0.0250
HUMAN_TISSUE_TESTIS	43	-0.481	-1.748	0.0067	0.0246
MYC_TARGETS	38	-0.492	-1.742	0.0092	0.0249
HESS_HOXAANMEIS1_DN	70	-0.432	-1.742	0.0000	0.0244
FSH_GRANULOSA_DN	66	-0.435	-1.735	0.0035	0.0257
BLEO_MOUSE_LYMPH_HIGH_24HRS_DN	32	-0.509	-1.730	0.0028	0.0262
CANCER_UNDIFFERENTIATED_META_UP	62	-0.438	-1.716	0.0067	0.0294
ET743_SARCOMA_24HRS_DN	87	-0.413	-1.715	0.0039	0.0289
HDACI_COLON_CLUSTER10	28	-0.525	-1.715	0.0000	0.0283
CMV_HCMV_TIMECOURSE_14HRS_UP	37	-0.487	-1.709	0.0030	0.0293
ADIP_DIFF_CLUSTER5	35	-0.489	-1.709	0.0113	0.0286
BCNU_GLIOMA_NOMGMT_48HRS_DN	26	-0.529	-1.703	0.0117	0.0292
LH_GRANULOSA_DN	66	-0.435	-1.694	0.0034	0.0309
IGFR_IR_UP	15	-0.602	-1.680	0.0136	0.0339
ET743_SARCOMA_48HRS_DN	148	-0.373	-1.674	0.0000	0.0347
UVC_HIGH_ALL_DN	234	-0.348	-1.673	0.0000	0.0343
REOVIRUS_HEK293_DN	188	-0.353	-1.651	0.0000	0.0410
ET743_SARCOMA_72HRS_DN	169	-0.346	-1.644	0.0000	0.0428
MENSSEN_MYC_UP	25	-0.503	-1.642	0.0137	0.0428
GAY_YY1_DN	270	-0.336	-1.633	0.0000	0.0451
BRENTANI_CELL_CYCLE	73	-0.404	-1.626	0.0000	0.0466
CANTHARIDIN_DN	45	-0.446	-1.622	0.0155	0.0473
FERRANDO_MLL_T_ALL_DN	72	-0.402	-1.622	0.0000	0.0468
P21_P53_ANY_DN	37	-0.458	-1.620	0.0142	0.0467

Table A1.5: Genes up- and down-regulated in prostate cancer cells expressing a dominant negative AMPKα1 versus empty vector - Zhou et al. (ref. 18) Tables 2 and 3

AMPK inactivation – UP	
Symbol	**Name**
MAGEC2	melanoma antigen family C, 2
EPHA3	EPH receptor A3
PRKAA1	protein kinase, AMP-activated, alpha 1 catalytic subunit
ITGB5	integrin, beta 5
FN1	fibronectin 1
EAF2	ELL associated factor 2
RHOU	ras homolog gene family, member U
IGF1	insulin-like growth factor 1 (somatomedin C)
MAP2	microtubule-associated protein 2
HIST2H2BE	histone cluster 2, H2be
GHR	growth hormone receptor
FGFR1OP2	FGFR1 oncogene partner 2
IGF1R	insulin-like growth factor 1 receptor
ID2	inhibitor of DNA binding 2, dominant negative helix-loop-helix protein
CDC42EP3	CDC42 effector protein (Rho GTPase binding) 3
PRKACB	protein kinase, cAMP-dependent, catalytic, beta
FKBP5	FK506 binding protein 5
CLU	clusterin
CENPF	centromere protein F, 350/400ka (mitosin)
TMEPAI	

AMPK inactivation – DOWN	
Symbol	**Name**
CD24	CD24 molecule; CD24 molecule-like 4
RND3	Rho family GTPase 3
MMP16	matrix metallopeptidase 16 (membrane-inserted)
TNFSF15	tumor necrosis factor (ligand) superfamily, member 15
GSTA1	glutathione S-transferase alpha 1
MATN2	matrilin 2
LITAF	lipopolysaccharide-induced TNF factor
PSMB8	proteasome (prosome, macropain) subunit, beta type, 8 (large multifunctional peptidase 7)
BIRC3	baculoviral IAP repeat-containing 3
BTG1	B-cell translocation gene 1, anti-proliferative
EGF	epidermal growth factor (beta-urogastrone)
LMO4	LIM domain only 4
TP53TG3	similar to TP53 target 3; TP53 target 3; similar to TP53TG3 protein
RGS2	regulator of G-protein signaling 2, 24kDa
GJB2	gap junction protein, beta 2, 26kDa
PTPRR	protein tyrosine phosphatase, receptor type, R
PLA2G2A	phospholipase A2, group IIA (platelets, synovial fluid)
MAGEA4	melanoma antigen family A, 4
EGLN3	egl nine homolog 3 (C. elegans)
OPHN1	oligophrenin 1
CDH3	cadherin 3, type 1, P-cadherin (placental)
CMKOR1	

Table A1.6: Genes up- and down-regulated 1.5 fold in mouse skeletal muscle cells following AICAR treatment versus vehicle control - Narkar et al. (ref. 17)

AICAR treatment – UP		**AICAR treatment – DOWN**	
Symbol	**Name**	**Symbol**	**Name**
IFI205	interferon activated gene 205	TCEAL7	transcription elongation factor A (SII)-like 7
PTPLB	predicted gene 7908; protein tyrosine phosphatase-like (proline instead of catalytic arginine), member b	CITED4	Cbp/p300-interacting transactivator, with Glu/Asp-rich carboxy-terminal domain, 4
SLC36A2	solute carrier family 36 (proton/amino acid symporter), member 2	KLF2	Kruppel-like factor 2 (lung)
ACP5	acid phosphatase 5, tartrate resistant	COQ10B	hypothetical protein LOC675736; coenzyme Q10 homolog B (S. cerevisiae); predicted gene 4899
HP	haptoglobin	ITGB6	integrin beta 6
SFXN1	sideroflexin 1	ETS1	E26 avian leukemia oncogene 1, 5' domain
CYP2E1	cytochrome P450, family 2, subfamily e, polypeptide 1	E2F2	E2F transcription factor 2
MT2	metallothionein 2	KLF10	Kruppel-like factor 10
FKBP5	FK506 binding protein 5	ATRX	alpha thalassemia/mental retardation syndrome X-linked homolog (human)
SCD1	stearoyl-Coenzyme A desaturase 1	SERBP1	serpine1 mRNA binding protein 1
MCF2L	mcf.2 transforming sequence-like	MYO10	myosin X
MT1	metallothionein 1	AQP4	aquaporin 4
TUSC5	tumor suppressor candidate 5	TFRC	transferrin receptor
AOC3	amine oxidase, copper containing 3	PRPF40A	PRP40 pre-mRNA processing factor 40 homolog A (yeast)
ORM1	orosomucoid 1	HSPA8	similar to heat shock protein 8; heat shock protein 8
RETN	resistin	TGFB2	transforming growth factor, beta 2
SULT1A1	sulfotransferase family 1A, phenol-preferring, member 1	LPP	LIM domain containing preferred translocation partner in lipoma
CIDEC	cell death-inducing DFFA-like effector c	RPL22L1	predicted gene 2157; similar to ribosomal protein L22 like 1; ribosomal protein L22 like 1
PIK3CD	phosphatidylinositol 3-kinase catalytic delta polypeptide; RIKEN cDNA 2610208K16 gene	XPR1	xenotropic and polytropic retrovirus receptor 1
FABP4	fatty acid binding protein 4, adipocyte	LNP	limb and neural patterns

AICAR treatment – UP		AICAR treatment – DOWN	
Symbol	**Name**	**Symbol**	**Name**
ADRB3	adrenergic receptor, beta 3	OTUD1	OTU domain containing 1
CFD	complement factor D (adipsin)	TNFAIP2	tumor necrosis factor, alpha-induced protein 2
IER5	immediate early response 5	PRKG1	protein kinase, cGMP-dependent, type I
ADIPOQ	adiponectin, C1Q and collagen domain containing	DUSP10	dual specificity phosphatase 10
ADH1	alcohol dehydrogenase 1 (class I)	SOCS2	suppressor of cytokine signaling 2; predicted gene 8000
AACS	acetoacetyl-CoA synthetase	PDE4B	phosphodiesterase 4B, cAMP specific
SLC7A8	solute carrier family 7 (cationic amino acid transporter, y+ system), member 8	ATP2B1	ATPase, Ca++ transporting, plasma membrane 1
SLC25A1	solute carrier family 25 (mitochondrial carrier, citrate transporter), member 1	HIST1H1E	histone cluster 1, H1e
PPARG	peroxisome proliferator activated receptor gamma	PFKFB3	6-phosphofructo-2-kinase/fructose-2,6-biphosphatase 3
ARRDC2	arrestin domain containing 2	LRRFIP1	leucine rich repeat (in FLII) interacting protein 1
DGAT2	diacylglycerol O-acyltransferase 2	SCD2	stearoyl-Coenzyme A desaturase 2
LEP	leptin	FOS	FBJ osteosarcoma oncogene
		ENSMUSG0000006916	3
CEBPA	CCAAT/enhancer binding protein (C/EBP), alpha	PREI4	
FMO2	flavin containing monooxygenase 2		
CHDH	choline dehydrogenase		
AGPAT2	1-acylglycerol-3-phosphate O-acyltransferase 2 (lysophosphatidic acid acyltransferase, beta)		
FASN	fatty acid synthase		
TRF	transferrin		
SLC7A10	solute carrier family 7 (cationic amino acid transporter, y+ system), member 10		
PPP1R3C	protein phosphatase 1, regulatory (inhibitor) subunit 3C		
ITGB1BP3	integrin beta 1 binding protein 3		
FOXO1	forkhead box O1		
PCK1	phosphoenolpyruvate carboxykinase 1, cytosolic		
MGST1	microsomal glutathione S-transferase 1		
UCP1	uncoupling protein 1 (mitochondrial, proton carrier)		
TKT	transketolase		

AICAR treatment – UP		AICAR treatment – DOWN	
Symbol	**Name**	**Symbol**	**Name**
CDO1	cysteine dioxygenase 1, cytosolic		
PYGL	liver glycogen phosphorylase		
ELOVL6	predicted gene 11295; ELOVL family member 6, elongation of long chain fatty acids (yeast)		
ADAMTSL4	ADAMTS-like 4		
MAP3K6	mitogen-activated protein kinase kinase kinase 6		
ANKRD2	ankyrin repeat domain 2 (stretch responsive muscle)		
TIMP4	tissue inhibitor of metalloproteinase 4		
XDH	xanthine dehydrogenase		
CYP2F2	cytochrome P450, family 2, subfamily f, polypeptide 2		
CAR3	carbonic anhydrase 3		
NNAT	neuronatin		
CIDEA	cell death-inducing DNA fragmentation factor, alpha subunit-like effector A		
CSRP3	cysteine and glycine-rich protein 3		
TMEM45B	transmembrane protein 45b		
ACLY	ATP citrate lyase		
LMOD2	leiomodin 2 (cardiac)		
THRSP	thyroid hormone responsive SPOT14 homolog (Rattus)		
LIPE	lipase, hormone sensitive		
MYL2	myosin, light polypeptide 2, regulatory, cardiac, slow		
PRKAR2B	protein kinase, cAMP dependent regulatory, type II beta		
SLC1A5	solute carrier family 1 (neutral amino acid transporter), member 5		
CD1D1	CD1d1 antigen; CD1d2 antigen		
SYP	synaptophysin		

Table A1.7: Genes differentially expressed in glucose deprived FOXO3A-/- MEFs re-expressing wild-type versus an inactive (non-phosphorylatable) 6A-mutant FOXO3A construct - Greer et al. (ref. 19) Figure 6

AMPK/FOXO3A – UP		AMPK/FOXO3A – DOWN	
Symbol	**Name**	**Symbol**	**Name**
TSPYL5	testis-specific protein, Y-encoded-like 5	LGALS2	lectin, galactoside-binding, soluble, 2
SQSTM1	sequestosome 1	SUV39H2	suppressor of variegation 3-9 homolog 2 (Drosophila)
CLEC14A	C-type lectin domain family 14, member a	NPR3	natriuretic peptide receptor C/guanylate cyclase C (atrionatriuretic peptide receptor C)
CXCR4	chemokine (C-X-C motif) receptor 4	LFNG	LFNG O-fucosylpeptide 3-beta-N-acetylglucosaminyltransferase
MT2	metallothionein 2	SORBS1	sorbin and SH3 domain containing 1
MLLT10	myeloid/lymphoid or mixed-lineage leukemia (trithorax homolog, Drosophila); translocated to, 10	HCK	hemopoietic cell kinase
LARP6	La ribonucleoprotein domain family, member 6	SIGLEC10	sialic acid binding Ig-like lectin 10
VAV3	vav 3 oncogene	DDAH1	dimethylarginine dimethylaminohydrolase 1
RAB27A	RAB27A, member RAS oncogene family	VCL	vinculin
TSC22D1	TSC22 domain family, member 1	SDPR	serum deprivation response (phosphatidylserine binding protein)
GRASP	GRP1 (general receptor for phosphoinositides 1)-associated scaffold protein	LIMS2	LIM and senescent cell antigen-like domains 2
RGS2	regulator of G-protein signaling 2	CDC42EP3	CDC42 effector protein (Rho GTPase binding) 3
DDIT3	DNA-damage inducible transcript 3	GJB2	gap junction protein, beta 2, 26kDa
ZFP467	zinc finger protein 467	AMOTL2	angiomotin like 2
MT1	metallothionein 1	RASGRP3	RAS guanyl releasing protein 3 (calcium and DAG-regulated)
SSTR2	somatostatin receptor 2	TNFRSF11B	tumor necrosis factor receptor superfamily, member 11b
ITGB2	integrin beta 2	MRVI1	murine retrovirus integration site 1 homolog
CAMK1D	calcium/calmodulin-dependent protein kinase ID	CYR61	cysteine-rich, angiogenic inducer, 61
KIFC2	kinesin family member C2	PKP2	plakophilin 2
GADD45A	growth arrest and DNA-damage-inducible 45 alpha	NEXN	nexilin (F actin binding protein)
LHFPL2	lipoma HMGIC fusion partner-like 2	ANKRD1	ankyrin repeat domain 1 (cardiac muscle)
AMPK/FOXO3A – UP		**AMPK/FOXO3A – DOWN**	
Symbol	**Name**	**Symbol**	**Name**

CCND3	similar to Cyclin D3; cyclin D3
VCAN	versican
APOD	apolipoprotein D
IGFBP5	insulin-like growth factor binding protein 5
ALDH3A1	aldehyde dehydrogenase family 3, subfamily A1
PCMTD1	protein-L-isoaspartate (D-aspartate) O-methyltransferase domain containing 1
PEG3	paternally expressed 3; antisense transcript gene of Peg3
SLC40A1	solute carrier family 40 (iron-regulated transporter), member 1
TXNIP	thioredoxin interacting protein
USP22	ubiquitin specific peptidase 22
ANPEP	alanyl (membrane) aminopeptidase
GSTM1	similar to Glutathione S-transferase Mu 1 (GST class-mu 1) (Glutathione S-transferase GT8.7) (pmGT10) (GST 1-1); predicted gene 5562; glutathione S-transferase, mu 1
WNT7B	wingless-related MMTV integration site 7B
ZFAND5	similar to zinc finger protein ZNF216; zinc finger, AN1-type domain 5
MAFB	v-maf musculoaponeurotic fibrosarcoma oncogene family, protein B (avian)
CD28	CD28 antigen; similar to CD28 antigen
HPS1	Hermansky-Pudlak syndrome 1 homolog (human)
CTE1	
RAMP	
UGP1A1	
NEBL	nebulette
TGM2	transglutaminase 2 (C polypeptide, protein-glutamine-gamma-glutamyltransferase)
RGS4	regulator of G-protein signaling 4
NES	nestin
JPH2	junctophilin 2
RRM2	ribonucleotide reductase M2 polypeptide
EHMT2	euchromatic histone-lysine N-methyltransferase 2
GADD45G	growth arrest and DNA-damage-inducible, gamma
SPATA3	spermatogenesis associated 3
LIPG	lipase, endothelial
LMOD1	leiomodin 1 (smooth muscle)
EGFL9	
CXCL7	
HNRPAB	